The Contribution of Spleen Tyrosine Kinase to the Pathobiology of Alzheimer's Disease

Thesis

PHD THESIS

OF

JONAS ELIAS SCHWEIG
(B.SC., M.SC.)

The Contribution of Spleen Tyrosine Kinase to the Pathobiology of Alzheimer's Disease

Discipline:
Neuroscience

Date of Submission:
September 10, 2018

Supervisors:
Dr. Daniel Paris & Dr. Michael Mullan

OU Personal Identifier: E5024232

ARC: The Roskamp Institute,
2040 Whitfield Avenue, Sarasota
34243, FL, USA

The Open University,
Walton Hall, Milton Keynes,
MK7 6AA, UK

Declaration

I hereby declare that the work presented in this thesis is my own, except for where stated. This work has not been submitted for any other degree of professional qualification.

Jonas Schweig

Abstract

Alzheimer's disease (AD) is a neurodegenerative disease that accounts for most cases of dementia. The pathological hallmarks of AD include extracellular Aβ plaques, intracellular tau accumulations or neurofibrillary tangles, as well as neuroinflammation. As of 2018, there exists no disease modifying treatment for AD and the cause of sporadic AD remains elusive. We investigated the contribution of the spleen tyrosine kinase (SYK) in AD pathobiology. Syk is well-known for its involvement in B-cell receptor (BCR) signaling but our previous data have demonstrated that SYK is also involved in tau hyperphosphorylation and Aβ production, therefore suggesting that SYK could contribute to the formation of AD pathological lesions.

The goals of our present studies were to determine whether SYK activation occurs in the brain of mouse models of AD and investigate whether the levels of SYK activation vary with the amount of AD pathological lesions. In addition, we aimed to examine the role of SYK in the autophagic degradation of tau via the mammalian target of rapamycin (mTOR) pathway *in vitro* and *in vivo*. We investigated SYK activation in different age-groups of Aβ and tau overexpressing mice, as well as human AD specimens. We characterized the activation of SYK in relation to AD pathological lesions including amyloid plaques, activated microglia and astroglia, as well as hyperphosphorylated tau. In addition, our mechanistic *in vitro* experiments delineated SYK as a regulator of autophagic tau degradation via the mTOR pathway. These data were confirmed in an *in vivo* study, assessing the effects of a 12-week chronic SYK inhibition on tau burden, neurodegeneration, behavior, and neuroinflammation in a mouse model with established tauopathy.

Identifying new targets like SYK that act downstream of Aβ and tau and in turn exacerbate these known pathologies, is crucial to find a treatment for AD.

Acknowledgements

Doing research and writing a doctoral thesis is so much more than just going to the lab and doing experiments. It is the daily interactions with the people that makes it a unique experience. I would like to thank all those people now.

First and foremost, I would like to thank my primary supervisor Dr. Daniel Paris. Daniel, thank you for selecting me three years ago out of all those applicants. Thank you for having faith in me and my work and supporting me with your wisdom during the last three years. Your guidance has been excellent and it allowed me to finish this piece of work. Thank you for letting me benefit from your years of scientific experience and for guiding me into the next chapter of my life. I am looking forward to many more exciting discussions about quantum physics and the purpose of life.

I would also like to thank my second supervisor Dr. Mike Mullan. Thank you Mike, for the great discussions about our research that formed the past research articles, that shaped this thesis and also formed me as a scientist. I am very grateful for your supervision and support. Your vast medical, scientific and business knowledge is still a mystery to me sometimes but I hope to achieve such a level of insight in the future.
And of course, I would like to thank Dr. Fiona Crawford. Thank you Fiona, for selecting and supporting me and all other students continuously during our research without ever failing to fulfill all those other countless obligations of yours. I admire your ambition, passion and perseverance in the pursuit of a greater well-being of humans and a flourishing Roskamp Institute.

I thank Dr. Hailan Yao and Kyle Coppola for great teamwork and for making the molecular biology lab a pleasant work place.
I thank all staff members of the Roskamp Institute.
I thank my friends, roommates, and fellow Ph.D. students Alex Morin and Utsav Joshi as well as Heather Langlois and Nicole Saltiel for fun times in and outside of work.
Thank you Robert & Diane Roskamp for founding the Roskamp Institute in the first place and giving young students like me the chance to do research that will reduce human suffering.
I would like to thank the Roskamp foundation for funding our research and for supporting us students even outside of work.
I also thank the James Hailey Veteran's Hospital for providing the funding for this research.
Thank you, all of you, the past three years will forever stay in my memory.

I would like to thank the most wonderful human being I know, Charis Ringland. Charis, you bring joy into my life like no one else. You are always there for me. You made it easier for me to write this thesis but you also made it easier for me to write my life.
Zuguterletzt möchte ich meinen Eltern Uwe und Ricarda Schweig, sowie meinen Großeltern Roselinde und Manfred Schmidtberger, sowie Gunda Schweig danken. Ich widme euch diese Doktorarbeit, weil ihr wirklich immer für mich da wart und alles dafür gegeben habt, damit es mir gut geht und ich die Zukunft haben kann, die ich mir erträumt habe. Ihr wart es, die es mir überhaupt erst ermöglicht habt diese Ausbildung anzustreben und dieses Wissen anzueignen, das mich das Leben etwas mehr verstehen laesst. Ich werde euch auf ewig dankbar für alles sein und ich wünschte, dass alle von euch noch hier wären, um diesen Moment mit mir zu feiern.

I would also like to thank the scientists that actively contributed to this thesis:

Chapter on the "Assessment of the activation pattern of SYK in 3 distinct mouse models of AD and human AD specimens"

1. Dr. Hailan Yao generated of SYK overexpressing SH-SY5Y Cells and did the WBs shown in Figure 16.
2. Dr. Benoit Mouzon provided paraffin sections of AD and non-demented controls.
3. Dr. Ghania Ait-Ghezala provided paraffin blocks of Tg Tau P301S mice.

Chapter on the "Mechanistic Assessment of the role of SYK in autophagy and the mTOR pathway in CNS-derived SH-SY5Y cells"

1. Dr. Daniel Paris performed the Puromycin Incorporation Assay, Immunoprecipitation (IP) and did the WBs shown in Figure 23A/C.
2. Dr. Hailan Yao did the Quantitative RT-PCR (Figure 23E), generated SYK knockdown SH-SY5Y cells and helped with the WBs shown in Figure 25A/B.

Chapter on the "Effects of chronic SYK inhibition in Tg Tau P301S mice"

1. Dr. Daniel Paris helped with the tissue collection following the *in vivo* study and the ELISAs for measuring PSD-95 and cytokines.

General:

1. Dr. Daniel Paris and Dr. Mike Mullan guided me through the preparation of the published/submitted manuscripts that are presented as the three main results chapters in this thesis. They furthermore guided and supervised the research presented in my thesis.
2. Dr. Daniel Paris and David Beaulieu-Abdelahad trained me in the lab and showed me all methods presented in my thesis.

Index

1 Introduction 14
1.1 Alzheimer's Disease 14
1.1.1 History 14
1.1.2 Demography & Etiology 15
1.1.3 Amyloid pathology 19
1.1.3.1 APP processing 21
1.1.4 Tau pathology 23
1.1.5 Neuroinflammation 32
1.1.6 Autophagy and the mTOR pathway 38
1.1.7 Mouse models of Alzheimer's disease 43
1.1.7.1 Tg APPsw mice (Tg 2576) 43
1.1.7.2 Tg PS1/APPsw mice 44
1.1.7.3 Tg Tau P301S mice (Line PS19) 45
1.2 The Spleen Tyrosine Kinase 47
1.2.1 The role of SYK in Alzheimer's disease 51
1.2.2 The role of SYK in Nasu-Hakola disease 53
1.3 Clinical trials for Alzheimer's disease 57
1.4 Aims of the studies 66
2 Assessment of the activation pattern of SYK in 3 distinct mouse models of AD and human AD specimens 67
2.1 Introduction 67
2.2 Materials & Methods 71
2.2.1 Animals 71
2.2.2 Tissue Processing 71
2.2.3 Immunofluorescence 72
2.2.4 Cell Culture 74
2.2.5 Generation of SYK overexpressing SH-SY5Y Cells 75
2.2.6 Immunoblotting 75
2.2.7 Statistical Analyses 76
2.3 Results 77
2.3.1 Cellular localization of Syk activation in brains of Tg PS1/APPsw, Tg APPsw mice and WT mice 77
2.3.2 SYK activation in dystrophic neurites of Tg PS1/APPsw and Tg APPsw mice 79

2.3.3 Age-dependent and amyloid deposition-dependent increase of SYK activation in Tg PS1/APPsw and Tg APPsw compared to WT mice 81
2.3.4 Age-dependent and tau dependent SYK activation pattern in Tg Tau P301S mice 84
2.3.5 Tau species-dependent SYK activation 92
2.3.6 SYK upregulation promotes tau accumulation in neuron-like SH-SY5Y cells.... 105
2.3.7 Increased SYK activation in human AD specimen compared to non-demented controls 108
2.4 Discussion 112
3 Mechanistic assessment of the role of SYK in autophagy and the mTOR pathway in CNS-derived SH-SY5Y cells 117
3.1 Introduction 117
3.2 Methods 120
3.2.1 Cell Culture 120
3.2.2 Cell Culture Treatments 120
3.2.3 Puromycin Incorporation Assay 120
3.2.4 Immunoprecipitation (IP) 121
3.2.5 Quantitative RT-PCR 121
3.2.6 Generation of SYK knockdown SH-SY5Y Cells 122
3.2.7 Immunoblotting 122
3.2.8 Statistical Analyses 123
3.3 Results 124
3.3.1 SYK inhibition decreases p-tau, as well as total tau levels and reverses the effects of the Akt activator SC79 on the mTOR pathway 124
3.3.2 SYK inhibition reverses the effects of the mTOR activator MHY1485 and mimics the effects of the mTOR inhibitor KU0063794 127
3.3.3 SYK inhibition increases the autophagic flux and decreases tau levels in the presence of the lysosomal inhibitor chloroquine 130
3.3.4 SYK inhibition does not affect tau translation or transcription 134
3.3.5 Suppression of SYK expression mimics pharmacological inhibition of SYK and decreases total tau levels 140
3.4 Discussion 143
4 Effects of chronic SYK inhibition in Tg Tau P301S mice 148
4.1 Introduction 148
4.1.1 Study design 151
4.2 Methods 152
4.2.1 Animals 152

4.2.2 In vivo treatment 152
4.2.3 Behavioral Analysis 153
4.2.4 Tissue Processing 154
4.2.5 Immunoblotting 155
4.2.6 Total protein concentration (BCA) 156
4.2.7 ELISA for PSD-95 and cytokine levels 156
4.2.8 Statistical Analyses 156
4.3 Results 157
4.3.1 Chronic SYK inhibition reduces p-SYK and t-SYK levels in Tg Tau P301S mice, rescues neuronal and synaptical loss and decreases mTOR activity 157
4.3.2 Chronic SYK inhibition reduces tau accumulation and improves motor performance in Tg Tau P301S mice 160
4.3.3 Chronic SYK inhibition decreases neuroinflammation in Tg Tau P301S mice ... 163
4.4 Discussion 166
4.4.1 Excursion: Tg Tau P301S organotypic vibrosections: brain cytokine levels following ex-vivo SYK inhibition 172
4.4.1.1 Introduction 172
4.4.1.2 Materials and Methods 173
4.4.1.2.1 Animals 173
4.4.1.2.2 Treatment of organotypic vibrosections 173
4.4.1.2.3 ELISA for cytokine levels 174
4.4.1.2.4 Total protein concentration (BCA) 174
4.4.1.2.5 Statistical Analyses 175
4.4.1.3 Results 175
4.4.1.4 Discussion 181
5 Conclusion 186
6 Future Directions 193
7 Publication bibliography 195
8 Appendix: Published Research Articles 229



Table of Figures

Figure 1: APP Processing 22
Figure 2: Tau isoforms 24
Figure 3: p-SYK is increased in activated microglia and non-glial cells associated with Aβ-plaques in Tg APPsw and Tg PS1/APPsw mice. 79
Figure 4: p-SYK is increased in dystrophic neurites of Aβ-overexpressing mice 80
Figure 5: Cortical p-SYK burden is age-dependently increased in Aβ-overexpressing mice, particularly in microscopic fields containing Aβ deposits, compared to wild-type littermates 83
Figure 6: p-SYK is increased in hippocampal neurons of Tg Tau P301S mice compared to wild-type littermates 86
Figure 7: p-SYK is increased in cortical neurons of Tg Tau P301S mice compared to wild-type littermates 87
Figure 8: p-SYK is increased age-dependently in hippocampal neurons of Tg Tau P301S mice compared to wild-type littermates 89
Figure 9: p-SYK is increased age-dependently in cortical neurons of Tg Tau P301S mice compared to wild-type littermates 91
Figure 10: The degree of co-localization of p-SYK and tau differs for various tau epitopes 94
Figure 11: The amount of MC1 tau conformers and p-SYK (Y525/526) levels cross-influence each other 96
Figure 12: tau phosphorylation at Y18 and Syk activation (Y525/526) cross-influence each other 98
Figure 13: Syk activation (p-SYK (Y525/526) influences the level of tau phosphorylation at S396/404 100
Figure 14: SYK activation (Y525/526) influences the level of tau oligomerization (TOC1) 102
Figure 15: Syk activation (Y525/526) influences the level of tau phosphorylation at S202 104
Figure 16: Syk overexpression increases tau phosphorylation and total tau levels in SH-SY5Y cells 107
Figure 17: p-SYK is increased in cortical neurons immunopositive for p-tau (Y18) of human AD compared to non-demented controls 109
Figure 18: p-SYK is increased in cortical neurons immunopositive for MC1 pathogenic tau conformers in AD compared to brain sections from a non-demented control 110
Figure 19: p-SYK is increased in dystrophic neurites associated with β-amyloid plaques of human AD patients compared to healthy controls 111
Figure 20: SYK inhibition decreases p-tau, as well as total tau levels and reverses the effects of the Akt activator SC79 on the mTOR pathway 126
Figure 21: SYK inhibition reverses the effects of the mTOR activator MHY1485 and mimics the effects of the mTOR inhibitor KU0063794 129
Figure 22: SYK inhibition increases the autophagic flux and decreases tau levels in the presence of the lysosomal inhibitor chloroquine 133
Figure 23: SYK inhibition does not alter transcription or translation levels of tau in vitro 137
Figure 24: S6K inhibition by PF4708671 has similar effects as SYK inhibition on the mTOR pathway and tau levels 139
Figure 25: SYK knockdown mimics pharmacological inhibition of SYK and decreases total tau levels 142
Figure 26: Schematic depiction of the role of SYK in the mTOR pathway and autophagy 147

Figure 27: Study design for 12-week chronic SYK inhibition 151
Figure 28: Chronic SYK inhibition reduces p-SYK and t-SYK levels in Tg Tau P301S mice, rescues neuronal and synaptic loss and decreases mTOR activity 159
Figure 29: Chronic SYK inhibition reduces insoluble and soluble tau levels and improves motor performance in Tg Tau P301S mice 162
Figure 30: Chronic SYK inhibition decreases microgliosis and reduces pro-inflammatory cytokines in Tg Tau P301S mice 165
Figure 31: Cytokine production in organotypic vibrosections of Tg Tau P301S mice and WT littermates following LPS exposure and SYK inhibition 180
Figure 32: Relationships between SYK and the main AD pathologies 191

Abbreviations

3/4R	3/4 Repeat
AAALAC	Association for Assessment and Accreditation of Laboratory Animal Care International
AD	Alzheimer's Disease
ADAS	Alzheimer's Disease Assessment Scale
AICD	APP Intracellular Domain
Akt	Protein Kinase B
ALL	Acute Lymphoblastic Leukemia
aMCI	Amnestic Mild Cognitive Impairment
AMPK	5' Adenosine Monophosphate-Activated Kinase
ApoE	Apolipoprotein E
APP	Amyloid Precursor Protein
APP	Amyloid Precursor Protein
ARIA-E	Amyloid-Related Imaging Abnormalities-Edema
ASO	Anti-sense Oligonucleotides
Atg	Autophagy-Related Proteins
AVMA	American Veterinary Medical Association
AVs	Autophagic Vesicles
Aβ	β-amyloid
Aβ	Amyloid β
BACE	Beta-secretase
BBB	Blood Brain Barrier
BCR	B-Cell Receptor
BUADC	Boston University Alzheimer's Disease Center
CdK5	Cyclin-Dependent Kinase 5
CDR-SB	Clinical Dementia Rating Scale Sum of Boxes
CIN85	CbI-interacting 85-kDa multi-adaptor protein
cKO	Conditional Knockout
CLL	Chronic Lymphocytic Leukemia
CNS	Central Nervous System
CNS	Central Nervous System
CQ	Chloroquine
CREB	cAMP Response Element-Binding Protein
CSF	Cerebrospinal Fluid
CTFα/β	C-terminal Fragment α/β
DAD	Disability Assessment for Dementia
DAP12	DNAX-activation Protein 12
DHP	Dihydropyridine
DMT	Disease Modifying Therapies
DNs	Dystrophic Neurites
EIF 4EBP1	Eukaryotic Translation Initiation Factor 4E-binding Protein
EOAD	Early Onset Alzheimer's Disease

ERK	Extracellular signal-regulated Kinase
FcγR	Fragment crystallizable (Fc) of immunoglobulin G receptor
FcεRI	Fragment crystallizable (Fc) of immunoglobulin E receptor I
FDA	Food and Drug Administration
FLT-3	FMS-like Tyrosine Kinase 3
FTD	Frontotemporal Dementia
FTDP-17	Frontotemporal Dementia and Parkinsonism
Fyn	Proto-oncogene Tyrosine Kinase
GFAP	Glial Fibrillary Acidic Protein
GRN	Granulin
GSK-3	Glycogen Synthase Kinase 3
Iba-1	Ionized Calcium-Binding Adapter Molecule-1
IF	Intermediate Filaments
IL	Interleukin
iNOS	Inducible Nitric Oxide Synthase
IP	Immunoprecipitation
ITAM	Immunoreceptor Tyrosine-Based Activating Motifs
ITP	Immune Thrombocytopenia
JAK	Janus Kinase
LAMP-1	Lysosomal-Membrane Associated Protein-1
LC3	Microtubule-Associated Protein 1 Light Chain 3
LCC	L-type Calcium Channel
LcK	Lymphocyte-specific Protein Tyrosine Kinase
LMTM	Leuco-Methylthioninium-Bis(Hydromethanesulfonate)
LOAD	Late Onset Alzheimer's Disease
LRP1	Low Density Lipoprotein Receptor-Related Protein 1
MAP	Microtubule Associated Protein
MAPK	Mitogen-Activated Protein Kinases
MAPT	Microtubule Associated Protein Tau
MMSE	Mini-Mental State Examination
MOA	Mechanism of Action
MPER	Mammalian Protein Extraction Reagent
MS	Multiple Sclerosis
MTBD	Microtubule Binding Domain
mTOR	Mammalian Target of Rapamycin
mTORC1	mTOR complex 1
NFTs	Neurofibrillary Tangles
NHD	Nasu-Hakola Disease
PBS	Phosphate Buffered Saline
PCR	Polymerase Chain Reaction
PD	Parkinson's Disease
PDK1	3-Phospoinositide-Dpendent Protein Kinase 1
PE	Phosphatidylethanolamine
PET	Positron Emission Tomography

PFA	Paraformaldehyde
PHF	Paired Helical Filaments
PI3K	Phosphoinositide 3-Kinase
PKA	cAMP-Dependent Protein Kinas A
PKC	Protein Kinase C
PLC	Phospholipase C
PNS	Peripheral Nervous System
PP2A	Protein Phosphatase 2A
PRD	Proline-Rich Domain
PS1/2	Presenilin 1/2
PSD-95	Post Synaptic Density-95
PSP	Progressive Nuclear Palsy
p-SYK	Phosphorylated SYK
PTK	Protein Tyrosine Kinase
PYK	Protein Tyrosine Kinase 2
R/R AML	Relapsed or Refractory Acute Myelogenous Leukemia
RAWM	Radial Arm Water Maze
Rheb	Ras Homolog Enriched in Brain
S6K	Ribosomal Protein S6 Kinase
SEM	Standard Error of the Mean
SH2	Src-Homology Domains 2
SH3	Src-homology Domain
shRNA	Short Hairpin RNA
STAT	Signal Transducer and Activator of Transcription
SUnSET	Surface Sensing of Translation
SYK	Spleen Tyrosine Kinase
SYK-OX	SYK overexpressing
TAI	Tau Aggregation Inhibitor
TBI	Traumatic Brain Injury
TDP-43	TAR DNA-binding protein
TFEB	Transcription Factor EB
TLRs	Toll-Like Receptors
TNFα	Tumor Necrosis Factor α
TREM2	Triggering Receptor Expressed on Myeloid Cells 2
TSC1/2	Tuberous Sclerosis Protein ½
t-SYK	Total SYK
UPS	Ubiquitin-Proteasome System
VLDLR	Very Low Density Lipoprotein Receptor
WHO	World Health Organization
WT	Wild-Type

Research Articles

Schweig, Jonas Elias; Yao, Hailan; Beaulieu-Abdelahad, David; Ait-Ghezala, Ghania; Mouzon, Benoit; Crawford, Fiona et al. (2017): Alzheimer's disease pathological lesions activate the spleen tyrosine kinase. In *Acta neuropathologica communications* 5 (1), p. 69. DOI: 10.1186/s40478-017-0472-2.

Schweig, Jonas Elias; Yao, Hailan; Coppola, Kyle; Jin, Chao; Crawford, Fiona et al. (2018): Spleen Tyrosine Kinase inhibition increases autophagic tau degradation via the mTOR pathway *in vitro* and *in vivo*. *The Journal of biological chemistry*; Under review, as of September 2018

Schweig, Jonas Elias; Yao, Hailan; Coppola, Kyle; Jin, Chao; Crawford, Fiona et al. (2018): Spleen Tyrosine Kinase inhibition decreases neuroinflammation in organotypic vibrosections of Tg Tau P301S mice. *Neuroscience Letter*; In preparation, as of September 2018

Conference Presentations

Poster:

Abnormal Accumulation of Activated SYK in Microglia & Dystrophic Neurites in Mouse Models of Alzheimer's Disease. **Jonas E. Schweig**, David Beaulieu-Abdelahad, Yong Lin, Michael Mullan, Fiona Crawford, Daniel Paris (AAIC, Toronto, 2016)

Aberrant SYK Kinase Activation Associated with tau and b-amyloid Pathologies in Mouse Models of Alzheimer's Disease. **Jonas E. Schweig**, David Beaulieu-Abdelahad, Ghania Ait-Ghezala, Michael Mullan, Fiona Crawford, Daniel Paris (VA Research Day, Tampa, 2017)

The Spleen Tyrosine Kinase (SYK) as a novel target for the treatment of Alzheimer's Disease. **Jonas E. Schweig**, Hailan Yao, Michael Mullan, Fiona Crawford, Daniel Paris (VA Research Day, Tampa, 2018)

Symposium:

Abnormal Activation of the Spleen Tyrosine Kinase (SYK) in Microglia and Neurons of Different Mouse Models of Alzheimer's Disease. **Jonas E. Schweig**, Hailan Yao, David Beaulieu-Abdelahad, Michael Mullan, Fiona Crawford, Daniel Paris (SfN, San Diego, 2016)

The pivotal role of spleen tyrosine kinase (SYK) in the pathobiology of Alzheimer's disease. **Jonas E. Schweig**, Hailan Yao, David Beaulieu-Abdelahad, Ghania Ait-Ghezala, Benoit Mouzon, Michael Mullan, Fiona Crawford, Daniel Paris (SfN, Washington D.C., 2017)

Chair:

Preclinical Therapeutic Strategies for Neurodegenerative Disease I.
Jonas E. Schweig (SfN, Washington D.C., 2017)

1 Introduction

1.1 Alzheimer's Disease

1.1.1 History

Alzheimer's disease (AD) is the most common form of dementia, accounting for 60-70% of all dementia cases as of 2018 (WHO). The pathology of AD was first described by the eponym Alois Alzheimer at a conference in Tübingen, Germany in 1906 and in his subsequent research article "Über eine eigenartige Erkrankung der Hirnrinde" (Alois Alzheimer 1907). In his research article, he delineates the three major hallmarks of AD that are still used for diagnosis today. He describes the psychological changes of a 51 year old woman including increased memory loss and formation, temporal and spatial disorientation and many other behavioral and cognitive abnormalities (Alois Alzheimer 1907). After 4.5 years, his patient died and he further described the pathological changes in the brain including brain atrophy and arteriosclerosis of the larger vessels (Alois Alzheimer 1907). In his analysis, he speaks of "merkwürdige Veränderungen der Neurofibrillen" (strange changes of the neurofibrils) that lead to a degeneration of the cell, thereby referring to what we now know as neurofibrillary tangles of the microtubule-associated protein (MAP) tau. He hypothesized that a "chemical transformation of the fibril substance took place" and that this "chemical transformation seems to go hand in hand with the deposition of a not yet investigated, pathological metabolite into the (ganglion) cell" (Alois Alzheimer 1907). In addition, Alzheimer described the pathological hallmark that is today known as Aβ-plaques (or β-amyloid plaques). He mentions that there were "miliare Herdchen" (miliar nidi) caused by "deposition of a strange substance into the cortex", even visible without staining. Furthermore, the "glia formed plenty of fibers" and show "big fat bags" (Alois Alzheimer 1907). This was his description of the neuroinflammation that we now know is the third major pathological hallmark of the disease

named after him. In summary, Alois Alzheimer already described the extracellular Aβ-plaques, intracellular neurofibrillary tau tangles and neuroinflammation (microgliosis and astrogliosis) that are today's standard for the pathological description of the disease.

1.1.2 Demography & Etiology

Nearly, 112 years after Alzheimer's first public description of his findings, there is still no cure for the devastating disease and the numbers of AD cases are rapidly increasing (Alzheimer's disease facts and figures 2018). Today (2018), there are approximately 5.7 million living with AD in the US and approximately 50 million people are affected worldwide. Estimates suggest that these numbers could increase to 14 million in the US and 130 million worldwide by 2050 (Alzheimer's disease facts and figures 2018). AD is the 6th leading cause of death in the US, as one in three seniors dies with AD or another dementia. Not only does AD negatively affect the lives of millions of people, but it also represents a major burden for the governments. The medical and care costs are as high as 277 billion dollars in the US and could increase to 1.1 trillion dollars by 2050 (Alzheimer's disease facts and figures 2018). These facts imply the undisputed need for a cure for AD. However, most recent clinical trials aiming to remove the Aβ and tau pathologies failed to meet their endpoint criteria (Watt et al. 2014; St-Amour et al. 2016; Rosenblum 2014) (for a more detailed discussion and review on clinical trials see chapter 1.3).

AD can be divided into a familial and sporadic forms. The familial form is caused by genetic mutations. In the early 1990s, the first genetic mutations were found to cause AD. These mutations include point/missense mutations in the gene encoding the amyloid precursor protein (*APP*) (e.g. APP V717I (London) (Goate et al. 1991), APP KM670/671NL (Swedish) (Mullan et al. 1992). In the following years, many more studies found various other mutations in the *APP*

gene that lead to an early onset of AD (EOAD). Interestingly, one variant (APP A673T (Icelandic)) was identified in 1993 (Peacock et al. 1993) and later confirmed to be protective against AD and age-related cognitive decline (Jonsson et al. 2012). Since the A673T mutation is in close proximity to the beta-secretase (BACE) cleavage site, the substrate characteristic of APP changes, resulting in lower Aβ production levels by BACE (Jonsson et al. 2012). In addition to mutations in the *APP* gene, mutations in genes encoding subunits of the γ-secretase, *presenilin 1* and *2* (*PS1, PS2*), represent another cause of EOAD by affecting the cleavage of APP (Strooper et al. 1998; Wolfe et al. 1999), while *PS1* mutations are the most common and *PS2* mutations are the least common cause of EOAD (Sherrington et al. 1995; Sherrington et al. 1996; Cai et al. 2015). More than 180 mutations in *PS1/2* have been reported so far (http://www.molgen.ua.ac.be/ADMutations/). The γ-secretase cleaves type I transmembrane proteins including APP, leading to the production of Aβ. Presenilin mutations cause a shift towards longer Aβ peptides that have a higher tendency to aggregate than shorter forms (Aβ42 compared to Aβ38), thereby contributing to the formation of amyloid aggregates (Duff et al. 1996; Citron et al. 1997; Borchelt et al. 1996).

Although intracellular neurofibrillary tangles (NFTs) composed of the microtubule associated protein tau (MAPT) are one of the main hallmarks of AD, mutations of the *MAPT* gene are only known to cause frontotemporal dementia (FTD) and not directly cause AD, although, a recent study showed the *MAPT* gene influences the AD risk (Desikan et al. 2015).

In contrast to the rare familial forms of AD that only comprise a very small percentage of all cases and lead to an early onset of the disease, the sporadic form of AD is much more common and is characterized by a late onset (LOAD) (Barber 2012). The etiology of LOAD is still not fully understood. However, there are several risk factors, including risk genes, for sporadic AD that have been identified. The greatest risk factor for LOAD remains age, as the risk for developing

AD doubles every five years after the age of 65 resulting in a nearly 50% chance at the age of 85 (Alzheimer's disease facts and figures 2018). Besides the deterministic genes mentioned above (*APP, PS1, PS2*), mutations in risk genes have been identified that increase the probability to develop LOAD.

In 1993, an isoform of the apolipoprotein E (ApoE) was found to increase the risk of AD and represents to date the highest genetic risk factor (Corder et al. 1993). ApoE is responsible for the binding and transport of lipids (Getz and Reardon 2009). Different variants of the genes encoding the apolipoprotein E exist (e.g. ApoE-ε1, ApoE-ε2, ApoE-ε3, and ApoE-ε4). ApoE has been found to associate with Aβ (Sanan et al. 1994) and enhance the fibril formation (Wisniewski et al. 1994). Furthermore, ApoE has been shown to disrupt the clearance of Aβ across the BBB in an isoform specific manner (Deane et al. 2008). The ApoE-ε4 isoform reduced the clearance of Aβ the most by shifting the clearance via the low density lipoprotein receptor-related protein 1 (LRP1) to the slower very-low-density-lipoprotein receptor (VLDLR) (Deane et al. 2008). In contrast, another study suggested that the interaction between ApoE and Aβ are minimal in the extracellular milieu and that ApoE and soluble Aβ compete for the LRP1-dependent uptake in astrocytes, thereby providing a different explanation for the impact of ApoE on Aβ metabolism (Verghese et al. 2013). Furthermore ApoE-ε4 has been suggested to exacerbate the tau pathology *in vivo (Shi et al. 2017)*. Heterozygous carriers of the *ApoE-ε4* gene exhibit a 2-4 fold risk of developing AD, while the risk for homozygous carriers increases up to 8-15 fold (Qian et al. 2017). Interestingly, the ApoE-ε2 seems to be protective and reduce the risk for AD by 2-4 fold (Corder et al. 1994).

In addition, mutations in the gene encoding the triggering receptor expressed on myeloid cells 2 (TREM2) are not only a known cause of the autosomal recessive early-onset dementia called Nasu-Hakola disease (NHD), but are also a known risk factor for AD and FTD (Borroni et al. 2014; Ulrich et al. 2017; Dardiotis et al. 2017). Variants of *TREM2* can increase the risk for AD 2-4 fold (Ulrich and Holtzman 2016). TREM2 is a known receptor that is expressed in monocytes (Fahrenhold et al. 2017) and the more differentiated microglia (Yao et al. 2016; Filipello et al. 2018) and infiltrating macrophages (Turnbull et al. 2006; Jay et al. 2015) in the brain, thereby mediating the inflammatory response and phagocytosis in the CNS. TREM2 has been shown to promote microglia-mediated phagocytosis of Aβ (Kim et al. 2017). However, the impact of TREM2 on the tau pathology remains controversial, as many studies show opposing results. TREM2 deficiency has been shown to exacerbate (Bemiller et al. 2017), as well as ameliorate (Leyns et al. 2017) tau pathology *in vivo*. Interestingly, ApoE has been shown to be a ligand of TREM2 (Atagi et al. 2015; Bailey et al. 2015), thereby linking two risk factors of AD to each other.

Besides these well-known deterministic genes and risk factors that result in the observed AD pathologies, the impaired degradation of intracellular proteins via the autophagy/lysosome pathway has been observed in AD and other forms of dementia and seems to play a key role in the formation of Aβ deposits and tau aggregates (Nilsson et al. 2013; Piras et al. 2016) (detailed information on autophagy can be found in chapter 1.1.6).

1.1.3 Amyloid pathology

The β-amyloid peptide (Aβ) that is now known to be a cleavage product of the APP and the building block of the extracellular plaques observed in AD (Masters et al. 1985), has first been isolated, purified and sequenced from the cerebrovasculature of AD and trisomy 21 patients (Glenner and Wong 1984a, 1984b). Glenner and Wong (1984a) already hypothesized that Aβ had to be a derivate of a precursor that was located on chromosome 21. Subsequent molecular cloning experiments confirmed their hypothesis (Kang et al. 1987; Goldgaber et al. 1987; Tanzi et al. 1987; Robakis et al. 1987). The knowledge about the apparent genetic link between APP, PS1/2 and the amyloid plaque pathology in AD (see also chapter 1.1.2) triggered the postulation of the amyloid hypothesis (Selkoe 1991; Hardy and Higgins 1992).

The amyloid hypothesis positions the known missense mutations of APP, PS1 and PS2 at the basis of its rationale (Hardy and Selkoe 2002). These mutations lead to an increased Aβ42 production and accumulation, resulting in Aβ oligomerization and deposition (Hardy and Selkoe 2002). The Aβ oligomers are said to cause synaptic and neuritic injury while microglia and astrocytes become activated (Hardy and Selkoe 2002). As an extension of the amyloid cascade hypothesis, the oligomer cascade hypothesis emerged, as an increasing amount of studies suggested that Aβ oligomers, rather than Aβ fibrils may initiate AD pathogenesis (Hayden and Teplow 2013). This, in turn, leads to changes in neuronal homeostasis, oxidative injury and importantly, to changes in kinase and phosphatase activity, resulting in tau hyperphosphorylation and ultimately, in tau tangles (Hardy and Selkoe 2002). At the end of the hypothesis stands the pervasive neuritic and neuronal dysfunction, along with cell death leading to dementia (Hardy and Selkoe 2002).

In their review ten years after their postulation of the amyloid hypothesis, the authors discuss advances and weaknesses but conclude that the weaknesses mainly point to knowledge gaps and that no alternative hypothesis has emerged so far that could explain the AD pathologies as well as the amyloid hypothesis does (Hardy and Selkoe 2002). Furthermore, they suggested treatments for AD including inhibition of β-and γ-secretases and Aβ immunization to enhance its clearance (Hardy and Selkoe 2002). In their review 25 years after the emergence of their hypothesis, the authors conclude that the dyshomeostasis of Aβ remains the most compelling therapeutic target that has been validated by numerous previous studies (Selkoe and Hardy 2016). In addition, they mention that the results of clinical trials that used Aβ antibodies to remove Aβ from the brain (e.g. solanezumab, crenezumab, and aducanumab) suggest that the cognitive decline was slowed in patients with mild AD (Selkoe and Hardy 2016). In regards to their endpoint criteria, however, all clinical trials involving Aβ immunization and BACE or γ-secretase inhibitors failed (Mehta et al. 2017; Mullard 2018). The failure of those studies caused many scientists in the field to propose tau as the main factor driving AD progression and development (Kametani and Hasegawa 2018).

However, the simple removal of one or both main pathologies after a profound metabolic dyshomeostasis has already been established in patients with full-blown AD, may not suffice to restore normal brain function and reverse cognitive decline. As recent clinical trials suggest, successful interventions at different stages of AD may have to differ in their approach and duration. Future therapies may have to act downstream of the main pathologies and focus on re-establishing a homeostasis in the brain in addition to stemming the main pathologies.



1.1.3.1 APP processing

In order to understand the amyloid pathology, the deposition of Aβ in the brain of AD patients and possible treatments that aim to reduce the amyloid pathology, it is crucial to understand the processing of the APP in detail.

The APP is a type I transmembrane protein and is expressed in large amounts in the brain. The processing of APP can be divided into two pathways that differ in the involvement of different sets of proteases: the amyloidogenic pathway and the non-amyloidogenic pathway. The names already imply that a shift towards the amyloidogenic pathway ultimately leads to the generation and accumulation of Aβ and a shift towards APP processing via the non-amyloidogenic pathway prevents said event (Webb and Murphy 2012) (Figure 1).

The non-amyloidogenic pathway is initiated by the α-secretase proteolytic cleavage of APP within the Aβ sequence, therefore preventing the formation of Aβ and leading to the release of the soluble ectodomain sAPPα and the membrane anchored C-terminal fragment α (CTFα). Following endocytosis of the CTFα, the γ-secretase localized in endosomes further cleaves CTFα into the APP intracellular domain (AICD) and P3 (Webb and Murphy 2012) (Figure 1).

In contrast to the non-amyloidogenic pathway described above, the amyloidogenic pathway is initiated by the endocytosis of APP and the proteolytic cleavage by the β-secretase (Webb and Murphy 2012) (Figure 1). In order to function properly, the β-secretase requires an acidic milieu (low pH), as it is found in endosomes (Das et al. 2013; Prasad and Rao 2015). The β-secretase cleaves APP into the soluble ectodomain sAPPβ and the C-terminal fragment β (CTFβ). The final step in the amyloidogenic pathway leads to the production of β-amyloid, as the γ-secretase further cleaves the CFTβ into AICD and Aβ. Following exocytosis, both Aβ and sAPPβ are released into the extracellular milieu (Webb and Murphy 2012) (Figure 1).

In conclusion, a shift in the equilibrium of the APP processing towards the amyloidogenic pathway, represents one mechanistic reason for the accumulation of soluble Aβ and later aggregation into Aβ plaques observed in AD.

However, the overproduction and aggregation of Aβ, represents just one of the hallmarks of AD. As mentioned before, the aggregation of hyperphosphorylated tau into intracellular NFTs is another known and well-described hallmark of the AD pathologies.

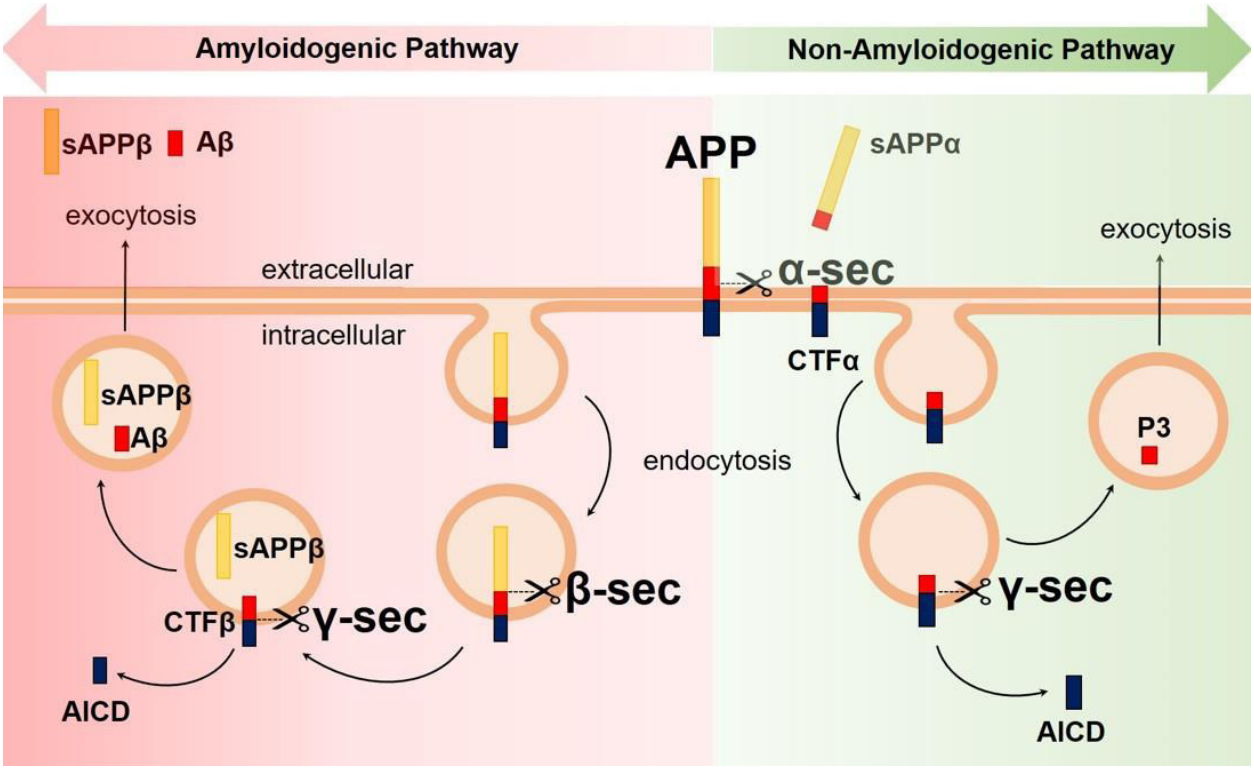

Figure 1: APP Processing
The amyloid precursor protein (APP) can be processed via the amyloidogenic or non-amyloidogenic pathway. The amyloidogenic pathway involves an endocytosis and a cleavage by the β-secretase resulting in CFTβ and sAPPβ and a subsequent cleavage by the γ-secretase, resulting in Aβ and AICD. The non-amyloidogenic pathway involves a cleavage by the α-secretase resulting in CFTα and sAPPα and a subsequent endocytosis and cleavage by the γ-secretase, resulting in P3 and AICD (as described by (Webb and Murphy 2012)).

1.1.4 Tau pathology

Tau is a microtubule associated protein (MAP). Under physiological conditions, tau stabilizes the microtubule network. The *MAPT* gene that encodes for human tau is located on chromosome 17 and comprises 16 exons (Andreadis 2006; Wang and Mandelkow 2016). Alternative splicing of the transcript leads to the generation of six distinct isoforms of tau (Guo et al. 2017). Each of those isoforms can be divided into N-terminus, the proline-rich domain (PRD), the microtubule binding domain (MTBD), and the C-terminus (Guo et al. 2017) (Figure 2). The different tau isoforms either comprise zero, one or two N-terminal inserts (0N, 1N, 2N) (Guo et al. 2017) (Figure 2). The PRD and the C-terminus remain the same for the six isoforms. Another difference between the tau isoforms is the existence of three or four repeats (3R or 4R) within the MTBD (Guo et al. 2017). Exons 9-12 of the *MAPT* gene encode for the four repeats (Guo et al. 2017). The second MTBD repeat is encoded by exon 10 and is missing in 3R tau isoforms (Guo et al. 2017) (Figure 2). The 3R and 4R tau isoforms are expressed in equal amounts in the adult human brain under physiological conditions (Goedert et al. 1989). In the brain of adult mice, however, the 4R isoforms are predominant (Kosik et al. 1989). The ratio of 0N, 1N, and 2N, however is not equally distributed, as the human CNS comprises 54% of 1N, 37% of 0N and only 9% of 2N tau isoforms (Goedert and Jakes 1990).

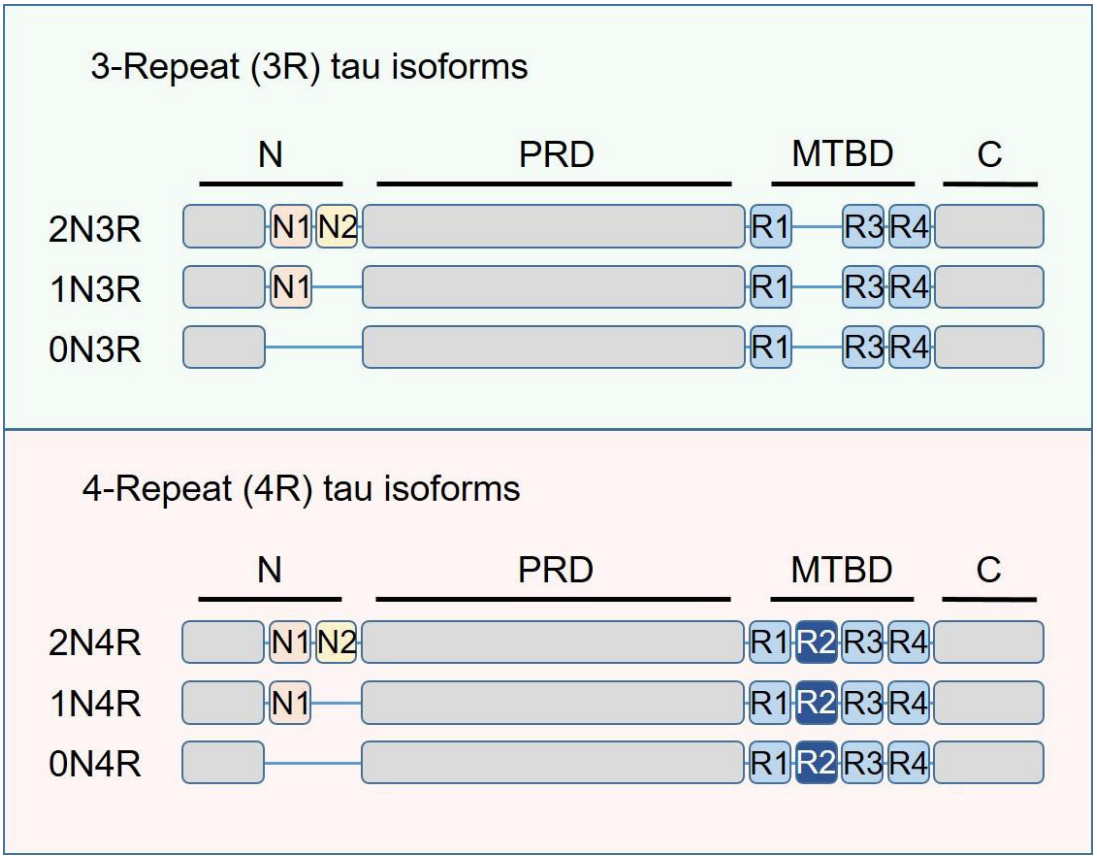

Figure 2: Tau isoforms
There are six different tau isoforms, comprising different numbers of repeat domains (R1-R4) in the MTBD and different numbers of N-terminal inserts (N0, N1, N2) (as described by (Guo et al. 2017)).

The PRD contains seven motifs comprised of Pro-X-X-Pro. These motifs can potentially be recognized by several kinases carrying a Src-homology-3 (SH3) domain, including the proto-oncogene tyrosine-protein kinase Fyn, lymphocyte-specific protein tyrosine kinase (LcK), phosphoinositide 3-kinase (PI3K), and phospholipase C (PLC) (Morris et al. 2011).

Many post-translational modifications of tau have been identified, including the most frequently investigated phosphorylation of tau but also acetylation, glycation, O-GlcNAcylation, nitration, sumoylation, ubiquitination (Martin et al. 2011; Morris et al. 2015). In total, 85

phosphorylation sites have been identified, including 45 at serine residues, 35 at threonine residues and 5 at tyrosine residues (Hanger et al. 2009). Increased phosphorylation or hyperphosphorylation of tau is associated with pathology and seen in various forms of dementia, including AD and FTD (Guo et al. 2017). In general, tau phosphorylation reduces its binding affinity to microtubules, leading to its detachment from microtubules and mislocalization (Guo et al. 2017). Soluble, hyperphosphorylated tau, detached from the microtubule network, can bind to tau instead of the microtubules and is therefore prone to oligomerization and aggregation (Guo et al. 2017; Iqbal et al. 2013). Phosphorylation of tau within the MTBD (e.g. at Ser262) decreases tau's binding affinity to microtubules (Drewes et al. 1995; Sengupta et al. 1998). Furthermore, the dissociation of tau from the microtubule network following phosphorylation at Thr231 and Ser235 has been shown in previous studies (Sengupta et al. 1998). In addition, tau phosphorylation at Ser356 by Nuak1, an AMPK-related kinase has been suggested to stabilize tau and promote its accumulation and aggregation, while Nuak1 reduction drastically decreased total tau levels *in vivo* (Lasagna-Reeves et al. 2016). Phosphorylation of tau within the PRD is said to lead to a disruption of microtubule assembly (Eidenmuller et al. 2001) and phosphorylation of tau within the C-terminal domain increases tau aggregation (Liu et al. 2007).

Tau hyperphosphorylation can occur if the activity of tau kinases is increased or the activity of tau phosphatases is decreased or both. Tau kinases are divided into three major groups including proline directed serine/threonine-protein kinases, non-proline-directed serine/threonine-protein kinases, and protein kinases that are specific for phosphorylation of tyrosine residues. Important representatives of the first group include mitogen-activated protein kinases (MAPKs), cyclin-dependent kinase-5 (Cdk5), glycogen synthase kinase 3 (GSK3)-α/β (Hanger et al. 2009; Guo et al. 2017). The protein kinase B (or Akt), cAMP-dependent protein kinase A (PKA), protein kinase

N, 5′ adenosine monophosphate-activated protein kinase (AMPK), and protein kinase C (PKC), belong to the second group of non-proline-directed serine/threonine-protein kinases (Guo et al. 2017). The third group is comprised of tyrosine kinases including proto-oncogene tyrosine-protein kinase Src, Fyn, and the spleen tyrosine kinase (SYK) (Guo et al. 2017; Martin et al. 2011).

GSK3-β plays a major role in the pathological phosphorylation of tau, as it seems to co-localize with pathological tau changes in AD (Pei et al. 1997; Leroy et al. 2002). Although GSK3-β inhibition has been shown to have positive effects on neuronal loss, tau phosphorylation and neurite degeneration in pre-clinical studies (Caccamo et al. 2007; Leroy et al. 2010; Serenó et al. 2009) in clinical trials, the inhibition of GSK3-β by lithium were not successful in a 12-month double-blind trial for amnestic mild cognitive impairment (aMCI) (Forlenza et al. 2011).

Tyrosine kinases like Src-family kinases, Lck, Fyn, and SYK can directly phosphorylate tau (Scales et al. 2011; Lebouvier et al. 2008). The effects of SYK on tau phosphorylation and AD pathologies are described in a different chapter of this thesis (1.2).

There are five known tyrosine residues at Tyr18, Tyr29, Tyr197, Tyr310, Tyr394 (Derkinderen et al. 2005a; Lebouvier et al. 2009). Tau phosphorylation at tyrosine residues has been shown to correlate with tau aggregation (Vega et al. 2005).

As mentioned before, the phosphorylation process of tau is not only mediated by kinases but also by phosphatases. One of the major phosphatases in the brain is the protein phosphatase 2A (PP2A) (Liu et al. 2005) which is also involved in regulating tau (de)phosphorylation (Gong et al. 2000). Interestingly, PP2A has been shown to be decreased in AD brains by approximately 50%, suggesting a possible contribution of PP2A to tau hyperphosphorylation in AD (Liu et al. 2007). An interplay between tau kinases and phosphatases has been observed, as well. PP2A dephosphorylates GSK3-β at its inhibitory Ser9 site, thereby rendering GSK3-β more active (Lee

et al. 2005). Furthermore, GSK3-β can inhibit PP2A (Yao et al. 2011). The inhibition of the mammalian target of rapamycin (mTOR), a serine/threonine kinase, activates PP2A (Meske et al. 2008). This may suggest an important regulatory role of key players of the mTOR pathway including GSK3-β, Akt and mTOR in interplay with PP2A in tau phosphorylation (Meske et al. 2008).

Pathological dyshomeostasis of tau kinases and phosphatases is one of the key post-translational mechanisms by which tau hyperphosphorylation can occur. In AD and other tauopathies, tau becomes hyperphosphorylated resulting in a detachment of tau from microtubules and increased cytosolic tau, finally leading to the formation of insoluble paired helical filaments (PHFs) and NFTs (Kidd 1963; Terry 1963; Šimić et al. 2016). Cytosolic tau, unbound to microtubules, can interact with several molecules, including ApoE, PS1, α-synuclein, and F-actin (Correas et al. 1990; Jensen et al. 1999; Huang et al. 1995; Takashima et al. 1998).

For characterization of the pathological progression of AD, six different so called Braak stages were proposed that describe a characteristic NFTs spread but the distribution of the neuritic amyloid plaques seemed to vary a lot between different individuals (Braak and Braak 1991). The tau pathology spreads from the transentorhinal/peripheral cortex (Braak I), to the CA1 of the hippocampus (Braak II), to the limbic system (Braak III), to the amygdala, claustrum and thalamus (Braak IV), isocortical areas (Braak V), and primary sensory, motor, and visual regions (Braak VI) (Braak and Braak 1991).

The spreading of the tau burden is an essential part of the disease progression. Neuroinflammation has been shown to enhance tau propagation. Activated microglia have been suggested to mediate tau propagation via exosomes, since inhibition of exosome synthesis and depletion of microglia can lead to a decreased tau spread *in vitro* and *in vivo* (Asai et al. 2015).

Tau can be secreted and exist extracellularly (Yamada 2017). There it can be recognized by microglia and activate the MAPK pathway which in turn leads to the release of pro-inflammatory cytokines including tumor necrosis factor alpha (TNFα), interleukin-6 (IL6), and interleukin-1β (IL-1β) (Kovac et al. 2011), which could further enhance neuronal tau phosphorylation (Quintanilla et al. 2004).

The tau pathology correlates best with the cognitive decline in AD, despite the proposed key role of Aβ plaques in AD pathogenesis (Bejanin et al. 2017; Nelson et al. 2012). However, synaptical loss and cognitive decline show the greatest correlation in AD (Masliah 1995).

The mechanism by which the Aβ and tau pathologies interact in the disease progression is not completely understood. The amyloid hypothesis proposes the Aβ pathology to be an upstream event of the tau pathology, as APP overexpressing mice show tau hyperphosphorylation and transgenic tau mice injected with Aβ exhibit an increased tau pathology (Götz et al. 2001; Lewis et al. 2001). In addition, there is no known tau mutation that causes AD, further highlighting the important role of Aβ in AD pathogenesis which is known to increase many years before the clinical onset of AD (Insel et al. 2017). However, autopsies of very young individuals that exhibited tau accumulations in the subcortical nuclei (e.g. locus coeruleus) have suggested that the tau pathology may emerge prior to the Aβ pathology (Braak and Del Tredici 2011; Jack et al. 2013).

The first mutation identified in the *MAPT* gene was the P301L mutation, associated with FTLD, that leads to neuronal loss caused by a dysfunction of tau (Hutton et al. 1998). Although many other tau mutations have been identified, importantly, none of these mutations has been shown to lead to the classical AD pathology.

The P301L mutation occurs within a six-residue segment within the MTBD called PHF6. The second and third repeat domains of the MTBD each contain such a six-residue segment that can form a β-sheet structure and therefore represents a basis for tau's propensity of self-aggregation (Bergen et al. 2001). Since 4R tau isoforms contain two six-residue segments (PHF6* and PHF6) instead of one that is present in 3R tau isoforms, the 4R tau isoforms are more likely to aggregate than 3R tau isoforms. In addition, the P301L mutation increases tau's propensity to form a β-sheet and thereby increases the probability of tau aggregation (Bergen et al. 2000).

It is important to mention, that the composition of NFTs varies depending on the type of tauopathy. In AD, the tangles were found to contain 3R, as well as 4R tau isoforms (Espinoza et al. 2008), while in FTLD the isoform ratio depends on the tau mutation causing the disease (Silva et al. 2006). Pick bodies in FTLD cases only contain 3R tau isoforms, while familial FTLD cases associated with exon 10, including P301L, exhibit 4R NFTs and the R406W mutation showed NFTs containing both 3R and 4R tau isoforms (Silva et al. 2006). Sporadic FTLD cases without Pick bodies exhibit 4R tau isoform pathology (Silva et al. 2006).

The toxicity of insoluble tau tangles is still subject of debate (Spires-Jones et al. 2011). However, the soluble tau species, including tau oligomers, seem to be more neurotoxic (Spires-Jones et al. 2011), as they have been suggested to activate the mitochondrial apoptotic pathway and inhibit the synaptic energy production via the mitochondrial complex I (Lasagna-Reeves et al. 2011).

Another important outcome of tauopathies is the impaired axonal transport resulting from a dysfunction of motor proteins and a compromised microtubule network. Impaired axonal and dendritic transport have been found in neurons bearing tau tangles (Millecamps and Julien 2013; Vos et al. 2008). It is known that the interaction of tau with microtubules can be disturbed

following certain post-translational modifications, like phosphorylation, ultimately leading to a destabilization of the microtubule network (Martin et al. 2011). Tau is mainly present in axons under physiological conditions. Early in the pathogenesis of AD, phosphorylated tau is mislocalized to dendrites, thereby contributing to the disruption of the axonal transport (Hoover et al. 2010). In addition, tau has an impact on the transport along the microtubule network by directly interacting with the motor proteins dynein and kinesin (Dixit et al. 2008; Vershinin et al. 2008). Interestingly, it has been shown that GSK3-β can phosphorylate kinesin and thereby cause an inhibition of anterograde transport *in vitro* and *in vivo* (Morfini et al. 2002).

In summary, tau can become hyperphosphorylated under pathological conditions, detach from microtubules and localize in dendrites of neurons, thereby destabilizing the microtubule network and impairing the intracellular transport via the microtubule network.

However, there are mechanisms by which pathological tau can be degraded and cleared from the brain including the ubiquitin-proteasome system (UPS) and the autophagic-lysosomal system. The autophagic degradation is described in another chapter of this thesis (1.1.6).

Tau has been the target of many different therapeutic interventions to treat AD. The aim was to target the tau pathology by preventing tau oligomerization or lowering tau aggregation. A recent phase III clinical trial that used of leuco-methylthioninium-bis(hydromethanesulfonate) (LMTM) to target aggregated tau has proven not to be successful as a treatment for mild to moderate AD (Gauthier et al. 2016). Besides using small molecules, tau has been targeted by active and passive immunization using tau polypeptides or antibodies against tau, respectively. One example for using active tau immunization (tau residues 294–305) is the ongoing phase II clinical trial of AADvac1 (Axon Neuroscience) for mild to moderate AD that will end in 2020. Examples of clinical trials using passive immunization with antibodies against tau include the phase Ib trial

for mild to moderate AD by AC Immune SA and Janssen that target the 393-408 residues of tau phosphorylated at Ser396/404 (ACI-35). Bristol-Myers Squibb uses an antibody targeting N-terminally truncated extracellular tau (residues 9-18) in a phase II clinical trial for progressive supranuclear palsy (PSP) and AC Immune SA, Genentech, and Hoffmann-La Roche use an antibody targeting phosphorylated tau at Ser409 in a phase I clinical trial for mild to moderate AD. AbbVie and C2N Diagnostics use an antibody targeting aggregated tau (residues 25-30) in two different phase II clinical trials for PSP and AD (more information on clinical trials for AD can be found in chapter 1.3).

These approaches using antibodies against tau have been criticized because tau is known to be mainly intracellular and also forms its aggregates intracellularly and the antibodies would have to enter the neurons in order to effectively label pathological tau and trigger its removal by microglia. However, it has also been shown that antibodies against tau can reduce tau spreading without microglia engagement and thereby prevent the progression of the disease in animal models (Lee et al. 2016). Nevertheless, the direct intervention at the presumed roots the diseases will still have to prove successful and the results of the abovementioned ongoing clinical trials will shed light on this topic.

1.1.5 Neuroinflammation

Inflammation generally describes the biological response following the exposure to harmful agents including exogenous pathogens like bacteria or viruses but also endogenous ones like misfolded or aggregated proteins. The immune response evoked by exogenous or endogenous signals can be described as either innate or adaptive. The innate immune response is considered to be an unspecific reaction mediated by a certain subset of cells, whereas the adaptive immune response is a specific answer of the organism to an antigen, involving a different subset of immune cells. Besides the categorization into innate and adaptive another temporal differentiation of the immune response has been introduced. The initial response in presence of the pathogen is called acute immune response. If the immune response and the resulting inflammation persists for a prolonged period of time, however, the affected organism can reach a state of dyshomeostasis that cannot be easily resolved and therefore enters a chronic inflammation (Kaur et al. 2013). Inflammation can be specific to certain tissues and is therefore differentiated spatially. The inflammation of the nervous system (central (CNS) or peripheral (PNS)) is called neuroinflammation. The CNS plays a special role, as it has specific immune cells compared to the periphery and is additionally protected from pathogens by the blood-brain-barrier (BBB). Insults to the BBB are therefore considered to be very harmful as the exposure of the CNS and therefore also the likelihood of an infection is increased.

Neuroinflammation is known to play an important role in traumatic brain injury (TBI) and in neurodegenerative diseases like AD. In AD, the quantity of endogenous pathogens like Aβ and hyperphosphorylated tau increases over time and their persistence can cause a chronic inflammation in the brain (Fuster-Matanzo et al. 2013).

The inflammatory response in the brain is mainly mediated by microglia and astroglia. The increased proliferation of astrocytes is called astrogliosis. Astrogliosis is also described by hypertrophy and increase in intermediate filaments (IF, e.g. glial fibrillary acidic protein (GFAP)). The activation of microglia involves a change in morphology, from ramified to amoeboid, resulting in a change of motility to enable their movement to affected brain areas. This process is called microgliosis and also involves an increased proliferation of microglia. The ionized calcium-binding adapter molecule 1 (Iba-1) is often used as a marker for microglial activation since its expression increases in activated microglia (Carson et al. 2006).

Both the initial astrogliosis and microgliosis are said to be neuroprotective events (Carson et al. 2006), but the role of prolonged microgliosis and astrogliosis in AD remains controversial, despite extensive research. While some studies support the necessity of microglia for Aβ clearance, others show the detrimental effects of the prolonged microgliosis in AD, including an increased neurodegeneration and an impaired Aβ clearance (Frautschy et al. 1998; Hickman et al. 2008; Rogers et al. 2002; Yoon and Jo 2012).

An increased number of microglia can be found around Aβ deposits in brains of AD patients, as well as AD mouse models (Frautschy et al. 1998; Perlmutter et al. 1990). In addition, it has been shown that microglia can phagocytose Aβ (Frackowiak et al. 1992). However, the same authors first estimated that the actual Aβ degradation by microglia to be low, as the phagosomal appearance of Aβ persisted after 20 days in culture (Frackowiak et al. 1992). The phagocytosis of Aβ by microglia was later confirmed *in vivo*, in addition to the migration of microglia and the extension of their processes towards β-amyloid deposits (Bolmont et al. 2008).

The notion of the microglial inability to phagocyte and thereby degrade Aβ deposits has been supported by later *in vivo* studies involving amyloid-overexpressing mouse models (Wegiel

et al. 2001; Wegiel et al. 2004). A following study has suggested that the microglial phagocytosis of Aβ is impaired by pro-inflammatory cytokines and can be relieved by treatment with anti-inflammatory cytokines or drugs (Koenigsknecht-Talboo and Landreth 2005). The same study showed that FcR-mediated phagocytosis is not impacted by pro-inflammatory cytokines (e.g. IL-1β, TNFα, IFNγ) and therefore the authors concluded that immunotherapies, involving antibodies directed against Aβ (IgG), can to successfully induce the microglial clearance of Aβ deposits (Koenigsknecht-Talboo and Landreth 2005; Schenk et al. 1999). One study has shown that ablation of microglia had no effect on the size or number of Aβ-deposits over a short timeframe (4 weeks), however, soluble Aβ was largely increased, suggesting that microglia may play a role in the clearance of soluble, rather than fibrillar Aβ (Grathwohl et al. 2009). However, another ablation study showed a 13% increase in plaque size after just one week, suggesting that microglia can limit the growth of Aβ deposits (Zhao et al. 2017). Differences in animal models and the agent used for ablation, as well as the age of the mice may account for the different findings but the role of microglia in Aβ plaque formation and maintenance still remains controversial.

Microglia not only respond to Aβ (Doens and Fernández 2014), but also to tau. Tau oligomers and fibrils have been shown to activate microglia (Morales et al. 2013) and in addition, microglia have been proposed to play an important role in the spread of the tau pathology (Perea et al. 2018). It has been suggested that excess tau could be released by neurons and internalized by microglia (Bolos et al. 2015) and that this internalization is, at least in part, mediated by the CX3CR1 receptor (Bolós et al. 2017). The ablation of microglia, as well as the inhibition of exosome synthesis resulted in a reduction of tau propagation over a time course of four weeks, further supporting the idea of the microglial involvement in tau propagation and highlighting the exosome secretion as a possible mechanism of tau propagation (Asai et al. 2015).

Microglia are known to produce signaling molecules called cytokines, including interferon (IFN) and interleukins (IL). Cytokines are often labelled as pro-inflammatory (e.g. IFNγ, IL-1β, TNFα, IL-6) or anti-inflammatory (e.g. IL-4, IL10), however, it has been argued that this categorization is too simplistic because the action of the respective cytokine may depend largely on other factors like the amount released, the timing, the target cell and the experimental model (Cavaillon 2001).

It is generally believed that microglia are overactive in AD brains and produce more pro-inflammatory and less anti-inflammatory cytokines (Su et al. 2016; Wang et al. 2015a), thereby creating an imbalance in the cytokine household and further contributing to the disease progression. The pro-inflammatory cytokines IL-1β, IL-6 and TNFα have been shown to be elevated in AD and may, at least in part, be caused by Aβ-induced microgliosis (Wang et al. 2015a). Pro-inflammatory cytokines can also contribute to abnormal phosphorylation of tau (Domingues et al. 2017). Lipopolysaccharide (LPS) has been shown to induce the release of pro-inflammatory cytokines by stimulating toll-like receptor 4 (TLR4) (Lu et al. 2008). TLR4 is also involved in the clearance of Aβ deposits (Tahara et al. 2006). Interestingly, SYK has been shown to associate with TLR4 and play a role in the TLR4 signaling cascade (Chaudhary et al. 2007; Dennehy et al. 2008). Therefore, SYK could be an important mediator of the LPS or Aβ-induced pro-inflammatory response and regulate the release of cytokines. LPS is not only known to evoke a release of cytokines but has also been shown to exacerbate the tau pathology *in vivo* (Kitazawa et al. 2005). The simultaneous activation of TLR4 and the IFNγ receptor resulted in neuronal dysfunction and neuronal death in organotypic brain slice cultures (Papageorgiou et al. 2016). This was found to be mainly mediated by an increased inducible nitric oxide synthase (iNOS) expression and subsequent nitric oxide (NO) release (Papageorgiou et al. 2016). This means that a pro-inflammatory signaling cascade in activated microglia, that could be induced by cytokines

and amyloid, can potentially cause neurodegeneration. NO is known to be a signaling molecule that can freely move across cell membranes (Sierra et al. 2014). It can be neuroprotective (Brown 2010; Mejia-Garcia and Paes-de-Carvalho 2007), however, in presence of NADPH oxidase, the production of peroxynitrite can lead to neuronal death (Mander and Brown 2005). Therefore, iNOS inhibition may have neuroprotective effects (Mander and Brown 2005). Genetic ablation of iNOS in mouse models of AD seemed to decrease the cerebral plaque load, microgliosis and astrogliosis (Nathan et al. 2005).

It is known that iNOS is also expressed in astrocytes and can be induced by certain cytokines including IFNγ and IL-1β (Jana et al. 2005; Saha and Pahan 2006). Similar to microglia that, for example, play an important role in synaptic pruning (Paolicelli et al. 2011) or neuroprotection (Chen and Trapp 2016), astrocytes support neuronal health under physiological conditions for example by engaging in neurotransmitter uptake (Kreft et al. 2012) or maintaining the integrity of the BBB (Cabezas et al. 2014). Astrocytes can also potentially regulate neurotransmission and play an active role in neuroplasticity by releasing gliotransmitters (e.g. glutamate or gamma-aminobutyric acid (GABA)) (Covelo and Araque 2018).

In neurodegenerative diseases like AD, however, the prolonged exposure to Aβ may alter the functional state of astrocytes (Thal 2012). Aβ can decrease the astrocytic glutamate uptake which could contribute to the NMDA receptor-mediated excitotoxicity observed in AD (Matos et al. 2008; Hynd et al. 2004). In addition, Aβ has been shown to induce astrocytic glutamate release, thereby further contributing to NMDA receptor-mediated synaptic damage (Talantova et al. 2013). The NMDA receptor antagonist memantine was able to prevent Aβ-induced synaptic damage (Talantova et al. 2013). The Aβ-induced activation of astrocytes can be mediated by the receptor for advanced glycation end products (RAGE) which can in turn activate the NFκB signaling

pathway that leads to the increased expression and release of pro-inflammatory cytokines (Gonzalez-Reyes and Rubiano 2018). Pro-inflammatory cytokines like TNFα, IFNγ and IL-1β can in turn increase BACE-1, APP and Aβ levels (Blasko et al. 2000; Zhao et al. 2011). Furthermore, it has been argued that Aβ can induce a production and exosomal release of astrocytic p-tau via the activation of the calcium sensing receptor (CaSR) (Chiarini et al. 2017), thereby linking both tau and amyloid pathology to astrocytes. Interestingly, astrocytes derived from Tg Tau P301S mice (1 week postnatal) (see chapter 1.1.7.3) seem to decrease the survival of neurons in a co-culture and their conditioned media decreased synaptophysin and PSD-95 in primary cortical neurons, implying early functional deficits of Tg Tau P301S astrocytes and a potential role of astrocytes in neurodegeneration (Sidoryk-Wegrzynowicz et al. 2017). Furthermore, the cytokine S100B produced by astrocytes has been found to increase tau phosphorylation via JNK and GSK3-β (Esposito et al. 2008).

Other studies have also argued that reactive astrocytes that cause neurotoxicity can be induced by activated microglia in neurodegenerative disorders, thereby implying a positive feedback between the two types of glial cells that exacerbates neuroinflammation (Liddelow et al. 2017). Interestingly, neuroinflammation has also been shown to impair the autophagic flux (Du et al. 2017) and may therefore additionally contribute to AD and proteinopathies in a different way. The next chapter will describe the mTOR pathway and its involvement in autophagy (1.1.6).



1.1.6 Autophagy and the mTOR pathway

Macroautophagy (hereafter called autophagy) describes the degradation of proteins and organelles and is essential to maintain the cellular homeostasis (Feng et al. 2014). The complex process of autophagy involves various autophagy-related (Atg) proteins for the initiation and sequestration of proteins (Feng et al. 2014). After autophagy initiation, autophagosomes fuse with late endosomes. Finally, the cargo of these amphisomes gets degraded by lysosomes (Sanchez-Wandelmer and Reggiori 2013).

During autophagy initiation, the cytosolic form of the microtubule-associated protein 1 light chain 3 (LC3-I) gets conjugated to phosphatidylethanolamine (PE) and turns into LC3-II (Ge et al. 2014) which mediates the formation of autophagosomes and remains associated with the membrane of the autophagic vesicles (AVs) until lysosomal degradation (Sarkar 2013). LC3-II is either degraded in the lumen after fusion with lysosomes or is de-lipidated and recycled on the surface of AVs (Sarkar 2013). Hence, the ratio of LC3-I and LC3-II is often used to monitor the level of autophagic flux (the rate of autophagy initiation and lysosomal degradation) but its correct interpretation remains controversial because it is influenced by autophagy initiation and lysosomal degradation (Tanida et al. 2008). Since increased LC3-II levels following a drug treatment could be indicative of either an increased in autophagy initiation or a decreased in lysosomal degradation, lysosome inhibitors like chloroquine (CQ) are often used to determine the rate of autophagy initiation, as previously described (Mizushima and Yoshimori 2007; Tanida et al. 2008). CQ accumulates in the lysosomes and raises their pH. Thereby, CQ decreases the functionality of lysosomal proteases and inhibits the fusion of lysosomes and autophagosomes. Therefore, CQ allows the observation of the conversion rate of LC3-I to LC3-II (autophagy initiation) by limiting the degradation of LC3-II.

Besides using LC3 as a marker, members of the mammalian target of rapamycin (mTOR) pathway are often monitored since mTOR and its downstream targets are major regulators of autophagy (Munson and Ganley 2015). The main triggers of autophagy are insulin, growth factors and amino acids (Efeyan and Sabatini 2013). Insulin and growth factors bind to cell surface receptors (e.g. insulin receptor (IR) or insulin-like growth factor 1 (IGF-1) receptor) and activate the phosphoinositide 3-kinase (PI3K) via insulin receptor substrates (IRS) (Boucher et al. 2014) which, in turn, leads to a downstream activation of the protein kinase B (PKB, also known as Akt) (Hemmings and Restuccia 2012). Akt inhibits the tuberous sclerosis complex 1/2 (TSC1/2) (Inoki et al. 2002) which, in turn, also has an inhibitory effect on a GTP-binding protein, the Ras homolog enriched in brain (Rheb) (Inoki et al. 2003a). Rheb activates mTOR and thereby inhibits autophagy (Bai et al. 2007). This means that each member of the mTOR pathway or upstream elements of the mTOR pathway can potentially interfere with autophagy.

mTOR can inhibit the eukaryotic translation initiation factor 4E-binding protein 1 (EIF 4EBP1) (Wu et al. 2017) and activate the ribosomal protein S6 kinase (S6K) (Easley et al. 2010). This means that mTOR can potentially regulate translation. S6K can initiate a negative feedback loop through inhibition of the insulin receptor substrate 1 (IRS1) (Zhang et al. 2008). The S6K phosphorylation level (T389) is often used to monitor mTOR activity (Sarkar 2013).

Amino acids can activate Rag GTPases which causes mTOR recruitment to the lysosomes, activation of mTOR and autophagy inhibition. In addition, the mTOR activation on the lysosomal surface causes sequestration of the transcription factor EB (TFEB) which is involved in transcription of autophagy-related and lysosomal genes (Sarkar 2013), additionally contributing to the inhibition of autophagy.

The pathways mentioned are complemented by activation of the 5' AMP-activated protein kinase (AMPK) and the corresponding AMPK/TSC/mTOR pathway that can be influenced by ATP (Sarkar 2013). It has been shown that AMPK phosphorylates (activates) TSC2 under energy starvation, thereby increasing autophagy via mTOR inhibition, which prevents energy deprivation-induced apoptosis (Inoki et al. 2003b). The same authors concluded in a subsequent study that the TSC2 phosphorylation mediated by AMPK represents a priming event for subsequent phosphorylation by GSK3-β (Inoki et al. 2006). This would have an opposing effect on the TSC1/2 inhibition mediated by Akt and thereby negatively modulate the PI3K/Akt/TSC/mTOR pathway (Inoki et al. 2006). However, these findings imply that inhibition of GSK3-β would decrease autophagy and several previous studies have shown the opposite, demonstrating that autophagy is increased (mTOR inhibited) following GSK3-β inhibition or knockdown (Ren et al. 2016; Weikel et al. 2016). It may be possible, that different results were obtained in those studies because different inhibitors were used. It is also possible, that GSK3-β inhibition enhances autophagy by phosphorylating the mTOR-associated scaffold protein raptor (regulatory-associated protein of mTOR) at the Ser859 site and thereby reduces the interaction of raptor and mTOR, leading to a decreased mTOR signaling and increased autophagic flux (Stretton et al. 2015). Furthermore, many studies have shown that GSK3-β can interact with various members of the mTOR pathway and therefore the effect of GSK3-β on the mTOR pathway has been described as very complex (Hermida et al. 2017). Additionally, some studies have shown that GSK3-β inhibition can increase lysosomal biogenesis and increase lysosomal acidification (Parr et al. 2012; Azoulay-Alfaguter et al. 2015), suggesting that GSK3-β can potentially affect the autophagy initiation, as well as the lysosomal degradation.

Autophagy and lysosomal degradation have been shown to be impaired in AD leading to an accumulation of autophagic vesicles in the large swellings of dystrophic neurites (Nixon et al. 2005; Piras et al. 2016). The accumulation of CTFβ (C99) in dystrophic neurites has been found to be both responsible for and the result of the autophagic and lysosomal impairment in 3xTg AD mice (Lauritzen et al. 2016). Furthermore, mutations in presenilin-1 (PS1) are likely to be a cause of the dysfunctional degradation of proteins in AD since PS1 is required for targeting the v-ATPase to lysosomes (Lee et al. 2010). Pathological alteration of this targeting caused by PS1 mutations may lead to impaired acidification of the autolysosomes and hence, an impairment of the lysosomal proteases (Lee et al. 2010). In fact, the inhibition of lysosomal proteolysis has been shown to disrupt the axonal transport of proteolytic vesicles and cause axonal dystrophy in cultures of murine primary cortical neurons (Lee et al. 2011). A different study identified that pathological tau phosphorylation, Aβ oligomers and decreased levels of kinesin and dynein are responsible for accumulation of AVs in dystrophic neurites (Sanchez-Varo et al. 2012). Interestingly, the ApoE-ε4 isoform has been associated with impaired astrocytic autophagy and reduced Aβ clearance (Simonovitch et al. 2016). ApoE-ε4 astrocytes were found to store rather than digest large amounts of Aβ protofibrils and releasing incompletely digested, toxic Aβ (Sollvander et al. 2016).

In AD, the PI3K/Akt/mTOR pathway and downstream targets such as p70S6K, 4EBP1, and GSK3-β are upregulated, resulting in a reduced level of autophagy (Tramutola et al. 2015). The upregulation of mTOR has been associated with increased cytosolic tau and increased tau secretion (Tang et al. 2015). Inhibition of mTOR by rapamycin, on the other hand, has been suggested to be protective against Aβ-induced synaptotoxicity in hippocampal neurons and to prevent tau-induced neuronal loss in Tg P301L mice (Ramirez et al. 2014; Siman et al. 2015). Another *in vivo* study showed that impaired autophagy not only leads to increased intracellular Aβ

accumulation but also to increased Aβ plaque formation due to an upregulated Aβ secretion in APP23 mice (Nilsson et al. 2013). Furthermore, rapamycin has been shown to prevent neuritic dystrophy in PC12 cells and superior cervical ganglion neurons (Yang et al. 2014).

Interestingly, the *in vivo* conditional knockout (cKO) of autophagy-related protein 7 (Atg7) in postnatal forebrain-specific neurons leads to an age-dependent neurodegeneration along with p62, GSK3-β and p-tau accumulations (Inoue et al. 2012). Since tau and GSK3-β are both known to regulate autophagy (Ren et al. 2016; Lin et al. 2003) these findings suggest a feedback loop in which autophagy defects can lead to accumulations of phosphorylated tau and GSK3-β which in turn influences the autophagy (Inoue et al. 2012).

It has been shown that the inhibition of lysosomal function by lysosomotropic agent chloroquine (CQ) that decreased the activities of cathepsins B, L and D led to the accumulation of tau in human neuroblastoma cells that inducibly express tau (Hamano et al. 2008). Pharmacological inhibition of autophagy also resulted in tau accumulation and aggregation (Hamano et al. 2008), suggesting that autophagy and lysosomal degradation are crucial for the degradation of tau and that a malfunction of the autophagic-lysosomal pathway may contribute to the formation of tau pathologies.

Furthermore, the inhibition of mTOR activity by rapamycin, which increases autophagy initiation, also decreased total and phosphorylated tau in Tg Tau P301S mice (Caccamo et al. 2013). Interestingly, heterozygous TSC2 +/- mice exhibited elevated total tau and phosphorylated tau because of an increased activation of mTOR signaling (Caccamo et al. 2013). As mentioned before TSC1/2 are known negative regulators of mTOR (Caccamo et al. 2013). The same study also showed an important link between GSK3-β and mTOR signaling. The phosphorylation at the inhibitory GSK3-β S9 site was decreased in heterozygous TSC2 +/- mice and increased after

rapamycin treatment of Tg Tau P301S mice, indicating that GSK3-β inhibition is linked to increased autophagy and decreased tau pathology (Caccamo et al. 2013).

In conclusion, the pharmacological induction of autophagy via suppression of the mTOR pathway represents a promising therapeutic approach against AD pathologies and pure tauopathies.

1.1.7 Mouse models of Alzheimer's disease

Many different transgenic mouse models of AD that recapitulate some of the pathological aspects of AD have been developed. This chapter will describe the three mouse models that we used in our studies.

1.1.7.1 Tg APPsw mice (Tg 2576)

The transgenic APPsw (Tg APPsw or Tg 2576) mice were used among two other mouse models to determine whether Aβ accumulation can affect of SYK activation in the CNS. Tg APPsw mice overexpress the Swedish mutation (KM670/671NL) of human APP695 under the control of the hamster prion protein promoter (Hsiao et al. 1996) and therefore exhibit elevated levels of Aβ and typically develop Aβ deposits at the age of 11 months (Irizarry et al. 1997). Tg APPsw mice develop Aβ deposits much later than the double transgenic Tg PS1/APPsw mice (described below). Tg APPsw mice also show a loss of dendritic spines in the CA1 region of the hippocampus as early as 4.5 months of age, before the formation of β-amyloid deposits (Lanz et al. 2003), suggesting that soluble forms of Aβ are synaptotoxic. Neuroinflammation becomes evident at 10-16 months in these mice, as Aβ plaque-associated microglia increase in abundance and size (Frautschy et al. 1998). Additionally, Tg APPsw mice develop dystrophic neurites in and around Aβ plaques and exhibit tau hyperphosphorylation without forming NFTs (Tomidokoro et al. 2001). The described

age-dependent pathological changes in Tg APPsw are also accompanied by behavioral abnormalities. At 3 months of age, the animals perform normally in learning and spatial memory tasks but display impairments at 9 months of age (Hsiao et al. 1996).

1.1.7.2 Tg PS1/APPsw mice

Tg PS1/APPsw mice that carry the APP KM670/671NL (Swedish) and the PSEN1 M146L mutations were also used for investigating the influence of the β-amyloid pathology on SYK activation in the CNS. Tg PS1/APPsw mice were generated by crossing Tg APPsw (Tg2576) mice with Tg PS1(M146L) mice. In all our studies, the mice were heterozygous for the for the *APP* and *PS1* transgenes. The overexpression of the human APPsw is driven by the hamster prion protein gene promoter, whereas the overexpression of the human PSEN1 M146L is driven by the PDGF-β promoter. The double transgenic mice develop cortical and hippocampal amyloid deposits at 6 months of age; much earlier than the single transgenic APPsw (described above). Furthermore, the total Aβ burden is increased in the double transgenic compared to the single transgenic mice (Holcomb et al. 1998). As in Tg APPsw mice, the Aβ deposits are associated with dystrophic neurites that occur at 12 months of age (Gordon et al. 2002). Additionally, these mice display an increase in Aβ plaque-associated microglia and astrocytes at 6 months of age, with increased microglial activity occurring at 12 months of age (Gordon et al. 2002). Although Tg PS1/APPsw mice do not overexpress tau like the Tg Tau P301S mice (see below) and do not form NFTs, hyperphosphorylated tau has been detected in some dystrophic neurites at 24 weeks of age (Kurt et al. 2003).

The accumulation of Aβ in the brain of these mice is also responsible for the development of cognitive impairment. Although their learning ability is still normal in the water maze at the age

of 9 months (Holcomb et al. 1999), their spatial memory assessed by the Y-maze seems to be impaired at 3 months. Moreover, memory acquisition and working memory have been shown to be impaired in 15 months old animals, as assessed by the Morris water maze and the radial arm water maze (Arendash et al. 2001).

1.1.7.3 Tg Tau P301S mice (Line PS19)

Besides the amyloid overexpressing mouse models described in the two previous subchapters, we used another mouse model overexpressing the human tau protein. The transgenic tau P301S (line PS19) mice were used, to investigate the possible impact of the tau pathology on SYK activation in the CNS. In addition, we used the Tg Tau P301S mice to determine the effects of chronic SYK inhibition on tau hyperphosphorylation and oligomerization, neurodegeneration, neuroinflammation, and behavioral deficits induced by the tau pathology. Tg Tau P301S mice overexpress the human tau with the P301S mutation.

The P301S mutation in the tau gene on chromosome 17 has been associated with autosomal dominantly inherited frontotemporal dementia and parkinsonism (FTDP-17) and the P301S mutation in exon 10 causes a reduced ability of tau to promote microtubule assembly and might furthermore contribute to tau hyperphosphorylation (Bugiani et al. 1999; Lossos et al. 2003; Sperfeld et al. 1999).

The expression of the P301S mutated tau is driven by the mouse prion protein promoter and fivefold higher than the endogenous mouse tau protein (Yoshiyama et al. 2007). The P301S tau overexpression leads to a progressive synaptic loss at 3 months and neuronal loss at 9 months of age, spreading from the hippocampus to the cortex. NFTs emerge at 6 months of age and also

spread from the hippocampus to the cortex. Microgliosis has been observed as early as 3 months of age, preceding astrogliosis (Yoshiyama et al. 2007).

As a consequence of these pathological changes, the behavior of these mice is also altered. Tg Tau P301S mice have been found to exhibit spatial learning and memory impairments at 6 months of age (Takeuchi et al. 2011). Apart from the cognitive deficits, the mice also display a progressive motor decline culminating in paralysis at approximately 10 months of age. This also leads to a mortality rate of 80% at 12 months (Yoshiyama et al. 2007). In contrast to Tg PS1/APPsw and APPsw mice (described above), the Tg Tau P301S mice do not develop β-amyloid plaques.

1.2 The Spleen Tyrosine Kinase

The spleen tyrosine kinase (SYK) is a non-receptor protein-tyrosine kinase (PTK) that mediates inflammatory responses (Geahlen 2014). PTKs like SYK are part of receptor-mediated signal transduction cascades that require their intracellular association with integral membrane receptors. These receptors contain cytoplasmic immunoreceptor tyrosine-based activating motifs (ITAMs). The SYK protein can be divided into different domains, including the N-terminal Src homology domains (SH2) that are linked by an interdomain A, and the C-terminal kinase domain that is linked to the SH2 domains by an interdomain B (Sada et al. 2001). SYK can be activated through autophosphorylation or binding to ITAM-containing receptors (Tsang et al. 2008).

SYK phosphorylation plays an important role in its activation. In the resting state, the kinase domain of SYK is inactive. It has been speculated that SYK adopts an autoinhibitory conformation in the absence of ITAM binding, similar to the ζ-chain-associated protein kinase of 70 kDa (ZAP-70) that is known as a SYK homologue (Mócsai et al. 2010). For activation of SYK, the N-terminal SH2 domains need to bind to the C-terminally phosphorylated tyrosines of the ITAM (Futterer et al. 1998; Mócsai et al. 2010) or the linker regions interdomain A or B need to be phosphorylated (Tsang et al. 2008). The latter activation enables SYK to stay active for a prolonged period of time, beyond the ITAM-mediated signaling (Tsang et al. 2008).

SYK autophosphorylation is also known to influence its activation. Several autophosphorylation sites of SYK have been identified: Tyr130, Tyr290, Tyr317, Tyr 342, Tyr346, Tyr358, Tyr519/520, Tyr525/526 and Tyr623/624/625 (Mócsai et al. 2010; Furlong et al. 1997; Tsang et al. 2008; Zhang et al. 2000). The phosphorylation sites Tyr519/520 and Tyr525/526 play an important role in the activation of SYK and the propagation of receptor-mediated signaling events, as they are part of the kinase activation loop that regulates the enzymatic activity of SYK



(Zhang et al. 2000; Tsang et al. 2008). In the non-activated SYK, the tyrosines of the activation loop occupy the catalytic center and prevent ATP or substrate binding, while phosphorylation of those tyrosines induces a conformational change that allows the binding of ATP and substrate (Zhang et al. 2000). Since tyrosine phosphorylation in the activation loop has been shown to be the best indicator for functional activation of SYK (Zhang et al. 2000), in this thesis, we focused on the Tyr525/526 phosphorylation site for assessment of SYK activation. Many previous studies have used the Tyr525/526 phosphorylation site to monitor SYK activation (Feldman et al. 2008; Speich et al. 2008; Aouar et al. 2016; Satoh et al. 2012).

Several receptors are known to activate SYK. Amongst these are toll-like receptors (TLRs). TLRs can, for example, mediate the host defense against infections and initiate the innate immune response. The TLR-triggered inflammatory response has been shown to activate SYK and PI3K (Han et al. 2010). SYK has also been shown to be required for the collaborative response of TLR2 and the β-glucan receptor Dectin-1 that are involved in the cytokine response in macrophages (Dennehy et al. 2008).

SYK has also been shown to be activated by FcεRI (high-affinity receptor for the fragment crystallizable (Fc) of immunoglobulin E (IgE)) receptor as part of the Lyn-SYK-Akt pathway leading to AMPK inhibition (Lin et al. 2016).

SYK has also been suggested to play a role in the FcεRI-initiated histamine release from basophils during an allergic response (Youssef et al. 2002). The same study found that a ubiquintin/proteasome-dependent mechanism regulates SYK levels in human basophils (Youssef et al. 2002). The CbI-interacting 85-kDa multi-adaptor protein (CIN85), a negative regulator of FcεRI-mediated degranulation that is involved in endocytosis and vesicle trafficking, could decrease SYK levels by increasing the ubiquitin-proteasome degradation (Peruzzi et al. 2007).

The CD40 receptor is known to play an important role in B-cell proliferation and activation (Faris et al. 1994). It has been shown that the CD40 signaling pathway involves PTKs, including Lyn, Fyn, and SYK (Faris et al. 1994; Ying et al. 2011). Interestingly, the CD40 expression in microglia has been found to be increased after treatment with Aβ and in microglia derived from Tg APPsw mice (Tan et al. 1999). Since SYK is involved in CD40 signaling, this could suggest that SYK also plays a role in Aβ-induced signaling via CD40. It has also been shown that CD40 deficiency leads to a decreased amyloid burden and decreased tau hyperphosphorylation *in vivo* (Laporte et al. 2006), suggesting that CD40 signaling is involved in amyloid and tau pathogenesis and microglial activation. This could imply a role of SYK in the generation of the amyloid and tau pathology and microgliosis seen in AD via the CD40 receptor.

SYK has also been shown to be involved in TNFR-mediated signaling (Takada and Aggarwal 2004). In T-cells, TNF activated SYK and resulted in a downstream signaling cascade involving JNK, MAPK and NFκB (Takada and Aggarwal 2004). Furthermore, pharmacological SYK inhibition and knockdown of SYK using shRNA led to the suppression of the TNFR signaling cascade (Takada and Aggarwal 2004).

In addition, two engulfment receptors, Jedi-1 and MEGF10, expressed in glial precursor cells and involved in phagocytosis, have been shown to recruit and activate SYK through their ITAMs (Scheib et al. 2012). The same study suggested that SYK was involved in phagocytosis of apoptotic neurons by glial precursor cells, as SYK inhibition by BAY61-3606 and knockdown of STK blocked the phagocytosis (Scheib et al. 2012).

SYK activation can also be induced by integrin receptors (Jakus et al. 2007) that are involved in cell adhesion. APP has been shown to co-localize with β1-integrin receptors (Yamazaki et al. 1997), suggesting an involvement of APP in neuronal adhesion processes.

Interestingly, one study has demonstrated that APP is involved in β1-integrin-mediated adhesion in murine microglia and human monocytes leading to a recruitment of Lyn and SYK, mediating a pro-inflammatory response (Sondag and Combs 2004). This suggests that APP may be able to act as a pro-inflammatory receptor in monocytes and further links SYK to the pathobiology of AD. TREM2 is another receptor expressed in microglia that can mediate SYK activation (TREM2 mediated activation of SYK is described in the chapter 1.2.2).

SYK is mainly localized at the plasma membrane but is also actively transported to the centrosomes, suggesting a role of SYK in cell division (Zyss et al. 2005). This transport depends on the phosphorylation site Tyr130 of SYK (Zyss et al. 2005). It has also been shown that SYK co-localizes with γ-tubulin, persists during interphase and is degraded by the proteasome during mitosis, suggesting an inhibitory effect of SYK on cell division (Zyss et al. 2005). However, SYK activity is also known to be increased and act as a pro-survival factor in certain rapidly proliferating tumor cells and SYK inhibition has therefore been suggested as a therapeutic strategy for targeting certain types of cancer, especially hematopoietic malignancies (Geahlen 2014).

In addition, SYK is involved in ERK (extracellular signal-regulated) activation during differentiation of neuron-like P19 cells (Tsujimura et al. 2001). In neurons, SYK is also involved in axonal growth cone collapse and acts as a switch between adhesive and repulsive responses during axonal outgrowth (Noraz et al. 2016).

SYK was shown to phosphorylate microtubules which could have an effect on microtubule polymerization or the interaction of signaling molecules with the microtubule network (Faruki et al. 2000). Hence, Tsujimura et al. (2001) argue that microtubule phosphorylation by SYK may affect the formation of supernumerary neurites. Furthermore, pharmacological SYK inhibition has been found to stabilize microtubules through dephosphorylation of microtubules and microtubule-

associated proteins (MAPs) (Yu et al. 2015). In the same study, the authors found that SYK inhibition by small molecules (R406) or shRNA and paclitaxel co-treatment had a synergistic cytotoxic effect on ovarian cells (Yu et al. 2015). Certain tumor cells were previously found to express higher levels of SYK (Yu et al. 2015). In B-cell lymphoma cells for example, inhibition of SYK by cerdulatinib resulted in blockage of Janus kinase (JAK)/signal transducer and activator of transcription (STAT) signaling and subsequent cell death (Ma et al. 2015), suggesting that SYK regulates the JAK/STAT pathway.

1.2.1 The role of SYK in Alzheimer's disease

The previous work in our laboratory with the antihypertensive dihydropyridine (DHP) nilvadipine has led to the identification of SYK as a potential target for AD (Paris et al. 2011; Paris et al. 2014). Nilvadipine is a known L-type calcium channel (LCC) antagonist (Paris et al. 2011; Paris et al. 2014). Nilvadipine is a racemic compound consisting of equal amounts of (+)-nilvadipine and (-)-nilvadipine. The (+) enantiomer is a potent LCC antagonist, while the (-) enantiomer is a much weaker LCC blocker (Paris et al. 2014). Interestingly, both enantiomers decrease Aβ production and increase Aβ clearance across the blood-brain barrier (BBB) *in vitro* to the same extent (Bachmeier et al. 2011; Paris et al. 2011; Paris et al. 2014). In addition, both enantiomers decrease Aβ accumulation in the brains of Tg PS1/APPsw mice with similar potency and improve learning and spatial memory (Paris et al. 2011; Bachmeier et al. 2011; Paris et al. 2014). Interestingly, other L-type calcium channel blockers were unable to lower Aβ levels (Paris et al. 2011). Taken together, these findings suggests that the effects of nilvadipine on Aβ are independent of LCC inhibition and mediated by another target (Paris et al. 2014). Subsequent mechanistic experiments with nilvadipine revealed SYK as a target by showing a direct binding of nilvadipine to SYK and

a consequential inhibition of SYK activity in a cell-free assay (Paris et al. 2014). This implies that SYK inhibition by nilvadipine could be responsible for its Aβ-lowering activity (Paris et al. 2014). Indeed, our previous studies showed that pharmacological inhibition of SYK, as well as genetic suppression of SYK, downregulate Aβ production and BACE-1 expression in SH-SY5Y cells, thereby mimicking the effects of nilvadipine (Paris et al. 2014). Furthermore, our previous studies showed that acute treatments with (-)-nilvadipine or with the Syk inhibitor BAY61-3606 reduced tau hyperphosphorylation in Tg Tau P301S mice (Paris et al. 2014).

Importantly, the acute pharmacological inhibition of SYK with the selective inhibitor BAY61-3606 had the same effects as the treatment with (-)-nilvadipine and increased phosphorylation of GSK3-β at the inhibitory Ser9 site and reduced p-Akt (Ser473) levels significantly (Paris et al. 2014), thereby confirming the hypothesis that the Aβ-lowering activity of nilvadipine may be mediated by SYK inhibition. The impact on GSK3-β was found to be mediated by the cAMP-dependent protein kinase (PKA) which also phosphorylates the cAMP response element-binding protein (CREB), involved in neuronal plasticity (Paris et al. 2014). SYK also has a major impact on neuroinflammation since it acts upstream of NFκB, which is known to control the inflammatory response but also regulates BACE-1 expression, the rate-limiting enzyme in Aβ production (Paris et al. 2014). In fact, BACE-1 expression was significantly decreased following SYK inhibition (Paris et al. 2014). SYK inhibition by BAY61-3606 also increased Aβ clearance across the blood-brain barrier (BBB) like nilvadipine and reduced Aβ levels in Tg PS1/APPsw mice, thereby recapitulating the different biological effects of nilvadipine observed on Aβ and tau (Paris et al. 2014). More specifically, the acute treatment with BAY61-3606 had a profound impact on tau hyperphosphorylation at Ser396/404 (PHF-1), Ser202 (CP13) and partially prevented Tyr18 (9G3) phosphorylation in Tg Tau P301S mice (Paris et al. 2014). SYK and Src

family kinases have been shown to phosphorylate tau directly at Tyr18 (Lebouvier et al. 2009) which could explain the partial inhibition of tau Tyr18 phosphorylation observed following SYK inhibition. Tau tyrosine phosphorylation is considered an early pathological change in AD (Derkinderen et al. 2005b; Lebouvier et al. 2009).

In addition to our previous experiments, *in vitro* experiments performed by other groups have shown that Aβ oligomers can activate and trigger an inflammatory response in cultured primary microglial and monocytic cells. This response was mediated by the tyrosine kinases Lyn and SYK and elicited an intracellular calcium release that triggered the activation of the protein kinase C (PKC) (Combs et al. 1999; McDonald et al. 1997). The calcium-sensitive tyrosine kinase PYK2 then triggered the activation of the mitogen-activated protein kinases (MAPKs) and the extracellular signal-regulated kinases 1 and 2 (ERK1/2) (Combs et al. 1999). Importantly, SYK inhibition resulted in a reduced Aβ-mediated neurotoxicity *in vitro* (Combs et al. 1999). A subsequent study also showed that SYK was the mediator of the Aβ-induced elevated cytokine production in microglia, including tumor necrosis factor alpha (TNFα) and interleukin 1 beta (IL-1β) via a NFκB-dependent mechanism (Combs et al. 2001).

1.2.2 The role of SYK in Nasu-Hakola disease

In addition to the receptors mentioned above, TREM2 can also mediate the recruitment and activation of SYK (Lanier and Bakker 2000). TREM2 is a type I transmembrane protein and part of the immunoglobulin (Ig) receptor superfamily. An adaptor protein DNAX-activating protein of 12 kDa (DAP12, also known as TYROBP) is needed for TREM2 signal transduction, since TREM2 does not have any cytoplasmic signaling motifs. DAP12 interacts with the transmembrane domain of TREM2 and the cytoplasmic domain of DAP12 contains an ITAM (see above 1.2).

Nasu-Hakola disease (NHD) is a rare autosomal recessive disorder that is caused by a loss-of-function mutation of TREM2 or DAP12 (Paloneva et al. 2002). Symptoms of NDH include multifocal bone cysts and presenile dementia. In contrast to AD patients, the onset of dementia occurs very early in NHD patients (30 years of age) (Paloneva et al. 2001). Interestingly, NHD specimens show β-amyloid pathology and tau pathology (NFTs) but too a much lesser extent than AD specimens (Ghezzi et al. 2017; Satoh et al. 2018). However, considering the fact that the homozygous TREM2 or DAP12 mutations lead to death at the age of 40 (Paloneva et al. 2001), the period of exposure to the disease-causing mutations is not long enough to build up full-blown AD-like pathologies. Nevertheless, these studies suggest that TREM2 mutations could promote the development of AD pathological lesions and further highlight the importance of myeloid cells (microglia, macrophages, monocytes) in the pathogenesis of AD. Importantly, SYK activity is increased in NHD neurons compared to controls (p-SYK, Tyr525/526) (Satoh et al. 2012). The authors also found p-SYK to be mainly present in microglia and macrophages but not in astrocytes or oligodendrocytes. This further supports the idea that SYK plays an important role in TREM2-mediated signaling and implies a contribution of SYK to the pathobiology of NHD.

A described before (1.1.3, 1.1.4), TREM2 mutations have been associated with neurodegenerative diseases including AD (Finelli et al. 2015), Parkinson's disease (PD) (Benitez and Cruchaga C 2013) and frontotemporal dementia (FTD) (Borroni et al. 2014), thereby suggesting that microglia and neuroinflammation play important roles in these diseases, as TREM2 is exclusively expressed in myeloid cells. Although rare, heterozygous TREM2 variants are associated with an increased risk for developing AD (Kober et al. 2016). TREM2 immunoreactivity is upregulated in Aβ plaque-associated microglia and neurites of human AD temporal cortices (Lue et al. 2015).

Additionally, increased TREM2 expression positively correlated with tau phosphorylation and caspase 3 activity (Lue et al. 2015).

TREM2 has been shown to be a receptor for Aβ (Zhao et al. 2018). They furthermore found, that Aβ enhanced the interaction of TREM2 and DAP12, thereby regulating the activation of downstream kinases including SYK and GSK3-β (Zhao et al. 2018). Since TREM2 is an established risk factor for AD, this Aβ-induced SYK activation mediated by TREM2 further highlights SYK as an important kinase in the pathobiology of AD.

Interestingly, ApoE has been found to be a ligand of TREM2 (Atagi et al. 2015; Bailey et al. 2015). It has been shown that ApoE modulates the Aβ clearance in mouse models of AD. Binding of ApoE to TREM2 induces microglial phagocytosis of apoptotic N2a cells (Atagi et al. 2015). Interestingly, the missense TREM2-R47H mutation that is associated with AD in particular, exhibited reduced binding of all ApoE isoforms, thereby linking two risk factors of AD (Atagi et al. 2015).

In APP23 transgenic mice, expressing human APP containing the Swedish mutation under the murine Thy1 promoter, TREM2 appears to be upregulated in microglia associated with β-amyloid plaques (Frank et al. 2008). However, the effects of TREM2 deficiency on AD pathological lesions in animal models remains highly controversial (see introduction on tau for more examples 1.1.4). TREM2 deficiency has been shown to reduce inflammation, ameliorate amyloid and tau pathologies in AD mouse models (APPPS1-21 and 5xFAD) (Jay et al. 2015). The opposite has been shown in two studies by Jiang et al. (2014a; 2015) in which they conclude that TREM2 upregulation ameliorates the neuropathology and rescues the spatial cognitive impairment in APPsw/PS1ΔE9 and Tg Tau P301S mice. In a subsequent study, they also suggested that

TREM2 overexpression causes downregulation of GSK3-β, cyclin-dependent kinase (CDK5) and a suppression of neuroinflammation through M2 activation of microglia (Jiang et al. 2016).

APPPS1-21 mice, expressing only one copy of TREM2, exhibit altered microglial phenotypes and a decrease in microglia around Aβ plaques (Ulrich et al. 2014). This suggest an important role of TREM2 in the Aβ-mediated microglial response (Ulrich et al. 2014). Interestingly, no differences in β-amyloid plaque burden were detected (Ulrich et al. 2014). In contrast, Wang et al. (2015b) and Yuan et al. (2016) found that TREM2 deficiency and haploinsufficiency exacerbate amyloid pathology in AD mouse models.

Although TREM2 has been established as a well-known risk factor for AD, the abovementioned contradicting results show that its function is not fully understood and remains subject of debate. Nevertheless, given that TREM2 is known to mediate SYK activation and that certain TREM2 mutations have been shown to induce SYK activation in neurons and microglia in NHD, this could suggest that a dysregulation of SYK activity plays a role in the development of AD.

1.3 Clinical trials for Alzheimer's disease

To date, there is no cure available to AD patients, as none of the drugs approved by the food and drug administration (FDA) halts the cognitive decline. There are five approved AD drugs (as of August 2018), three of which are acetylcholine esterase inhibitors (donepezil, galantamine, rivastigmine), one NMDA receptor antagonist (memantine) and one drug that combines donepezil and memantine, meaning that there are just two different forms drugs in terms of mechanism of action (MOA) that are currently approved by the FDA. Memantine has been the last drug approved by the FDA in 2003, meaning that there has been no approval of a drug for AD during the last 15 years. Furthermore, the currently approved drugs are not disease-modifying therapies (DMT) that will prevent or delay the onset or slow the progression of the disease but are categorized as symptomatic cognitive enhancers. While symptomatic cognitive enhancers may help patients in the short term by boosting their cognitive performance, they do not alter the advance of the disease in the long term. Therefore, FDA approved DMTs are needed to successfully treat AD.

As of the beginning of 2018, there were 112 drugs in the pipeline according to clinicaltrials.gov (Cummings et al. 2018). Of those 112 drugs only 63% were DMTs. 17 DMTs were in phase III and the drugs targeted amyloid (14 drugs), had a tau-related target (1 drug), involved neuroprotection (1 drug), or had a metabolic MOA (Cummings et al. 2018). Six of the DMTs were immunotherapies targeting amyloid, five BACE inhibitors, and three drugs aiming to prevent the amyloid aggregation (Cummings et al. 2018).

Passive immunotherapies against Aβ include for example the antibodies solanezumab, aducanumab and BAN2401. Solanezumab is a humanized monoclonal IgG1 antibody directed against the Aβ mid-domain. The antibody recognizes soluble monomeric Aβ but not fibrillar Aβ. Solanezumab has been in many phase II and phase III clinical trials but the last phase III was

terminated because of "insufficient scientific evidence that solanezumab would likely demonstrate a meaningful benefit to participants with prodromal AD as defined by study protocol" (clinical trials.gov; NCT02760602). The previous solanezumab phase III trial for mild AD failed to meet the primary endpoints (Doody et al. 2014; Honig et al. 2018). However, there is a phase III trial ongoing that enrolled asymptomatic or very mildly symptomatic individuals that may be at risk for memory loss because of biomarker evidence of brain amyloid deposition (NCT02008357).

The aducanumab trials involve a fully human IgG1 monoclonal antibody directed against aggregated Aβ (conformational epitope). The antibodies are derived from aged, healthy, cognitively normal donors who were said to have successfully resisted AD. The phase I aducanumab trial that started in 2012 and involved 166 prodromal or mild AD individuals is still ongoing (NCT01677572) and one year of monthly aducanumab intravenous infusions seemed to dose- and time-dependently reduce brain Aβ and slow the clinical decline, as measured by CDR-SB and MMSE (Sevigny et al. 2016). However, the ongoing two phase III clinical trials (NCT02477800, NCT02484547), both involving 1350 mild MCI or mild AD patients, will show if aducanumab is suitable as a treatment for AD.

BAN2401 is a humanized IgG1 antibody directed against large, soluble Aβ protofibrils. The phase II clinical trial that enrolled 856 MCI or mild AD patients (MMSE ≥22) showed a dose dependent reduction of amyloid PET values and, more importantly, slowing in cognitive decline after 18 months of treatment with the highest dose (ADAS-cog, 47%) (NCT01767311). However, APOE-ε4 carriers are prone to develop amyloid related imaging abnormalities-edema (ARIA-E) following Aβ antibody treatment and therefore a significant number of APOE-ε4 individuals were moved out of the highest dose arm. APOE-ε4 carriers are at higher risk for developing AD and

exhibit a faster progression, Therefore, the positive results of the phase II BAN2401 trial have to be considered with caution.

The CAD106 trials involve an active immunization strategy using the Aβ1-6 peptide derived from the N-terminal B-cell epitope of Aβ, coupled to a bacteriophage Qβ (virus-like) particle. An ongoing phase II/III study that enrolled 1340 homozygous APOE-ε4 carriers (60-75 years of age) not only aims to test CAD106 but also compare it to the BACE inhibitor CNP520 (NCT02565511).

BACE inhibitors aim to limit the production of Aβ. The phase III clinical trial of the BACE inhibitor verubecestat (NCT01739348) failed to slow cognitive and functional decline in individuals with mild-to-moderate AD despite target engagement (90% reduction of Aβ production with the highest dose) and another phase III including individuals with prodromal AD (NCT01953601) was terminated in 2018 because it was unlikely to have a positive benefit/risk.

Nevertheless, other phase III BACE inhibitors continue. Elenbecestat, for example, is currently being tested in two phase III trials (NCT02956486, NCT03036280) that both enrolled 1350 MCI and prodromal AD patients. Previously elenbecestat had shown a 70% reduction of CSF Aβ in a phase II clinical trial (NCT02322021). An interesting approach is also the combination of BACE inhibitors and Aβ antibodies. TRAILBLAZER (NCT03367403) is the name of the study that will test LY3002813, a humanized IgG1 antibody directed against a N-terminally truncated pyro-glutamate modified Aβ (specifically localized in Aβ plaques), and the LY3202626 BACE inhibitor, in order to achieve maximal target engagement of the amyloid pathway. Interestingly, this trial enrolls early symptomatic AD patients based on amyloid and tau burden (PET).

The first drugs targeting tau were aiming to reduce tau aggregation and failed to meet their primary endpoints. TRx0237, also known as LMT-X, methylene blue or tau aggregation inhibitor

(TAI) is the chemical methylthioninium chloride (MTC) and is a drug that predates the FDA and is a re-purposed malaria drug. Between the years there were three different phase III clinical trials for all-cause dementia or mild AD (NCT01689233), mild to moderate AD (NCT01689246), and the behavioral variant of frontotemporal dementia (NCT01626378). All phase III TRx0237 trials failed to meet their primary endpoints. Nevertheless, another phase II/III TRx0237 for all-cause dementia and AD is underway and will end in 2019 (NCT03446001). There are only a few clinical trials involving small molecules whose MOA involves tau. In fact, besides TRx0237 there is no other small molecules in a phase III and only four in a phase II clinical trial, including ANAVEX2-73, a sigma-1 receptor agonist, nicotinamide (vitamin B3), the re-purposed drug nilotinib (FDA-approved to treat adult chronic myeloid leukemia), is said to inhibit the tyrosine kinase Abl, and another compound with a similar MOA, AZD0530 or saracatinib (NCT02167256), an inhibitor of the Src/Abl family of kinases. The rational of using AZD0530 is mainly based on targeting Fyn and thereby decreasing the phosphorylation of tau and Aβ burden (Nygaard et al. 2014). Therefore, the use of AZD0530 for the treatment of AD represents an approach that is, to some extent, similar to targeting SYK. The 12-months phase II clinical trial that included 152 AD patients (MMSE 18-26 and 18F-Florbetapir PET scan with evidence of elevated Aβ) ended in February 2018 and the analysis will give additional information about the efficacy of targeting a tyrosine kinase similar to SYK in the brain of AD patients.

However, there are currently active and passive tau immunotherapies in phase I and II trials. Among the tau immunotherapies in phase II trials are active immunotherapy AADvac-1 (NCT02579252), passive immunotherapy ABBV-8E12 (NCT02880956), antisense oligonucleotides (ASO) based IONIS-MAPTRx or BIIB092 (NCT03186989), and passive immunotherapy BIIB092 (NCT03352557). The AADvac-1 trial involves a treatment with a

synthetic peptide derived from amino acids 294 to 305 of the tau sequence. The peptide is supposed to evoke an immune response against pathologically modified forms of tau protein because tau cleavage has been found to generate N-terminally truncated fragments (Kontsekova et al. 2014; Paholikova et al. 2015). The results of the 24-months phase II trial including 185 mild-to-moderate AD patients will presumably be available in 2019 and give first hints about the efficacy of an active tau vaccination. The ABBV-8E12 trial involves a treatment with a humanized IgG4 antibody directed against aggregated, extracellular tau species, in order to prevent or reduce the transneuronal tau propagation (Braak and Del Tredici 2011; Clavaguera et al. 2009). Therefore, its MOA does not require a neuronal uptake. The phase II 96-weeks-long trial included 400 AD patients (CDR 0.5, MMSE≥22) and is currently ongoing. The IONIS-MAPTRx or BIIB092 trial is the first clinical approach using antisense oligonucleotides (ASO) to target tau expression (DeVos et al. 2013; DeVos et al. 2017). The phase I/II trial will assess adverse events and pharmacokinetic parameters and will end in 2020. The BIIB092 trial involves the use of another a humanized IgG4 monoclonal anti-tau antibody. Similar to the ABBV-8E12 approach, the antibody is directed against extracellular, N-terminally fragmented forms of tau. The phase 2 trial started in May 2018, involves 528 mild MCI and mild AD patients with positive amyloid PET scan and will end in 2021.

None of the DMTs in phase III enrolled patients with severe AD in their studies and only one phase II DMT included severe AD patients, while six trials of symptoms-reducing small molecules in phase II and III enrolled patients with severe AD (Cummings et al. 2018). Cummings et al. state that there is trend towards enrolling patients with milder forms of AD (also mild cognitive impairment (MCI), prodromal AD) or even cognitively normal individuals with signs of amyloid pathology as measured in the cerebrospinal fluid (CSF) or by positron emission

tomography (PET). The approach of developing DMTs only for milder or moderate forms of AD bears the danger of neglecting patients with severe AD although there are millions of people with AD dementia worldwide (Cummings et al. 2018). Considering that there are currently no DMTs approved that could slow down the progression of AD, this means that many mild-to-moderate AD patients will soon have progressed into the severe AD stage. Another important factor to consider for studies only including patients in the earliest stages of AD is trial length. The earlier clinical trials aim to intervene, the longer the clinical trials have to be – an approach that increases the costs for clinical trials dramatically and increases the time from patent filing to drug approval, thereby making it financially less attractive for pharmaceutical companies to work on drugs for AD. Failures of previous anti-amyloid clinical trials enrolling more severe cases of AD lead to the belief that it is too late to intervene during a state of established dementia when neurodegeneration has already progressed (Sperling et al. 2011).

As mentioned before, nilvadipine is an anti-hypertensive drug, a L-type CCB of the dihydropyridine (DHP) group (Rosenthal 1994) that our team found to inhibit SYK (Paris et al. 2014) and it was also found to increase cerebral blood flow in rats (Furuichi et al. 1992), mouse models of AD (Tg APPsw) (Paris et al. 2004), as well as humans (Ogasawara et al. 2003). Anti-hypertensive drugs have been associated with lower incidence of AD (Khachaturian et al. 2006). Nilvadipine has been re-purposed and shown to prevent cognitive decline in a small study including MCI patients with essential hypertension, as nilvadipine is lipophilic and can cross the BBB (Hanyu et al. 2007). Pre-clinical studies performed by our team have shown that nilvadipine facilitates the clearance of Aβ across the BBB (Bachmeier et al. 2011), inhibits Aβ production *in vitro* and decreased Aβ burden *in vivo* (Paris et al. 2011), and furthermore, reduced tau hyperphosphorylation *in vivo* (Paris et al. 2014).

The Roskamp Institute team was involved in launching a European multicenter double-blind placebo-controlled 18-months phase III clinical trial for AD, including 511 mild-to-moderate AD patients treated with 8mg of nilvadipine daily and the trial ended in 2017 (NILVAD, NCT02017340). Primary outcome measures included Alzheimer's Disease Assessment Scale (ADAS)-Cog 12. Secondary outcome measures included Clinical Dementia Rating Scale Sum of Boxes (CDR-SB) and Disability Assessment for Dementia (DAD).

The pre-specified primary outcome measure did not show any treatment benefit of nilvadipine for individuals with mild-to-moderate AD and the decline from baseline in ADAS-Cog 12 on placebo was 0.79 (95% CI: -0.07 to 1.64) at 13 weeks, 6.41 (5.33 to 7.49) at 52 weeks, and 9.63 (8.33 to 10.93) at 78 weeks and on nilvadipine was 0.88 (0.02 to 1.74) at 13 weeks, 5.75 (4.66 to 6.85) at 52 weeks, and 9.41 (8.09 to 10.73) at 78 weeks. However, there were some limitations to the study, as more severe AD cases were enrolled and, as in many other clinical trials, there was a lack of biomarker confirmation (PET scans or CSF amyloid measurements) for the diagnosis of AD. In addition, the dose of 8mg daily may have been too low.

Nevertheless, the sub-group exploratory analyses showed interesting results, as there was less cognitive decline in the mild AD group (MMSE ≥20 at baseline) on nilvadipine compared to placebo and a greater decline seen in the moderate AD group (MMSE ≤19 at baseline) treated with nilvadipine, furthermore indicating that earlier interventions may yield a more favorable outcome (Sperling et al. 2011). In the NILVAD trial, males showed less cognitive decline than females on nilvadipine compared to placebo. Furthermore, APOE4 carriers showed less cognitive decline than non-carriers on nilvadipine. In summary, the results of the exploratory analyses suggest that the treatment with nilvadipine may be beneficial for individuals in the early stage of AD. These findings have to be confirmed in future clinical trials with nilvadipine.

Interestingly, nilvadipine has also been shown to impact cytokine and T-cell levels in systemic autoimmune disorders complicated with hypertension (Kagawa et al. 1999). Patients treated with nilvadipine over a period of six months exhibited lower levels of IL-1β, IL-2, IL-6 and TNFα, while levels of helper/activated T-cells decreased in the peripheral blood, suggesting that nilvadipine inhibits the cytokine production in T lymphocytes. It is very likely that this effect on the immune system is mediated by SYK, as the racemic compound nilvadipine is also a SYK inhibitor (Paris et al. 2014).

The findings mentioned in the previous paragraphs further underline the importance of investigating and advancing new potential DMTs to the clinic and because of the data presented in this thesis, the development of specific SYK inhibitors represents a new and promising treatment strategy for AD. To this date, there have only been oral SYK inhibitors in clinical trials or FDA approved that aim to treat conditions like rheumatoid arthritis, autoimmune thrombocytopenia, autoimmune hemolytic anemia, IgA nephropathy, and lymphoma (fostamatinib/R788/R406), relapsed or refractory chronic lymphocytic leukemia (CLL), acute lymphoblastic leukemia (ALL) or non-Hodgkin lymphoma (entospletinib/GS-9973) (Liu and Mamorska-Dyga 2017; Sharman et al. 2015). There have also been clinical trials for CLL investigating the dual SYK/JAK1/2 inhibitor cerdulatinib/PRT062070 (Blunt et al. 2015), and for advanced solid tumors or lymphoma or relapsed or refractory acute myelogenous leukemia (R/R AML), investigating the dual SYK/FMS-like tyrosine kinase 3 (FLT-3) inhibitor TAK-659 (Liu and Mamorska-Dyga 2017) and for urticaria and cutaneous lupus erythematosus, investigating GSK2646264. Fostamatinib became the first FDA approved SYK inhibitor in 2018 for the treatment of chronic immune thrombocytopenia (ITP). This means that past and present clinical trials have investigated specific SYK inhibitors mainly for the treatment of cancer and autoimmune diseases. Only a small number



of teams have been working on SYK as a target for the treatment of CNS diseases, thereby mainly focusing on AD. However, the scientific field around SYK inhibitors may expand in the near future, as the role of SYK in several important processes within the CNS becomes more apparent to the scientific community.

1.4 Aims of the studies

The aims of the studies were to further elucidate the role of SYK in the pathobiology of AD and to investigate SYK as a possible target for the treatment of AD.

This thesis can be divided into 3 major parts:

1) The first aim was to determine whether SYK activation occurs in different animal models of AD, and in human AD specimen in relation to the β-amyloid and tau pathologies.

2) The second aim was to study the impact of SYK inhibition on tau and to delineate the molecular mechanism responsible for the effects of SYK on tau *in vitro*.

3) The third aim was to conduct an *in vivo* study to investigate the effects of a 12-week-long chronic pharmacological SYK inhibition on tau phosphorylation and tau accumulation, as well as neuroinflammation in Tg Tau P301S mice and determine whether some of the molecular pathways mediating the effects of SYK on tau (identified in aim 2) are also triggered following SYK inhibition *in vivo*.

2 Assessment of the activation pattern of SYK in 3 distinct mouse models of AD and human AD specimens

2.1 Introduction

SYK is a known to be involved in BCR and in some cases TCR-signaling (Geahlen 2014) and is therefore a regulator of the peripheral immune response. However, very little is known about the role of SYK in the CNS. The knowledge about the functional role of SYK in the CNS is limited to *in vitro* studies involving cultured microglia and macrophages (Combs et al. 1999; Combs et al. 2001; McDonald et al. 1997), as well as experiments involving neuronal cell cultures that suggested a SYK-dependent regulation of the early neuronal neuritogenesis (Angibaud et al. 2011; Richards et al. 2006). Our previous findings that highlighted SYK as a potential target for the treatment of AD (see 1.2.1 for further information), triggered us to investigate the cellular expression and activation of SYK in human AD brains and mouse models of AD, including Tg PS1/APPsw, Tg APPsw and Tg Tau P301S mice AD (see 1.1.7 for further information) in relation to the development of Aβ and tau pathologies. The data and conclusions presented in this chapter have been peer-reviewed and published (Schweig et al. 2017).

As described in the introduction of this thesis, the AD pathological hallmarks include extracellular amyloid deposits, intracellular tau aggregates and neuroinflammation. Various studies have emphasized the importance of the Aβ-induced neuroinflammation in the pathogenesis of AD and suggested that a therapeutic strategy can only be successful if it counteracts the neurotoxicity caused by neuroinflammation (McGeer and McGeer 2013; Prokop et al. 2013).

Aβ oligomers have been shown to trigger an inflammatory response in primary microglial and monocytic cells via an activation of the tyrosine kinases Lyn and SYK (Combs et al. 1999; McDonald et al. 1997). Importantly, SYK inhibition appears to prevent Aβ-mediated neurotoxicity



in vitro (Combs et al. 1999). A subsequent study also showed that SYK mediates the Aβ-induced cytokine production including tumor necrosis factor alpha (TNFα) and interleukin 1 beta (IL-1β) by activated microglia (Combs et al. 2001), suggesting that SYK may be a key kinase responsible for the pro-inflammatory activity of Aβ. Furthermore, SYK was suggested to play a role microglial phagocytosis (Hadas et al. 2012). Recruitment and activation of SYK can also be mediated by activation of TREM2 which is known to be expressed in microglia (Lanier and Bakker 2000). Several TREM2 variants are associated with an increased risk to develop AD and have been shown to alter AD pathology including Aβ deposition, tau hyperphosphorylation, neuroinflammation and synaptic loss in AD mouse models (Kober and Brett 2017).

The *in vitro* studies mentioned in the previous paragraph strongly suggest a role of SYK in microglia and the Aβ-induced immune response of the CNS. Moreover, we have shown previously that pharmacological inhibition of SYK appears to reduce Aβ production by decreasing BACE-1 expression *in vitro* in SH-SY5Y neuron-like cells (Paris et al. 2014). Therefore, one of our goals of this study was to investigate the possible expression of SYK in microglia *in vivo* and if the activation of SYK differs in activated versus non-activated microglia *in vivo*. Another part of this experiment was to analyze SYK activation in close proximity to Aβ-deposits observed in AD and mouse models thereof.

As stated in detail in the first chapter (1.1.4), there exist many different tau phosphorylation sites and various kinases responsible for tau hyperphosphorylation have been identified as contributors to tau pathogenesis. Tau tyrosine phosphorylation is considered an early pathological change in AD (Derkinderen et al. 2005b; Lebouvier et al. 2009). SYK and Src family kinases have been shown to phosphorylate tau directly at Y18 (Lebouvier et al. 2009; Nisbet et al. 2015). SYK has also been shown to phosphorylate microtubules which could have an effect on microtubule



polymerization or the interaction of signaling molecules with the microtubule network (Faruki et al. 2000). In addition, pharmacological SYK inhibition has been found to stabilize microtubules through dephosphorylation of microtubules and microtubule associated proteins (MAPs) (Yu et al. 2015). Our previous studies revealed that SYK regulates the activation of GSK3-β, one of the main tau kinase that phosphorylates tau at multiple sites present in neurofibrillary tangles (Paris et al. 2014). Furthermore, we have shown that pharmacological inhibition of SYK appears to reduce tau hyperphosphorylation both *in vitro* and *in vivo* (Paris et al. 2014).

Taking into consideration that SYK has been found to phosphorylate tau and the microtubule network, and regulate the activity of other tau kinases, we were prompted to also examine the expression and activation of SYK in neurons, especially in neurons displaying the tau pathology.

SYK activation can, at least in part, be regulated by phosphorylation (see 1.2 for more information). Since tyrosine phosphorylation in the kinase activation loop has been shown to be the best indicator for functional activation of SYK (Zhang et al. 2000), we therefore focused on the SYK phosphorylation site Y525/526 to monitor SYK activation and analyzed its association with AD pathological hallmarks in the present study. The Y525/526 phosphorylation sites are located within the activation loop of the SYK kinase domain which means, when SYK is catalytically active, it is phosphorylated at these sites. Many previous studies have used the Tyr525/526 phosphorylation site to monitor SYK activation (Feldman et al. 2008; Speich et al. 2008; Aouar et al. 2016; Satoh et al. 2012).

Our analysis of images, obtained by high-resolution confocal microscopy, revealed that SYK activation is increased in a subset of activated microglia and in dystrophic neurites around Aβ plaques of Tg APPsw and Tg PS1/APPsw mice. Interestingly, p-SYK (Y525/526) is also age-

dependently increased in neurons of Tg Tau P301S mice, presenting tau pathological lesions. The degree of co-localization between p-SYK and tau is largely dependent on the tau epitope investigated and differs between various p-tau epitopes and tau oligomers/conformers. The level of SYK activation, as measured by fluorescence intensity, correlates with the amount of pathological tau species detected. In addition, we show that SYK overexpression in a human neuroblastoma cell line (SH-SY5Y) results in increased total tau and tau phosphorylation levels at multiple epitopes suggesting the activation of SYK contributes to the formation of tau pathological lesions.

In summary, our results show that β-amyloid and tau pathological species both activate SYK *in vivo* and conversely, that SYK is involved in microglial activation, plays a role in the pathogenesis of dystrophic neurites (DNs) and contributes to the formation of pathological tau species therefore exacerbating the formation of AD pathological lesions. Interestingly, human AD brain sections exhibit the same pattern of SYK activation as the mouse models of β-amyloidosis and tauopathy combined. Human AD brain sections show an increase in p-SYK (Y525/526) levels in DNs around β-amyloid plaques and in neurons immunopositive for hyperphosphorylated tau (Y18) and pathological tau conformers (MC1), whereas brain sections from non-demented controls do not show any p-SYK increase. Altogether, these data suggest a crucial role of SYK in the pathobiology of AD and further highlight SYK as a promising therapeutic target in AD.



2.2 Materials & Methods

2.2.1 Animals

Tg PS1/APPsw, Tg APPsw, Tg Tau P301S and wild-type mice were generated and maintained in a C57BL/6 genetic background as previously described (Paris et al. 2014). All mice were maintained under specific pathogen free conditions in ventilated racks in the Association for Assessment and Accreditation of Laboratory Animal Care International (AAALAC) accredited vivarium of the Roskamp Institute. All experiments involving mice were reviewed and approved by the Institutional Animal Care and Use Committee of the Roskamp Institute before implementation and were conducted in compliance with the National Institutes of Health Guidelines for the Care and Use of Laboratory Animals.

2.2.2 Tissue Processing

All mice were humanely euthanatized and their brains were collected and fixed in 4% paraformaldehyde (PFA) for 48 hours. The method of euthanasia used follow the AVMA (American Veterinary Medical Association) guidelines for the euthanasia of animals. Briefly, mice were rendered unconscious through inhalation of 5% isoflurane in oxygen using a vaporizer and a gas chamber. While under anesthesia, after verifying the absence of reflexes, mice were euthanatized by exsanguination (blood was withdrawn from cardiac puncture).

Subsequently, the hemispheres were processed in a Sakura Tissue-Tek VIP (Leica Biosystems Inc., IL, USA) vacuum infiltration processor. Brains were then embedded in paraffin with the Sakura Tissue-Tek (Leica Biosystems Inc., IL, USA) and stored at 4˚C for two days for subsequent cutting with a Leica RM2235 microtome (Leica Biosystems Inc., IL, USA). All brains

were cut at a thickness of 12µm. Sagittal slices were mounted on glass slides and dried for 48 hours at 37˚C for subsequent immunofluorescence staining and confocal imaging.

2.2.3 Immunofluorescence

Paraffin sections were washed in two baths of histoclear (National Diagnostics, USA) and progressively rehydrated with ethanol gradients and phosphate buffered saline (PBS, Sigma Aldrich, MO, USA). Brain sections were subjected to antigen retrieval for seven minutes in citric acid buffer (pH 6) at 100˚C. All sections were treated with 0.05% Sudan Black in 70% ethanol to quench autofluorescence. Sections were then blocked in PBS containing 10% donkey serum (Abcam, MA, USA) for one hour. Sections were incubated in PBS containing 1% donkey serum and the respective panel of primary antibodies overnight at 4˚C. The following antibodies were used: CP13 (anti(α)-phospho-tau (p-tau) S202, 1:200, Dr. Peter Davies' Lab), MC1 (α-conformational tau, 1:200, Dr. Peter Davies' Lab), TOC1 for detection of tau oligomers (1:200, Dr. Lester Binder's Lab), PHF-1 (α -p-tau S396/404, 1:200, Dr. Peter Davies' Lab), 9G3 (α-p-tau Y18, 1:200, MediMabs Inc., QC, Canada), DA9 (α-total-tau (t-tau), 1:200, Dr. Peter Davies' Lab), α-BACE1 (1:200 Cell Signaling, MA, USA), α-sAPPβ with Swedish mutation (1:100 Immuno-Biological Laboratories Co, Ltd., Japan), α-Iba1 (1:300, Abcam, MA, USA), α-GFAP (1:5000, Aves Labs, OR, USA), α-p-SYK (Y525/526, 1:200, Cell Signaling, MA, USA). In addition to the α-p-SYK (Y525/526, 1:200, Cell Signaling, MA, USA), we used the α-p-SYK (Y525/526, 1:100, Abgent, CA, USA) and obtained similar results. After three washing steps in PBS for five minutes, sections were incubated in a solution containing PBS, 1% donkey serum and the respective panel of secondary antibodies for one hour in the dark at room temperature in a humidified chamber. The following secondary antibodies were used: donkey α-rabbit, α-goat, α-mouse conjugated to

Alexa 488, 568 and 647, respectively (1:500, Life technologies). After three washing steps in PBS for five minutes, sections were mounted in Fluoroshield with or without DAPI (Sigma Aldrich, MO, USA). All images were acquired using the confocal microscope LSM 800 (Carl Zeiss AG, Germany), the ZEN Blue 2.1 (Carl Zeiss AG, Germany) software and a 20x or 63x objective. The acquisition settings were kept the same for all genotypes within the same experiment.

For qualitative analysis of the p-SYK burden in Tg PS1/APPsw and Tg APPsw mice compared to age-matched WT littermates (n=6 for each genotype, equal amount of male and female), 116±13.5 (AVG±SEM) weeks of age were stained and analyzed as described above (Figure 3).

For qualitative analysis of the p-SYK burden in Tg Tau P301S mice compared to WT littermates, hippocampi and cortices of sixteen male and female mice ranging from 8 to 56 weeks of age were stained and analyzed as described above.

For the quantitative analysis of the p-SYK burden (Figure 5), 140 randomly-selected microscopic fields of four non-consecutive brain slices (containing the hippocampus) from six animals per genotype (equal number of male and female) were acquired. The area covered with the p-SYK immunopositive staining was quantified with Fiji (Schindelin et al. 2012) in microscopic fields containing Aβ plaques as well as in microscopic fields not containing Aβ deposits. The PS1/APPsw, APPsw and WT mice of the younger cohort were on average 45±0.3 (AVG±SEM) weeks old. The average age of the mice of the older cohort was 116±13.5 weeks (±SEM). The p-SYK burden of the transgenic mice was normalized to the level of p-SYK burden quantified in wild-type littermates of the respective age-group. As a negative control, primary antibodies were omitted to determine background and autofluorescence (not shown).

For the quantitative analysis of the co-localization of p-SYK and different tau epitopes (Figure 10) between 400 and 570 cortical fields (50,000 μm^{2-}per field) from four male Tg Tau P301S animals (average age 47±3.1 (SEM) weeks) were analyzed for each tau epitope. To quantify the percentage of the immunopositive neurons a total of 2546 microscopic fields and 21800 neurons were counted using the Zen Blue 2.1 software (Carl Zeiss AG, Germany).

The fluorescence intensities (Figure 11-Figure 15) of 30 to 40 neurons immunopositive for p-SYK, p-tau or both (co-localized) were determined for each tau epitope (total of 90 neurons per epitope) using Zen Blue 2.1 (Carl Zeiss AG, Germany). The male Tg Tau P301S mice (n=4) used for quantification were on average 47±3.1 weeks old (AVG±SEM).

In addition, the different immunostainings mentioned above were performed on paraffin-embedded tissue sections (10µm, dorsolateral frontal cortex) from a 67-year-old, male patient with AD (Braak VI) and a 102-year-old, male non-demented control that were provided by Dr. Ann McKee (Boston University, MA, USA). Institutional review board approval for brain donation was obtained through the Boston University Alzheimer's Disease Center (BUADC, Boston, MA, USA).

2.2.4 Cell Culture

SH-SY5Y cells were purchased from American Type Culture Collection (VA, USA). SH-SY5Y cells were grown in DMEM/F12 medium (Thermo Fisher Scientific, MA, USA) supplemented with 10% fetal bovine serum (Thermo Fisher Scientific, MA, USA), GlutaMAX and 1% penicillin/streptomycin/fungizone.

2.2.5 Generation of SYK overexpressing SH-SY5Y Cells

A human cDNA ORF Clone of the human SYK gene (NM_003177, transcript variant 1) was purchased from OriGene Technologies (MD, USA). The cDNA fragment encoding human SYK was amplified by PCR using PfuUltra II Fusion HS DNA polymerase (Agilent Genomics, CA, USA) and subcloned into the p3xFLAG-Myc-CMV™-26 Expression Vector (Sigma-Aldrich, MO, USA) to generate the pCMV-SYK-Flag plasmid. The entire reading frame of the plasmid was confirmed by DNA sequencing. SH-SY5Y cells were maintained in advanced DMEM/F-12 medium supplemented with 10% fetal bovine serum, 1% GlutaMAX, 1% penicillin/streptomycin (Thermo Fisher Scientific, MA, USA) and incubated in a humidified 5% CO_2 atmosphere at 37˚C. For stable transfection, SH-SY5Y cells were grown in 6-wells cell culture plates until reaching 70-80% confluence and transfected with 3 µg of empty pCMV vector (control cells) or pCMV-SYK-Flag plasmids per well using lipofectamine 2000 (Thermo Fisher Scientific, MA, USA). After 48 hours, the medium surrounding transfected cells was replaced with fresh medium containing 0.2mg/ml of G418 for selection. After 14 days of selection, G418 resistant cells were trypsinized and expanded. The expression efficiency of SYK was analyzed by Western blot using antibodies against SYK (4D10 SYK antibody, Santa Cruz Biotechnology, TX, USA) and the Flag tag (Sigma-Aldrich, MO, USA).

2.2.6 Immunoblotting

SH-SY5Y cells were cultured in 24-well-plates for 24 hours and subsequently lysed with mammalian protein extraction reagent (MPER, Thermo Fisher Scientific, MA, USA) containing Halt protease & phosphatase single use inhibitor/EDTA (Thermo Fisher Scientific, MA, USA) and 1 mM PMSF. Proteins of cell lysates were separated by 10% tris-glycine-SDS-PAGE using 1 mm

Criterion TGX gels (Bio-Rad Laboratories, CA, USA) and electro-transferred onto 0.2 µm PVDF membranes (Bio-Rad Laboratories, CA, USA). Membranes were blocked in TBS containing 5% non-fat dried milk for 1h and were hybridized with the primary antibody (α-SYK (4D10, 1:1000, Santa Cruz, TX, USA), α-p-tau S396/404 (PHF-1, 1:1000, Dr. Peter Davies' Lab), α-t-au (DA9, 1:1000, Dr. Peter Davies' Lab), α-p-tau Y18 (9G3, 1:1000, MediMabs Inc., QC, Canada,) overnight at 4˚C. Subsequently, the membranes were incubated for 1h in HRP-conjugated α-mouse secondary antibody (1:1000, Cell Signaling, MA, USA). Western blots were visualized using chemiluminescence (Super Signal West Femto Maxium Sensitity Substrate, Thermo Fisher Scientific, MA, USA). Signals were quantified using ChemiDoc XRS (Bio-Rad Laboratories, CA, USA) and densitometric analyses were performed using Quantity One (Bio-Rad Laboratories, CA, USA) image analysis software.

2.2.7 Statistical Analyses

The data were analyzed and plotted with GraphPad Prism (GraphPad Software, Inc., CA, USA). The Shapiro-Wilk test for normality was used to test for Gaussian distribution. Statistical significance was determined by either Kruskal-Wallis followed by Dunn's post-hoc test or the non-parametric Mann-Whitney test. All data are presented as mean ± the standard error of the mean (SEM) and $p<0.05$ was considered significant.

2.3 Results

2.3.1 Cellular localization of Syk activation in brains of Tg PS1/APPsw, Tg APPsw mice and WT mice

To investigate whether pathological SYK activation occurs in the brain of AD mouse models, we analyzed the brains of 116-week-old wild-type, Tg APPsw and Tg PS1/APPsw mice using high-resolution confocal microscopy and immunofluorescence. All transgenic mice (Figure 3b-e) exhibit an increased Iba-1 and GFAP reactivity compared to wild-type littermates (Figure 3a). Moreover, some of the activated amoeboid microglia that are observed in transgenic mice are also strongly positive for p-SYK (Figure 3b-d). In contrast, we did not detect any p-SYK immunoreactivity in astrocytes (Figure 3). In addition, we observed that p-SYK immunoreactivity is upregulated near Aβ plaques but neither co-localizes with microglia nor astrocytes suggesting that it could be of neuronal origin. (Figure 3e). We further investigated the cellular origin of these p-SYK accumulations by immunofluorescence staining and confocal microscopy (Figure 4).

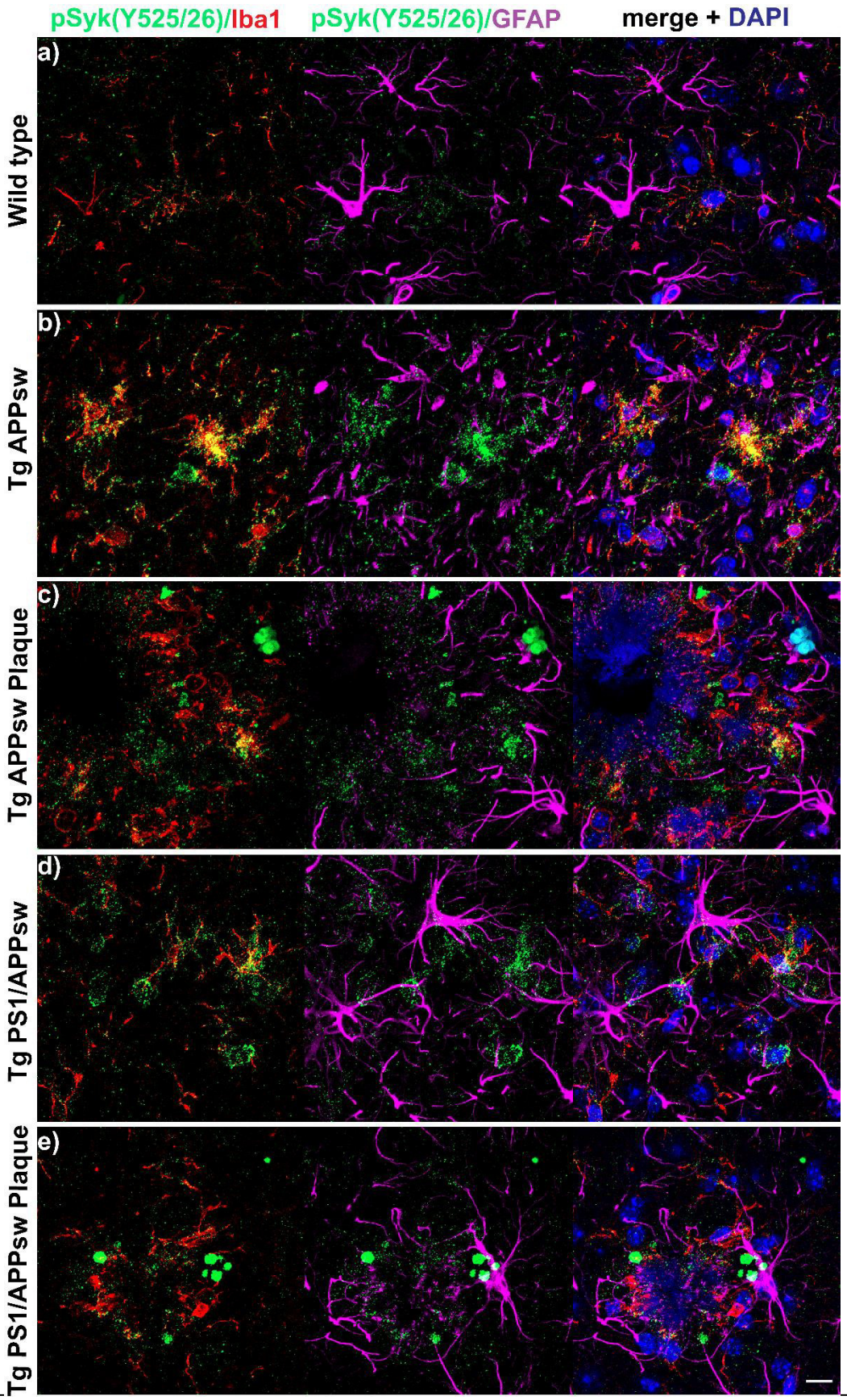
pSyk(Y525/26)/Iba1
pSyk(Y525/26)/GFAP
merge + DAPI
a)
Wild type
b)
Tg APPsw
c)
Tg APPsw Plaque
d)
Tg PS1/APPsw
e)
Tg PS1/APPsw Plaque

Figure 3: p-SYK is increased in activated microglia and non-glial cells associated with Aβ-plaques in Tg APPsw and Tg PS1/APPsw mice.

a) Spatial distribution and cellular localization of activated/phosphorylated SYK were investigated in the cortex of 116 ± 13.5-week-old (avg. ± SEM) wildtype mice (n = 6) by triple-immunostaining of p-SYK (Y525/526, green), microglia (Iba1, red) and astrocytes (GFAP, purple). Nuclei were stained with DAPI (blue). b) Syk activation in wild-type animals was compared to age-matched Tg APPsw (n = 6) (b-c) and Tg PS1/APPsw littermates (n = 6) (d-e). Plaque-associated cortical areas (c, e) were compared to non-plaque-associated areas (b, d). Qualitative image analysis of orthogonal projections and 3D-image analysis (not-shown) revealed an increased p-SYK burden in transgenic (b-e) compared to wild-type mice (a) and a co-localization of p-SYK and Iba1 but not GFAP in Aβ-overexpressing animals (b-d). Large, non-glial spherical accumulations of p-SYK were observed in plaque-associated areas (e). The scale bar represents 10 µm.

2.3.2 SYK activation in dystrophic neurites of Tg PS1/APPsw and Tg APPsw mice

To further characterize the cellular origin of p-SYK accumulations near Aβ plaques, we tested different markers of dystrophic neurites (BACE-1 and sAPPβ) (Sadleir et al. 2016) and found a strong co-localization between p-SYK and sAPPβ (Figure 4a) around Aβ deposits. The sAPPβ staining clearly reveals dystrophic swellings of neurites (Figure 4a) which are a known hallmark of AD. Most of the dystrophic neurites are positive for p-SYK (Figure 4a). Additionally, we found a strong co-localization between sAPPβ and BACE-1 (Figure 4b) which are often used as markers of dystrophic neurites. Both sAPPβ and BACE-1 exhibit circular accumulations near Aβ plaques (Figure 4b), highly reminiscent of the pattern observed for activated SYK.

In conclusion, activated SYK is not only found in microglia but also in neurons near Aβ deposits, particularly in dystrophic neurites of Tg APPsw and Tg PS1/APPsw mice supporting a possible role of SYK activation in the formation of dystrophic neurites. Dystrophic neurites are characterized by an accumulation of BACE-1 and sAPPβ (Sadleir et al. 2016) and our previous work (Paris et al. 2014) has shown that SYK regulates BACE-1 expression and sAPPβ levels suggesting that SYK upregulation in dystrophic neurites could contribute to the accumulation of BACE-1 and sAPPβ.

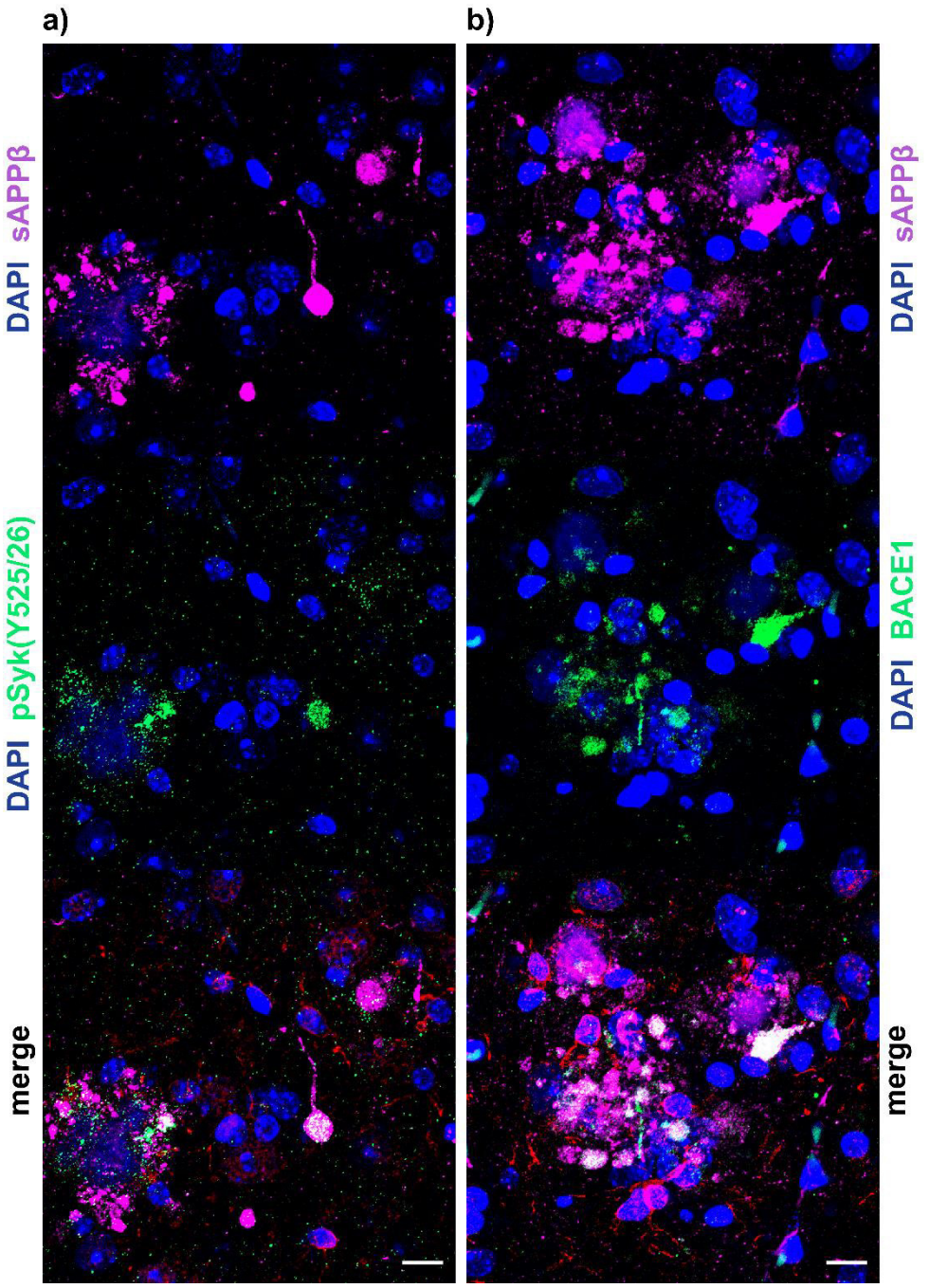

Figure 4: p-SYK is increased in dystrophic neurites of Aβ-overexpressing mice Representative confocal image depicting the cortex of 116.5 ± 13.5-week-old Tg PS1/APPsw mice stained for sAPPβ (purple), p-SYK (green, a), BACE1 (green, b), Iba-1 (red). Nuclei were stained with DAPI (blue). a) p-SYK was accumulated in dystrophic neurites positive for sAPPβ (a) and BACE1 (b). The scale bars represent 10 µm.

2.3.3 Age-dependent and amyloid deposition-dependent increase of SYK activation in Tg PS1/APPsw and Tg APPsw compared to WT mice

We also quantified the p-SYK burden in the cortex of Tg APPsw, Tg PS1/APPsw and wild-type (WT) littermates (Figure 3-Figure 4). Two different age-groups were investigated: younger animals, 45 weeks of age and older animals 116 weeks of age in average. In 45-week-old Tg APPsw mice, we did not observe significant β-amyloidosis (only three Aβ plaques were found in the cohort of mice analyzed) (data not shown) showing that, at that age, the Aβ plaque pathology is almost inexistent in these mice. We differentiated between microscopic fields containing Aβ deposits and microscopic fields not containing Aβ deposits for the quantification of the p-SYK burden in Tg PS1/APPsw and older Tg APPsw mice. 45-week-old Tg APPsw and Tg PS1/APPsw mice do not show any significant difference in p-SYK burden in fields without Aβ deposits compared to WT mice. The p-SYK burden of 45-week-old Tg APPsw mice is identical to that of the WT mice (100±6.76% compared to 80.85±11.77%; Figure 5a). The p-SYK burden in fields not containing Aβ plaques in Tg PS1/APPsw mice is not statistically significantly elevated (153.48±18.47%), compared to the WT littermates, although a trend for an increase was observed. As expected, 45-week-old Tg PS1/APPsw mice exhibited a significantly higher p-SYK burden in fields containing Aβ plaques (410.19±46.46%) compared to WT and Tg APPsw mice (Figure 5).

The analysis of the p-SYK burden in the cortex of older animals (average age: 116 weeks) revealed large differences between genotypes. The p-SYK burden of 116-week-old Tg APPsw (216.32±45.23%) mice in microscopic fields without plaques is not significantly increased compared to WT mice (100±7.78%) (Figure 5b). In contrast, microscopic fields of older Tg APPsw mice containing Aβ deposits exhibit a strong increase in p-SYK burden (799.95±130.19%) compared to age-matched WT mice. 116-week-old Tg PS1/APPsw mice also exhibit a statistically significant increase in p-SYK burden in microscopic fields that do not contain Aβ deposits

(458.1±109.68) compared to age-matched WT controls. In addition, a much greater p-SYK burden is found in Tg PS1/APPsw in microscopic fields containing Aβ deposits. In these fields, the p-SYK burden is increased by 1157.31±129.68% compared to WT littermates (Figure 5b).

In conclusion, our data show that the p-SYK burden is highly associated with Aβ plaques and increases with age in Tg PS1/APPsw and Tg APPsw mice whereas no activation of SYK is observed in the brain of WT littermates. The upregulation of SYK activation observed in the brains of Tg APPsw and Tg PS1/APPsw is mainly attributable to p-SYK accumulations in dystrophic neurites that are associated with Aβ plaques and increase with age and Aβ burden.

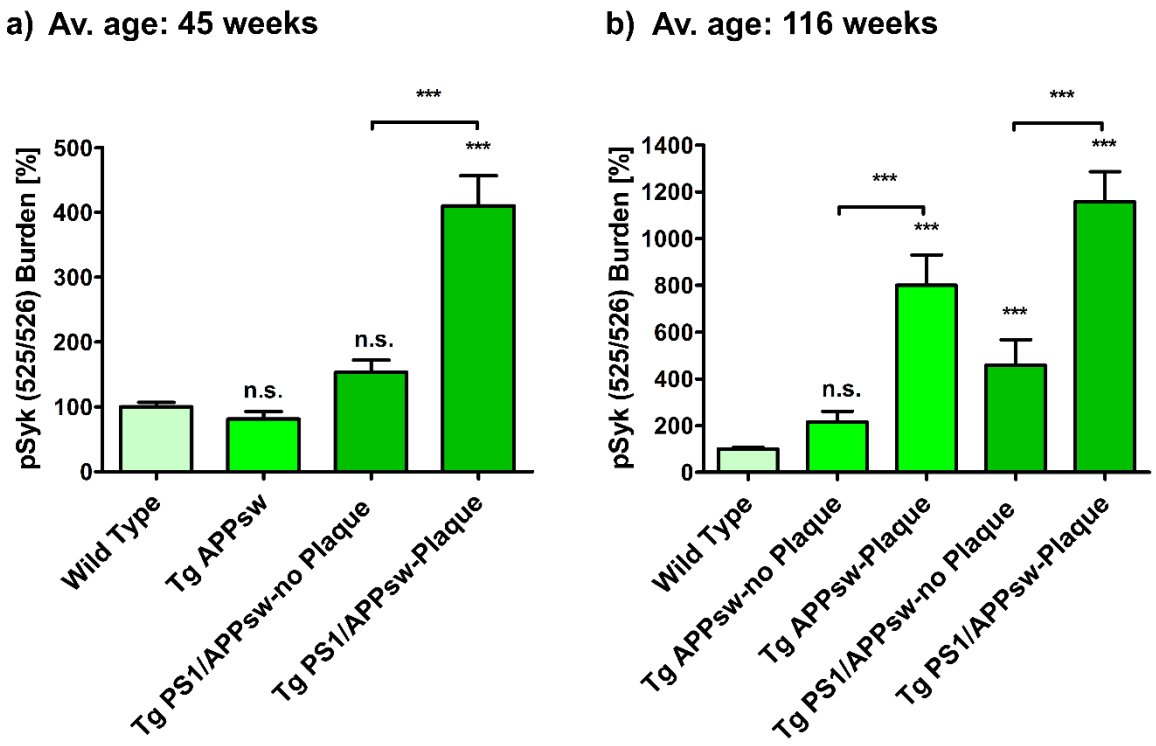

Figure 5: Cortical p-SYK burden is age-dependently increased in Aβ-overexpressing mice, particularly in microscopic fields containing Aβ deposits, compared to wild-type littermates
Cortical p-SYK burden (area covered) of immunofluorescence images (Figure 3) was quantified in 45 ± 0.3-weekold (avg. ± SEM) (a) and 116 ± 13.5-week-old (avg. ± SEM) (b) Tg APPsw (n = 6) and Tg PS1/APPsw mice (n = 6), compared and normalized to wildtype littermates (n = 6). Microscopic fields containing Aβ deposits were distinguished from microscopic fields not containing Aβ deposits as described in the materials and methods section. Kruskal-Wallis and post-hoc Dunn's multiple comparison test revealed a significant increase ($p < 0.001$) in p-SYK in fields containing Aβ deposits in younger Tg PS1/APPsw animals compared to age-matched wild-type littermates (a). p-SYK burden in older Tg APPsw and Tg PS1/APPsw mice was statistically significantly increased in cortical microscopic fields containing Aβ deposits compared to age-matched wildtype littermates ($p < 0.001$). Older Tg PS1/APPsw mice also exhibited a statistically significant p-SYK burden increase in microscopic fields not containing Aβ deposits ($p < 0.001$), whereas the p-SYK burden in Tg APPsw in microscopic fields not containing Aβ deposits was not statistically different from wild-type littermates ($P > 0.05$). Six animals per genotype were analyzed. Error bars represent SEM

2.3.4 Age-dependent and tau dependent SYK activation pattern in Tg Tau P301S mice

Having shown that Aβ-overexpressing mouse models of AD exhibit an increased SYK activation in microglia and dystrophic neurites, we investigated whether SYK activation also occurs in Tg Tau P301S mice (a pure model of tauopathy) using immunofluorescence and confocal microscopy. Hippocampal neurons of Tg Tau P301S mice exhibit a high level of tau hyperphosphorylation (Figure 6b) as well as an accumulation of pathogenic tau conformers (MC1, not shown) compared to WT littermates (Figure 6a). Most importantly, pathological tau species clearly co-localize with p-SYK (Y525/526) in hippocampal neurons (Figure 6b). The p-SYK burden is particularly prominent in hippocampal neurons of Tg Tau P301S mice (Figure 6b) whereas WT littermates do not exhibit any p-SYK immunoreactivity in the hippocampus (Figure 6a).

Cortical neurons of Tg Tau P301S mice also exhibit an increased level of tau hyperphosphorylation (Figure 7b) compared to wild-type littermates (Figure 7a). We observed a co-localization between p-SYK and p-tau (S202) immunoreactivities in cortical neurons. Interestingly, we also observed neurons that are singly immunopositive for tau or for p-SYK. We addressed this observation by performing additional analyses (Figure 10-Figure 17).

We also analyzed the temporal changes of p-SYK and tau levels in hippocampi and cortices of Tg Tau P301S mice between the age of 8 and 56 weeks (Figure 8-Figure 9). WT mice do not exhibit any detectable tau phosphorylation (Figure 8f) or tau oligomerization at any age (not shown). We then focused on the dentate gyrus of the hippocampus and found an age-dependent increase of tau phosphorylation (Figure 8, S202, left panels) in Tg Tau P301S mice. Tau phosphorylation at S202 in the dentate gyrus was already detectable in 8-week-old Tg Tau P301S mice, however, p-SYK immunoreactivity was not observed. Neurons immunopositive for p-SYK (Y525/526) and p-tau (S202) or tau conformers (MC1, not shown) were observed in the dentate gyrus of 42-week-old

Tg Tau P301S mice (Figure 8d). The neuronal p-SYK burden also increases with age in Tg Tau P301S mice and is mainly restricted to the neuronal cell body (Figure 8). Interestingly, microglia and neurites did not exhibit activated SYK in the hippocampus of tau P301S mice (Figure 8). Abnormal SYK activation seems to follow tau hyperphosphorylation (S202) in the hippocampus of Tg P301S mice (Figure 8), as well as the formation of MC1-tau pathological conformers (data not shown here but MC1 and p-SYK co-localization were quantified below).

Cortical neurons of Tg Tau P301S mice also show an increase in tau hyperphosphorylation and p-SYK with age (Figure 9). Interestingly, the onset of abnormal SYK activation occurs earlier (16 weeks of age) in the cortex than in the hippocampus (Figure 9b compared to Figure 8d). In conclusion, both p-SYK and tau pathology in Tg Tau P301S mice increase with age but the progression is different in the hippocampus and the cortex. Many cortical neurons exhibit a co-localization of p-SYK and p-tau (S202) (Figure 9b-c, e) but as mentioned earlier, there are also neurons that are singly immunopositive for p-SYK or p-tau.

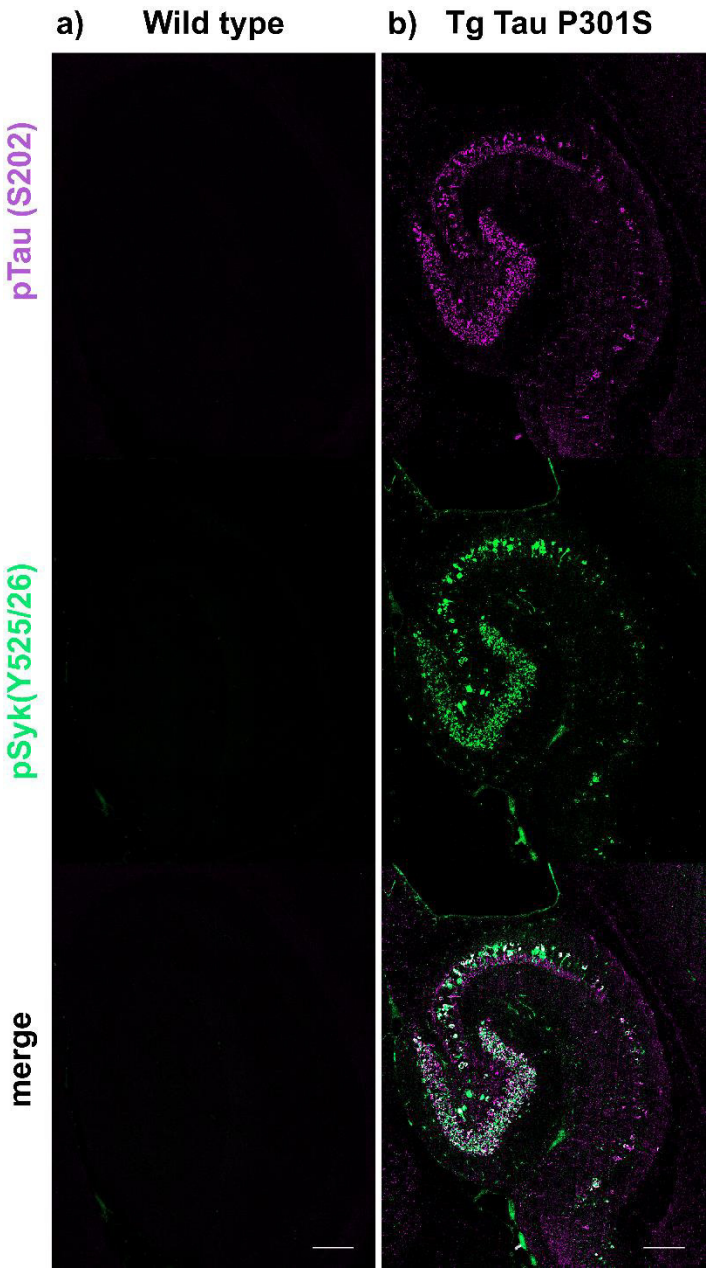

Figure 6: p-SYK is increased in hippocampal neurons of Tg Tau P301S mice compared to wild-type littermates
Representative confocal image depicting 56 week-old male Tg Tau P301S and wild-type mice stained with antibodies against p-tau (S202, purple) and p-SYK (Y525/526, green). a) Wild-type mice did not exhibit any tau phosphorylation nor Syk activation in their hippocampi. b) tau-overexpressing Tg Tau P301S mice exhibited a prominent tau phosphorylation at S202 that co-localized with SYK activation in hippocampal neurons. The scale bars represent 200 µm.

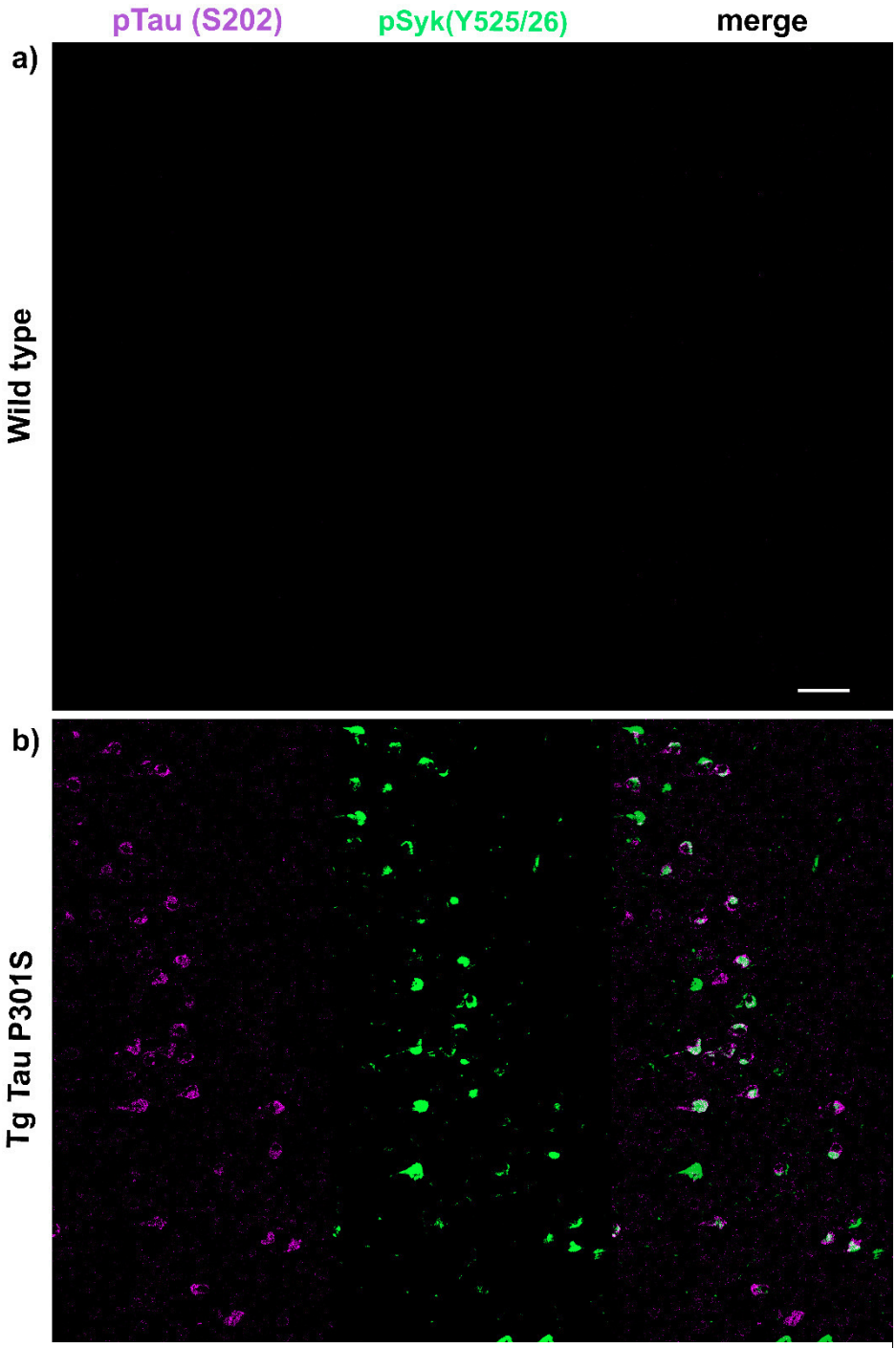

Figure 7: p-SYK is increased in cortical neurons of Tg Tau P301S mice compared to wild-type littermates

Representative confocal image depicting 56 week-old male Tg Tau P301S and wild-type mice stained with antibodies against p-tau (S202, purple), p-SYK (Y525/526, green). a) wild-type mice did not exhibit any tau phosphorylation nor Syk activation in their cortices. b) tau-overexpressing Tg Tau P301S mice exhibited a prominent tau phosphorylation at S202 that co-localized with Syk activation in cortical neurons. The scale bars represent 100 µm

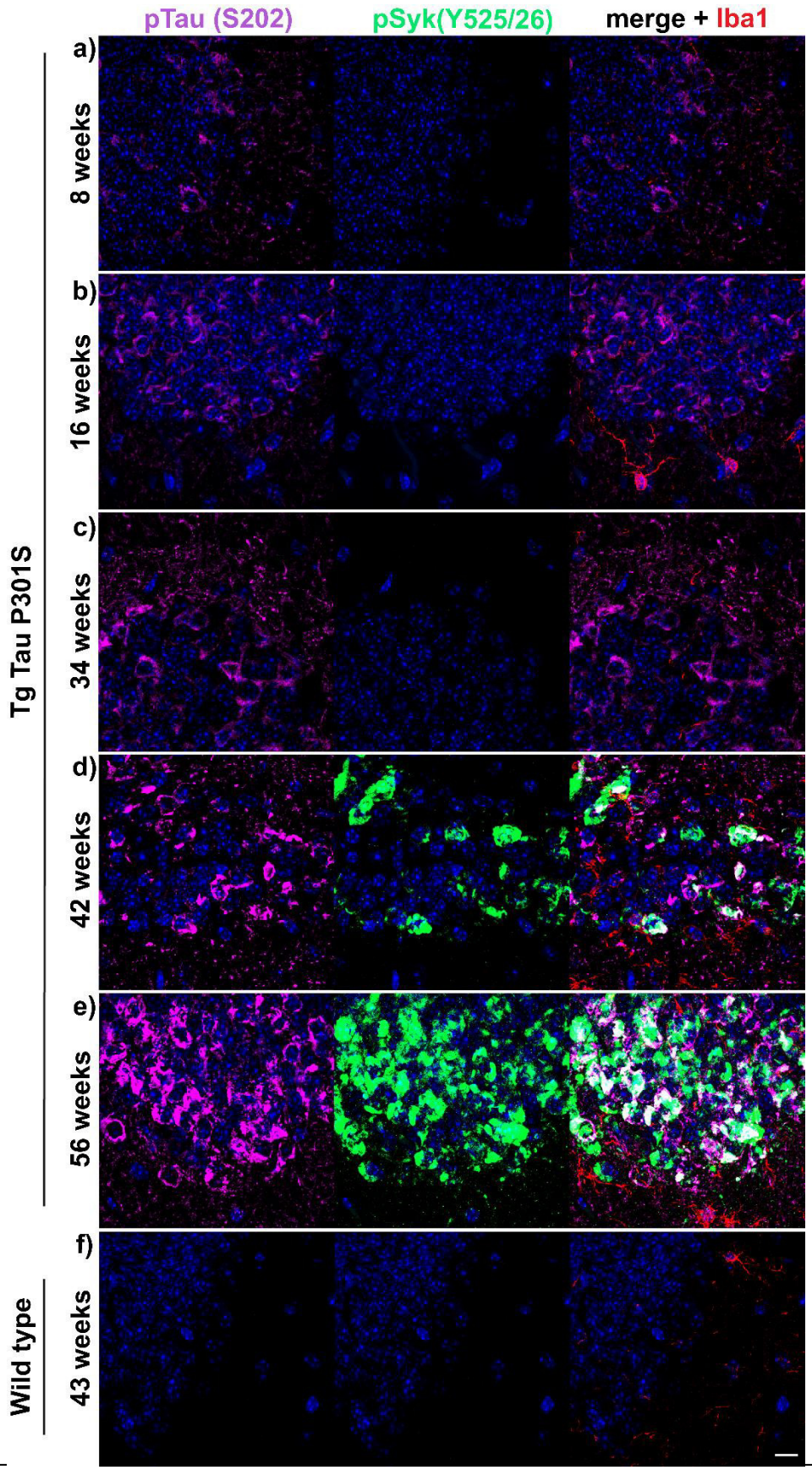
pTau (S202)
pSyk(Y525/26)
merge + Iba1
a)
8 weeks
b)
16 weeks
c)
34 weeks
d)
42 weeks
e)
56 weeks
f)
43 weeks
Tg Tau P301S
Wild type

Figure 8: p-SYK is increased age-dependently in hippocampal neurons of Tg Tau P301S mice compared to wild-type littermates

Representative confocal image depicting Tg Tau P301S and wild-type mice (n = 16) stained with antibodies against p-tau (S202, purple), p-SYK (Y525/526, green) and Iba-1 (red). Nuclei were stained with DAPI. a-e) tau-overexpressing Tg Tau P301S mice exhibited a prominent tau phosphorylation (S202) that increased with age and co-localized with Syk activation in hippocampal neurons. f) Wild-type mice did not exhibit any tau phosphorylation nor SYK activation in their hippocampi. The scale bar represents 10 μm.

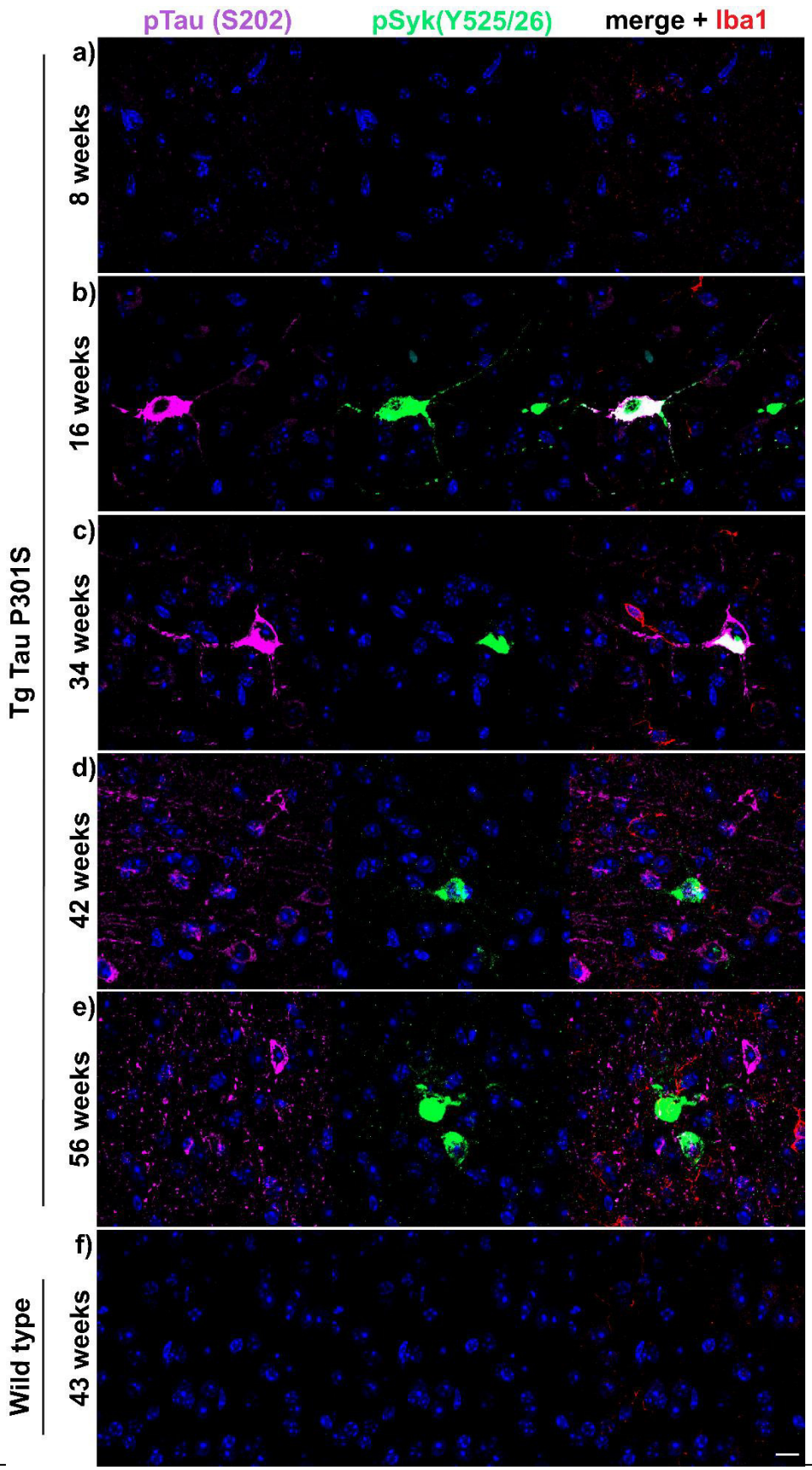
pTau (S202)
pSyk(Y525/26)
merge + Iba1
a)
8 weeks
b)
16 weeks
c)
34 weeks
d)
42 weeks
e)
56 weeks
f)
43 weeks
Tg Tau P301S
Wild type

Figure 9: p-SYK is increased age-dependently in cortical neurons of Tg Tau P301S mice compared to wild-type littermates

Representative confocal image depicting Tg Tau P301S and wild-type mice (n = 16) stained with antibodies against p-tau (S202, purple), p-SYK (Y525/526, green) and Iba-1 (red). Nuclei were stained with DAPI. a-e) tau-overexpressing Tg Tau P301S mice exhibited a prominent tau phosphorylation (S202) that increased with age and partially co-localized with Syk activation in cortical neurons. f) Wild-type mice did not exhibit any tau phosphorylation nor Syk activation in their cortices. The scale bar represents 10 μm.

2.3.5 Tau species-dependent SYK activation

We further quantified the number of neurons that are singly p-SYK immunopositive, singly immunopositive for tau pathogenic species and neurons immunopositive for both p-SYK and tau pathogenic species in the cortex of 47-week-old Tg Tau P301S mice (Figure 10). We calculated the percentages of neurons singly immunopositive for either p-SYK, pathogenic tau species or neurons immunopositive for both. The sum of all cortical neurons counted was standardized to 100% including neurons positive for p-SYK and the respective tau epitope and neurons immunopositive for both. For all the tau epitopes tested, we found that only a small fraction of the neurons is singly immunopositive for p-SYK (9.7±4.4% (p-tau, Y18); 2.5±1.2% (p-tau, S202); 9.2±1.6% (MC1 pathogenic tau conformers); 9.6±6.3% (p-tau, S396/404); 4.8±2.0% (TOC1 (tau oligomers)). Interestingly, a larger percentage of neurons is immuno-reactive for both p-SYK and tau pathogenic species (44.7±8.6% (MC1); 39.7±12.4% p-tau Y18; 22.5±18.6% (PHF-1, p-tau S396/404); 12.4±8.1% (TOC1, tau oligomers) but only 5.7±2.2% for p-tau (S202)). The neurons singly immunopositive for tau complement these observations with relative values of 46.1±8.2% (MC1), 50.6±16.3% (Y18), 67.9±24.9% (S396/404), 82.8±10.1% (TOC1), and 91.8±3.2% (S202) (Figure 10). The differences in relative co-localization between p-SYK and specific tau pathologic species suggest that specific pathogenic forms of tau may have a different impact on SYK activation or that SYK activation may contribute to the formation of specific tau pathogenic species (Figure 10). We therefore subsequently measured the fluorescent intensities of p-SYK and of the different tau epitopes to determine whether the level of SYK activation correlates with the amount of specific tau pathogenic species. In general, we found that neurons that exhibit a high level of p-SYK immunoreactivity also demonstrate a higher level of tau pathogenic species whereas neurons that are weakly immunopositive for p-SYK show less tau pathology (Figure 11-

Figure 15). In addition, neurons that are singly immunopositive for tau pathogenic species (including hyperphosphorylated tau and misfolded tau) show also less intense tau pathologies, as measured by fluorescent intensities, than neurons that are displaying both p-SYK and tau pathology, further supporting a role of SYK in the formation of tau pathogenic species. For instance, the level of pathogenic tau conformers (MC1) is significantly increased in neurons that are also strongly immunopositive for p-SYK compared to neurons that are singly immunopositive for MC1 (Figure 11d, $p<0.05$). Interestingly, the level of p-SYK is also significantly increased in neurons that display an accumulation of MC1 pathogenic conformers compared to neurons that are singly immunopositive for p-SYK (Figure 11e, $p<0.01$). These data suggest that pathogenic tau conformers and SYK activation may promote each other. We found that tau phosphorylation at Y18 is significantly increased in neurons that are also immunopositive for p-SYK (Figure 12d, $p<0.05$) which is consistent with previous data showing that *in vitro* SYK can phosphorylates tau at Y18. We have previously shown that SYK positively regulates GSK3-β activity *in vitro*. It is therefore consistent with our observation that the GSK3-β-dependent phospho-tau epitope (S396/404, PHF-1) is also increased in neurons that display SYK activation (Figure 13d, $p<0.0001$). The p-SYK level, however, is not statistically significantly increased in neurons that are immunopositive for both PHF-1 and p-SYK compared to neurons that are singly immunopositive for p-SYK suggesting that PHF-1 phosphorylated tau species do not induce SYK activation (Figure 13e). Similar observations were obtained for tau oligomers (Figure 14, TOC1) and tau species phosphorylated at S202 (Figure 15, CP13). Altogether, these data suggest that only certain pathogenic forms of tau (MC1, Y18) promote SYK activation, whereas SYK activation appears to directly induce tau phosphorylation at Y18 and to indirectly regulate tau phosphorylation at multiple epitopes (S396/404, S202) as well as tau misfolding (MC1, TOC1).

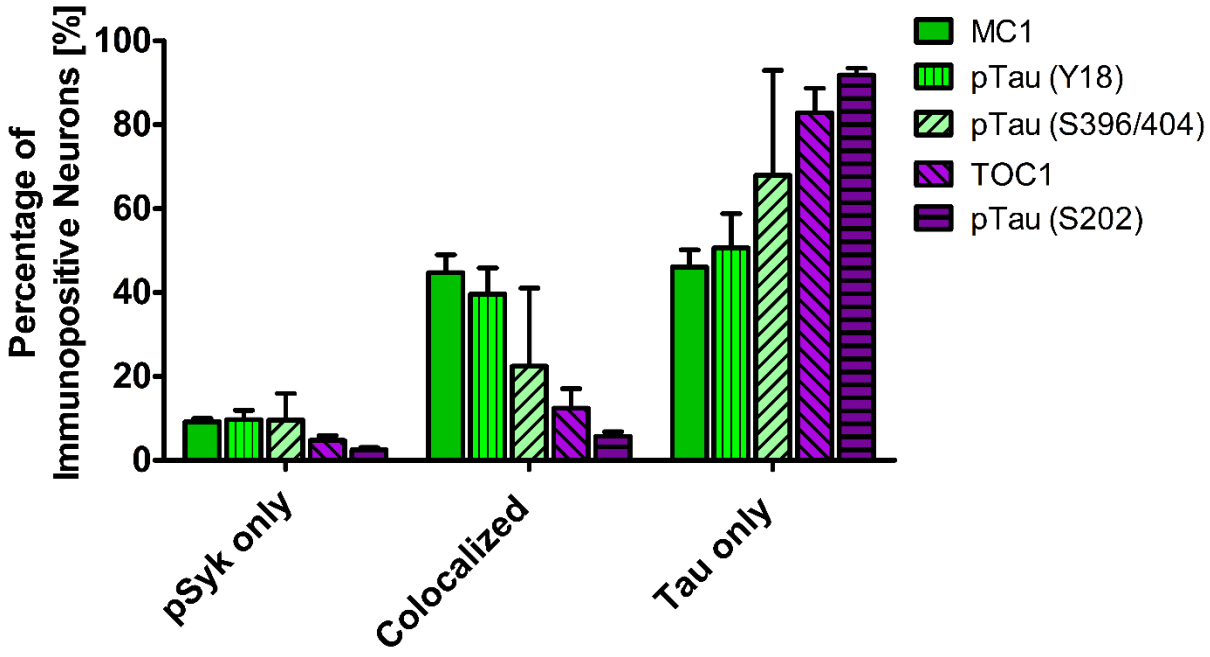

Figure 10: The degree of co-localization of p-SYK and tau differs for various tau epitopes
Sections from Tg Tau P301S mice (n = 4, 47 ± 3.1-week-old) were stained with antibodies against p-tau (S202, S396/404, Y18), tau oligomers (TOC1) or tau conformers (MC1) and p-SYK (Y525/526, green). The cortices were divided in ROIs (each at a size of 50,000µm2) and neurons singly immunopositive for p-SYK, singly immuno-reactive for the respective tau epitope and the neurons immunopositive for both p-SYK and the respective tau epitope (co-localized) were counted and the percentages of each neuronal fraction calculated using Zen Blue 2.1 (Zeiss) and Excel (MS Office), respectively. In average, 509 cortical fields were analyzed for each epitope (total of 21,800 neurons counted). The percentage of neurons singly immunopositive for p-SYK was at a similar level for all tau epitopes investigated (p-SYK only). MC1 and p-tau Y18 show the highest co-localization with p-SYK whereas the incidence of neurons immunopositive for both p-SYK and tau oligomers (TOC1) or p-tau S202 was much lower (co-localized fraction). The error bars represent SEM.

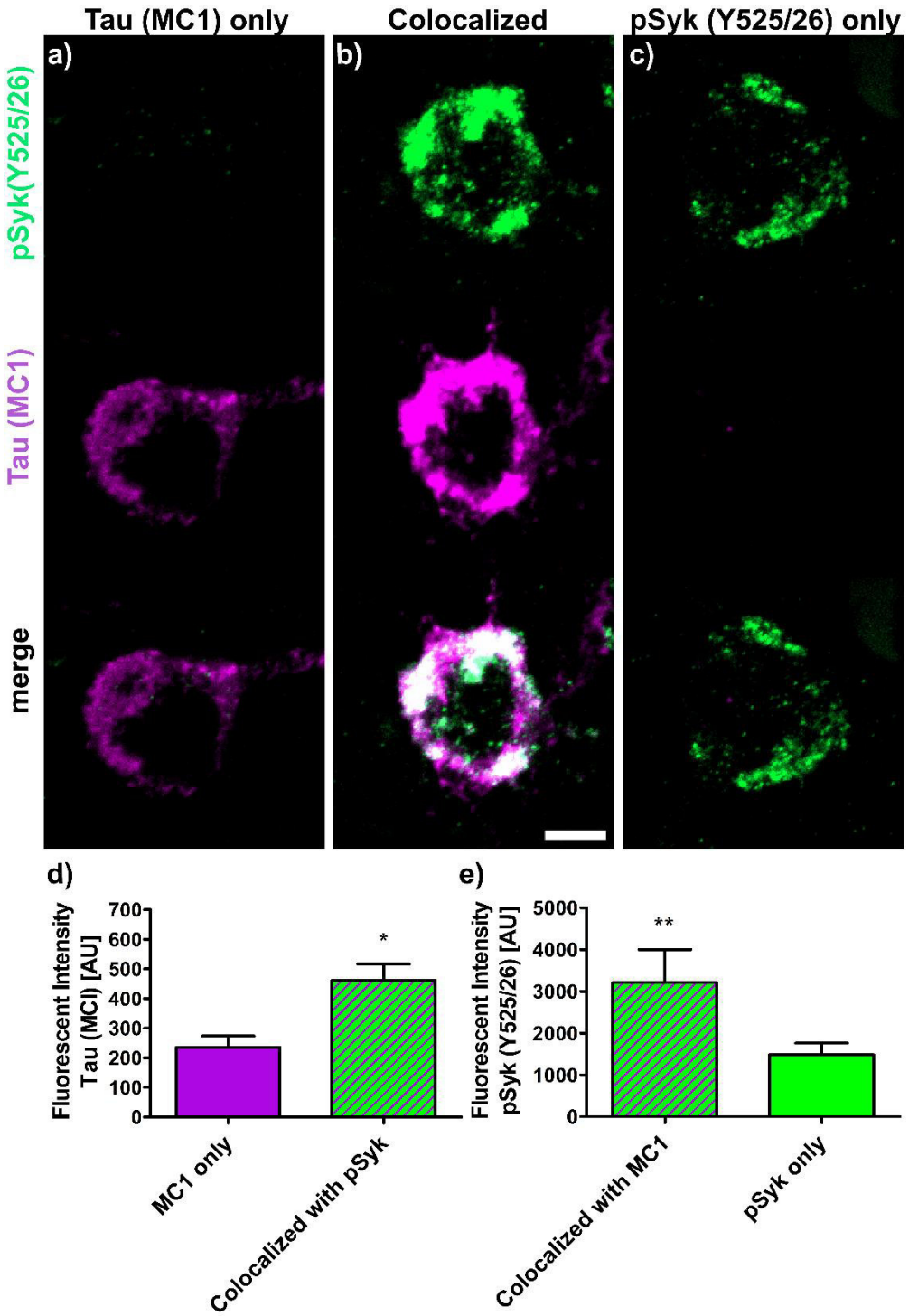
Tau (MC1) only
Colocalized
pSyk (Y525/26) only
a)
b)
c)
pSyk(Y525/26)
Tau (MC1)
merge
d)
Fluorescent Intensity Tau (MCI) [AU]
700
600
500
400
300
200
100
0
*
MC1 only
Colocalized with pSyk
e)
Fluorescent Intensity pSyk (Y525/26) [AU]
5000
4000
3000
2000
1000
0
**
Colocalized with MC1
pSyk only

Figure 11: The amount of MC1 tau conformers and p-SYK (Y525/526) levels cross-influence each other

Sections from Tg Tau P301S (n = 4, 47 ± 3.1-week-old) were stained with antibodies against tau conformers (MC1, purple) and p-SYK (Y525/526, green). Fluorescent intensities of MC1 and p-SYK were measured using Zen Blue 2.1 (Zeiss). Three different neuronal fractions were differentiated: a) neurons singly immunopositive for MC1, (b) neurons singly immunopositive for p-SYK and (c) neurons immunopositive for both MC1 and p-SYK (co-localized). d) Fluorescent intensities of MC1 were compared between neurons singly MC1 positive (purple) and neurons exhibiting a co-localization of MC1 and p-SYK (purple-green-striped). Two-tailed Mann–Whitney test revealed a significant increase ($p < 0.05$) of MC1 fluorescent intensity in neurons exhibiting a co-localization of MC1 and p-SYK compared to neurons singly immunopositive for MC1. e) Fluorescent intensities of p-SYK were compared between neurons singly immunopositive for p-SYK (green) and neurons that show an immunoreactivity for both p-SYK and MC1 (purple-green-striped). Two-tailed Mann–Whitney test revealed a significant increase ($p < 0.01$) of p-SYK fluorescent intensity in neurons immuno-reactive for both p-SYK and MC1 compared neurons that are singly immunopositive for p-SYK. The scale bar represents 10 µm. The error bars represent SEM.

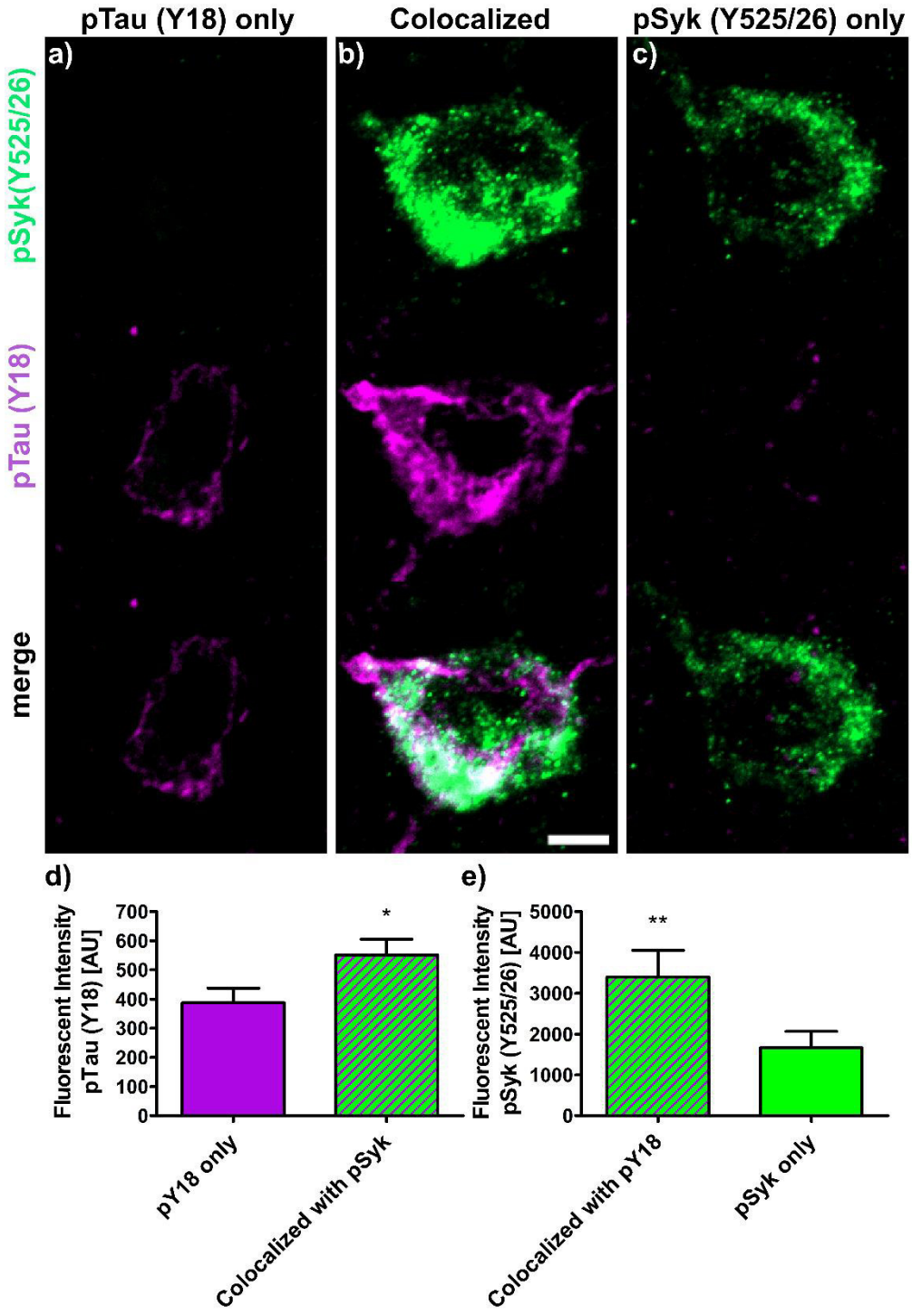
pTau (Y18) only
Colocalized
pSyk (Y525/26) only
a)
b)
c)
pSyk(Y525/26)
pTau (Y18)
merge
d)
Fluorescent Intensity pTau (Y18) [AU]
700
600
500
400
300
200
100
0
*
pY18 only
Colocalized with pSyk
e)
Fluorescent Intensity pSyk (Y525/26) [AU]
5000
4000
3000
2000
1000
0
**
Colocalized with pY18
pSyk only

Figure 12: tau phosphorylation at Y18 and Syk activation (Y525/526) cross-influence each other

Sections from Tg Tau P301S (n = 4, 47 ± 3.1-weekold) were stained with antibodies against phosphorylated tau (Y18, purple) and p-SYK (Y525/526, green). Fluorescent intensities of p-tau (pY18) and p-SYK were measured using Zen Blue 2.1 (Zeiss). Three different neuronal fractions were differentiated: a) neurons singly immunopositive for pY18, (b) neurons singly immunopositive for p-SYK and (c) neurons immunopositive for both (co-localized). d) Fluorescent intensities of pY18 tau were compared between singly pY18 immunopositive and the double immunopositive neurons (co-localized, purple-green-striped). Two-tailed Mann–Whitney test revealed a significant increase ($p < 0.05$) of pY18 fluorescent intensity for neurons exhibiting a co-localization compared to the neurons singly immunopositive for pY18 tau. e) Fluorescent intensities of p-SYK were compared between singly p-SYK immunopositive neurons (green) and double immunopositive neurons for p-SYK and pY18 tau (purple-green-striped). Two-tailed Mann–Whitney test revealed a significant increase ($p < 0.01$) of p-SYK fluorescent intensity in neurons double immunopositive for p-SYK and pY18 tau compared to singly p-SYK immunopositive neurons. The scale bar represents 10 µm. The error bars represent SEM.

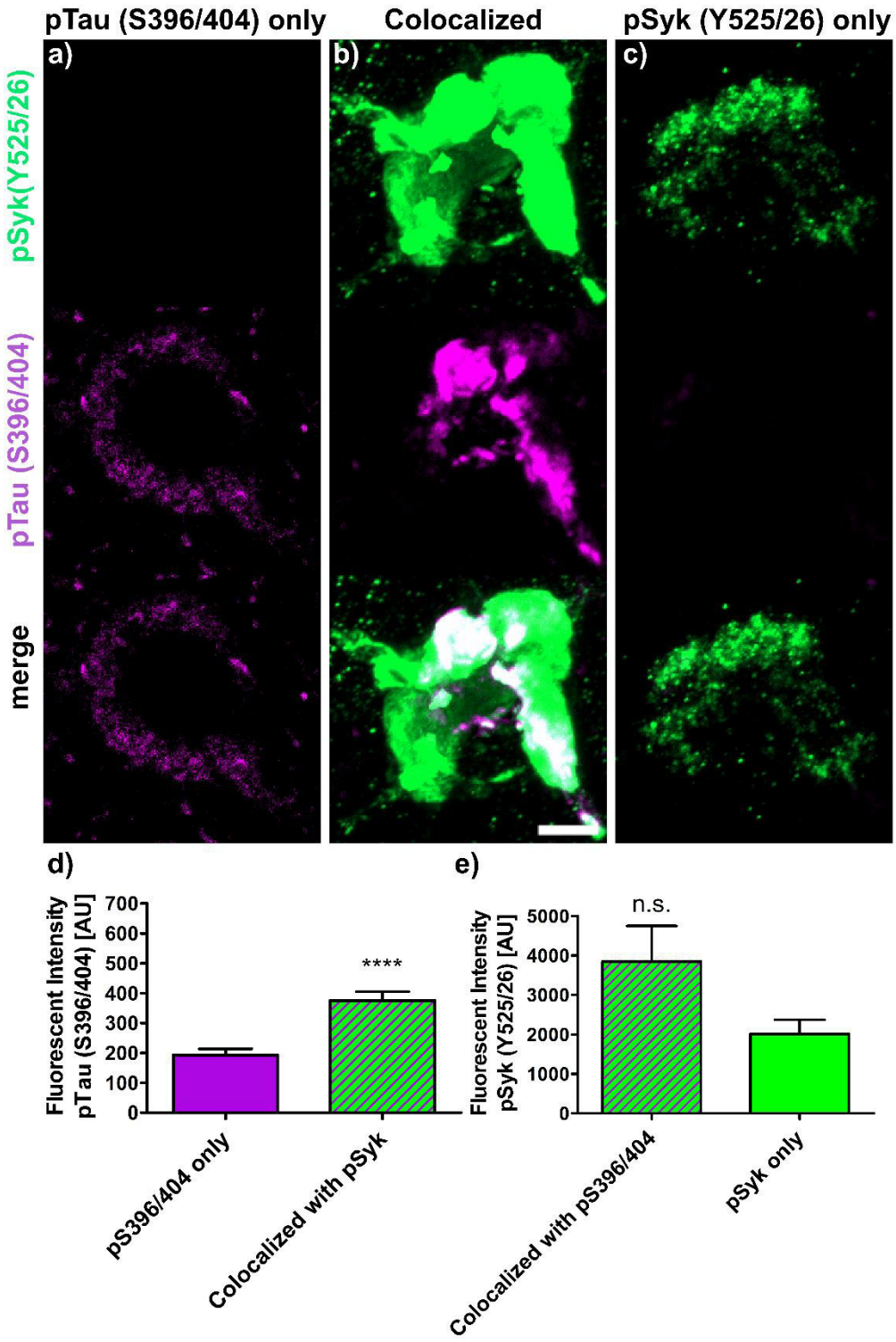
pTau (S396/404) only
Colocalized
pSyk (Y525/26) only
a)
b)
c)
pSyk(Y525/26)
pTau (S396/404)
merge
d)
e)
Fluorescent Intensity pTau (S396/404) [AU]
700
600
500
400
300
200
100
0
****
pS396/404 only
Colocalized with pSyk
Fluorescent Intensity pSyk (Y525/26) [AU]
5000
4000
3000
2000
1000
0
n.s.
Colocalized with pS396/404
pSyk only

Figure 13: Syk activation (p-SYK (Y525/526) influences the level of tau phosphorylation at S396/404

Sections from Tg Tau P301S (n = 4, 47 ± 3.1-week-old) were stained with antibodies against phosphorylated tau (S396/404, purple) and p-SYK (Y525/526, green). Fluorescent intensities of p-tau (pS396/404) and p-SYK were measured using Zen Blue 2.1 (Zeiss). Three different neuronal fractions were differentiated: a) neurons singly immunopositive for pS396/404 tau, (b) neurons singly immunopositive for p-SYK and (c) neurons immunopositive for both (co-localized). d) Fluorescent intensities of pS396/404 tau were compared between neurons singly immunopositive for pS396/404 (purple) and the neurons exhibiting a co-localization of pS396/404 and p-SYK (purple-green-striped). Two-tailed Mann–Whitney test revealed a significant increase ($p < 0.0001$) of pS396/404 fluorescent intensity in the neurons exhibiting a co-localization compared to neurons singly immunopositive for pS396/404 tau. e) Fluorescent intensities of p-SYK were compared between singly p-SYK immunopositive neurons (green) and neurons exhibiting a co-localization of p-SYK and pS396/404 tau (purple-green-striped). Two-tailed Mann–Whitney test revealed no significant change of p-SYK fluorescent intensity in neurons exhibiting a co-localization compared to singly p-SYK immunopositive neurons. The scale bar represents 10 µm. The error bars represent SEM.

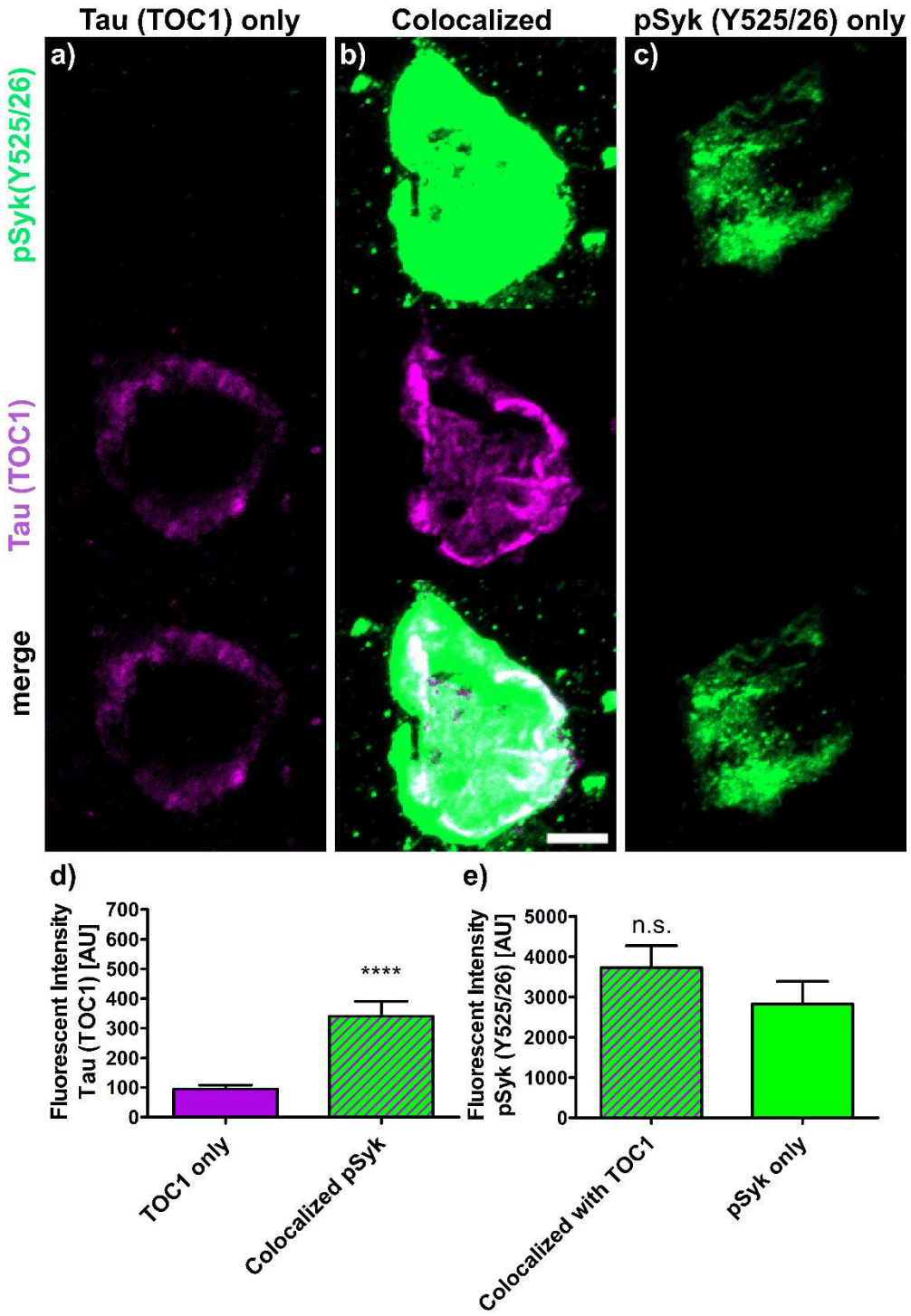
Tau (TOC1) only
Colocalized
pSyk (Y525/26) only
a)
b)
c)
pSyk(Y525/26)
Tau (TOC1)
merge
d)
Fluorescent Intensity Tau (TOC1) [AU]
700
600
500
400
300
200
100
0
****
TOC1 only
Colocalized pSyk
e)
Fluorescent Intensity pSyk (Y525/26) [AU]
5000
4000
3000
2000
1000
0
n.s.
Colocalized with TOC1
pSyk only

Figure 14: SYK activation (Y525/526) influences the level of tau oligomerization (TOC1)

Sections from Tg Tau P301S (n = 4, 47 ± 3.1-week-old) stained with antibodies against tau oligomers (TOC1, purple) and p-SYK (Y525/526, green). Fluorescent intensities of oligomerized tau (TOC1) and p-SYK were measured using Zen Blue 2.1 (Zeiss). Three different neuronal fractions were differentiated: a) neurons singly immunopositive for TOC1, (b) neurons singly immunopositive for p-SYK and (c) neurons immunopositive for both (co-localized). d) Fluorescent intensities of TOC1 were compared between neurons singly immunopositive for TOC1 (purple) and neurons exhibiting a co-localization of p-SYK and TOC1 (purple-green-striped). Two-tailed Mann–Whitney test revealed a significant increase ($p < 0.0001$) of TOC1 fluorescent intensity in neurons exhibiting a co-localization with p-SYK compared to singly TOC1 immunopositive neurons. e) Fluorescent intensities of p-SYK were compared between neurons singly immunopositive for p-SYK (green) and neurons exhibiting a co-localization pf TOC1 and p-SYK (purple-green-striped). Two-tailed Mann–Whitney test revealed no significant change of p-SYK fluorescent intensity in neurons exhibiting a co-localization compared to the singly p-SYK immunopositive neurons. The scale bar represents 10 µm. The error bars represent SEM.

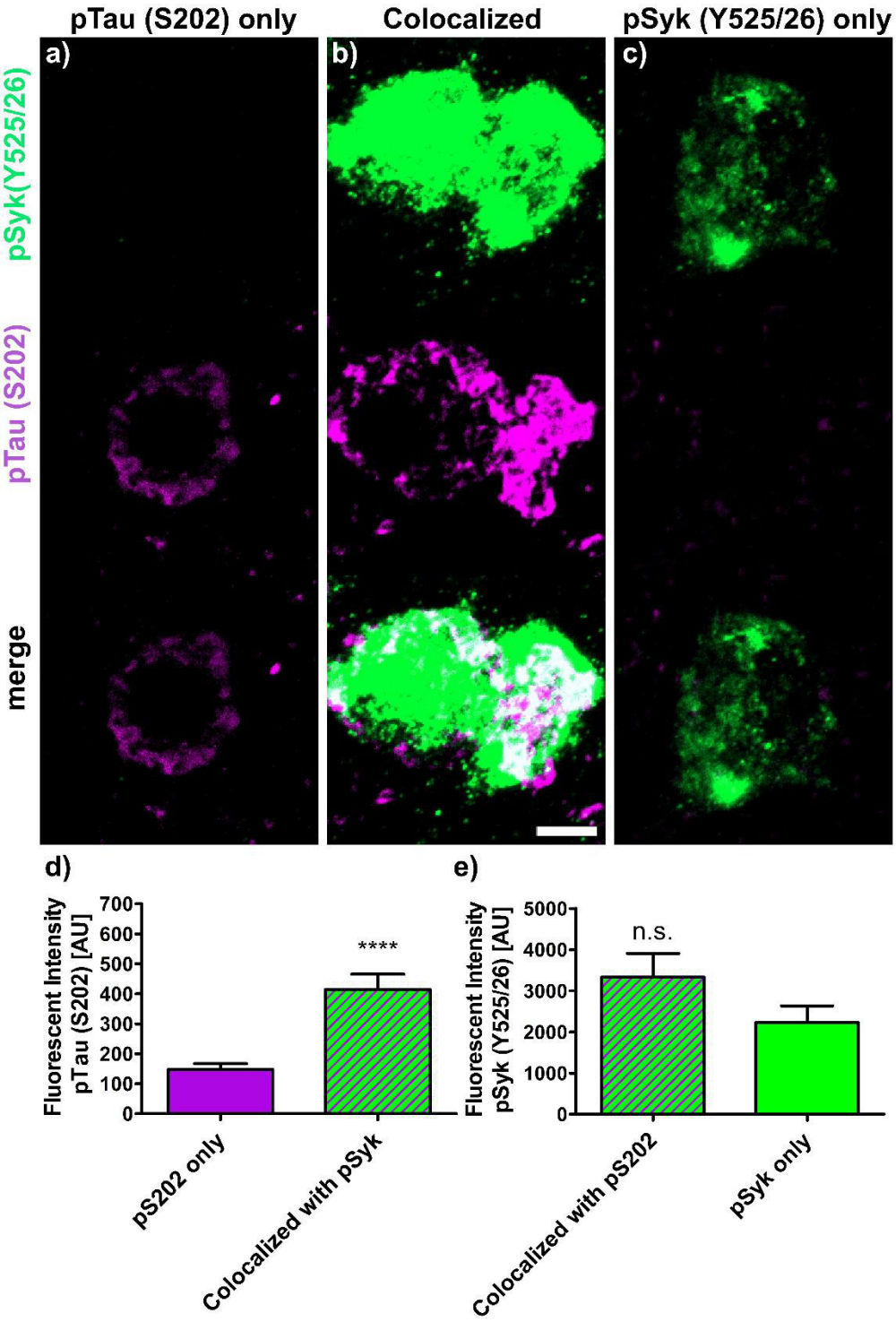
pTau (S202) only
Colocalized
pSyk (Y525/26) only
a)
b)
c)
pSyk(Y525/26)
pTau (S202)
merge
d)
e)
Fluorescent Intensity pTau (S202) [AU]
700
600
500
400
300
200
100
0
****
pS202 only
Colocalized with pSyk
Fluorescent Intensity pSyk (Y525/26) [AU]
5000
4000
3000
2000
1000
0
n.s.
Colocalized with pS202
pSyk only

⬆ Figure 15: Syk activation (Y525/526) influences the level of tau phosphorylation at S202

Sections from Tg Tau P301S (n = 4, 47 ± 3.1-week-old) stained with antibodies against phosphorylated tau (S202, purple) and p-SYK (Y525/526, green). Fluorescent intensities of p-tau (S202) and p-SYK were measured using Zen Blue 2.1 (Zeiss). Three different neuronal fractions were differentiated: a) neurons singly immunopositive for S202, (b) neurons singly immunopositive for p-SYK and (c) neurons immunopositive for both (co-localized). d) Fluorescent intensities of pS202 tau were compared between neurons singly pS202 immunopositive (purple) and neurons exhibiting a co-localization between pS202 and p-SYK (purple-green-striped). Two-tailed Mann–Whitney test revealed a significant increase ($p < 0.0001$) of pS202 fluorescent intensity in neurons exhibiting a co-localization compared to neurons singly immunopositive for pS202. e) Fluorescent intensities of p-SYK were compared between neurons singly immunopositive for p-SYK (green) and neurons exhibiting a co-localization of p-SYK and pS202 tau (purple-green-striped). Two-tailed Mann–Whitney test revealed no significant change of p-SYK fluorescent intensity in neurons exhibiting a co-localization compared to singly p-SYK immunopositive neurons. The scale bar represents 10 µm. The error bars represent SEM.

2.3.6 SYK upregulation promotes tau accumulation in neuron-like SH-SY5Y cells

To further investigate the impact of SYK on tau, we generated human neuronal-like (SH-SY5Y) cells overexpressing SYK (SYK-OX). SYK-OX SH-SY5Y cells show an approximate 17-fold increase in SYK expression compared to control SH-SY5Y cells transfected with the empty vector (Fig. 14b, $p<0.0001$). Interestingly, SYK upregulation in SH-SY5Y cells leads to a significant increase (1.7-fold) in phosphorylated tau at Y18 (Figure 16c, $p<0.01$) and at S396/404 (Figure 16d, 3-fold, $p<0.0001$) compared to control cells. Total tau levels are also significantly increased following SYK overexpression (Figure 16e, 4.2-fold, $p<0.0001$). We analyzed the possible impact of SYK on tau mRNA levels by quantitative RT-PCR and found that SYK does not affect tau transcription and translation (Figure 23: SYK inhibition does not alter transcription or translation levels of tau in vitro) suggesting that SYK may regulate tau degradation. In summary, these results show that the accumulation of tau pathogenic species can trigger SYK activation, as shown in Tg Tau P301S mice (Figure 10-Figure 15), whereas SYK itself appears to regulate total tau levels and tau phosphorylation at multiple epitopes (Figure 16) therefore influencing the development of the tau pathology.

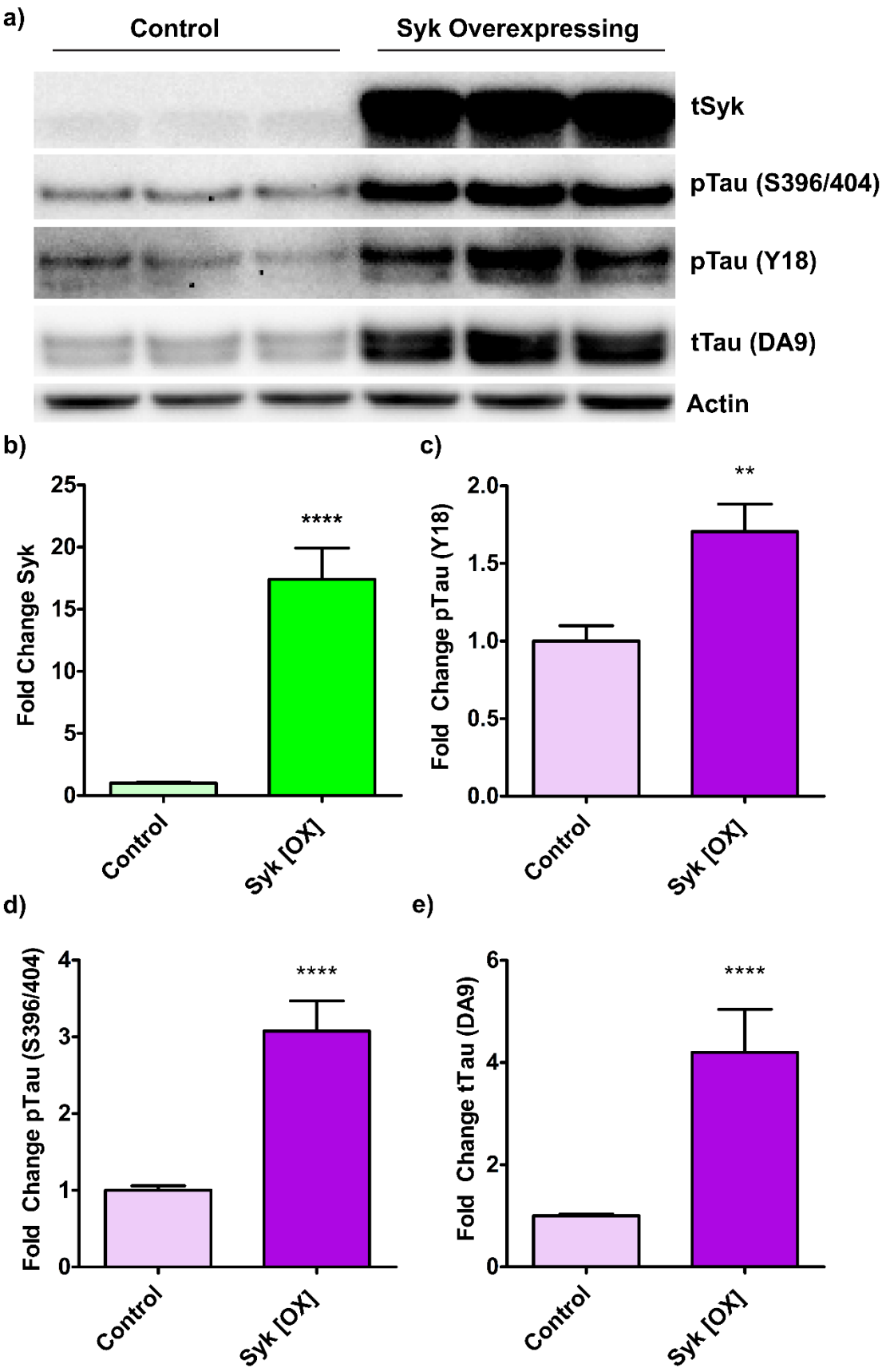
a)
Control
Syk Overexpressing
tSyk
pTau (S396/404)
pTau (Y18)
tTau (DA9)
Actin
b)
Fold Change Syk
****
Control
Syk [OX]
c)
Fold Change pTau (Y18)
**
Control
Syk [OX]
d)
Fold Change pTau (S396/404)
****
Control
Syk [OX]
e)
Fold Change tTau (DA9)
****
Control
Syk [OX]

Figure 16: Syk overexpression increases tau phosphorylation and total tau levels in SH-SY5Y cells

SH-SY5Y cells were transfected with either the empty plasmid as a control or with the same plasmid carrying the SYK sequence for overexpression (SYK OX). Proteins expressed by transfected SH-SY5Y cells were analyzed by Western-blotting. Western-blots chemiluminescent signals were quantified and results were tested for normal distribution using the Shapiro-Wilk test. A subsequent Mann–Whitney test was used to test for statistical significance. a Representative Western blots are shown. b) Level of Syk overexpression is in average 17.3 times higher than in control cells ($p \leq 0.0001$, $n = 18$). c) Level of tau phosphorylation at Y18 is 1.7 times higher in SYK overexpressing compared to control cells ($p \leq 0.01$, $n = 11$). d) Level of tau phosphorylation at S396/404 is 3 times higher in SYK overexpressing compared to control cells ($p \leq 0.0001$, $n = 17$). e) Level of total tau (DA9) is 4.1 times higher in SYK overexpressing compared to control cells ($p \leq 0.0001$, $n = 18$). The error bars represent SEM.

2.3.7 Increased SYK activation in human AD specimen compared to non-demented controls

We also performed different immunostainings against Aβ, p-SYK, GFAP, Iba-1, tau pathogenic conformers (MC1) and phosphorylated tau at Y18 using brain sections from human AD and non-demented controls. We found an increase in SYK activation in DNs surrounding Aβ deposits as well as in neurons displaying an accumulation of phosphorylated tau at Y18 and elevated levels of MC1 pathogenic tau conformers in AD brain sections whereas only weak immunoreactivity for p-SYK was observed in brain sections from a non-demented control (Figure 17-Figure 19). As observed in the AD mouse models, astrocytes did not exhibit SYK activation in neither the AD brain section nor the control. Only a subset of microglial cells exhibited a weak p-SYK signal. Most of the detected p-SYK signal was of neuronal origin and either localized in the somata or DNs. These data complement our observation in AD mouse models and reveal an association between SYK activation and typical AD pathological lesions in the human brain. Further studies will be required using a larger sample of AD pathological specimen to further clarify the role of SYK activation in AD brains.

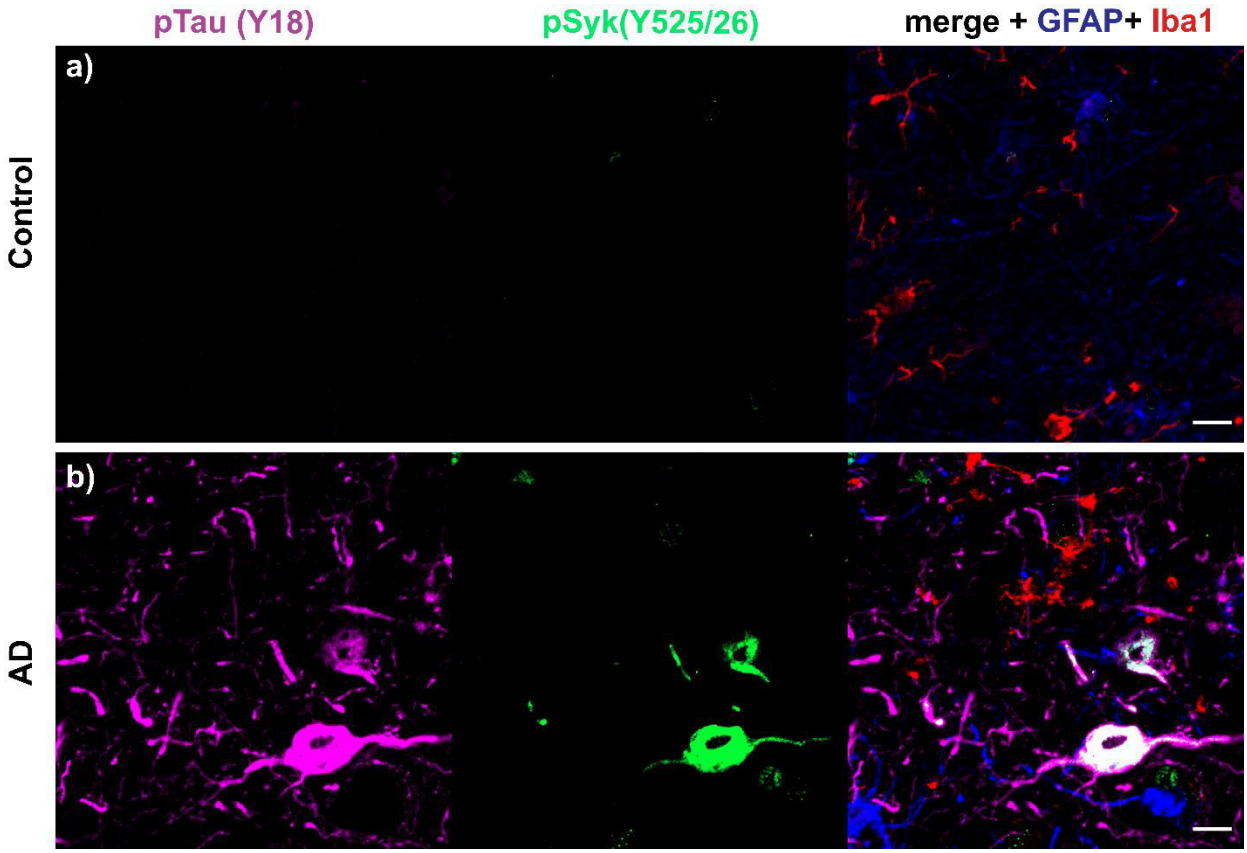

Figure 17: p-SYK is increased in cortical neurons immunopositive for p-tau (Y18) of human AD compared to non-demented controls

Representative confocal images of the dorsolateral frontal cortex sections of human AD (b) were stained with antibodies against p-tau (Y18) (purple), p-SYK (525/526) (green), Iba-1 (red) and GFAP (blue) and compared to control brain sections (a). a) The non-demented control (102-year-old, male) does not exhibit any tau phosphorylation nor increased SYK activation in the dorsolateral frontal cortex. b) The AD brain (67-year-old, male) exhibits a prominent tau phosphorylation at Y18 that co-localizes with Syk activation (Y525/526) in cortical neurons. The scale bars represent 10 µm.

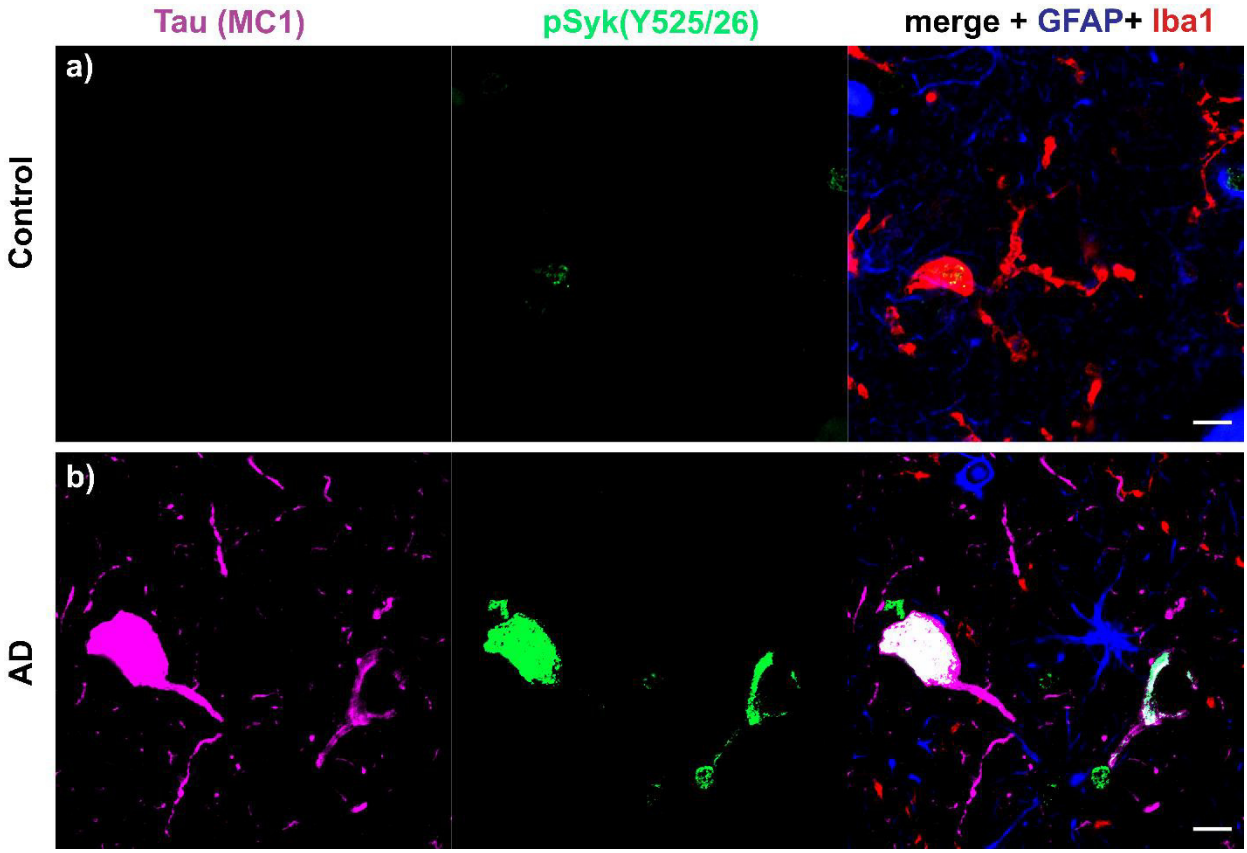

Figure 18: p-SYK is increased in cortical neurons immunopositive for MC1 pathogenic tau conformers in AD compared to brain sections from a non-demented control

Representative confocal images of the dorsolateral frontal cortex sections of human AD (b) were stained with antibodies against conformationally altered tau species (MC1) (purple), p-SYK (525/526) (green), Iba-1 (red) and GFAP (blue) and compared to non-demented control brain sections (a). a) The non-demented control (102-year-old, male) does not exhibit any cells immunopositive for MC1 nor increased in SYK activation in the dorsolateral frontal cortex. b) The AD brain (67-year-old, male) exhibits neurons strongly immunopositive for MC1 that co-localize with SYK activation (Y525/526) in cortical neurons. The scale bars represent 10 μm.

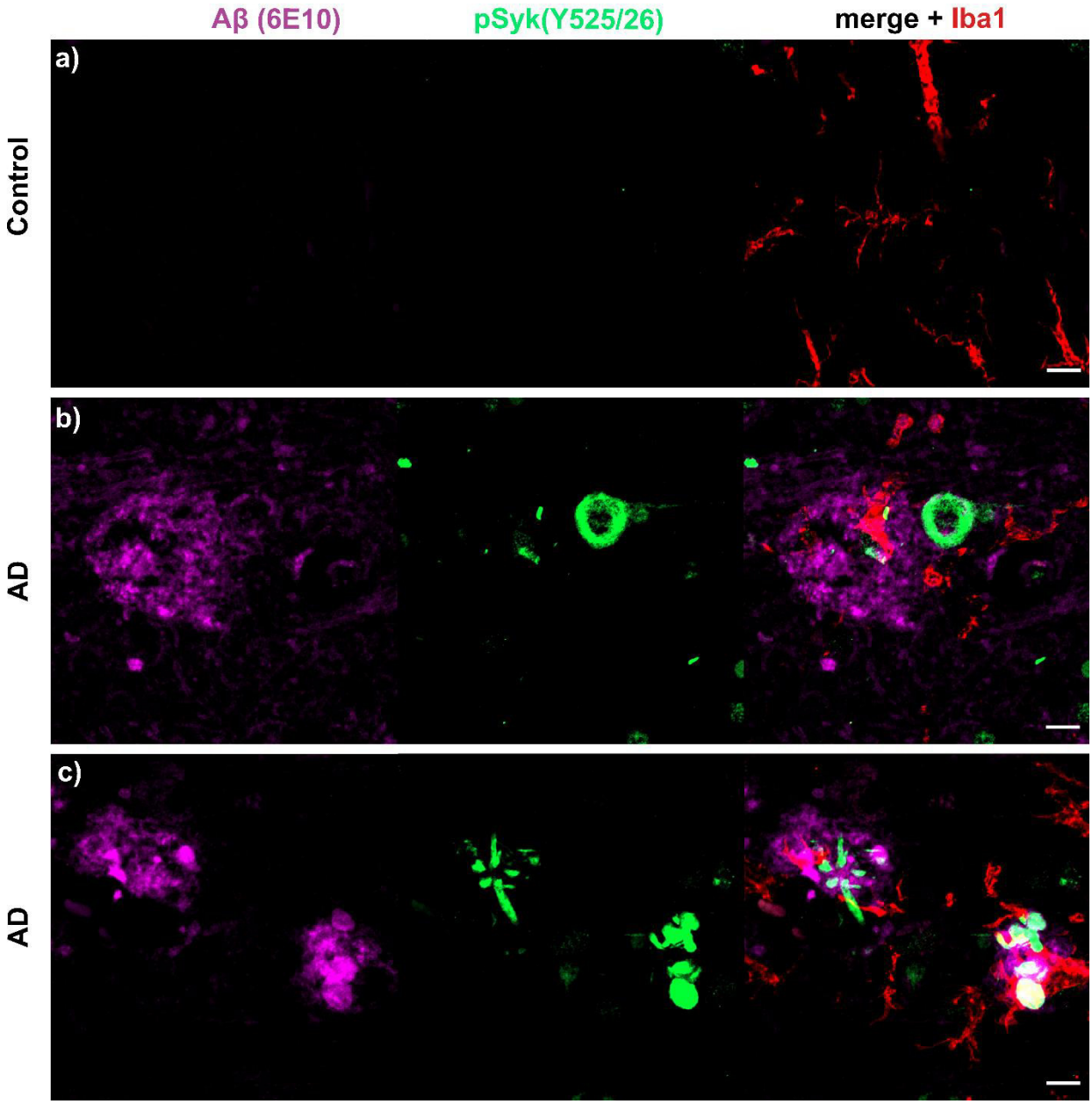

Figure 19: p-SYK is increased in dystrophic neurites associated with β-amyloid plaques of human AD patients compared to healthy controls

Representative confocal images of dorsolateral frontal cortex sections of human AD (b) were stained with antibodies against Aβ (6E10) (purple), p-SYK (525/526) (green), Iba-1 (red) and compared to non-demented control brain sections (a). a) The non-demented control (102-year-old, male) does not exhibit any Aβ deposits nor increased Syk activation in neurons. b) The AD brain (67-year-old, male) exhibits neurons strongly immunopositive for p-SYK (Y525/526). c) The AD brain also exhibits dystrophic neurites immunopositive for p-SYK (Y525/526) near/within Aβ deposits. The scale bars represent 10 µm.

2.4 Discussion

Our previous studies have shown that tau hyperphosphorylation, Aβ production and neuroinflammation are reduced following an acute inhibition of SYK (Paris et al. 2014). These data prompted us to investigate the level of SYK activation in different mouse models of AD and in brain sections from a non-demented control and AD patients. We found that SYK activation occurs in three different mouse models of AD, overexpressing Aβ or tau, showing that SYK activation is triggered by both Aβ deposits and tau pathological species. Most importantly, we made similar observations in human AD brain sections.

Recent late phase clinical trials targeting the major pathological hallmarks of AD, mainly extracellular Aβ plaques or intra-neuronal tau aggregates, have been unsuccessful so far and have failed to prevent cognitive decline and brain atrophy in AD patients (Siemers et al. 2016; Le Couteur et al. 2016; St-Amour et al. 2016; Gauthier et al. 2016). As PET scan imaging of AD patients reveals that Aβ deposits and pathological tau accumulation occur during the prodromal phase of AD (Ossenkoppele et al. 2011), it has been suggested that therapies that are targeting Aβ or pathological tau accumulation must be implemented decades before the appearance of the symptoms to be successful (Ossenkoppele et al. 2011). Hence, pharmacological intervention at downstream targets of Aβ and tau may represent a more promising therapeutic strategy for AD patients. However, therapeutic targets downstream of the Aβ and tau pathological lesions remain to be identified. Our work supports the view that SYK may be such a therapeutic target as it appears to be activated *in vivo* in response to β-amyloidosis and the formation of pathological tau species. In this chapter, we report a hyperactivation of SYK in the brains of three different AD mouse models versus wild-type littermate controls and human AD compared to non-demented controls. In Tg PS1/APPsw, Tg APPsw mice, SYK activity is largely increased in activated microglia and



in DNs around Aβ deposits. In addition, we observed an activation of SYK in DNs around Aβ deposits in an AD pathological specimen. In Tg Tau P301S mice and AD brain sections, SYK hyperactivation is co-localized with misfolded tau and hyperphosphorylated tau in neurons.

The strong increase in activated SYK observed in dystrophic neurites (DNs) surrounding Aβ deposits may suggest the involvement of SYK in the formation of these DNs that ultimately leads to the synaptic loss observed in AD (Sanchez-Varo et al. 2012). DNs are characterized by an accumulation of BACE-1 and sAPPβ which implies a contribution of DNs to Aβ production and accumulation (Sadleir et al. 2016). In fact, several *in vivo* studies have shown that BACE-1 immunopositive dystrophic neurites precede Aβ plaque formation in the brains of 3xTg-AD, 2xFAD and 5xFAD mice and therefore, represent an early pathological event in AD (Cai et al. 2012; Kandalepas et al. 2013; Zhang et al. 2009). Our previous *in vitro* and *in vivo* data have shown that SYK regulates Aβ and sAPPβ production via a modulation of BACE-1 expression (Paris et al. 2014) and therefore support a causative role of SYK activation in the accumulation of BACE-1 and sAPPβ in DNs.

The increased activation of SYK in activated microglia of Aβ-overexpressing mice further supports a role of SYK in microglial activation *in vivo* and suggests that Aβ accumulation can lead to an activation of SYK in microglia. Previous *in vitro* studies have shown that Aβ fibrils and oligomers can trigger a microglial inflammatory response mediated by SYK and leading to neurotoxicity (Combs et al. 1999; Combs et al. 2001; McDonald et al. 1997).

Recruitment and activation of SYK has been suggested to be mediated by activation of triggering receptor expressed on myeloid cells 2 (TREM2) (Lanier and Bakker 2000). TREM2 is a type I transmembrane protein and part of the immunoglobulin (Ig) receptor superfamily. Since TREM2 does not have any cytoplasmic signaling motifs, an adaptor protein DNAX-activating

protein of 12 kDa (DAP12, also known as TYROBP) is needed for TREM2 signal transduction. DAP12 interacts with the transmembrane domain of TREM2. The cytoplasmic domain of DAP12 contains an immunoreceptor tyrosine activation motif (ITAM) that provides docking sites for SYK activation. Interestingly, loss-of-function mutations in the DAP12 or TREM2 genes cause a rare autosomal recessive disorder called Nasu-Hakola disease (NHD) whereas heterozygous carriers of these mutations show an elevated risk to develop AD (Paloneva et al. 2002). Symptoms of NDH include multifocal bone cysts and presenile dementia. Interestingly, SYK activation (p-SYK, Y525/526) is increased in NHD neurons compared to controls (Satoh et al. 2012) and was found to be also present in microglia and macrophages but not in astrocytes or oligodendrocytes (Satoh et al. 2012) supporting a role of SYK activation in the development of NHD dementia.

SYK plays a key role in the activation of immune cells and the production of inflammatory cytokines. We have shown previously that activation of NFκB (nuclear factor kappa-light-chain-enhancer of activated B cells) which is known to play a regulatory role in neuroinflammation, is prevented following either pharmacological SYK inhibition or genetic knockdown of SYK. Hence, this suggests a role of SYK in the regulation of neuroinflammation. In addition, SYK has been shown to mediate the neuroinflammation and neurotoxicity caused by Aβ. Furthermore, the Aβ-induced cytokine production by microglia has been found to be mediated by SYK, suggesting that SYK is involved in the activation of microglia.

The pathological analysis of Tg Tau P301S mice shows that SYK activation is associated with the formation of hyperphosphorylated tau and misfolded tau in the hippocampus and cortex while our previous work has shown that acute SYK inhibition can reduce tau phosphorylation at multiple AD relevant epitopes (Paris et al. 2014). Interestingly, we show here that SYK upregulation in human neuronal like SH-SY5Y cells induces tau accumulation and tau

phosphorylation further confirming a role of SYK in the formation of tau pathogenic species. Altogether, our data suggest that SYK activation may also promote tau hyperphosphorylation and misfolding *in vivo* as neurons that show higher levels of SYK activation also show more accumulation of hyperphosphorylated tau and tau pathogenic conformers. Pathological tau species accumulation clearly results in SYK activation in Tg Tau P301S mice while SYK activation appears to be a mediator of the formation of tau pathogenic species, thereby implying the existence of a positive feedback loop resulting in an enhanced progression of tau pathology. Given that SYK is also present in DNs which exhibit tau accumulation and tau phosphorylation (Schmidt et al. 1994; Su et al. 1993), this further supports a pathological role of SYK in the formation of DNs and ultimately synaptical loss.

Our previous *in vivo* and *in vitro* data show decreased tau phosphorylation at multiple epitopes (S396/404, S202, Y18) following SYK inhibition (Paris et al. 2014). Interestingly, we show here that SYK overexpression in SH-SY5Y cells increases tau phosphorylation and total tau levels (Y18, S396/404, DA9). The increase in total tau levels following SYK upregulation is not caused by an increased transcription, as SYK does not impact tau transcription (Figure 23). Therefore, increased SYK levels may lead to a decreased degradation of tau. However, the molecular mechanisms responsible for the increased tau levels following SYK overexpression or decreased tau following SYK inhibition are delineated in the following chapter of this thesis.

In this study, we also provide evidence for an aberrant SYK activation in DNs around Aβ deposits and in neurons immunopositive for pathological tau species in human AD brain sections further validating the data obtained with different transgenic mouse models of AD. In conclusion, our data support a pathological role of SYK in the formation of Aβ deposits and misfolded tau and suggest additionally that reduction of SYK hyperactivity through pharmacological inhibition may be a promising therapeutic approach for the treatment of AD.

3 Mechanistic assessment of the role of SYK in autophagy and the mTOR pathway in CNS-derived SH-SY5Y cells

3.1 Introduction

Protein misfolding, aggregation and accumulation constitute a pathological hallmark of neurodegenerative proteinopathies including AD and frontotemporal lobar degeneration (FTLD). Many studies have suggested that neurodegeneration is, at least partly, caused by a dysfunctional degradation of proteins that are prone to aggregate. In fact, an impaired autophagic clearance of macromolecules has been widely accepted to be a major contributor to various neurodegenerative diseases (Nixon 2007; Nixon and Yang 2011; Ghavami et al. 2014; Menzies et al. 2015) by promoting the accumulation of misfolded proteins. The mammalian target of rapamycin (mTOR) is known to regulate autophagy (Jung et al. 2010). The members of the mTOR pathway including phosphatidylinositol-4,5-bisphosphate 3-kinase (PI3K), 3-phosphoinositide-dependent protein kinase 1 (PDK1), protein kinase B (Akt), Tuberous sclerosis 1/2 (TSC1/2), Ras homolog enriched in brain (Rheb), mTOR and ribosomal protein S6 kinase (S6K), thereby also indirectly control the autophagic degradation of proteins. AD and FTLD share the accumulation of tau as a common underlying pathology. In human AD and FTLD cases, as well as in mouse models of AD and pure tauopathy, autophagy has been found to be decreased (Zare-Shahabadi et al. 2015; Kragh et al. 2012; Wang et al. 2012) and to contribute to the pathological accumulation of tau aggregates. Impaired autophagy has been linked to an overactive mTOR pathway which acts as a regulator of autophagy initiation and lysosomal degradation, thereby controlling the autophagic flux (Jung et al. 2010; Puertollano 2014).

More specifically, in the frontotemporal dementia and parkinsonism linked to chromosome 17 (FTDP-17) mouse model that overexpresses mutant tau (Tg Tau P301S), direct inhibition of

mTOR with either rapamycin or temsirolimus attenuated tau pathology (Ozcelik et al. 2013; Jiang et al. 2014b). Furthermore, stimulation of autophagy by trehalose or by the overexpression of the transcription factor EB (TFEB) were both shown to be efficient in reducing neurodegeneration and mitigating tauopathy in Tg Tau P301S mice (Schaeffer et al. 2012; Wang et al. 2016) suggesting that inhibiting mTOR may have therapeutic value for the treatment of tauopathies.

SYK has also been suggested to phosphorylate microtubules in B-cells (Faruki et al. 2000), and furthermore, pharmacological SYK inhibition has been found to stabilize microtubules in paclitaxel-resistant tumor cells (Yu et al. 2015).

SYK has been shown to mediate the activation of microglial cells induced by Aβ oligomers (Combs et al. 1999; McDonald et al. 1997), while SYK inhibition has been shown to prevent Aβ-mediated neurotoxicity *in vitro* (Combs et al. 1999). A subsequent study also demonstrated that SYK was the mediator of the Aβ-induced elevated cytokine production including interleukin 1 beta (IL-1β) and tumor necrosis factor alpha (TNFα) which is responsible for increased iNOS expression resulting in apoptosis in primary mouse neuronal cultures (Combs et al. 2001). In addition, it has been suggested that SYK contributes to microglial dysfunction in AD (Ghosh and Geahlen 2015).

In our previous studies, we identified SYK as a novel target for the treatment of AD (Paris et al. 2014; Schweig et al. 2017). We found that SYK inhibition can decrease Aβ production and tau hyperphosphorylation *in vitro*, and *in vivo* in mouse models of AD and tauopathy following an acute treatment (Paris et al. 2014), in part, by promoting the phosphorylation of GSK3-β at the inhibitory Ser9 site and reducing BACE-1 expression (Paris et al. 2014).

We have shown that SYK activation, as measured by p-SYK (Y525/526) levels, is largely increased in dystrophic neurites and microglia of Aβ-overexpressing mouse models of AD (Tg

PS1/APPsw, Tg APPsw) and in neurons of a mouse model of tauopathy (Tg Tau P301S) displaying pathological tau species while neurons of wild-type animals showed no activation of SYK (Schweig et al. 2017), suggesting that SYK plays a key role in the formation of AD pathological lesions (see previous chapter). Similarly, we observed an increased SYK activation in dystrophic neurites and in neurons affected by the tau pathology in human AD specimens (Schweig et al. 2017). Interestingly, we have shown that SYK activation promotes tau accumulation but does not affect tau expression suggesting that SYK may affect tau clearance (Schweig et al. 2017). In the present study, we further investigated the SYK molecular mechanisms which drive tau accumulation *in vitro*. We show that SYK is a key regulator of the mTOR pathway and that SYK inhibition, as well as suppression of SYK expression, lead to an inhibition of the mTOR pathway, resulting in increased autophagic tau degradation. These data not only provide further evidence for an important role of SYK in the pathological impairment of protein degradation observed in AD and tauopathies but also illustrate that pharmacological SYK inhibition may represent a promising therapeutic strategy for the treatment of AD and other neurodegenerative proteinopathies associated with a defective autophagic clearance of misfolded proteins.

3.2 Methods

3.2.1 Cell Culture

SH-SY5Y cells were purchased from American Type Culture Collection (VA, USA). SH-SY5Y cells were grown in DMEM/F12 medium (Thermo Fisher Scientific, MA, USA) supplemented with 10% fetal bovine serum (Thermo Fisher Scientific, MA, USA), GlutaMAX and 1% penicillin/streptomycin/fungizone.

3.2.2 Cell Culture Treatments

SH-SY5Y cells were treated in 500µl medium for 24h using 24-well cell culture plates. The cells were treated with the following inhibitors/activators: SYK inhibitor BAY61-3606 (5-10µM, Sigma, MO, USA), Akt activator SC79 (20µM, Sigma, MO, USA), mTOR activator MHY1485 (4-12µM, Sigma, MO, USA), mTOR inhibitor KU0063794 (1-2µM, Sigma, MO, USA), S6K inhibitor PF4708671 (5-10µM, Tocris, MN, USA), lysosomal inhibitor chloroquine (CQ, 100-200µM, Tocris, MN, USA).

3.2.3 Puromycin Incorporation Assay

To investigate the possible impact of SYK inhibition on protein synthesis, we used the SUrface SEnsing of Translation (SUnSET) technique (Schmidt et al. 2009). This technique involves the use of the antibiotic puromycin (a structural analog of tyrosyl-tRNA), and anti-puromycin antibodies to detect the amount of puromycin incorporation into nascent peptide chains. Incorporation of puromycin into nascent polypeptides causes termination. Although a high concentration of puromycin is toxic because it can inactivate translation, at low concentrations it provides an accurate snapshot of protein synthesis without causing lethality. Confluent SH-SY5Y



cells were treated with BAY61-3606 and PF4708671 for 24 hours and with cycloheximide for 5 hours. Cells were then treated for 1 hour with 10 µg/ml of puromycin and lysed in ice-cold M-PER (Thermo Fisher Scientific, MA, USA) containing Halt protease & phosphatase single use inhibitor/EDTA (Thermo Fisher Scientific, MA, USA) and 1 mM PMSF. Levels of newly synthesized proteins containing puromycin were then detected by Western blot using an anti-puromycin antibody (1/1000 dilution, Millipore Sigma, MA, USA).

3.2.4 Immunoprecipitation (IP)

Following the SUnSET technique, cell lysates were centrifuged at 16,000g for 15 min at 4°C to remove the insoluble fractions. The resulting supernatants were subjected to IP with 2µg/ml anti-puromycin (Millipore Sigma, MA, USA) overnight at 4°C. Then 20µl protein A-magnetic beads (Thermo Fisher Scientific, MA, USA) were added for 2 hours at 4°C. The beads were carefully washed, and the proteins were eluted with reducing 2x Laemmli sample buffer (Bio-Rad Laboratories, CA, USA) at 95°C for 5min. The samples were then analyzed by Western blotting.

3.2.5 Quantitative RT-PCR

Total RNA was extracted from SH-SY5Y cells treated with DMSO or BAY61-3606 using the Trizol reagent (Invitrogen, CA, USA). RNA was reverse-transcribed into first-strand cDNA using the superScript™ III First-Strand Synthesis System (Invitrogen, CA, USA). Quantitative real-time PCR (qPCR) was performed with ssoAdvanced™ Universal SYBR® Green Supermix (Bio-Rad Laboratories, CA, USA) and analyzed on a CFX96 Touch™ Real-Time PCR Detection System (Bio-Rad Laboratories, CA, USA) as per the manufacturer's instructions. The mRNA levels in each sample were analyzed by normalizing the threshold cycle (Ct) value to that of internal loading

control, β-actin employing the primer sets used for human total and 3R tau detection that have been described previously (Fernández-Nogales et al. 2014).

3.2.6 Generation of SYK knockdown SH-SY5Y Cells

Short hairpin RNAs (shRNAs) were used to stably knockdown SYK gene expression in SH-SY5Y cells. GIPZ lentiviral vectors expressing SYK specific shRNAs (Paris et al. 2014) or nonsense control shRNAs were purchased from Origene. For stable transfection, SH-SY5Y cells were grown on 6-well plates until reaching 70-80% confluence and transfected with shRNAs plasmids using lipofectamine 2000 (Invitrogen, CA, USA). After 48 hours, transfected cells were placed into fresh medium in the presence of 1μg/ml puromycin for selection. After 14 days, the resistant cells were trypsinized and expanded. The knockdown efficiency of SYK was confirmed by western blot using antibodies against SYK (4D10, Santa Cruz, TX, USA).

3.2.7 Immunoblotting

Western blots were performed as previously described (Paris et al. 2014; Schweig et al. 2017). Briefly, SH-SY5Y cells were cultured in 24-well-plates, treated for 24 hours and subsequently lysed with mammalian protein extraction reagent (MPER, Thermo Fisher Scientific, MA, USA) containing Halt protease & phosphatase single use inhibitor/EDTA (Thermo Fisher Scientific, MA, USA) and 1 mM PMSF. Proteins of cell lysates were separated by 10% tris-glycine-SDS-PAGE using 1 mm Criterion TGX gels (Bio-Rad Laboratories, CA, USA) and electro-transferred onto 0.2 μm PVDF membranes (Bio-Rad Laboratories, CA, USA). Membranes were blocked in TBS containing 5% non-fat dried milk for 1h and were hybridized with the primary antibody (anti-SYK (4D10, 1:1000, Santa Cruz, TX, USA), anti-p-tau S396/404 (PHF-1, 1:1000, Dr. Peter Davies' Lab), anti-t-tau (DA9, 1:1000, Dr. Peter Davies' Lab), anti-p-tau S202 (CP13, 1:1000, Dr.

Peter Davies' Lab), anti-p-tau T231 (RZ3, 1:1000, Dr. Peter Davies' Lab), anti-conformer-tau (MC1, 1:1000, Dr. Peter Davies' Lab), anti-oligomeric-tau (TOC1, 1:1000, Dr. Lester Binder's Lab) anti-p-SYK (Y525/526), anti-p-mTOR (S2448), anti-p-S6K (T389/T412), anti-p-Akt (S473), anti-LC3b, anti-Actin, anti-NeuN, anti-LAMP-1, anti-iNOS (all 1:1000, Cell Signaling, MA, USA), anti-GFAP (1:5000, DAKO, USA), anti-Iba1 (1:1000, Abcam, MA, USA), anti-beta-tubulin (1:1000, BD Biosciences, CA, USA) overnight at 4˚C. Subsequently, the membranes were incubated for 1h in HRP-conjugated anti-mouse or anti-rabbit secondary antibody (1:1000, Cell Signaling, MA, USA). Western blots and Dot Blots were visualized using chemiluminescence (Super Signal West Femto Maxium Sensitity Substrate, Thermo Fisher Scientific, MA, USA). Signals were quantified using ChemiDoc XRS (Bio-Rad Laboratories, CA, USA) and densitometric analyses were performed using Quantity One (Bio-Rad Laboratories, CA, USA) image analysis software.

3.2.8 Statistical Analyses

The data were analyzed and plotted with GraphPad Prism (GraphPad Software, Inc., CA, USA). The Shapiro-Wilk test for normality was used to test for Gaussian distribution. Statistical significance was determined by either ANOVA (for comparisons of three or more groups) or t-tests (SYK knockdown). All data are presented as mean ± the standard error of the mean (SEM) and $p<0.05$ was considered significant (*$p<0.05$, **$p<0.01$, ***$p<0.001$, ****$p<0.0001$).



3.3 Results

Our previous data suggest that SYK may regulate tau clearance since we have observed that SYK upregulation promotes tau accumulation without affecting tau expression (Schweig et al. 2017). As tau clearance is known to be regulated via autophagy, we therefore investigated the possible impact of SYK inhibition on the mTOR pathway and autophagic degradation of tau in SH-SY5Y cells.

3.3.1 SYK inhibition decreases p-tau, as well as total tau levels and reverses the effects of the Akt activator SC79 on the mTOR pathway

We show that SYK inhibition using the selective SYK inhibitor BAY61-3606 (Yamamoto et al. 2003) decreases p-tau (S396/404) levels significantly (Figure 20A) in SH-SY5Y cells and reduces total tau levels (Figure 20A).

In parallel with the reduction of total tau levels induced by SYK inactivation with BAY61-3606, an inhibition of several members of the mTOR pathway was observed (Figure 20B). Compared to untreated control cells, p-Akt (S473) and p-S6K (T389, T412) levels were significantly lower following SYK inhibition (Figure 20B, $p<0.01$). As expected, the Akt activator SC79 stimulated the mTOR pathway, as it increases the phosphorylation levels of p-S6K (T389, T412) and p-mTOR (S2448) significantly (Figure 20B, $p<0.01$). We show that SYK inhibition reverses the effects of the Akt activator and decreases the phosphorylation levels of p-Akt (S473), p-S6K (T389, T412), p-mTOR (S2448) induced by SC79 (Figure 20B, $p<0.001$). Interestingly, baseline levels of mTOR phosphorylation remained unchanged following SYK inhibition but elevated mTOR phosphorylation following SC79 activation were brought back to baseline levels following SYK inhibition, suggesting that SYK inhibition can antagonize dysregulated mTOR phosphorylation (Figure 20B).

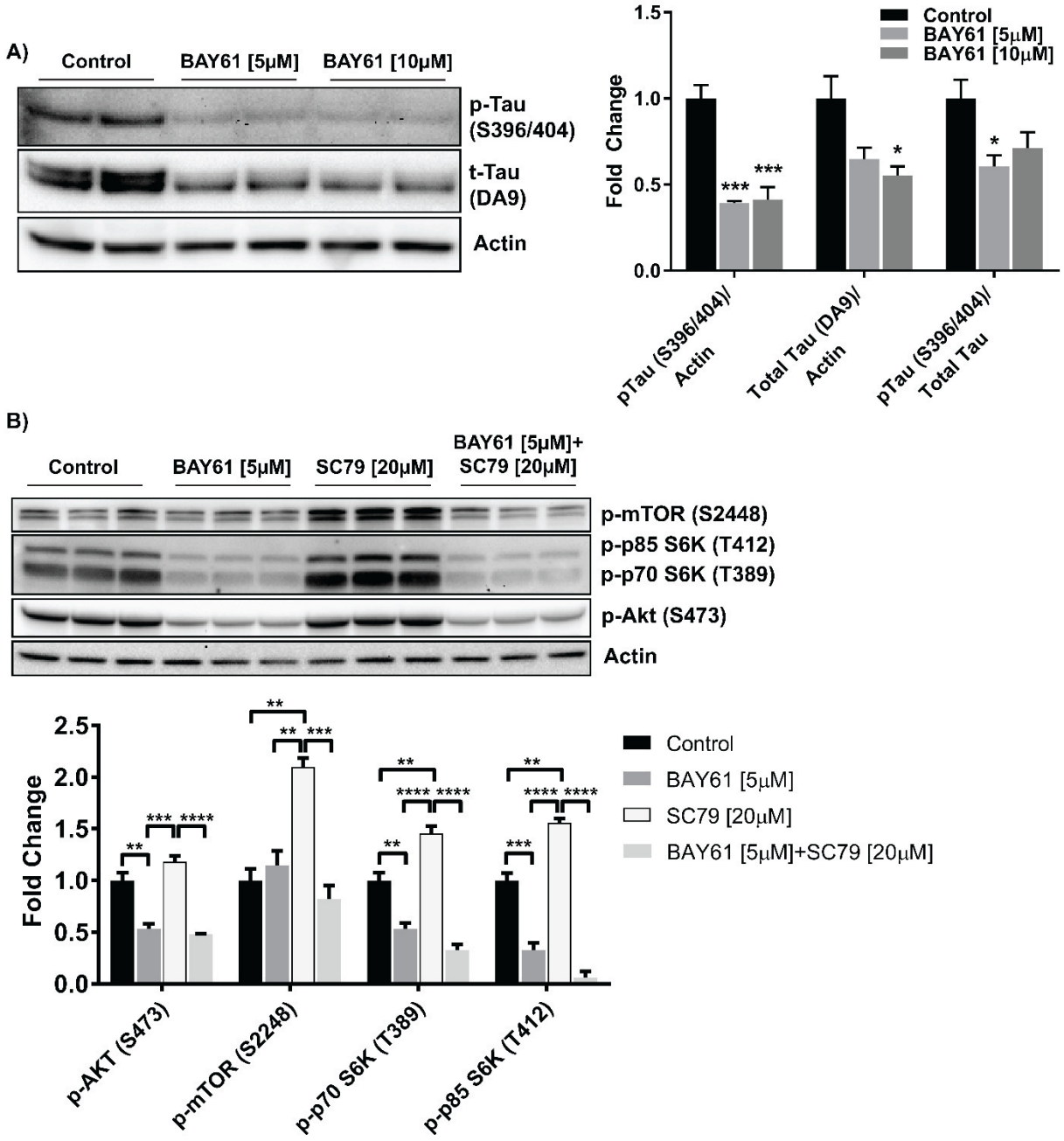
A)
Control
BAY61 [5μM]
BAY61 [10μM]
p-Tau (S396/404)
t-Tau (DA9)
Actin
Fold Change
1.5
1.0
0.5
0.0
Control
BAY61 [5μM]
BAY61 [10μM]
***
***
*
*
pTau (S396/404)/ Actin
Total Tau (DA9)/ Actin
pTau (S396/404)/ Total Tau
B)
Control
BAY61 [5μM]
SC79 [20μM]
BAY61 [5μM]+ SC79 [20μM]
p-mTOR (S2448)
p-p85 S6K (T412)
p-p70 S6K (T389)
p-Akt (S473)
Actin
Fold Change
2.5
2.0
1.5
1.0
0.5
0.0
Control
BAY61 [5μM]
SC79 [20μM]
BAY61 [5μM]+SC79 [20μM]
p-AKT (S473)
p-mTOR (S2248)
p-p70 S6K (T389)
p-p85 S6K (T412)

Figure 20: SYK inhibition decreases p-tau, as well as total tau levels and reverses the effects of the Akt activator SC79 on the mTOR pathway

A) Representative Western blots depicting p-tau (S396/404) and total tau are shown. Western blots chemiluminescent signals were quantified by densitometry and normalized to actin. The histogram represents the quantification of p-tau (S396/404) and t-tau following a 24h treatment of SH-SY5Y cells with 5µM or 10µM of the SYK inhibitor BAY61-3606. ANOVA with post-hoc Bonferroni test revealed significantly decreased tau phosphorylation at S396/404 ($p<0.001$) and total tau ($p<0.05$) levels following SYK inhibition (n=4 for each treatment condition).

B) Representative Western blots depicting p-mTOR (S2448), p-S6K (T389, T412) and p-Akt (S473) are shown. Western blots chemiluminescent signals were quantified by densitometry and normalized to actin. The histogram represents the quantification of p-mTOR (S2448), p-S6K (T389, T412) and p-Akt (S473) following a 24h treatment of SH-SY5Y cells with 5µM of the SYK inhibitor BAY61-3606 and 20µM of the Akt activator SC79 and a combination thereof. ANOVA with post-hoc Bonferroni test revealed significantly decreased p-Akt (S473) ($p<0.01$) and p-S6K (T389, T412) ($p<0.01$, $p<0.001$) levels following SYK inhibition (n=3) and also significantly increased p-mTOR (S2448) ($p<0.01$) and p-S6K (T389, T412) ($p<0.01$) levels following Akt activation. SYK inhibition reverses these effects significantly in the double treatment (n=3 for each treatment condition).

3.3.2 SYK inhibition reverses the effects of the mTOR activator MHY1485 and mimics the effects of the mTOR inhibitor KU0063794

We further investigated the effects of SYK inhibition on the mTOR pathway and determined whether SYK inhibition can overcome the impact of the mTOR activator MHY1485. We also tested the effects of the mTOR inhibitor KU0063794 on phosphorylated and total tau levels in SH-SY5Y cells to determine whether direct mTOR inactivation can mimic the effects of SYK inhibition. mTOR activation with MHY1485 significantly increased p-mTOR (S2448), p-S6K (T389, T412), and p-tau (S396/404) levels while mTOR inhibition with KU0063794 significantly decreased p-Akt (S473), p-S6K (T389, T412) and p-mTOR (S2448) levels compared to the untreated control cells (Figure 21A-B). The levels of t-tau, p-tau (S396/404) were also significantly lower in cells that were treated with the mTOR inhibitor than in cells that were treated with the mTOR activator (Figure 21A-B). In fact, mTOR inhibition appears to be mimicking the effects of SYK inhibition on the mTOR pathway (Figure 20-Figure 21). Interestingly, SYK inhibition was able to antagonize the increased p-tau (S396/404), p-S6K (T389, T412), p-mTOR (S2448) and p-Akt (S473) levels induced by MHY1485 (Figure 21C-D). A trend for an increase in total tau levels was observed following 24 hours of treatment with the mTOR activator MHY1485 which was also prevented by SYK inhibition (Figure 21C-D) showing that SYK inhibition can overcome the effects of a stimulation of the mTOR pathway. In summary, these results show that SYK inhibition and direct mTOR inhibition have similar effects on the mTOR pathway and tau levels. Furthermore, SYK inhibition can reverse the effects of mTOR activation on members of the mTOR pathway and tau, thereby underlining a role of SYK as an upstream modulator of the mTOR pathway and regulator of autophagic tau degradation.

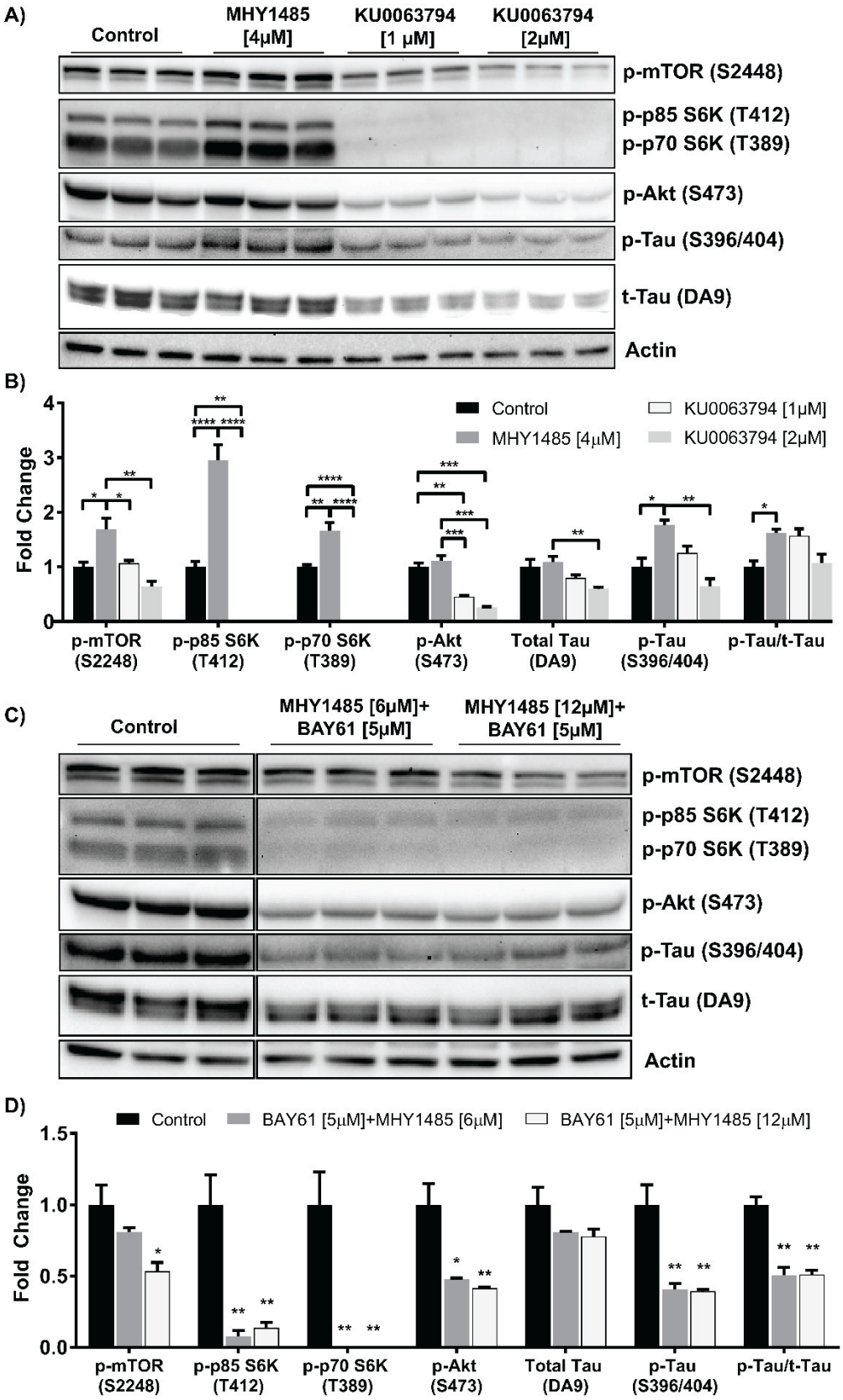
A)
Control
MHY1485 [4μM]
KU0063794 [1 μM]
KU0063794 [2μM]
p-mTOR (S2448)
p-p85 S6K (T412)
p-p70 S6K (T389)
p-Akt (S473)
p-Tau (S396/404)
t-Tau (DA9)
Actin
B)
Control
MHY1485 [4μM]
KU0063794 [1μM]
KU0063794 [2μM]
Fold Change
p-mTOR (S2248)
p-p85 S6K (T412)
p-p70 S6K (T389)
p-Akt (S473)
Total Tau (DA9)
p-Tau (S396/404)
p-Tau/t-Tau
C)
Control
MHY1485 [6μM]+ BAY61 [5μM]
MHY1485 [12μM]+ BAY61 [5μM]
p-mTOR (S2448)
p-p85 S6K (T412)
p-p70 S6K (T389)
p-Akt (S473)
p-Tau (S396/404)
t-Tau (DA9)
Actin
D)
Control
BAY61 [5μM]+MHY1485 [6μM]
BAY61 [5μM]+MHY1485 [12μM]
Fold Change
p-mTOR (S2248)
p-p85 S6K (T412)
p-p70 S6K (T389)
p-Akt (S473)
Total Tau (DA9)
p-Tau (S396/404)
p-Tau/t-Tau

Figure 21: SYK inhibition reverses the effects of the mTOR activator MHY1485 and mimics the effects of the mTOR inhibitor KU0063794

SH-SY5Y cells were treated for 24h with A-B) 4μM of the mTOR activator MHY1485 or 1-2μM of the mTOR inhibitor KU0063794 or C-D) a combination of 6-12μM of the mTOR activator MHY1485 and 5μM of the SYK inhibitor BAY61-3606.

A) Representative Western blots depicting p-mTOR (S2448), p-S6K (T389, T412), p-Akt (S473), p-tau (S396/404) and t-tau are shown.

B) Western blots chemiluminescent signals were quantified by densitometry, normalized to actin and presented as histograms. ANOVA with post-hoc Bonferroni test revealed significantly increased p-mTOR (S2448) ($p<0.05$), p-S6K (T389, T412) ($p<0.01$, $p<0.0001$) and p-tau (S396/404) ($p<0.05$) levels compared to untreated control cells following mTOR activation by MHY1485, whereas mTOR inhibition by KU0063794 decreased p-S6K (T389, T412) ($p<0.0001$, $p<0.01$) and p-Akt (S473) ($p<0.01$) levels significantly compared to control (n=3 for each treatment condition).

C) Representative Western blots depicting p-mTOR (S2448), p-S6K (T389, T412), p-Akt (S473), p-tau (S396/404) and t-tau are shown.

D) Western blots chemiluminescent signals were quantified by densitometry, normalized to actin and presented as histograms. ANOVA with post-hoc Bonferroni test revealed that the combination of the mTOR activator and the SYK inhibitor results in significantly decreased p-mTOR (S2448) ($p<0.01$), p-S6K (T389, T412) ($p<0.01$), p-Akt (S473) ($p<0.01$) and p-tau (S396/404) ($p<0.01$) levels compared to untreated control cells (n=3 for each treatment condition).

3.3.3 SYK inhibition increases the autophagic flux and decreases tau levels in the presence of the lysosomal inhibitor chloroquine

Having shown that SYK acts upstream of mTOR and thereby influences the autophagic degradation of tau, we investigated whether SYK inhibition could impact the autophagic flux by quantifying the amount of the microtubule-associated protein 1A/1B-light chain (LC3). During autophagy initiation, soluble cytosolic LC3-I gets lipidated and the resulting LC3-II becomes associated with the inside and outside of autophagosomal membranes (Kabeya et al. 2000). After the fusion of autophagosomes with lysosomes, LC3-II is degraded. Hence, the ratio of unlipidated LC-I to lipidated LC3-II can be used to measure the autophagic flux, the rate of autophagy initiation and lysosomal degradation (Mizushima and Yoshimori 2007; Pugsley 2017). Since an increased in LC3-II levels following a drug treatment could be indicative of either an increased in autophagy initiation or a decreased in lysosomal degradation, we employed a lysosome inhibitor (chloroquine (CQ)) to determine the rate of autophagy initiation, as previously described (Mizushima and Yoshimori 2007; Tanida et al. 2008). CQ accumulates in the lysosomes and raises their pH. Thereby, CQ decreases the functionality of lysosomal proteases and inhibits the fusion of lysosomes and autophagosomes. Therefore, CQ allows the observation of the conversion rate of LC3-I to LC3-II (autophagy initiation) by limiting the degradation of LC3-II. We treated SH-SY5Y cells for 24h with two different doses of CQ (100µM and 200µM) alone or in combination with 5µM of the SYK inhibitor BAY61-3606. CQ treatment significantly increased, p-S6K (T389), p-mTOR (S2448) and t-tau levels (Fig. 3A-B) showing an inhibition of lysosomal t-tau degradation. As expected, CQ treatment also increased the ratio of LC3-II/I by decreasing the degradation of LC3-II (Figure 22C). Importantly, the increased levels of p-S6K (T389), p-mTOR (S2448) and t-tau levels induced by CQ were significantly reduced following SYK inhibition (Figure 22A-B). The ratio of LC3II/I was further increased after a double treatment with CQ and

BAY61-3606 compared to CQ alone (Figure 22C). Since the degradation of LC3-II is inhibited by CQ, the additional increase of LC3-II observed in cells treated with CQ and the SYK inhibitor suggests that SYK inhibition accelerates the conversion of LC3-I into LC3-II and therefore stimulates the autophagic flux. The increased degradation of t-tau following the co-treatment with CQ and the SYK inhibitor compared to CQ alone (Figure 22) suggests that SYK inhibition not only increases autophagy initiation but may also increase the lysosomal degradation of tau which was antagonized by CQ.

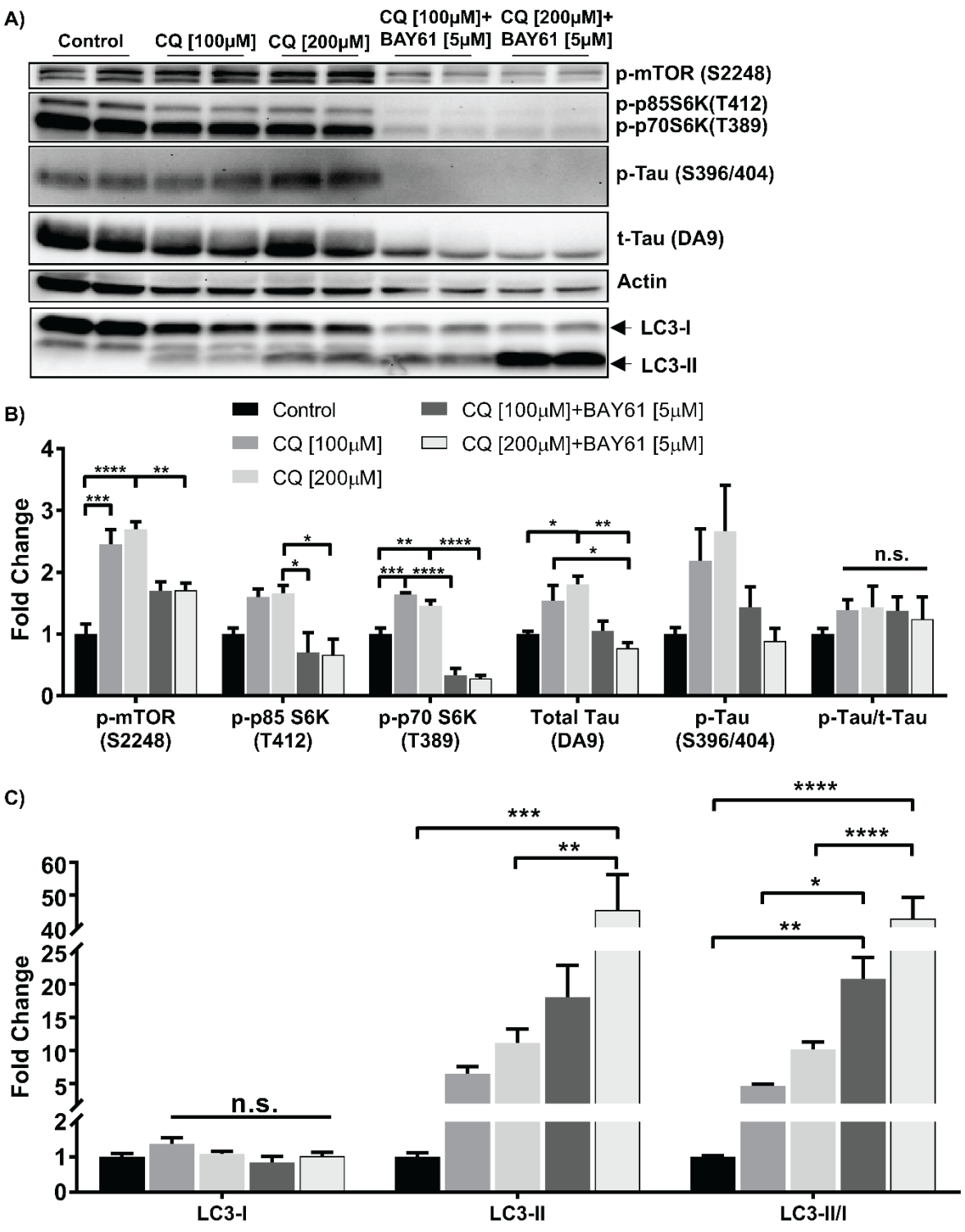
A)
Control
CQ [100μM]
CQ [200μM]
CQ [100μM]+ BAY61 [5μM]
CQ [200μM]+ BAY61 [5μM]
p-mTOR (S2248)
p-p85S6K(T412)
p-p70S6K(T389)
p-Tau (S396/404)
t-Tau (DA9)
Actin
LC3-I
LC3-II
B)
Control
CQ [100μM]
CQ [200μM]
CQ [100μM]+BAY61 [5μM]
CQ [200μM]+BAY61 [5μM]
Fold Change
p-mTOR (S2248)
p-p85 S6K (T412)
p-p70 S6K (T389)
Total Tau (DA9)
p-Tau (S396/404)
p-Tau/t-Tau
n.s.
C)
Fold Change
n.s.
LC3-I
LC3-II
LC3-II/I

Figure 22: SYK inhibition increases the autophagic flux and decreases tau levels in the presence of the lysosomal inhibitor chloroquine

SH-SY5Y cells were treated for 24h with 100-200μM of the lysosomal inhibitor chloroquine (CQ) or a combination of 100-200μM of CQ and 5μM of the SYK inhibitor BAY61-3606.

A) Representative Western blots depicting p-mTOR (S2448), p-S6K (T389, T412), p-tau (S396/404), t-tau, and LC3-I/II are shown.

B-C) Western blots chemiluminescent signals were quantified by densitometry, normalized to actin and presented as histograms.

B) ANOVA with post-hoc Bonferroni test revealed significantly increased p-mTOR (S2448) ($p<0.001$), p-S6K (T389) ($p<0.001$) and t-tau ($p<0.05$) levels compared to untreated control cells following lysosomal inhibition by CQ, whereas a combination of CQ and the SYK inhibitor reverses the effects of CQ, leading to significantly decreased p-mTOR (S2448) ($p<0.01$), p-S6K (T389, T412) ($p<0.0001$, $p<0.05$) and t-tau ($p<0.01$) levels compared to CQ alone (n=4 for each treatment condition).

C) ANOVA with post-hoc Bonferroni test revealed that the combination of the lysosomal and the SYK inhibitor results in significantly increased autophagic flux compared to CQ alone (CQ [100μM]+BAY61-3606, $p<0.05$, CQ [200μM]+BAY61-3606, $p<0.0001$), as measured by LC3II/I while LC3-I levels are not altered significantly (n=4 for each treatment condition).

3.3.4 SYK inhibition does not affect tau translation or transcription

Since SYK acts upstream of the mTOR pathway and the downstream kinase S6K is known to be involved in translation, we investigated whether SYK inhibition and S6K inhibition could impact tau translation (Figure 23). We show that the reduction in t-tau protein level following SYK inhibition is not caused by a reduction of t-tau transcription as measured by RT-PCR (mRNA) (Figure 23). We then assessed protein translation in SH-SY5Y cells that were treated for 24h with either 5µM or 10µM of the SYK inhibitor BAY61-3606 or 5µM, 10µM of the S6K inhibitor PF4708671 or 20µM cycloheximide (inhibitor of protein translation used as a positive control) (Figure 23A). Protein translation was quantified using the SUrface SEnsing of Translation (SUnSET) techniques (Schmidt et al. 2009) by monitoring puromycin incorporation in newly synthesized proteins. Both SYK inhibition and S6K inhibition significantly decreased puromycin incorporation, particularly in proteins of higher molecular weight (Figure 23A). This may suggest a general effect of SYK inhibition on translation that is possibly mediated by S6K inhibition, since SYK inhibition completely prevents S6K phosphorylation and since a direct S6K inhibition mimics the impact of SYK inhibition on protein translation (Figure 23A-B). However, isolation of newly synthesized proteins by immunoprecipitation using an anti-puromycin antibody followed by Western-blot analysis using a total tau antibody (DA9) to quantify the amount of nascent tau, reveals no impact of SYK inhibition (Figure 23C-D) on tau protein translation. In addition, t-tau and 3R mRNA levels in SH-SY5Y cells are not impacted by SYK inhibition with 5µM BAY61-3606 for 4h, 8h, 12h and 24h (Figure 23E-F) showing that SYK inhibition does not affect tau expression at the mRNA level. These data further demonstrate that the decrease in t-tau level, observed following SYK inhibition, is mainly caused by an increase in autophagic tau degradation, rather than a decreased level of tau translation or transcription.



In a subsequent experiment, we tested the effects of S6K inhibition by PF4708671 on the mTOR pathway and tau degradation. S6K inhibition using 10μM of PF4708671 leads to a significant reduction in p-mTOR (S2448) and p-S6K (T389, T412) levels (Figure 24A-B). p-Akt (S473) levels remain unchanged following S6K inhibition. This could imply the existence of a feedback mechanism following S6K inhibition on the mTOR pathway, as S6K is a downstream kinase of mTOR. In fact, S6K has been shown to phosphorylate mTOR (S2448) (Chiang and Abraham 2005) and the reduction in mTOR phosphorylation that we observed with PF4708671 are consistent with that observation. A non-significant trend for a decrease in p-tau (S396/404) and t-tau levels was observed in SH-SY5Y cells (Figure 24A, C) following 24 hours of treatment with the S6K inhibitor, suggesting that the S6K inhibition observed following SYK inactivation does not play a major role in the increased tau clearance induced by SYK inhibition.

In summary, these *in vitro* data show an upstream modulatory role of SYK on the mTOR pathway in SH-SY5Y cells and suggest that SYK is a major kinase that regulates the autophagic degradation of tau. Our data suggest that SYK inhibition increases tau degradation in SH-SY5Y cells by inhibiting the mTOR pathway and increasing the autophagic flux.

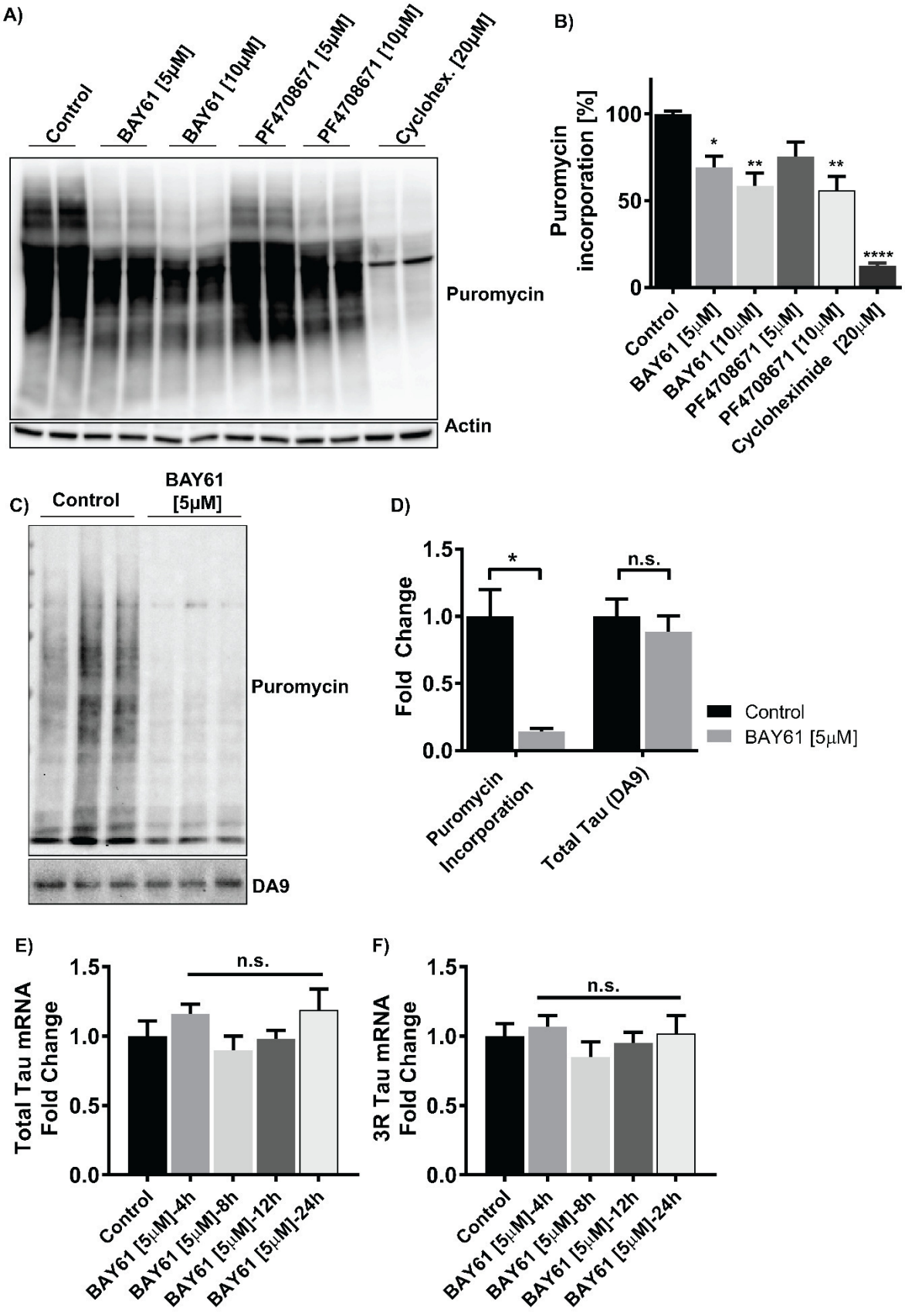
A)
Control
BAY61 [5μM]
BAY61 [10μM]
PF4708671 [5μM]
PF4708671 [10μM]
Cyclohex. [20μM]
Puromycin
Actin
B)
Puromycin incorporation [%]
100
50
0
*
**
**
****
Control
BAY61 [5μM]
BAY61 [10μM]
PF4708671 [5μM]
PF4708671 [10μM]
Cycloheximide [20μM]
C)
Control
BAY61 [5μM]
Puromycin
DA9
D)
Fold Change
1.5
1.0
0.5
0.0
*
n.s.
Control
BAY61 [5μM]
Puromycin Incorporation
Total Tau (DA9)
E)
Total Tau mRNA Fold Change
1.5
1.0
0.5
0.0
n.s.
Control
BAY61 [5μM]-4h
BAY61 [5μM]-8h
BAY61 [5μM]-12h
BAY61 [5μM]-24h
F)
3R Tau mRNA Fold Change
1.5
1.0
0.5
0.0
n.s.
Control
BAY61 [5μM]-4h
BAY61 [5μM]-8h
BAY61 [5μM]-12h
BAY61 [5μM]-24h

Figure 23: SYK inhibition does not alter transcription or translation levels of tau in vitro

A-B) The SUrface SEnsing of Translation (SUnSET) technique (Schmidt et al., 2009) was used to assess the impact of SYK inhibition on protein translation. SH-SY5Y cells were treated with 5-10μM of the SYK inhibitor BAY61-3606 or 5-10μM of the S6K inhibitor PF4708671 for 24 hours or with cycloheximide for 5 hours. Cells were then treated for 1 hour with 10 μg/ml of puromycin. Levels of newly synthesized proteins containing puromycin were then detected by Western blot using an anti-puromycin antibody.

A) Representative Western blots depicting puromycin and actin are shown. B) Western blots chemiluminescent signals were quantified by densitometry, normalized to actin and presented as histograms. ANOVA with post-hoc Bonferroni test revealed total levels of translation are significantly reduced following SYK inhibition (5μM $p<0.05$; 10μM $p<0.01$) or S6K inhibition (10μM $p<0.01$) or following cycloheximide treatment (20μM $p<0.0001$) (n=4 for each treatment condition).

C-D) Anti-puromycin antibodies and protein A-magnetic beads were used for immunoprecipitation of the cell lysate following treatment with 5μM of BAY61-3606. Western blot analysis with anti-puromycin and anti-t-tau antibodies, quantification (as in A-B) and subsequent unpaired t-test (D) revealed no significant difference in total tau translation levels following SYK inhibition while puromycin levels were significantly decreased ($p<0.05$) (n=3 for each treatment condition).

E-F) mRNA levels of total tau and 3R tau were measured by RT-PCR following different durations of treatment with 5μM of the SYK inhibitor BAY61-3606. ANOVA with post-hoc Bonferroni test revealed no significant difference of tau mRNA levels treated with BAY61-3606 for 4, 8, 12 or 24h versus untreated control (n=4 for each treatment condition).

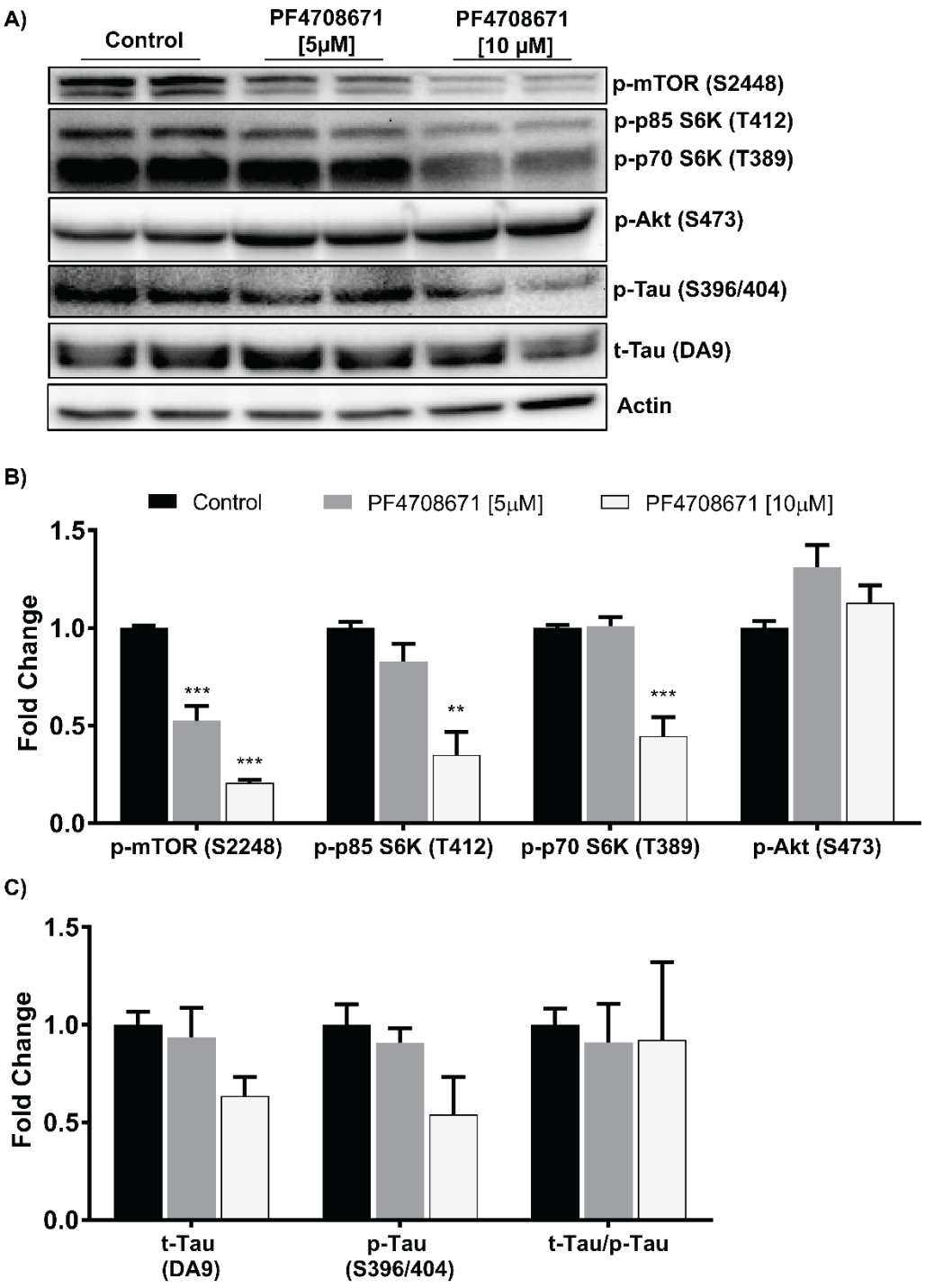
A)
Control
PF4708671 [5μM]
PF4708671 [10 μM]
p-mTOR (S2448)
p-p85 S6K (T412)
p-p70 S6K (T389)
p-Akt (S473)
p-Tau (S396/404)
t-Tau (DA9)
Actin
B)
Control
PF4708671 [5μM]
PF4708671 [10μM]
Fold Change
1.5
1.0
0.5
0.0
***
***
**
***
p-mTOR (S2248)
p-p85 S6K (T412)
p-p70 S6K (T389)
p-Akt (S473)
C)
Fold Change
1.5
1.0
0.5
0.0
t-Tau (DA9)
p-Tau (S396/404)
t-Tau/p-Tau

Figure 24: S6K inhibition by PF4708671 has similar effects as SYK inhibition on the mTOR pathway and tau levels

SH-SY5Y cells were treated for 24h with 5-10μM of the S6K inhibitor PF4708671. Western blots were quantified, normalized to actin and expressed relative to the untreated control cells.

A) Representative Western blots depicting p-mTOR (S2448), p-S6K (T389, T412), p-Akt (S473), p-tau (S396/404), and t-tau are shown. B-C) Western blots chemiluminescent signals were quantified by densitometry, normalized to actin and presented as histograms. B) ANOVA and post-hoc Bonferroni test revealed that p-mTOR (S2448) ($p<0.001$) and p-S6K (T389, T412) ($p<0.001$, $p<0.01$) levels were reduced significantly compared to control following S6K inhibition. P-Akt levels remained unchanged. C) Total tau and p-tau (S396/404) were slightly reduced at the highest dose of PF4708671 (n=4 for each treatment condition).

3.3.5 Suppression of SYK expression mimics pharmacological inhibition of SYK and decreases total tau levels

To validate the data obtained following pharmacological inhibition of SYK with BAY61-3606 and ensure that the effects observed were mediated by SYK inhibition, we knocked down SYK by stably overexpressing a SYK shRNA in SH-SY5Y cells. As expected, a significant decrease in total SYK (t-SYK) (Figure 25) was observed in the SYK knockdown SH-SY5Y cells compared to control SH-SY5Y cells that were stably transfected with a non-sense shRNA using the same vector. We show that SYK knockdown significantly decreases p-mTOR (S2248), p-S6K (T389), p-Akt (S473), p-tau (S396/404) and t-tau levels (Figure 25A-B) mimicking the effects of the SYK inhibitor BAY61-3606 in SH-SY5Y cells. Interestingly, LC3-I and LC3-II were both significantly decreased in the SYK knockdown cells while their ratio remained unchanged (Fig. 6A). These data suggest that genetic suppression of SYK expression leads to an increased autophagy initiation (LC3-I conversion to LC3-II) and an enhancement of lysosomal LC3-II degradation. To further test this hypothesis, we treated both control and SYK knockdown cells for 24h with 200μM of the lysosomal inhibitor chloroquine (CQ). In presence of CQ, the SYK knockdown cells exhibited a significantly increased ratio of LC3-II/I as observed in SH-SY5Y cells treated with CQ and BAY61-3606, implying an increased autophagic flux and suggesting that SYK may impact both the autophagy initiation and lysosomal degradation (Figure 25C).

Overall our data show that the knockdown of SYK mimics the data obtained following pharmacological inhibition of SYK in SH-SY5Y cells resulting in an inhibition of key members of the mTOR pathway and further establishes a key role of SYK as an upstream modulator of the mTOR pathway.

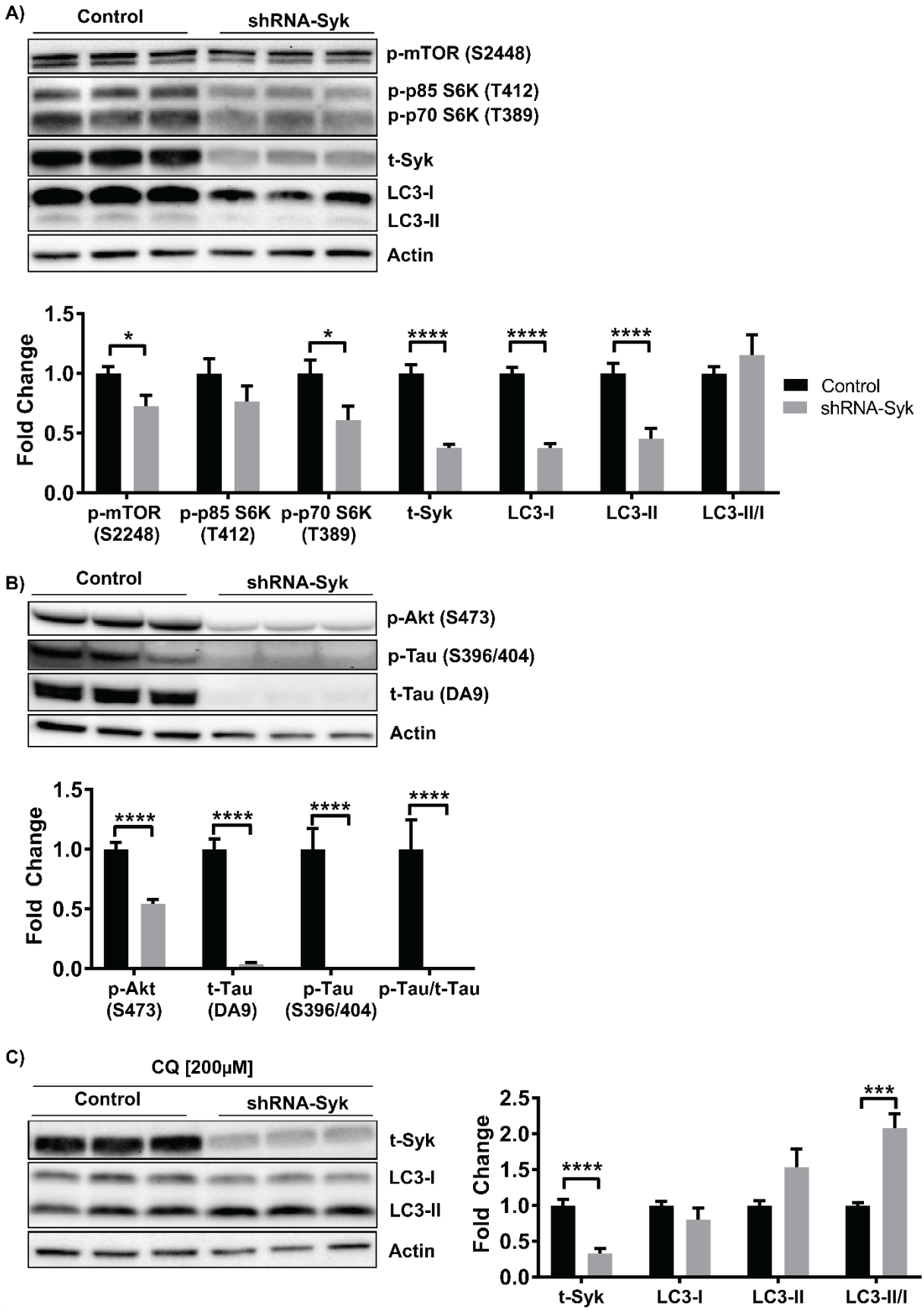
A)
Control
shRNA-Syk
p-mTOR (S2448)
p-p85 S6K (T412)
p-p70 S6K (T389)
t-Syk
LC3-I
LC3-II
Actin
Fold Change
1.5
1.0
0.5
0.0
*
*
****
****
****
p-mTOR (S2248)
p-p85 S6K (T412)
p-p70 S6K (T389)
t-Syk
LC3-I
LC3-II
LC3-II/I
Control
shRNA-Syk
B)
Control
shRNA-Syk
p-Akt (S473)
p-Tau (S396/404)
t-Tau (DA9)
Actin
Fold Change
1.5
1.0
0.5
0.0
****
****
****
****
p-Akt (S473)
t-Tau (DA9)
p-Tau (S396/404)
p-Tau/t-Tau
C)
CQ [200μM]
Control
shRNA-Syk
t-Syk
LC3-I
LC3-II
Actin
Fold Change
2.5
2.0
1.5
1.0
0.5
0.0
****
***
t-Syk
LC3-I
LC3-II
LC3-II/I

Figure 25: SYK knockdown mimics pharmacological inhibition of SYK and decreases total tau levels

Lentiviral vectors expressing SYK specific shRNAs or nonsense control shRNAs were used to stably knockdown SYK gene expression in SH-SY5Y cells.

A-B) Representative Western blots depicting p-mTOR (S2448), p-S6K (T389, T412), t-SYK, and LC3-I/II, as well as p-Akt (S473), p-tau (S396/404), and t-tau are shown. Western blots chemiluminescent signals were quantified by densitometry, normalized to actin and presented as histograms. Unpaired t-tests revealed that in SYK knockdown cells in which t-SYK was decreased significantly ($p<0.0001$), p-mTOR (S2448) ($p<0.05$), p-S6K (T389) ($p<0.05$), p-Akt (S473) ($p<0.0001$), t-tau ($p<0.0001$) and p-tau (S396/404) ($p<0.0001$) levels were also significantly decreased ($n=6$). LC3-I and LC3-II levels were significantly decreased in SYK knockdown cells compared to control ($p<0.0001$) but the ratio of both remains unchanged.

C) Both SYK knockdown and control cells were treated for 24h with 200µM of the lysosomal inhibitor chloroquine (CQ). Representative Western blots depicting t-SYK, and LC3-I/II are shown. Western blots chemiluminescent signals were quantified by densitometry, normalized to actin and presented as histograms. Unpaired t-tests revealed that in SYK knockdown cells in which t-SYK was decreased significantly ($p<0.0001$), the ratio of LC3-II/I was significantly increased ($p<0.001$) ($n=6$ for each treatment condition).

3.4 Discussion

Our previous data have shown that SYK is upregulated in the brain of AD patients and in mouse models of AD (Schweig et al. 2017). In particular, we have shown that SYK is overactivated in neurons affected by the tau pathology and that SYK upregulation promotes tau accumulation without affecting tau expression (Schweig et al. 2017). In the present study, we show that SYK inhibition as well as genetic suppression of SYK expression lower total tau levels in SH-SY5Y cells without impacting tau expression at the mRNA level or tau protein translation, suggesting that other mechanisms are responsible for the increased tau clearance observed following SYK inhibition. Therefore, we investigated the possible effects of SYK inhibition on the mTOR pathway and autophagic degradation of tau in SH-SY5Y cells as autophagy plays a pivotal role in tau degradation (Chesser et al. 2013).

We show for the first time that SYK can regulate the mTOR pathway in neuronal like SH-SY5Y cells and promote the autophagic clearance of tau. These data are consistent with previous studies that have highlighted the role of SYK on the mTOR pathway in immune and cancerous cells (Bartaula-Brevik et al. 2018; Carnevale et al. 2013; Choi et al. 2015; Fruchon et al. 2012; Gao et al. 2017; Krisenko et al. 2015; Leseux et al. 2006). Autophagy is crucial for maintaining the intracellular homeostasis by regulating the turnover of misfolded or damaged proteins, organelles and eliminating dysfunctional components. A decreased functionality of the autophagic degradation system has therefore been linked to aging and neurodegenerative diseases (Cuervo 2008; Eskelinen and Saftig 2009; Funderburk et al. 2010; Ghavami et al. 2014; Lee et al. 2010; Menzies et al. 2015; Nixon 2007; Nixon and Yang 2011). Many studies have now demonstrated the beneficial effects of mTOR inhibition in mouse models of AD and tauopathy, resulting in increased autophagy and in an amelioration of tau pathologies (Jiang et al. 2014b; Ozcelik et al.

2013; Schaeffer et al. 2012; Wang et al. 2016), suggesting that manipulating the mTOR pathway may represent an attractive therapeutic strategy for the treatment of neurodegenerative proteinopathies.

In this study, we demonstrate that SYK inhibition leads to an increased total tau degradation via the mTOR-dependent autophagy pathway while transcription and translation levels of tau remain unchanged. By examining the effects of SYK inhibition on members of the mTOR pathway, using selective inhibitors and activators of the mTOR pathway in combination with the SYK inhibitor BAY61-3606, we confirmed that SYK acts upstream of the mTOR pathway and thereby modulates autophagy in a neuron-like cell line (SH-SY5Y). We show, for example, that the dysregulation of the mTOR pathway, as well as the tau accumulation induced by the AKT stimulator SC79 or by MHY1485 (a direct activator of mTOR) can be reversed by SYK inhibition. We also confirm that inhibition of mTOR with KU0063794 can mimic the effects of SYK inhibition and increase the clearance of tau in SH-SY5Y cells. In addition, the treatment with CQ in combination with the SYK inhibitor revealed an increased autophagic flux following SYK inhibition, as measured by an increase in the LC3II/I ratio, as well as mTOR and S6K inhibition and increased tau degradation. To validate the data obtained with the SYK inhibitor BAY61-3606, we also generated an SH-SY5Y cell line in which SYK has been stably knocked down. We confirm that tau degradation is stimulated and that the mTOR pathway is also inhibited in this SYK knockdown cell line, showing that the effects of BAY61-3606 on tau clearance are recapitulated by genetic suppression of SYK expression and are therefore attributable to an inhibition of SYK.

The data presented in this chapter illustrate that SYK acts as a regulator of autophagy in cells derived from the CNS. The observations made in this study not only provide further evidence for an important role of SYK in the pathogenesis of AD and the development of tau pathologies but also demonstrate that pharmacological SYK inhibition may represent a promising therapeutic strategy for the treatment of AD and other neurodegenerative proteinopathies.



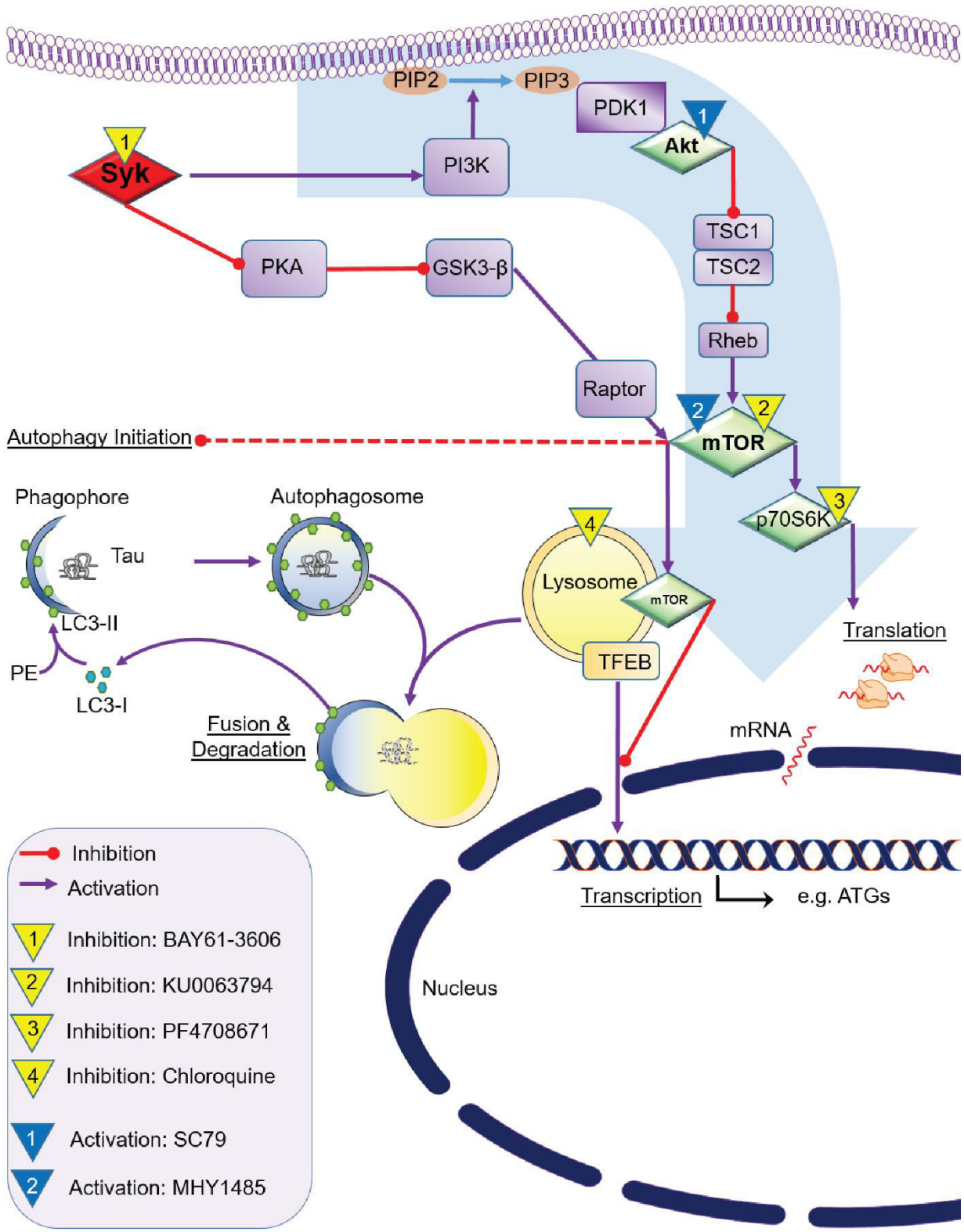
PIP2
PIP3
PDK1
Akt
Syk
PI3K
TSC1
TSC2
PKA
GSK3-β
Rheb
Raptor
mTOR
Autophagy Initiation
Phagophore
Autophagosome
Tau
LC3-II
PE
LC3-I
Lysosome
mTOR
TFEB
p70S6K
Translation
Fusion &
Degradation
mRNA
Transcription
e.g. ATGs
Nucleus
Inhibition
Activation
Inhibition: BAY61-3606
Inhibition: KU0063794
Inhibition: PF4708671
Inhibition: Chloroquine
Activation: SC79
Activation: MHY1485

Figure 26: Schematic depiction of the role of SYK in the mTOR pathway and autophagy
The schematic describes the role of SYK in the mTOR pathway and autophagic tau degradation and highlights the findings presented in this chapter. The mTOR pathway including PI3K, PDK1, Akt, TSC1/2, Rheb, mTOR and S6K and their role in regulation of autophagy have been well described in the literature (for review see (Sarkar, 2013). Our previous studies revealed SYK as an upstream regulator of PKA, GSK3-β, and PI3K (Paris et al., 2014). PI3K is recognized as an upstream member of the mTOR pathway and GSK3-β is known to regulate raptor which is known to form a complex with mTOR (C1) and enhance its downstream signaling. In this present study, we used different activators and inhibitors of members of the mTOR pathway (see legend) to elucidate the effect of SYK inhibition on the mTOR pathway. Our mechanistic experiments lead to the conclusion that SYK acts upstream of the mTOR pathway and thereby influences the activity levels of different members of that pathway and the autophagic degradation of tau. mTOR itself is known to inhibit autophagy. mTOR prevents the transcription factor EB (TFEB) from entering the nucleus, thereby preventing the transcription of autophagy related genes (ATGs), leading to a decreased autophagy initiation. Furthermore, the kinase S6K downstream of mTOR is involved in translation. Our results show that SYK inhibition leads to a decreased activation of the mTOR pathway and results in an increased autophagic flux (LC3-I to LC3-II conversion), leading to an increased lysosomal degradation of tau.

4 Effects of chronic SYK inhibition in Tg Tau P301S mice

4.1 Introduction

In the previous chapter we delineated the role of SYK in the autophagic degradation of tau in a neuroblastoma cell line (SH-SY5Y). Our mechanistic *in vitro* studies identified SYK as an upstream regulator of the mTOR pathway and autophagic tau degradation and showed that an inhibition of SYK may be beneficial for the treatment of tauopathies. Therefore, we investigated the effects of pharmacological SYK inhibition in a chronic treatment paradigm over twelve weeks in a mouse model with established tauopathy (30-week-old Tg Tau P301S) and age-matched wild-type littermates (Figure 27). We assessed the effects of SYK inhibition on key members of the mTOR pathway, tau pathology, behavior (motor and learning), and neuroinflammation.

As mentioned in the previous chapter, the neurodegeneration observed in proteinopathies is, at least partly, caused by a dysfunctional degradation of proteins that are prone to aggregate and an impaired autophagic clearance of macromolecules has been widely accepted to be a major contributor to various neurodegenerative diseases by promoting the accumulation of misfolded proteins (Nixon 2007; Nixon and Yang 2011; Ghavami et al. 2014; Menzies et al. 2015). mTOR is known to regulate autophagy (Jung et al. 2010). AD and FTLD share the accumulation of tau as a common underlying pathology. In human AD and FTLD cases, as well as in mouse models of AD and pure tauopathy, autophagy has been found to be decreased (Zare-Shahabadi et al. 2015; Kragh et al. 2012; Wang et al. 2012) and to contribute to the pathological accumulation of tau aggregates. Impaired autophagy has been linked to an overactive mTOR pathway which acts as a regulator of autophagy initiation and lysosomal degradation, thereby controlling the autophagic flux (Jung et al. 2010; Puertollano 2014).

Previous studies of other research groups have investigated the effects of autophagy activation (pharmacological mTOR inhibition or autophagy initiation by trehalose or TFEB) in tau mouse models. More precisely, in Tg Tau P301S mice direct inhibition of mTOR with either rapamycin or temsirolimus attenuated tau pathology (Ozcelik et al. 2013; Jiang et al. 2014b). Furthermore, stimulation of autophagy by trehalose or by the overexpression of the transcription factor EB (TFEB) were both shown to be efficient in reducing neurodegeneration and mitigating tauopathy in Tg Tau P301S mice (Schaeffer et al. 2012; Wang et al. 2016) suggesting that inhibiting mTOR may have therapeutic value for the treatment of tauopathies.

The involvement of SYK in microglial activation and cytokine production has been investigated in previous *in vitro* studies by other groups. For example, SYK has been shown to mediate the activation of microglial cells induced by Aβ oligomers (Combs et al. 1999; McDonald et al. 1997), while SYK inhibition has been shown to prevent Aβ-mediated neurotoxicity *in vitro* (Combs et al. 1999). A subsequent study also demonstrated that SYK was the mediator of the Aβ-induced elevated cytokine production including interleukin 1 beta (IL-1β) and tumor necrosis factor alpha (TNFα) which is responsible for increased iNOS expression resulting in apoptosis in primary mouse neuronal cultures (Combs et al. 2001). In addition, it has been suggested that SYK contributes to microglial dysfunction in AD (Ghosh and Geahlen 2015). Therefore, we also aimed to investigate the effects of chronic SYK inhibition *in vivo* on neuroinflammation, including microglial and astroglial markers, as well as cytokine levels in brain and plasma.

In our previous studies, we found that SYK inhibition can decrease tau hyperphosphorylation *in vitro*, and *in vivo* in mouse models of tauopathy following an acute treatment (Paris et al. 2014), in part, by promoting the phosphorylation of GSK3-β at the inhibitory Ser9 site (Paris et al. 2014). In addition, we have shown that SYK activation, as measured by p-



SYK (Y525/526) levels, is largely increased subsets of activated microglia of Aβ-overexpressing mouse models of AD (Tg PS1/APPsw, Tg APPsw) and in neurons of a mouse model of tauopathy (Tg Tau P301S) displaying pathological tau species while neurons of wild-type animals showed no activation of SYK (Schweig et al. 2017), suggesting that SYK plays a key role in the formation of AD pathological lesions. Similarly, we observed an increased SYK activation in dystrophic neurites and in neurons affected by the tau pathology in human AD specimens (Schweig et al. 2017).

In the previous chapter we have shown that key members of the autophagic pathway including Akt, mTOR and S6K can be largely influenced by SYK, thereby implying an indirect control of SYK over the autophagic degradation of proteins and providing an explanation for the decreased total tau levels observed following SYK inhibition. Therefore, we wanted to investigate the long-term effects of a chronic SYK inhibition *in vivo* on mTOR and S6K, as well as on tau pathological species.

In this chapter, we show that chronic SYK inhibition lowers pathological tau accumulation in Tg Tau P301S mice by inhibiting hyperactive mTOR. Furthermore, chronic SYK inhibition reduces the levels of pro-inflammatory cytokines, neuronal and synaptic loss and improves locomotor deficits in Tg Tau P301S mice.

These data not only provide further evidence for an important role of SYK in the pathogenesis of AD and the development of tauopathies but also illustrate that pharmacological SYK inhibition may represent a promising therapeutic strategy for the treatment of AD and other neurodegenerative proteinopathies associated with a defective autophagic clearance of misfolded proteins.

4.1.1 Study design

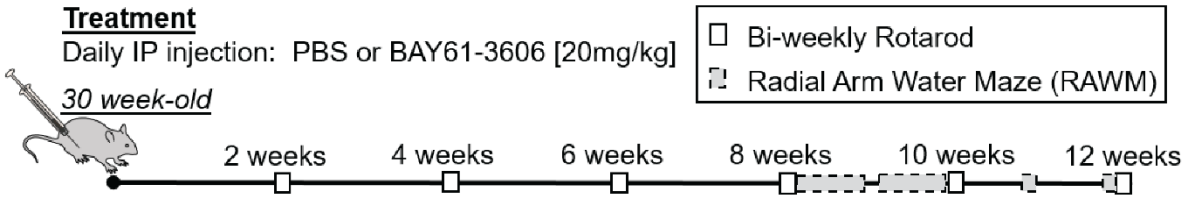

Figure 27: Study design for 12-week chronic SYK inhibition

30-week-old Tg Tau P301S mice and wild-type (WT) littermates were injected intraperitoneally with either PBS (vehicle) or 20mg/kg of the SYK inhibitor BAY61-3606 five consecutive days per week for a total of 12 weeks. 45 animals were treated in total (WT-PBS (n=11), WT-BAY61-3606 (n=11), Tg Tau P301S-PBS (n=11), Tg Tau P301S-BAY61-3606 (n=12)). The motor performance was assessed with the rotarod every 14 days and the spatial memory was assessed on five consecutive days starting in week 8 and an additional probe day 14 days after the last test day. After 12 weeks of treatment, brain homogenates were used to assess target engagement (t-SYK and p-SYK levels), as well as pathological tau species (soluble and insoluble), neuroinflammation (Iba-1, GFAP, iNOS, cytokines), neurodegeneration (NeuN, PSD-95), and effects on autophagic and lysosomal markers (mTOR, S6K, LAMP-1).

4.2 Methods

4.2.1 Animals

All mice were maintained under specific pathogen free conditions in ventilated racks in the Association for Assessment and Accreditation of Laboratory Animal Care International (AAALAC) accredited vivarium of the Roskamp Institute. All experiments involving mice were reviewed and approved by the Institutional Animal Care and Use Committee of the Roskamp Institute before implementation and were conducted in compliance with the National Institutes of Health Guidelines for the Care and Use of Laboratory Animals. Tg Tau P301S (Yoshiyama et al. 2007) mice were obtained from the Jackson Laboratories (ME, USA) and bred with C57BL/6J mice to produce the Tg Tau P301S and wild-type littermates used in this study.

4.2.2 In vivo treatment

30-week-old Tg Tau P301S mice and wild-type (WT) littermates were injected with either PBS (vehicle) or 20mg/kg of the SYK inhibitor BAY61-3606 five consecutive days per week for a total of 12 weeks. 45 animals were treated in total (WT-PBS (n=11), WT-BAY61-3606 (n=11), Tg Tau P301S-PBS (n=11), Tg Tau P301S-BAY61-3606 (n=12)). 2-(7-(3,4-dimethoxyphenyl) imidazo[1,2-c] pyrimidin-5-ylamino) nicotinamide hydrochloride hydrate (BAY61-3606) was synthetized as previously described (Takeshi Yura, Arnel B. Concepcion, Gyoonhee Han, Makiko Marumo, Hiroko Katsumata, Norihiro Kawamura, Toshio Kokubo, Hiroshi Komura, Yingfu Li, Timothy B. Lowinger, Muneto Mogi, Noriyuki Yamamoto, Nagahiro Yoshida, Scott Miller, Margaret A. Popp, Aniko M. Redmann, Martha E. Rodriguez, William J. Scott, Ming Wang 2001). The identity and purity of the compound obtained was analyzed by tandem mass spectroscopy (MS (ESI, pos. ion) m/z: 391.1 (M+1)). The activity of the synthesized BAY61-3606 was further

compared against a batch of BAY61-3606 obtained by a commercial vendor (Sigma-Aldrich, MO, USA) by assessing its potency for inhibiting p65-NFκB and STAT3 phosphorylation induced by TNFα in SH-SY5Y cells as previously described (Paris et al. 2014) (data not shown).

4.2.3 Behavioral Analysis

The spatial memory of the mice was assessed after 8 weeks of treatment with either PBS or 20mg/kg of the SYK inhibitor BAY61-3606 using the radial arm water maze (RAWM). The mice underwent 9 trials per day for a total of five consecutive days plus an additional probe day two weeks after the fifth day of testing (day 20). The RAWM consists of six arms that are distinguishable by unique visual cues. The mice were placed into one of the five arms and had to find the hidden platform in the sixth arm. Each trial ended after one minute and errors were calculated after tracking the movements using the EthoVision software (Noldus, VA, USA). Motor performance was assessed using a Rotarod apparatus every 14 days. The mice were placed onto a horizontally oriented, rotating cylinder. The baseline level was set to 5 rpm. The speed of the rotation of the cylinder was set up to increase to 50 rpm within 1 minute. The latency to fall was measured in seconds. Each mouse underwent 3 trials per day and the average latency to fall was calculated. Mice showing signs of partial paralysis of the hind limbs were excluded from the behavioral assessments.

4.2.4 Tissue Processing

All mice were humanely euthanatized and their brains were collected, snap-frozen in liquid nitrogen and stored at -80˚C until processing. The method of euthanasia used follows the AVMA (American Veterinary Medical Association) guidelines for the euthanasia of animals. Briefly, mice were rendered unconscious through inhalation of 5% isoflurane in oxygen using a vaporizer and a gas chamber. While under anesthesia, after verifying the absence of reflexes, mice were euthanatized by exsanguination (blood was withdrawn from cardiac puncture).

Subsequently, the brains were homogenized in Mammalian Protein Extraction Reagent (M-PER™, Thermo Fisher Scientific, MA, USA) containing Halt protease & phosphatase single use inhibitor/EDTA (Thermo Fisher Scientific, MA, USA) and 1 mM PMSF. Brain homogenates were centrifuged at 4˚C, 21,817xG for 30 minutes. The supernatant (detergent soluble fraction) was collected and stored at -80˚C until being assayed for total tau and phosphorylated tau as described below. The pellet (detergent insoluble fraction) was re-suspended by sonication in M-PER (1v:1v). A portion of this detergent insoluble fraction was treated with an equal volume of 5M guanidine isothiocyanate to dissociate and re-solubilize tau aggregates and quantify the amount of detergent insoluble total tau and phosphorylated tau at multiple epitopes as described below. The remaining portion of the detergent insoluble fraction was used to assess the levels of tau oligomers and tau pathogenic conformers under native conditions as described below.

4.2.5 Immunoblotting

For dot blots, 3µl of each sample were pipetted onto a nitrocellulose membrane (pore size 45µm, Bio-Rad Laboratories, CA, USA). Membranes were blocked in TBS containing 5% non-fat dried milk for 1h and were hybridized with the primary antibody (anti-SYK (4D10, 1:1000, Santa Cruz, TX, USA), anti-p-tau S396/404 (PHF-1, 1:1000, Dr. Peter Davies' Lab), anti-t-tau (DA9, 1:1000, Dr. Peter Davies' Lab), anti-p-tau S202 (CP13, 1:1000, Dr. Peter Davies' Lab), anti-p-tau T231 (RZ3, 1:1000, Dr. Peter Davies' Lab), anti-conformer-tau (MC1, 1:1000, Dr. Peter Davies' Lab), anti-oligomeric-tau (TOC1, 1:1000, Dr. Lester Binder's Lab), anti-p-SYK (Y525/526), anti-p-mTOR (S2448), anti-p-S6K (T389/T412), anti-NeuN, anti-LAMP-1, anti-iNOS (all 1:1000, Cell Signaling, MA, USA), anti-GFAP (1:5000, DAKO, USA), anti-Iba1 (1:1000, Abcam, MA, USA), anti-beta-tubulin (1:1000, BD Biosciences, CA, USA) overnight at 4˚C. Subsequently, the membranes were incubated for 1h in HRP-conjugated anti-mouse or anti-rabbit secondary antibody (1:1000, Cell Signaling, MA, USA). Western blots and Dot Blots were visualized using chemiluminescence (Super Signal West Femto Maxium Sensitity Substrate, Thermo Fisher Scientific, MA, USA). Signals were quantified using ChemiDoc XRS (Bio-Rad Laboratories, CA, USA) and densitometric analyses were performed using Quantity One (Bio-Rad Laboratories, CA, USA) image analysis software. All quantifications were normalized to beta-tubulin levels.

4.2.6 Total protein concentration (BCA)

Total protein levels of *in vivo* samples were determined using the Pierce BCA Protein Assay Kit (Thermo Fisher Scientific, MA, USA). The samples were prepared and measured as directed by the manufacturer's handbook.

4.2.7 ELISA for PSD-95 and cytokine levels

For quantification of *in vivo* PSD-95 and cytokine levels the MESO QuickPlex SQ 120 and the appropriate ELISA kits were used (Meso Scale Diagnostics, MD, USA). The samples were prepared and measured as directed by the manufacturer's instructions. 16 wells were used for the standard. 10 samples (brain homogenates) from each treatment group were randomly selected. The values for all brain samples were normalized to total protein level as determined by the BCA method.

4.2.8 Statistical Analyses

The data were analyzed and plotted with GraphPad Prism (GraphPad Software, Inc., CA, USA). The Shapiro-Wilk test for normality was used to test for Gaussian distribution. Statistical significance was determined by either ANOVA (for comparisons of three or more groups), 2-way ANOVA (behavioral test) or t-tests (SYK knockdown) or the non-parametric Kruskal-Wallis (Cytokine ELISA), where appropriate for data that were not normally distributed. The ROUT test (Q=1%) was used for the identification or rejection of statistical outliers. All data are presented as mean ± the standard error of the mean (SEM) and $p<0.05$ was considered significant (*$p<0.05$, **$p<0.01$, ***$p<0.001$, ****$p<0.0001$).



4.3 Results

4.3.1 Chronic SYK inhibition reduces p-SYK and t-SYK levels in Tg Tau P301S mice, rescues neuronal and synaptical loss and decreases mTOR activity

Following the *in vitro* studies presented in the previous chapter, we investigated the effects of chronic SYK inhibition on tau levels, neurodegeneration, inflammation and behavior *in vivo* using a tauopathy mouse model. 30-week-old Tg Tau P301S mice and age-matched wild-type (WT) littermates were treated for 12 weeks with 20 mg/kg of the SYK inhibitor BAY61-3606 or PBS as a vehicle control (Figure 28). As we previously demonstrated (Schweig et al. 2017) SYK activation, as measured by p-SYK (Y525/526) levels, is significantly higher in Tg Tau P301S-PBS mice compared to WT controls (Figure 28).

Importantly, the chronic treatment with the SYK inhibitor significantly reduced the elevated levels of p-SYK (Y525/526) (Figure 28) confirming target engagement following treatment with BAY61-3606. t-SYK levels were also increased in Tg Tau P301S-PBS mice compared to WT littermates and were significantly decreased following chronic SYK inhibition (Figure 28).

The neuron-specific protein NeuN (Mullen et al. 1992) has been used previously as a marker for neurodegeneration or neuronal loss (Wolf et al. 1996; Maximova et al. 2010). Neuronal loss revealed by a reduction in NeuN has been described previously in Tg Tau P301S mice (Schaeffer et al. 2012; Wang et al. 2012). Post-synaptic density-95 (PSD-95) has been shown to promote the stabilization of synapses and to regulate synaptic transmission (Béïque and Andrade 2003; Chen et al. 2011; Taft and Turrigiano 2014). In addition, it has been established that levels of PSD-95 are significantly reduced in Tg Tau P301S mice and reflect synaptic loss (Yoshiyama et al. 2007; Leyns et al. 2017). We therefore investigated whether chronic inhibition of SYK with BAY61-3606 was able to affect NeuN and PSD-95 levels in Tg Tau P301S mice. Our data show



that PSD-95 and NeuN levels were reduced in Tg Tau P301S-PBS mice compared to WT littermates (Figure 28) confirming previous observations (Yoshiyama et al. 2007; Leyns et al. 2017). Interestingly, the chronic treatment with the SYK inhibitor, was able to considerably increase PSD-95 and NeuN levels in Tg Tau P301S mice (Figure 28), suggesting that SYK inhibition prevents neuronal and synaptic loss in Tg Tau P301S mice.

P-mTOR (S2448) levels were significantly increased in Tg Tau P301S-PBS mice compared to WT littermates (Figure 28), suggesting there might be an associated reduction in autophagy. As observed in our *in vitro* experiments, SYK inhibition was able to significantly decrease the abnormally high p-mTOR (S2448) levels observed in Tg Tau P301S brains bringing them back to the levels observed in WT littermates (Figure 28). P-S6K (T389) levels were slightly elevated in Tg Tau P301S-PBS mice compared to WT littermates and chronic SYK inhibition was able to significantly decrease p-S6K (T389) levels in the brain of Tg Tau P301S mice (Figure 28), confirming an inhibition of the mTOR pathway. Interestingly, the lysosomal-membrane associated protein 1 (LAMP-1) was also significantly increased in Tg Tau P301S-PBS mice compared to WT littermates while chronic SYK inhibition was able to significantly reduce LAMP-1 levels in the brains of Tg Tau P301S mice (Figure 28).

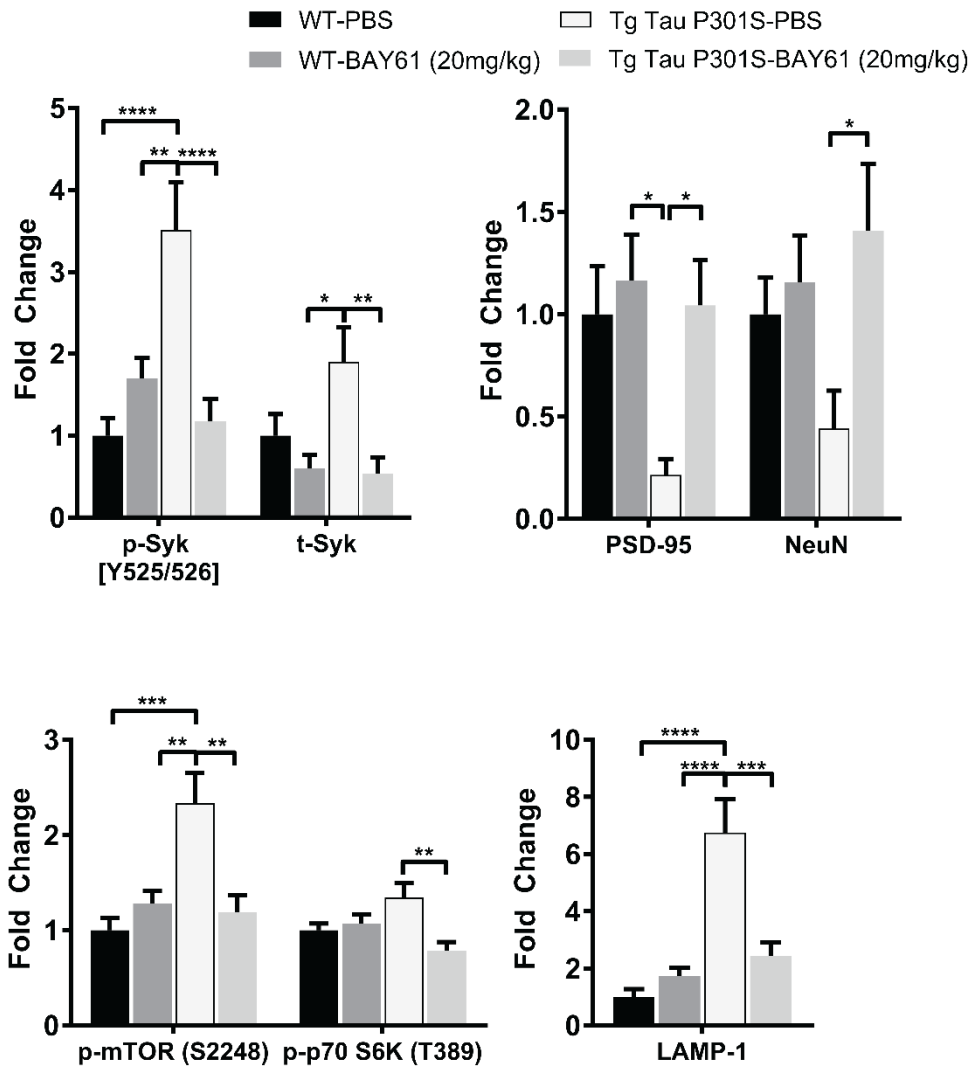

Figure 28: Chronic SYK inhibition reduces p-SYK and t-SYK levels in Tg Tau P301S mice, rescues neuronal and synaptic loss and decreases mTOR activity

PSD-95 levels were measured by ELISA. Levels of p-SYK, t-SYK, NeuN, p-mTOR (S2448), p-S6K (T389) and LAMP-1 were obtained by dot blots whose chemiluminescent signals were quantified and normalized to β-tubulin levels. All values are presented relative to WT-PBS (control).

Upper panel: ANOVA with post-hoc Bonferroni test revealed that SYK activation, as measured by p-SYK (Y525/526) levels, was significantly increased in Tg Tau P301S-PBS mice compared to WT controls ($p<0.0001$). Chronic treatment with 20mg/kg of the SYK inhibitor BAY61-3606 reduced these levels significantly ($p<0.0001$). T-SYK levels were also significantly reduced following treatment in Tg Tau P301S mice ($p<0.01$). PSD-95 and NeuN levels were significantly increased ($p<0.05$) following treatment with BAY61-3606 in Tg Tau P301S mice compared to untreated (PBS) controls.

Lower panel: ANOVA with post-hoc Bonferroni test revealed that mTOR activation, as measured by p-mTOR (S2248) levels, was significantly increased in Tg Tau P301S-PBS mice compared to WT controls ($p<0.001$). Chronic treatment with 20mg/kg of the SYK inhibitor BAY61-3606 reduced these levels significantly ($p<0.01$). LAMP-1 levels were also significantly increased in Tg Tau P301S-PBS mice compared to WT controls ($p<0.0001$). Chronic treatment with 20mg/kg of the SYK inhibitor BAY61-3606 reduced these levels significantly ($p<0.001$). The treatment also reduced p-S6K (T389) levels significantly in Tg Tau P301S mice ($p<0.01$).

4.3.2 Chronic SYK inhibition reduces tau accumulation and improves motor performance in Tg Tau P301S mice

Following the assessment of target engagement, we investigated the effects of chronic SYK inhibition on detergent soluble and insoluble tau levels in the brains of Tg Tau P301S mice. We found that chronic SYK inhibition over a 12-week period significantly reduced the levels of t-tau, p-tau (S396/404 and S202) and tau oligomers (TOC1) in the detergent insoluble fraction of brain homogenates compared to PBS-treated Tg Tau P301S mice. A trend for a reduction in detergent insoluble p-tau (S231) and tau conformers (MC1) was also observed following chronic SYK inhibition (Figure 29A). Detergent soluble total tau levels were also reduced following SYK inhibition compared to PBS-treated Tg Tau P301S mice, however, only soluble p-tau (S231) was significantly impacted by SYK inhibition (Figure 29B).

In addition to the reduced tau burden, a significant improvement in locomotor coordination, measured by a decreased latency to fall in the rotarod apparatus, was observed in Tg Tau P301S mice following chronic inhibition of SYK (Figure 29C). Furthermore, Tg Tau P301S mice receiving the Syk inhibitor, performed better after four days of training in the radial arm water maze (RAWM) compared to PBS-treated controls (Figure 29D). After 20 days, following the last training trial in the RAWM, the performance of the mice was reevaluated to determine whether the mice were able to remember the position of the hidden platform. On day 20, Tg Tau P301S mice treated with BAY61-3606 were making less errors to find the hidden platform than placebo treated Tg Tau P301S.

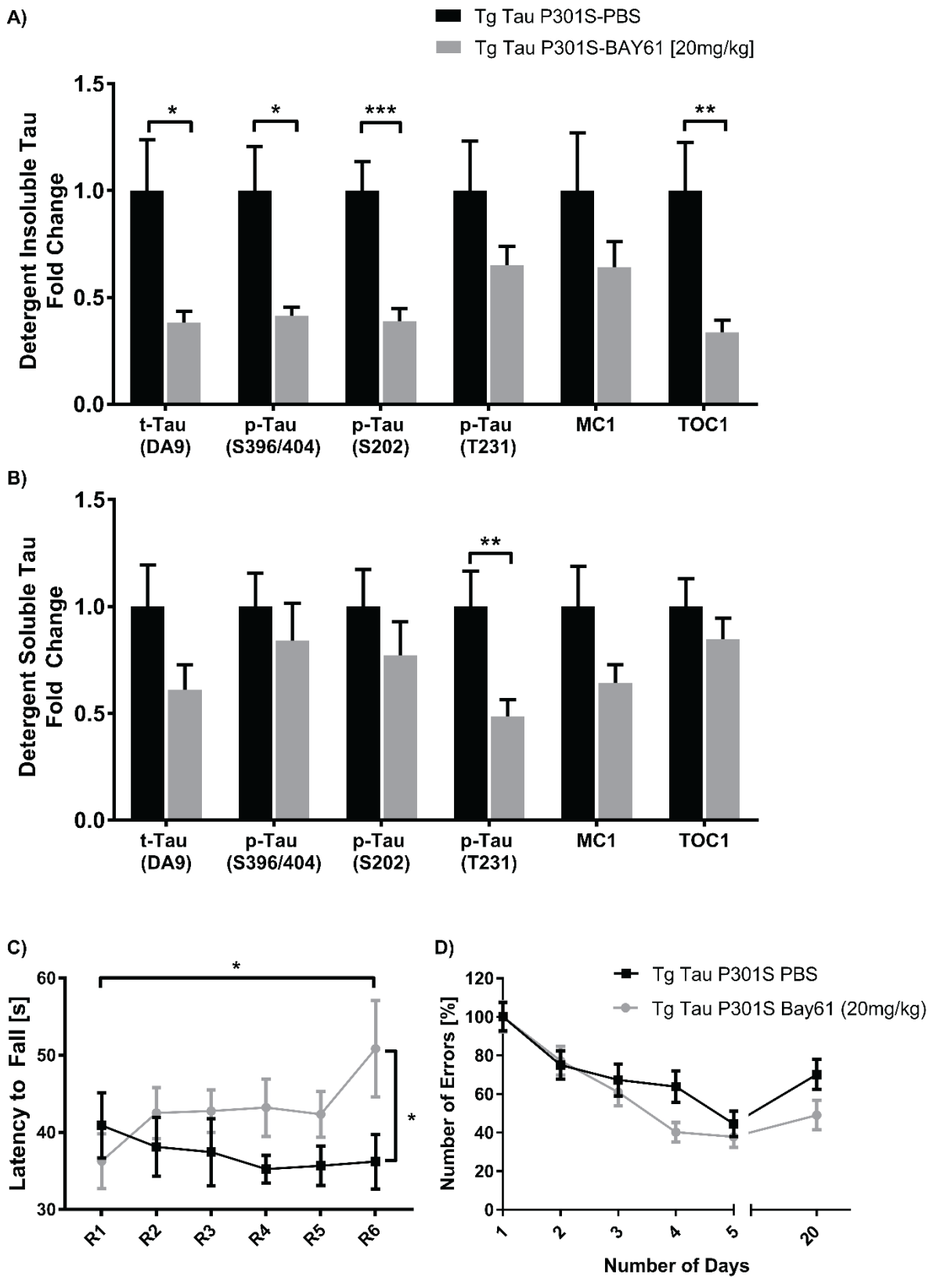
A)
Tg Tau P301S-PBS
Tg Tau P301S-BAY61 [20mg/kg]
Detergent Insoluble Tau Fold Change
1.5
1.0
0.5
0.0
*
*
***
**
t-Tau (DA9)
p-Tau (S396/404)
p-Tau (S202)
p-Tau (T231)
MC1
TOC1
B)
Detergent Soluble Tau Fold Change
1.5
1.0
0.5
0.0
**
t-Tau (DA9)
p-Tau (S396/404)
p-Tau (S202)
p-Tau (T231)
MC1
TOC1
C)
Latency to Fall [s]
60
50
40
30
*
*
R1
R2
R3
R4
R5
R6
D)
Tg Tau P301S PBS
Tg Tau P301S Bay61 (20mg/kg)
Number of Errors [%]
120
100
80
60
40
20
0
1
2
3
4
5
20
Number of Days

Figure 29: Chronic SYK inhibition reduces insoluble and soluble tau levels and improves motor performance in Tg Tau P301S mice

30-week-old Tg Tau P301S mice and wild-type (WT) littermates were treated for 12 weeks with either PBS (control) or 20mg/kg of the SYK inhibitor BAY61-3606 (administered IP) Tg Tau P301S-PBS (n=11), Tg Tau P301S-BAY61-3606 (n=12).

A) Detergent (M-PER) insoluble, as well as B) detergent (M-PER) soluble tau levels were obtained by dot blots whose chemiluminescent signals were quantified, normalized to β-tubulin levels and expressed as a fold change of the average tau values quantified in placebo treated Tg Tau P301S mice. A) Unpaired t-tests revealed that insoluble total tau levels ($p<0.05$), as well as p-tau (S396/404 ($p<0.05$), S202 ($p<0.001$)) and tau oligomers (TOC1) ($p<0.01$) were significantly reduced following chronic SYK inhibition. B) Soluble p-tau (S231) levels were reduced significantly following treatment with BAY61-3606.

C) The animals' motor performance was tested using the rotarod every 14 days following the initiation of the BAY61-3606 treatment. Two-way ANOVA with post-hoc Bonferroni revealed a significant difference in motor performance for the last day (R6) between the control (Tg Tau P301S-PBS) mice and the mice treated with the SYK inhibitor. Motor performance of Tg Tau P301S-BAY61-3606 mice improved significantly between the first and last day (R1-R6) of assessment but not in control.

D) There was no statistically significant difference between Tg Tau P301S mice treated with PBS and BAY61-3606 in percentage of errors made as measured by two-way ANOVA with post-hoc Bonferroni. However, the mice that received the treatment with the Syk inhibitor performed better on days 4 and 20.

4.3.3 Chronic SYK inhibition decreases neuroinflammation in Tg Tau P301S mice

Since SYK is known to be involved in the activation of microglia (McDonald et al. 1997; Combs et al. 1999), we investigated the effects of chronic SYK inhibition on neuroinflammation in Tg Tau P301S mice. As expected, the microglial marker Iba-1 was significantly increased in Tg Tau P301S-PBS mice compared to WT littermates (Figure 30A). Chronic SYK inhibition was able to decrease Iba-1 levels significantly in Tg Tau P301S mice (Figure 30A). We also investigated the levels of inducible nitric oxide synthase (iNOS) which is known to be elevated in activated microglia (Cherry et al. 2014). iNOS levels were found to be significantly increased in Tg Tau P301S-PBS mice compared to WT littermates (Figure 30A). Chronic SYK inhibition appeared to significantly lower iNOS levels in Tg Tau P301S mice (Figure 30A). Levels of the astrocytic marker, glial fibrillary acidic protein (GFAP) were similar with or without BAY61-3606 treatment in wild-type and Tg Tau P301S mice (Figure 30A). We also quantified by ELISA the amount of various pro-inflammatory cytokines in the brain and plasma. Overall, pro-inflammatory cytokine levels for most of the cytokines analyzed were higher in Tg Tau P301S-PBS mice compared to WT littermates and decreased in the Tg Tau P301S-BAY61-3606 treatment group (Figure 30B).

In summary, these data show that chronic SYK inhibition over a course of twelve weeks, leads to significant reduction in neuronal and synaptic loss, inhibition of hyperactive mTOR, decreased tau burden, improved motor performance and suppression of neuroinflammation in Tg Tau P301S mice. Importantly, the decreased t-tau and p-mTOR levels observed suggest that *in vivo*, SYK inhibition also triggers the degradation of tau via an autophagy-dependent mechanism similar to the one observed *in vitro*.

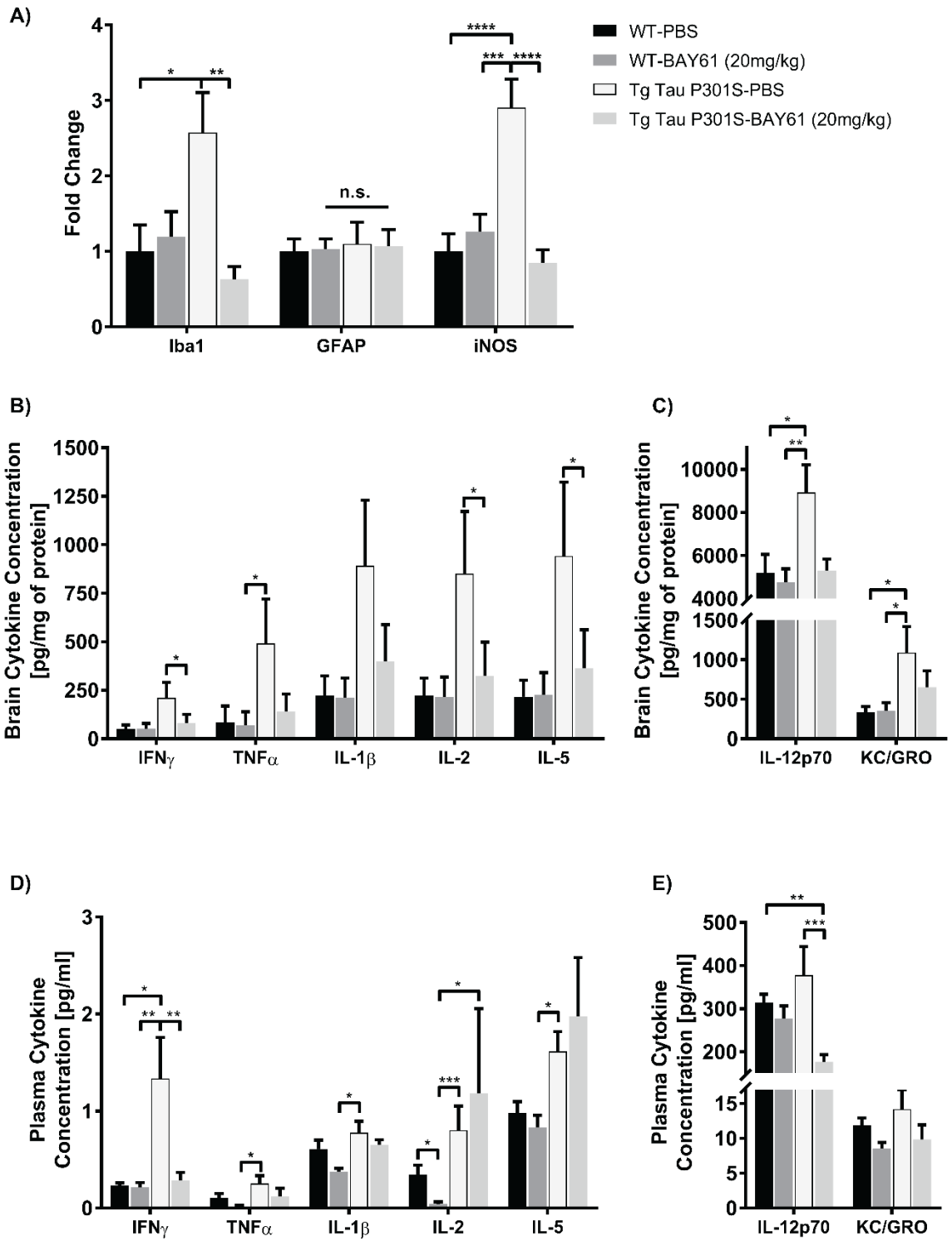
A)
Fold Change
WT-PBS
WT-BAY61 (20mg/kg)
Tg Tau P301S-PBS
Tg Tau P301S-BAY61 (20mg/kg)
n.s.
Iba1
GFAP
iNOS
B)
Brain Cytokine Concentration [pg/mg of protein]
IFNγ
TNFα
IL-1β
IL-2
IL-5
C)
Brain Cytokine Concentration [pg/mg of protein]
IL-12p70
KC/GRO
D)
Plasma Cytokine Concentration [pg/ml]
IFNγ
TNFα
IL-1β
IL-2
IL-5
E)
Plasma Cytokine Concentration [pg/ml]
IL-12p70
KC/GRO

Figure 30: Chronic SYK inhibition decreases microgliosis and reduces pro-inflammatory cytokines in Tg Tau P301S mice

30-week-old Tg Tau P301S mice and wild-type (WT) littermates were treated for 12 weeks with either PBS (control) or 20mg/kg of the SYK inhibitor BAY61-3606 (administered IP) WT-PBS (n=11), WT-BAY61-3606 (n=11), Tg Tau P301S-PBS (n=11), Tg Tau P301S-BAY61-3606 (n=12).

A) Iba-1, GFAP and iNOS levels were obtained by dot blots whose chemiluminescent signals were quantified, normalized to β-tubulin levels and expressed as a fold change of the average tau values quantified in placebo treated Tg Tau P301S mice. ANOVA with Bonferroni tests revealed that Iba-1 ($p<0.05$) and iNOS ($p<0.0001$) levels were significantly increased in Tg Tau P301S-PBS mice compared to WT-PBS mice suggesting that microglia are activated in Tg Tau P301S mice. Chronic SYK inhibition significantly reduced Iba-1 ($p<0.01$) and iNOS ($p<0.0001$) levels in Tg Tau P301S mice. GFAP levels did not differ significantly between the groups.

B-E) Brain and plasma cytokine levels were quantified by ELISA. Brain cytokine levels were normalized to total protein levels. B-C) Kruskal-Wallis test revealed that the elevated brain cytokine levels observed in Tg Tau P301S-PBS (control) mice were significantly reduced following chronic SYK inhibition (Tg Tau P301S-BAY61-3606) for IFNγ ($p<0.05$), IL-2 ($p<0.05$), IL-5 ($p<0.05$) and IL12p70, KC/GRO levels were significantly increased ($p<0.05$) in Tg Tau P301S-PBS mice compared to WT controls.

D-E) Kruskal-Wallis test revealed that the elevated plasma cytokine levels observed in Tg Tau P301S-PBS (control) mice were significantly reduced following chronic SYK inhibition (Tg Tau P301S-BAY61-3606) for IFNγ ($p<0.01$), IL-12p70 ($p<0.001$) and IFNγ levels were significantly increased ($p<0.05$) in Tg Tau P301S-PBS mice compared to WT controls.

4.4 Discussion

Our previous data have shown that SYK is upregulated in the brain of AD patients and in mouse models of AD (Schweig et al. 2017). In particular, we have shown that SYK is overactivated in neurons affected by the tau pathology and that SYK upregulation promotes tau accumulation without affecting tau expression (Schweig et al. 2017). Furthermore, in the previous chapter we have shown *in vitro* that SYK acts upstream of the mTOR pathway, thereby indirectly influencing the autophagic degradation of tau. SYK inhibition as well as genetic suppression of SYK expression lowered total tau levels in SH-SY5Y cells without impacting tau expression at the mRNA level or tau protein translation suggesting that other mechanisms are responsible for the increased tau clearance observed following SYK inhibition. Therefore, we investigated the possible effects of SYK inhibition on the mTOR pathway and autophagic degradation of tau in Tg Tau P301S following a chronic treatment with the SYK inhibitor BAY61-3606.

Autophagy is a crucial mechanism for maintaining the intracellular homeostasis by regulating the turnover of misfolded or damaged proteins, organelles and eliminating dysfunctional components. Therefore, a decreased autophagic degradation has been linked to aging and neurodegenerative diseases (Cuervo 2008; Eskelinen and Saftig 2009; Funderburk et al. 2010; Ghavami et al. 2014; Lee et al. 2010; Menzies et al. 2015; Nixon 2007; Nixon and Yang 2011). Many studies have now demonstrated the beneficial effects of mTOR inhibition in mouse models of AD and tauopathy, resulting in increased autophagy and in an amelioration of tau pathologies (Jiang et al. 2014b; Ozcelik et al. 2013; Schaeffer et al. 2012; Wang et al. 2016), suggesting that manipulating the mTOR pathway may represent an attractive therapeutic strategy for the treatment of neurodegenerative proteinopathies.

In this chapter, we demonstrate that chronic SYK inhibition in a mouse model of pure tauopathy leads to an increased total tau degradation via the mTOR-dependent autophagy pathway, thereby recapitulating the results obtained from *in vitro* experiments, presented in the previous chapter.

SYK inhibition was initiated in 30-week-old Tg Tau P301S mice. By that age, Tg Tau P301S already show significant tau accumulation and hyperphosphorylation as well as neuroinflammation and synaptic loss (Yoshiyama et al. 2007). We treated Tg Tau P301S mice for 12 weeks with BAY61-3606 and observed that the treatment was well tolerated. Behavioral analyses revealed that locomotor performances of the Tg Tau P301S mice were improved following SYK inhibition in the rotarod apparatus. Our biochemical characterizations of the brain of these mice, confirmed our previous findings that SYK activation is increased in Tg Tau P301S mice (Schweig et al. 2017), and revealed target engagement following BAY61-3606 treatment, as the phosphorylation of SYK in the activation loop of the kinase (Y525/526) was significantly reduced in Tg Tau P301S mice treated with BAY61-3606. We found that mTOR activation was increased in Tg Tau P301S mice compared to WT littermates, suggesting that autophagy could be decreased and contribute to pathological tau accumulation in Tg Tau P301S mice. Tg Tau P301S mice treated with the SYK inhibitor showed a reduction of mTOR activation confirming the *in vitro* data showing the impact of SYK on the regulation of the mTOR pathway.

We analyzed the impact of SYK inhibition on the accumulation of tau pathogenic species in the soluble and insoluble detergent fractions of Tg Tau P301S brain homogenates. Detergent insoluble tau species have been shown to generally contain tau aggregates that contribute to neurodegeneration (Fatouros et al. 2012; Yanamandra et al. 2015) while hyperphosphorylated tau in the detergent soluble fraction has previously been associated with synaptic loss (Kimura et al. 2010). We found that t-tau levels, as well as p-tau (S396/404, S202) levels and tau oligomers



(TOC1) were significantly decreased in the detergent insoluble fraction, following SYK inhibition in Tg Tau P301S mice. Given that mTOR phosphorylation was reduced following SYK inhibition in Tg Tau P301S mice, these data further suggest that the decreased accumulation of pathological tau species observed, results in part, from an increased tau degradation via the restored mTOR-autophagy pathway.

It is well known that tauopathies including AD and frontotemporal dementia with parkinsonism-17 (FTDP-17) lead to neurodegeneration. In mouse models of tauopathy including the Tg Tau P301S mice, reduced levels of the neuronal marker NeuN have been found and interpreted as evidence of neurodegeneration (Schaeffer et al. 2012; Wang et al. 2016). Interestingly, it has been shown (Schaeffer et al. 2012; Wang et al. 2016) that NeuN levels were restored in Tg Tau P301S mice following stimulation of autophagy. In addition, it was found that stimulation of autophagy in Tg Tau P301S mice can decrease insoluble tau, as well as p-tau (AT100 and PHF-1) levels (Schaeffer et al. 2012; Wang et al. 2016). The results of our study are in line with these findings. We also observed decreased levels of synaptic and neuronal markers PSD-95 and NeuN in Tg Tau P301S mice which were considerably increased following chronic SYK inhibition, suggesting that SYK inhibition can prevent neurodegeneration and synaptic loss induced by tau pathogenic species in Tg Tau P301S mice.

Neuroinflammation has been shown previously to be increased in Tg Tau P301S mice (Bellucci et al. 2004; Yoshiyama et al. 2007) and is likely to exacerbate the neurodegeneration and tau pathology (Bellucci et al. 2004). We carefully investigated the impact of chronic SYK inhibition on neuroinflammation in Tg Tau P301S mice by analyzing the levels of various pro-inflammatory cytokines and by quantifying Iba-1 and iNOS levels as markers of microgliosis (Korzhevskii and Kirik 2016; Xu et al. 2017), as well as GFAP to measure astrogliosis (Sofroniew

and Vinters 2010). We found that Iba-1, iNOS and various pro-inflammatory cytokine levels were markedly increased in Tg Tau P301S mice compared to WT littermates, while GFAP levels were unchanged. Chronic SYK inhibition appeared to significantly reduce Iba-1, iNOS and pro-inflammatory cytokine levels in Tg Tau P301S mice suggesting that SYK plays a key role in the induction of neuroinflammation by tau pathogenic species. Pro-inflammatory cytokines produced by activated microglia have been shown to promote tau hyperphosphorylation (Bernhardi et al. 2010; Wang et al. 2015a) and therefore SYK inhibition by directly targeting the activation of microglia could also contribute to the decreased tau hyperphosphorylation observed.

Several studies have linked neuroinflammation and a deficit of autophagy in the context of neurodegenerative diseases. It has been shown, for example, that mTOR or S6K inhibition by rapamycin or PF4708671, respectively, prevents neuroinflammation in a mouse model of cerebral palsy (Srivastava et al. 2016). In that mouse model, the mice were subjected to hypoxia-ischemia and LPS-induced inflammation on day 6 after birth. Zheng et al. (2013) showed that 5 mg/kg LPS injected intraperitoneally into C57BL/6J mice at 3 and 16 months of age not only leads to increased neuroinflammation but also to an autophagic impairment. Zhou *et al.* (2011) demonstrated that GSK3-β inhibition suppressed neuroinflammation in the cortices of rats subjected to ischemic brain injury by activating autophagy. In another study, it was observed that neuroinflammation can block the autophagic flux in rats subjected to stress-induced hypertension (Du et al. 2017). It has also been suggested that glial cells play a major role in the development of autophagy deficits observed in HIV-associated dementia (Alirezaei et al. 2008). In conclusion, these studies suggest that a pathological disruption of autophagy can cause an initiation or exacerbation of neuroinflammation and conversely, neuroinflammation can induce an autophagic deficit further contributing to neurodegeneration. Our data show that SYK is involved in both the regulation of

autophagy, as well as neuroinflammation and suggest that SYK may represent an important therapeutic target for the treatment of neurodegenerative proteinopathies.

We found increased LAMP-1 levels in Tg Tau P301S compared to wild-type littermates which could be indicative of a lysosomal defect in Tg Tau P301S. Interestingly, LAMP-1 levels were reduced in Tg Tau P301S mice following SYK inhibition which could suggest that lysosomal functions were also improved by the treatment. Bain et al. (2018) found that in some cases the pathological mechanism in FTLD-tau may be attributed to lysosomal deficiencies and impaired transport, as LAMP-1 levels were increased suggesting the presence of more lysosomes. They concluded that FTLD cases with an underlying GRN (granulin) mutation show TAR DNA-binding protein (TDP-43) aggregates because of a lysosomal dysfunction (impaired degradation) rather than a lysosomal deficiency (lack of lysosomes). In our study, we show that Tg Tau P301S mice exhibit elevated levels of LAMP-1, along with increased tau levels compared to WT littermates. Since LAMP-1 levels are increased and suggest higher numbers of lysosomes or increased lysosomal surface area, a lysosomal defect or a dysfunctional transport, as suggested by Bain et al. (2018), could also contribute to the accumulation of tau in Tg Tau P301S mice. It is possible that the increased LAMP-1 levels observed in Tg Tau P301S mice represents a compensatory mechanism, initiated to counteract the lysosomal dysfunction. Interestingly, the treatment with the SYK inhibitor decreased tau, as well as LAMP-1 levels significantly, suggesting an improvement of lysosomal functions. The analysis of the ratio of LC3-II/I in stable SYK knockdown cells alone and in the presence of the lysosome inhibitor CQ also indicate a possible role of SYK in lysosomal degradation (previous chapter). The role of SYK in lysosomal functions will need to be further delineated in future experiments.



The data presented in this chapter illustrate the dual role of SYK as a regulator of neuroinflammation and autophagy in the CNS. The observations made in this study not only provide further evidence for an important role of SYK in the pathogenesis of AD and the development of tau pathologies but also demonstrate that pharmacological SYK inhibition may represent a promising therapeutic strategy for the treatment of AD and other neurodegenerative proteinopathies.

4.4.1 Excursion: Tg Tau P301S organotypic vibrosections: brain cytokine levels following ex-vivo SYK inhibition

4.4.1.1 Introduction

As stated previously, SYK is known as a modulator of the immune response in the periphery. More specifically, SYK has been shown to be involved in B-cell receptor (BCR) and T-cell receptor (TCR) signaling (Kurosaki et al. 1994; Latour et al. 1997).

Our previous studies have revealed that SYK does not only play a major role in the periphery but is also present in CNS. More precisely, we have shown that SYK activation, is largely increased in subsets of microglia and in dystrophic neurites in AD mouse models, as well as in neurons of Tg Tau P301S mice, compared to wild-type (WT) animals that did not exhibit activation SYK activation (Schweig et al. 2017). We observed a similar increase in SYK activation in dystrophic neurites and neurons in human AD specimens.

This means that SYK activity is increased in neurons displaying the tau pathology but not in microglia of Tg Tau P301S. However, Tg Tau P301S mice are known to exhibit microgliosis (see previous chapter (Iba-1) and (Yoshiyama et al. 2007)) which implies that neuronal tau pathology can promote the activation of microglia but the mechanism remains elusive and implies a cross-talk between neurons and microglia. Given that SYK is upregulated in neurons in these mice, and since SYK has been shown to regulate inflammatory pathways in microglia *in vitro* (Combs et al. 1999; Combs et al. 2001; Lovering et al. 2012; McDonald et al. 1997), we were prompted to investigate whether blocking SYK activity could influence tau-induced neuroinflammation using organotypic vibrosections from Tg Tau P301S brains. By studying the effects of SYK inhibition on cytokine production *ex vivo* in organotypic vibrosections, we were able to directly assess the impact of SYK inhibition on the CNS and avoid peripheral effects of SYK inhibition on immune cells.

To our knowledge, no other studies have examined the immediate effects of SYK inhibition on neuroinflammation in the CNS. Therefore, we investigated the effect of SYK inhibition on cytokine production under normal conditions and in presence of LPS in culture media *ex vivo*, in organotypic brain vibrosections of a mouse model of tauopathy (Tg Tau P301S) and WT littermates.

4.4.1.2 Materials and Methods

4.4.1.2.1 Animals

All mice were maintained under specific pathogen free conditions in ventilated racks in the Association for Assessment and Accreditation of Laboratory Animal Care International (AAALAC) accredited vivarium of the Roskamp Institute. All experiments involving mice were reviewed and approved by the Institutional Animal Care and Use Committee of the Roskamp Institute before implementation and were conducted in compliance with the National Institutes of Health Guidelines for the Care and Use of Laboratory Animals. Tg Tau P301S (Yoshiyama et al. 2007) mice were obtained from the Jackson Laboratories (ME, USA) and bred with C57BL/6J mice to produce the Tg Tau P301S and wild-type littermates used in this study.

4.4.1.2.2 Treatment of organotypic vibrosections

Adult Tg Tau P301S mice and age-matched WT littermates were rapidly sacrificed after 3 minutes of 3% isoflurane anesthesia and their brains dissected in pre-cooled (4˚C) HBSS. Coronal, 250µm thick brain sections were cut at a speed of 0.3mm/s in pre-cooled (4˚C) HBSS using the Leica VT 1200S (Leica Inc., IL, USA) vibratome attached to the Julabo FL300 (Julabo Inc., PA, USA) recirculating cooler. Each brain section was immediately transferred into a well of a 24-well plate

with 500µl of DMEM/F12 media containing 10% FBS (Thermo Fisher Scientific, MA, USA), 1% GlutaMAX and 1% penicillin/streptomycin/fungizone.

The sections were incubated at 37˚C in a humidified 5% CO_2 atmosphere. The organotypic coronal vibrosections of 43-week-old Tg Tau P301S mice and age-matched WT littermates were treated with 5µM BAY61-3606 or 500ng/ml LPS or a combination of both for 24 hours. After 24h the supernatant was collected and stored at -80˚C for subsequent analysis of cytokine levels. The brain sections were lysed in 100µl MPER containing Halt protease inhibitors and also stored at -80˚C for subsequent analysis of total protein levels. Two animals for each genotype and five to ten organotypic vibrosections per treatment were analyzed and compared to untreated control slices using the MSD ELISA for multiple cytokines.

4.4.1.2.3 ELISA for cytokine levels

For quantification of *ex vivo* cytokine levels, the MESO QuickPlex SQ 120 and the appropriate ELISA kits were used (Meso Scale Diagnostics, MD, USA). The samples were prepared and measured as directed by the manufacturer's instructions. The values for all brain samples were normalized to total protein level as determined by the BCA method.

4.4.1.2.4 Total protein concentration (BCA)

Total protein levels of *ex vivo* samples were determined using the Pierce BCA Protein Assay Kit (Thermo Fisher Scientific, MA, USA). The samples were prepared and measured as directed by the manufacturer's handbook.

4.4.1.2.5 Statistical Analyses

The data were analyzed and plotted with GraphPad Prism (GraphPad Software, Inc., CA, USA). The Shapiro-Wilk test for normality was used to test for Gaussian distribution. Statistical significance was determined by ANOVA and post-hoc Bonferroni test. All data are presented as mean ± the standard error of the mean (SEM) and $p<0.05$ was considered significant (*$p<0.05$, **$p<0.01$, ***$p<0.001$, ****$p<0.0001$).

4.4.1.3 Results

In our previous studies we revealed that SYK is hyperactivated in neurons and microglia of AD brains and AD mouse models. Having established a possible role of SYK in the CNS and given that SYK is a well-known modulator of the peripheral immune response, we investigated the role of SYK in neuroinflammation directly in the CNS. We measured the release of pro-inflammatory and anti-inflammatory cytokines in the media of 250µm thick organotypic brain vibrosections of 43-week-old Tg Tau P301S mice and age-matched WT littermates following a 24h treatment with either 5µM of the SYK inhibitor BAY61-3606 or 500ng/ml LPS or a combination of both.

The baseline levels of TNFα were more than 2.5 times higher in Tg Tau P301S (227.71 pg/mg) compared to WT (85.86 pg/mg) vibrosections (Ctl) (Figure 31). The TNFα release was significantly increased in Tg Tau P301S following LPS treatment compared to untreated control (Ctl) ($p<0.0001$). In the double treatment, SYK inhibition significantly reduced the elevated TNFα levels ($p<0.001$). The LPS-induced TNFα release was significantly higher in organotypic vibrosections of Tg Tau P301S (1125.12 pg/mg) brains compared to WT littermates (316.15 pg/mg) ($p<0.001$). This means that the LPS-induced TNFα level was approximately 5 times higher in Tg Tau P301S vibrosections compared to baseline, while WT vibrosections exhibited less than

a 4-fold increase in TNFα following LPS treatment. Both WT and Tg Tau P301S vibrosections showed a decrease in TNFα following SYK inhibition with BAY61-3606 alone and in presence of LPS.

Similar to the TNFα data, the baseline levels of IL-1β were nearly 3 times higher in Tg Tau P301S (3.41 pg/mg) compared to WT (1.15 pg/mg) vibrosections (Ctl) (Figure 31). The IL-1β release was significantly increased in Tg Tau P301S following LPS treatment compared to untreated control (Ctl) ($p<0.001$). In the double treatment, SYK inhibition significantly reduced the elevated IL-1β levels ($p<0.001$). The LPS-induced IL-1β release was significantly higher in organotypic vibrosections of Tg Tau P301S brains (9.38 pg/mg) compared to WT littermates (1.88 pg/mg) ($p<0.0001$). This means that the LPS treatment lead to a 2.75-fold increased IL-1β release in Tg Tau P301S vibrosections compared to baseline, while WT vibrosections exhibited a 1.6-fold increase in IL-1β following LPS treatment. Both WT and Tg Tau P301S vibrosections showed a decrease in IL-1β following SYK inhibition with BAY61-3606 alone and in presence of LPS.

Interestingly, the anti-inflammatory IL-4 release was different to the pro-inflammatory TNFα and IL-1β release. The baseline levels of IL-4 were similar in Tg Tau P301S (0.065 pg/mg) and WT (0.056 pg/mg) vibrosections (Ctl) (Figure 31). ANOVA with post-hoc Bonferroni test revealed a significant increase in IL-4 release following LPS treatment compared to untreated control (Ctl) vibrosections in WT ($p<0.001$), however, not in the Tg Tau P301S mice. The increase in IL-4 release in the presence of LPS suggests the initiation of anti-inflammatory feedback loop following the induction of the pro-inflammatory response. The LPS-induced IL-4 release was also significantly lower in organotypic vibrosections of Tg Tau P301S brains compared to WT littermates ($p<0.05$). In fact, we observed a 6.76-fold increase in LPS-induced IL-4 levels in WT vibrosections compared to untreated control, while in Tg Tau P301S we only observed a 2.45-fold



increase in IL-4 release (Figure 31). This suggests a decreased anti-inflammatory response in Tg Tau P301S compared to WT mice. Both WT and Tg Tau P301S vibrosections showed a decrease in IL-4 following SYK inhibition with BAY61-3606 alone and in presence of LPS. This suggests that the initiation of the anti-inflammatory feedback loop mediated by IL-4 is suppressed following SYK inhibition because of a decreased pro-inflammatory response.

ANOVA with post-hoc Bonferroni test did not reveal any significant difference in IL-5 levels between transgenic and WT mice or following any treatment. This suggests that IL-5 does not play a role in LPS-induced inflammation or in the neuroinflammation observed in Tg Tau P301S mice.

The baseline release of IL-6 from Tg Tau P301S vibrosections (Ctl, 6171.53 pg/mg) was approximately 1.5-fold higher compared to WT vibrosections (Ctl, 4025.04 pg/mg). The release of IL-6 was not impacted by LPS. However, the IL-6 release was significantly lower in vibrosections of Tg Tau P301S mice double-treated with LPS and BAY61-3606 compared to LPS alone ($p<0.05$). Both WT and Tg Tau P301S vibrosections showed a decrease in IL-6 following SYK inhibition with BAY61-3606 alone and in presence of LPS (Figure 31).

The baseline levels of IL-10 were 2.6 times higher in Tg Tau P301S (2.31 pg/mg) compared to WT (0.87 pg/mg) vibrosections (Ctl) (Fig. 1). The IL-10 release was significantly increased in Tg Tau P301S double-treated with LPS and BAY61-3606 compared to LPS alone ($p<0.05$). Although the LPS-induced IL-10 release was significantly higher in organotypic vibrosections of Tg Tau P301S brains (3.88 pg/mg) compared to WT littermates (1.74 pg/mg) ($p<0.05$), the relative increase was lower in Tg Tau P301S compared to WT vibrosections (Figure 31). In fact, the LPS treatment lead to a 1.7-fold increased IL-10 release in Tg Tau P301S vibrosections compared to baseline, while WT vibrosections exhibited a 2-fold increase in IL-10 following LPS treatment.

Both WT and Tg Tau P301S vibrosections showed a decrease in IL-10 following SYK inhibition with BAY61-3606 alone and in presence of LPS.

The baseline levels of KC-GRO were 1.86 times higher in Tg Tau P301S (712.98 pg/mg) compared to WT (382.7 pg/mg) vibrosections (Ctl) (Figure 31). The KC-GRO release was significantly decreased in Tg Tau P301S vibrosections treated with BAY61-3606 compared to the untreated control ($p<0.05$). The KC-GRO release was not significantly altered following treatment with LPS in WT vibrosections (402.48 pg/mg). However, LPS decreased the KC-GRO release in Tg Tau P301S vibrosections (520.4 pg/mg). Both WT and Tg Tau P301S vibrosections showed a decrease in KC-GRO following SYK inhibition with BAY61-3606 alone and in presence of LPS. Tg Tau P301S IL-12p70 baseline levels (41.34 pg/mg) are slightly higher than WT vibrosections (29.04 pg/mg) IL-12p70 baseline levels. Although ANOVA with post-hoc Bonferroni test did not reveal a significant difference in IL-12p70 levels, both LPS and BAY61-3606 seem to reduce the release of IL-12p70 (Figure 31).

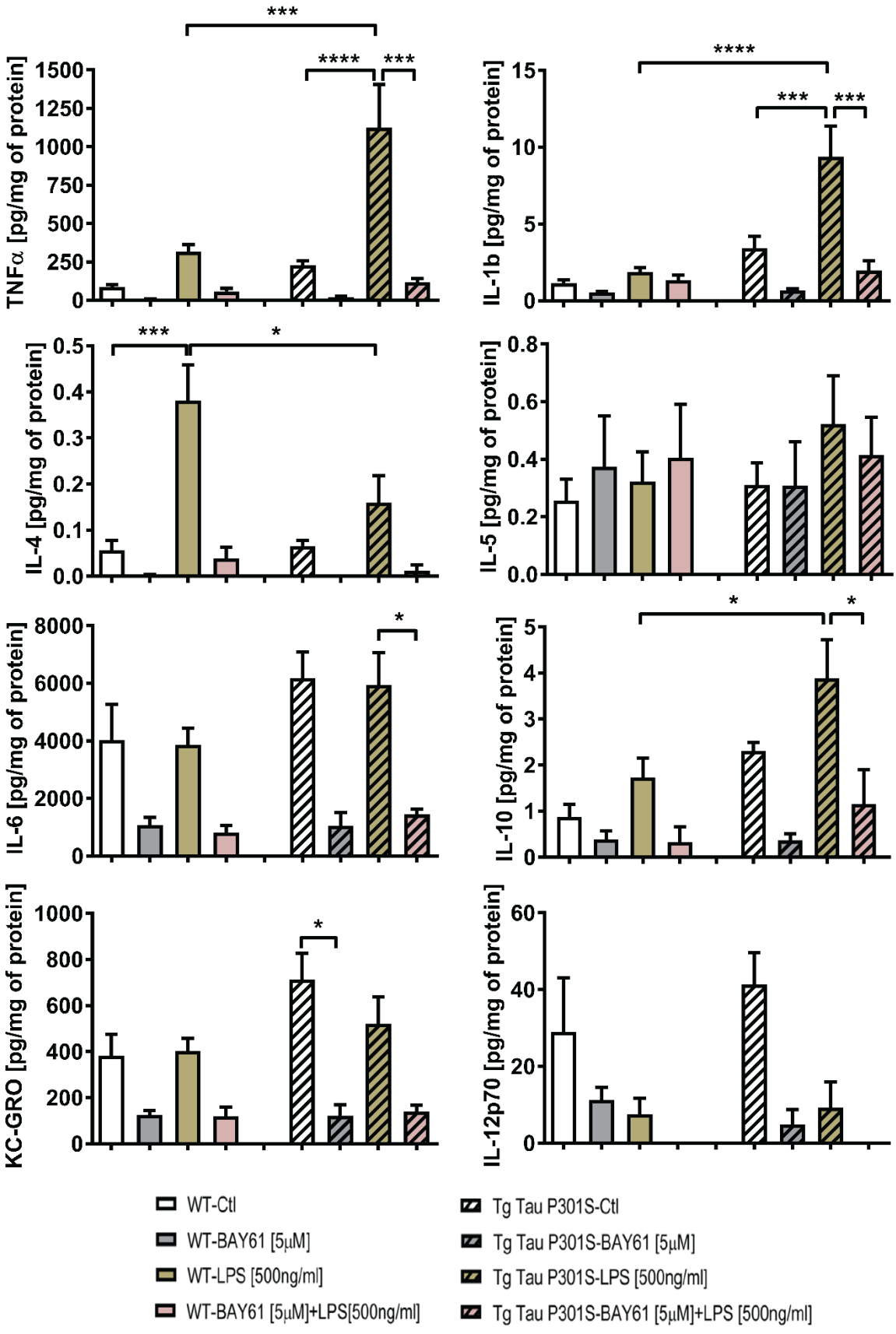
TNFα [pg/mg of protein]
IL-1b [pg/mg of protein]
IL-4 [pg/mg of protein]
IL-5 [pg/mg of protein]
IL-6 [pg/mg of protein]
IL-10 [pg/mg of protein]
KC-GRO [pg/mg of protein]
IL-12p70 [pg/mg of protein]
WT-Ctl
WT-BAY61 [5μM]
WT-LPS [500ng/ml]
WT-BAY61 [5μM]+LPS[500ng/ml]
Tg Tau P301S-Ctl
Tg Tau P301S-BAY61 [5μM]
Tg Tau P301S-LPS [500ng/ml]
Tg Tau P301S-BAY61 [5μM]+LPS [500ng/ml]

Figure 31: Cytokine production in organotypic vibrosections of Tg Tau P301S mice and WT littermates following LPS exposure and SYK inhibition

250µm thick brain sections of 43-week-old Tg Tau P301S mice and age-matched WT littermates were treated in 24-well plates for 24h with either 5µM of the SYK inhibitor BAY61-3606 or 500ng/ml LPS or a combination of both. Cytokine levels of the culture media were analyzed by ELISA.

ANOVA with post-hoc Bonferroni test revealed a significant increase in TNFα release in Tg Tau P301S following LPS treatment compared to untreated control (Ctl) ($p<0.0001$). In the double treatment, SYK inhibition significantly reduced the elevated TNFα levels ($p<0.001$). The LPS-induced TNFα release was significantly higher in organotypic vibrosections of Tg Tau P301S brains compared to WT littermates ($p<0.001$).

ANOVA with post-hoc Bonferroni test revealed a significant increase in IL-1β release in Tg Tau P301S following LPS treatment compared to untreated control (Ctl) vibrosections ($p<0.001$). In the double treatment, SYK inhibition significantly reduced the elevated IL-1β levels ($p<0.001$). The LPS-induced IL-1β release was significantly higher in organotypic vibrosections of Tg Tau P301S brains compared to WT littermates ($p<0.0001$).

ANOVA with post-hoc Bonferroni test revealed a significant increase in IL-4 release in WT following LPS treatment compared to untreated control (Ctl) vibrosections ($p<0.001$). The LPS-induced IL-4 release was significantly lower in organotypic vibrosections of Tg Tau P301S brains compared to WT littermates ($p<0.05$).

ANOVA with post-hoc Bonferroni test did not reveal a significant difference in IL-5 levels.

ANOVA with post-hoc Bonferroni test revealed a significant decrease in IL-6 release in vibrosections of Tg Tau P301S mice double-treated with LPS and BAY61-3606 compared to LPS alone ($p<0.05$).

ANOVA with post-hoc Bonferroni test revealed a significant decrease in IL-10 release in vibrosections of Tg Tau P301S mice double-treated with LPS and BAY61-3606 compared to LPS alone ($p<0.05$). The LPS-induced IL-10 release was significantly higher in organotypic vibrosections of Tg Tau P301S brains compared to WT littermates ($p<0.05$).

ANOVA with post-hoc Bonferroni test revealed a significant decrease in KC-GRO release in vibrosections of Tg Tau P301S mice treated with BAY61-3606 compared to the untreated control ($p<0.05$).

ANOVA with post-hoc Bonferroni test did not reveal a significant difference in IL-12p70 levels.

All cytokine levels were normalized to total protein measured. All data are presented as mean ± SEM. For all graphs WT and Tg Tau P301S Ctl, LPS; n=10, WT and Tg Tau P301S BAY61-3606, BAY61-3606+LPS; n=5 vibrosections were analyzed.

4.4.1.4 Discussion

Although SYK is a known regulator of the peripheral immune response, here we report, for the first time, a SYK-dependent release of various pro-inflammatory and anti-inflammatory cytokines in the CNS of WT and Tg Tau P301S mice. Since our previous studies suggested that SYK can regulate NFκB which is known to regulate neuroinflammation and cytokine production (Paris et al. 2014), we investigated the cytokine release in *ex vivo* experiments using brain organotypic vibrosections in addition to the *in vivo* experiments described in the previous chapter, in order to avoid possible confounding effects arising from SYK inhibition in the periphery and therefore enabling us to directly assess SYK inhibition in the CNS.

More precisely, we show that the baseline levels of pro-inflammatory cytokines including TNFα and IL-1β largely differ between WT and Tg Tau P301S mice, providing further evidence for the known cerebral neuroinflammation observed in Tg Tau P301S mice. Tg Tau P301S also exhibited a much stronger release of TNFα and IL-1β following LPS stimulation, suggesting that the neuroinflammation in Tg Tau P301S mice triggers a stronger pro-inflammatory response in those mice compared to WT littermates. Since LPS has been shown to induce the release of pro-inflammatory cytokines by stimulating (TLR4) (Lu et al. 2008), this could also suggest that TLR4 signaling is enhanced in Tg Tau P301S mice. Both TNFα and IL-1β baseline levels, as well as LPS-induced increases, were largely reduced following SYK inhibition in Tg Tau P301S mice, suggesting a SYK-dependent release of these pro-inflammatory cytokines. The roles of the pro-inflammatory cytokines TNFα and IL-1β, along with IL-6 in the brain have been extensively studied and elevated levels of those pro-inflammatory cytokines are often related to sickness, depression, and neurodegenerative disorders like AD (Griffin et al. 1989; Hull et al. 1996; Dantzer et al. 2008). IL-1β has been found to be increased in the hippocampus in 12-months-old Tg Tau

P301S mice compared to non-transgenic mice (Yoshiyama et al. 2007). The authors argue that neuroinflammation, and microgliosis in particular, may be the one of the earliest pathological changes observed in neurodegenerative tauopathies and that an inhibition of the neuroinflammatory response to tau could delay the progression of the tau pathology (Yoshiyama et al. 2007).

Interestingly, baseline levels of the anti-inflammatory cytokine IL-4 were similar in Tg Tau P301S mice compared to WT littermates but LPS stimulation induced a significantly smaller anti-inflammatory feedback response in Tg Tau P301S mice compared to WT littermates, suggesting an impaired anti-inflammatory response in Tg Tau P301S mice. This can be explained by the predominant neuroinflammation in Tg Tau P301S mice and could suggest that an increased pro-inflammatory baseline caused by the tau overexpression results in a decreased LPS-induced anti-inflammatory response. The effects of overexpression of IL-4 in amyloid overexpressing animal models remains controversial, as it has been shown to either attenuate or exacerbate the amyloid pathology, suggesting that more research needs to be done to assess the effects of IL-4 on the AD pathology (Kiyota et al. 2010; Chakrabarty et al. 2012). Significantly increased plasma IL-4 and IL-10 levels have been associated with a faster cognitive decline (ADA-cog.) in human AD patients, suggesting a correlation of anti-inflammatory cytokines and disease severity (Leung et al. 2013). However, a more recent study showed the exact opposite and stated that decreased IL-4 plasma levels were associated with increased disease severity in human AD patients (King et al. 2018), also suggesting that more research needs to be done to clarify the role of IL-4 in AD.

Some cytokines, including IL-5, did neither show a major difference between WT and Tg Tau P301S mice, nor a LPS-induced release, implying that IL-5 does not play a major role in the mediation of neuroinflammation in WT or Tg Tau P301S mice. The amount of released IL-12p70



was also similar in WT and Tg Tau P301S mice. Both LPS and the SYK inhibitor BAY61-3606 seemed to reduce the IL-12p70 release. Plasma IL-12 levels have been found to be vary at different stages of AD. Patients with mild AD exhibited the highest IL-12 levels, whereas patients with severe AD did not exhibit higher IL-12 levels compared to non-demented controls (Motta et al. 2007).

The release of IL-6 was also not altered by LPS, neither in WT nor in Tg Tau P301S mice. Only the baseline levels of IL-6 were slightly higher in Tg Tau P301S mice compared to WT littermates. In AD patients the levels of IL-6 in the serum has been found to significantly higher than in the control group (Cojocaru et al. 2011), whereas another study showed that CSF levels of IL-6 were decreased in dementia with Lewy bodies compared to AD and controls and that IL-6 levels negatively correlated with MMSE scores (Wennström et al. 2015).

The release of KC-GRO following LPS treatment was only slightly reduced compared to the untreated control in the Tg Tau P301S mice but did not differ for the WT littermates. KC-GRO is a ligand of the CXCR2 receptor and has been shown to be involved in triggering ERK1/2 and PI3K pathways resulting in tau hyperphosphorylation (Xia and Hyman 2002). The increase KC-GRO baseline levels that we observed in Tg Tau P301S compared to WT mice could therefore also contribute to the tau pathology.

The baseline level, as well as the LPS-induced release of IL-10 was also increased in Tg Tau P301S mice compared to WT littermates and Syk inhibition decreased IL-10 levels both in WT and Tg Tau P301S mice. IL-10 deficiency has been shown to mitigate AD pathology in APP/PS1 mice and was elevated in AD patient brains (Guillot-Sestier et al. 2015). It has therefore been suggested that IL-10 suppression may be a therapeutic approach to treat AD (Guillot-Sestier

et al. 2015). However, other studies have argued that increasing IL-10 could be a potential treatment strategy for AD, as IL-10 reduced pro-inflammatory cytokines (Magalhaes et al. 2017). Various pro-inflammatory and anti-inflammatory cytokines were reduced following SYK inhibition with BAY61-3606, even in the presence of LPS, including TNFα, IL-1β, IL-4, IL-6, IL-10, KC-GRO and IL-12p70. This suggests that SYK plays a regulatory role in the release of pro-inflammatory and anti-inflammatory cytokines in the CNS. Our findings also imply that the neuroinflammation observed in Tg Tau P301S mice, as well as LPS induced inflammation, can be controlled and brought back to baseline levels by inhibiting SYK.

Our studies presented in the previous three chapters found increased levels of SYK activation in subsets of activated microglia in Aβ-overexpressing animal models of AD, as well as in neurons of tau-overexpressing Tg Tau P301S mice. However, so far we found no evidence for increased SYK activation in microglia of Tg Tau P301S mice, although we confirmed the well-known microgliosis in this chapter. Therefore, we hypothesize that SYK could be a key kinase controlling the cross-talk between neurons carrying tau pathological species and microglia responding with a release of cytokines in Tg Tau P301S mice. Although glial cells are known to be the main source of cytokines (Hanisch 2002; Wang et al. 2015a), there is evidence that supports a cytokine release by neurons (Acarin et al. 2000; Bartfai and Schultzberg 1993; Sei et al. 1995). In fact, increased IL-1β levels have been observed in pyramidal neurons of the hippocampus in Tg Tau P301S mice while it was nearly absent in non-transgenic control mice (Yoshiyama et al. 2007). This means that, potentially, the cytokines could, at least partially, originate from neurons and SYK inhibition could prevent this neuronal release. Furthermore, even though we did not directly detect an elevated SYK activation in microglia of Tg Tau P301S mice, this does not mean that SYK inhibition could not directly influence the microglial cytokine release, as SYK may still be

present and activated to a lesser degree in those microglia. However, future studies have to determine the exact origin of the cytokines detected in this study and elucidate the exact mechanism by which SYK represses the tau- and LPS-induced cytokine release.

In conclusion, our data show a definite and direct involvement of SYK in the regulation of cytokine release in the CNS. This means that our previously observed hyperactivation of SYK in microglia and neurons in AD brains and AD mouse models is likely to contribute to the known neuroinflammation in AD. Hence, a pharmacological intervention targeting SYK may represent a promising approach to reduce neuroinflammation in AD and other diseases of the CNS with an underlying neuroinflammatory component.



5 Conclusion

Earlier work by our Roskamp Institute team had identified SYK as a target of the L-type calcium channel blocker and known anti-hypertensive drug nilvadipine (Paris et al. 2014). Nilvadipine is a racemic compound and was found to not only lower blood pressure but also to be a potential treatment for AD (see below for more information) (Paris et al. 2004; Paris et al. 2011; Bachmeier et al. 2011; Paris et al. 2014; Hanyu et al. 2007). Our team found in a previous study that treatment with nilvadipine resulted in a reduction of tau hyperphosphorylation, Aβ production and neuroinflammation (Paris et al. 2014; Paris et al. 2011). Interestingly, the (-)-enantiomer of nilvadipine does not exhibit anti-hypertensive activities, but still has comparable effects on AD pathologies compared to the racemic mixture and was found to inhibit SYK (Paris et al. 2014), suggesting that the positive impact of nilvadipine on AD pathologies was not mediated by its anti-hypertensive or L-type calcium channel blocker activities. Therefore, our team hypothesized that SYK inhibition with a selective Syk inhibitor should mimic the effects of nilvadipine and reduce the known AD pathologies. In fact, treatment with a specific SYK inhibitor BAY61-3606 resulted in reduction of tau hyperphosphorylation, Aβ production and neuroinflammation *in vitro* and in acute *in vivo* treatment paradigms (Paris et al. 2014), mimicking the effects of nilvadipine. Previous mechanistic studies in our lab have shown that SYK inhibition results in an inactivation of GSK3-β leading to a decreased tau phosphorylation at GSK3-β-dependent epitopes in addition to a partial reduction of tau phosphorylation at Tyr18 directly mediated by SYK. Furthermore, SYK was shown to regulate BACE-1 transcription and BACE-1 protein levels, by preventing p65-NFκB activation, resulting in a decreased Aβ and sAPPβ production (Paris et al. 2014). Altogether, these findings suggested an involvement of SYK in the formation of tau and β-amyloid pathologies in AD (Paris et al. 2014).



In this thesis, we report a hyperactivation of SYK in the brains of three different AD mouse models compared to age-matched wild type littermates. In Tg PS1/APPsw and Tg APPsw mice, SYK activity was largely increased in activated microglia and in dystrophic neurites around β-amyloid deposits. In Tg Tau P301S mice, SYK hyperactivation was co-localized with pathological tau species in hippocampal and cortical neurons. Similarly, human AD specimens exhibited increased SYK activation in neurons immunopositive for pathological tau species and dystrophic neurites.

The increased activation of SYK in activated microglia of Aβ-overexpressing mice supports a possible role of SYK in microglial activation *in vivo* and suggests that Aβ accumulation can lead to an activation of SYK *in vivo* in microglia and in dystrophic neurites around β-amyloid deposits. In this regard, previous *in vitro* studies have shown that Aβ oligomers can trigger a microglial inflammatory response mediated by SYK and leading to neurotoxicity (Combs et al. 1999; Combs et al. 2001; McDonald et al. 1997; Sondag et al. 2009).

The strong increase in activated SYK in dystrophic neurites (DNs) may suggest the involvement of SYK in the formation of these DNs that ultimately lead to the synaptic loss observed in AD (Sanchez-Varo et al. 2012). The DNs are characterized by an accumulation of BACE-1 and sAPPβ which implies a contribution of DNs to Aβ production and accumulation. In fact, several *in vivo* studies have shown that BACE-1 immunopositive dystrophic neurites precede Aβ plaque formation in the brains of 3xTg-AD, 2xFAD and 5xFAD mice and therefore, represent an early pathological event in AD (Cai et al. 2012; Kandalepas et al. 2013; Zhang et al. 2009). Our previous *in vitro* and *in vivo* data showing that SYK regulates Aβ production via a modulation of BACE-1 expression (Paris et al. 2014) support the contribution of SYK upregulation to BACE-1/ sAPPβ accumulation in DNs.

The impaired autophagy observed in AD is suggested to be at least partially caused by an impaired axonal transport that contributes to the formation of DNs. Accumulations of autophagic vesicles (AVs) contribute to the axonal swellings. AVs accumulate in DNs, at least in part, because of an impaired transport along the axon. The axonal transport may be impaired because of decreased levels of kinesin-1 and dynein motor proteins (Sanchez-Varo et al. 2012) resulting in a decreased lysosomal degradation of AVs. It has been shown that Aβ oligomers could associate with AVs and interact with dynein motor proteins, thereby impairing dynein recruitment to amphisomes and finally leading to an impaired retrograde transport (Tammineni et al. 2017). The impairment of the axonal transport along the microtubule network could also be caused by SYK hyperactivity since it has been shown that pharmacological SYK inhibition stabilizes microtubules through decreased phosphorylation of microtubules and microtubule-associated proteins (MAPs) (Yu et al. 2015).

The induction of autophagy, as well as the lysosomal degradation are strongly dependent on the key regulator mTOR. The mTOR pathway, including downstream targets like p70-S6K and 4EBP1 are upregulated in brains of AD patients (Tramutola et al. 2015). This upregulation has also been associated with increased cytosolic tau and increased tau secretion (Tang et al. 2015). Tau-induced neuronal loss, as well as Aβ-induced synaptotoxicity have been shown to be prevented by pharmacological inhibition of mTOR *in vivo* (Ramirez et al. 2014; Siman et al. 2015). Interestingly, the data presented in this thesis show that SYK inhibition has pronounced effects on the mTOR pathway and autophagic tau degradation *in vitro*, as well as *in vivo*. SYK inhibition lowers pharmacologically induced mTOR and Akt activity placing SYK as an upstream regulator of the mTOR pathway and ultimately as a regulator of autophagy and lysosomal degradation in neuron-like cells. Importantly, we confirmed these findings *in vivo* using a mouse model of tauopathy. Chronic SYK inhibition over 12 weeks significantly lowered pathological tau species

via mTOR inhibition, improved motor performance and decreased neuroinflammation in Tg Tau P301S mice, suggesting that targeting SYK could have a major impact on several key pathologies observed in AD patients.

Furthermore, the involvement of SYK in autophagy additionally supports the role of SYK in the formation of DNs, as it has been reported that pharmacological inhibition of mTOR can prevent neuritic dystrophy in PC12 cells and superior cervical ganglion neurons (Yang et al. 2014). The pathological analysis of Tg Tau P301S mice shows that SYK activation occurs concomitantly with the formation of hyperphosphorylated tau oligomers/aggregates in the cortex. This may suggest a possible involvement of SYK activation in tau oligomerization and aggregation *in vivo*. Pathological tau conformers may induce SYK activation but SYK activation could also be required for the establishment of tau pathologies, thereby inducing a positive feedback loop resulting in an enhanced progression of tau pathology. This is supported by our data showing that SYK upregulation in SH-SY5Y cells promotes tau accumulation *in vitro*.

Given that SYK is also present in DNs which exhibit tau accumulation and tau phosphorylation (Schmidt et al. 1994; Su et al. 1993), this further supports a pathological role of SYK in the formation of DNs and ultimately synaptical loss. Our *in vivo* study showed that chronic inhibition of SYK results in increased NeuN and PSD-95 levels in Tg Tau P301S mice compared to vehicle treated controls, suggesting a decreased neuronal and synaptic loss in treated Tg Tau P301S mice. This means that SYK inhibition could potentially counteract the neurodegeneration induced by pathological tau species and therefore represents a promising treatment strategy for AD.

Our previous findings show that SYK regulates GSK3-β activity which is a known tau-kinase (Paris et al. 2014; Hooper et al. 2008). In addition, mTOR and its downstream kinase S6K

can also directly phosphorylate tau (Pei et al. 2006; Sonoda et al. 2016; Tang et al. 2013). Both mTOR and S6K activation were decreased following pharmacological SYK inhibition *in vitro* and *in vivo*. Hence, mTOR and S6K represent additional targets of SYK inhibition that possibly contribute to the reduction of tau phosphorylation. Our previous and present data show decreased tau phosphorylation at multiple epitopes including S396/404, Ser202, T231, and Y18, as well as decreased tau oligomers (TOC1) and pathological tau conformers (MC1) following SYK inhibition (Paris et al. 2014) (and chapter 4).

In summary, SYK inhibition targets and reduces the activity of multiple tau-kinases and could therefore ameliorate tau pathology. Additionally, stimulation of tau degradation via increased autophagy may also contribute to the amelioration of the tau pathology following SYK inhibition which may explain why SYK inhibition has such a drastic impact on tau.

The results of this thesis show increased SYK activation in neurons of tau overexpressing mice and in dystrophic neurites and in microglia of Aβ overexpressing mice, indicating that both Aβ and tau can elicit a downstream activation of SYK. In addition, SYK overexpression increased tau phosphorylation and total tau levels implying a positive feedback loop between SYK and tau. SYK does not only exacerbate the tau pathology by directly phosphorylating tau at Y18 and indirectly by activating other downstream kinases (e.g. GSK3-β, S6K, Akt), thereby contributing to tau hyperphosphorylation but also by regulating the autophagic degradation of tau (Figure 32). Taken together, the results of the three main chapters, as well as the results from previous studies (Paris et al. 2014), suggest that both the tau and Aβ pathologies could exacerbate each other via the activation of SYK since SYK regulates tau hyperphosphorylation, tau degradation, Aβ production and neuroinflammation through downstream pathways, thereby creating positive feedback loops between Aβ, tau and SYK (as described in Figure 32).



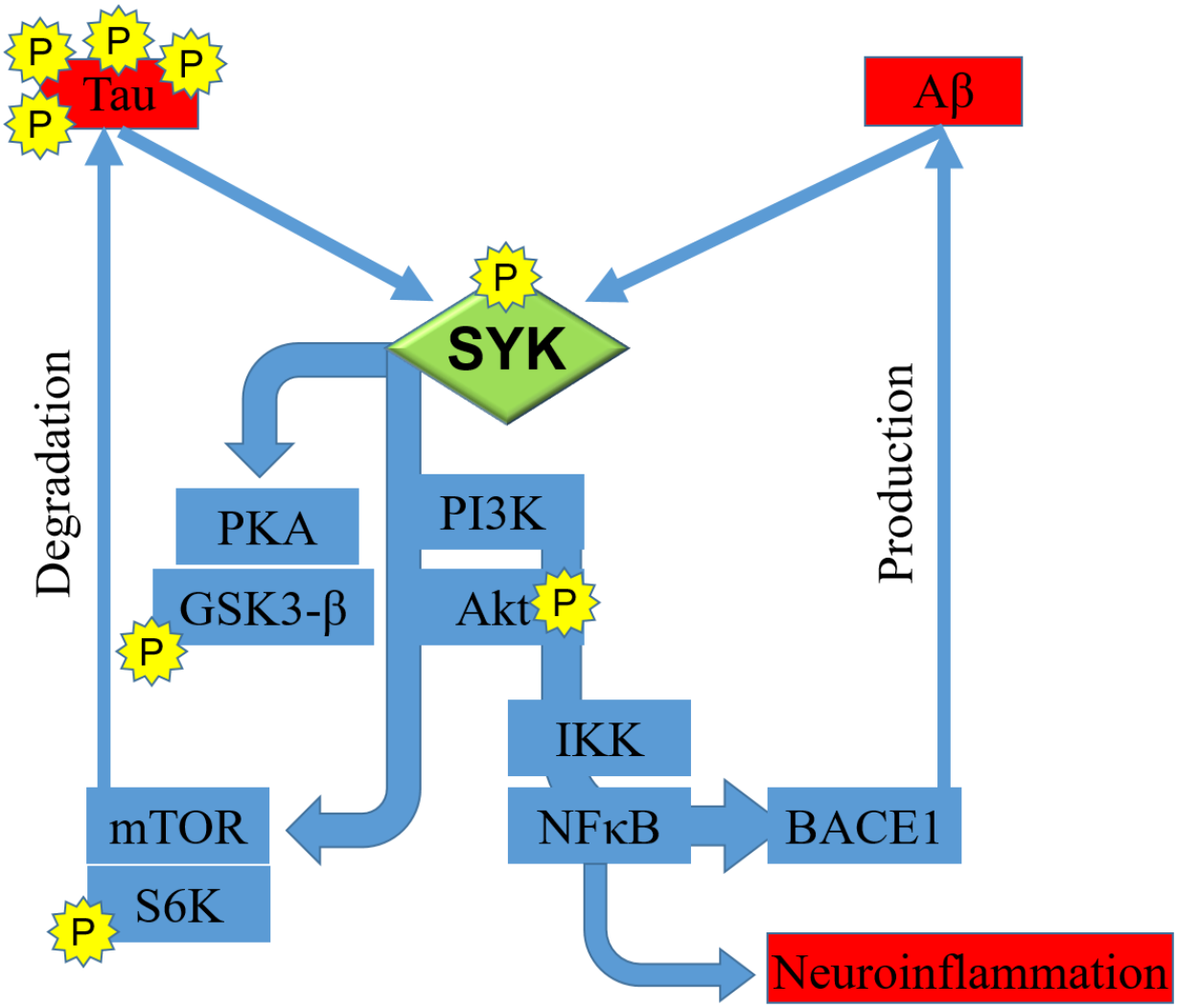

Figure 32: Relationships between SYK and the main AD pathologies

In the first chapter of this thesis, we have shown that SYK is activated in AD mouse models overexpressing Aβ, as well as mouse models overexpressing P301S tau. Therefore, SYK activation occurs downstream of Aβ and tau pathologies. Our present and previous studies (Paris et al. 2014) have shown that SYK activation causes activation of downstream kinases and conversely, SYK inhibition causes inhibition of certain kinases that are known to phosphorylate tau including GSK3-β, Akt, S6K and SYK itself (yellow star, P = phosphorylation of tau), thereby possibly exacerbating tau hyperphosphorylation. In addition, the second and third chapter of this thesis show that SYK acts upstream of the mTOR pathway and thereby influences the tau degradation, creating another and possibly stronger positive feedback loop between the tau pathology and SYK. Furthermore, our previous studies have shown that SYK impacts the expression of BACE1, the rate-limiting enzyme in Aβ production, via NFκB thereby closing the positive feedback loop between Aβ and SYK. NFκB is known to be involved in neuroinflammation and since we have shown SYK activation occurs in microglia, SYK is likely to contribute to neuroinflammation. Taken together our findings indicate that SYK activation is a downstream event of the Aβ and tau pathologies but also exacerbates these known AD pathologies and could therefore represent a promising target for the treatment of AD.

As described in detail in the introduction (1.3), to date, there is no cure available to AD patients, as none of the drugs approved by the FDA halts the cognitive decline but are just considered symptomatic cognitive enhancers. While symptomatic cognitive enhancers may help patients in the short term by boosting their cognitive performance, they do not alter the advance of the disease in the long term. Therefore, FDA approved disease modifying therapies (DMTs) are needed to successfully treat AD.

The findings mentioned in chapter 1.3, underline the importance of investigating and advancing new potential DMTs to the clinic and because of the data presented in this thesis, the development of specific SYK inhibitors represents a new and promising treatment strategy for AD. To this date, there have been only oral SYK inhibitors in clinical trials or FDA approved that aim to treat conditions like cancer and autoimmune diseases. Only a small number of teams have been working on SYK as a target for the treatment of CNS diseases, thereby mainly focusing on AD. In the near future, however, the scientific field around SYK inhibitors may expand to CNS-related disorders, as the role of SYK in several important processes within the nervous system becomes more apparent to the scientific community.

In conclusion, our previous data, as well as the data presented in this thesis support a pathological role of SYK in the formation of Aβ deposits, tau aggregates, and neuroinflammation and furthermore, suggest that prevention of SYK hyperactivity through pharmacological inhibition may be a promising therapeutic approach for Alzheimer's disease, pure tauopathies and potentially other neurodegenerative diseases with an underlying autophagic impairment or neuroinflammatory component.

6 Future Directions

In the first chapter of this thesis we focused on describing the activation of SYK in different cell types of the CNS and compared human AD specimens to non-demented controls, as well as AD mouse models overexpressing tau and Aβ to wild-type littermates. The second and third chapters mainly focused on the relationship between SYK and the tau pathology *in vitro* and in a chronic *in vivo* treatment paradigm.

However, we already performed experiments that investigated the effects of chronic SYK inhibition on AD mouse models overexpressing Aβ (Tg APPsw and Tg PS1/APPsw). We investigated two different age-groups that were treated with 20mg/kg BAY61-3606 or placebo; 70-week-old and 90-week-old transgenic mice were each compared to age-matched wild-type littermates. The two chronic treatments lasted for 14 weeks (70-week-old cohort) and 7 weeks (90-week-old cohort). The studies aimed to investigate the behavior (spatial memory, learning, anxiety, and social memory), as well as AD-related pathological changes on a molecular level, including Aβ burden, neuroinflammation, neurodegeneration, and synaptical changes using different techniques like ELISA, immunoblotting, and immunofluorescence microscopy. The analyses of these studies are still ongoing as of 2018 and will further elucidate the impact of chronic SYK inhibition on the Aβ pathology in two different mouse models of AD and additionally give valuable information about the best time point of intervention with a SYK inhibitor.

In addition to the two studies mentioned above, it will be interesting to add another, younger, age-group and treat 45-week-old Aβ-overexpressing mice chronically with the SYK inhibitor BAY61-3606. This study will provide us with more detailed information about the time of intervention with a SYK inhibitor.

As mentioned in the previous chapter (5) and the introduction (1.3), there are already a few SYK inhibitors in clinical trials and they generally have a good safety profile, but none of them has been designed for the treatment of neurological disorders. Therefore, the next crucial step on the way to successful SYK-based therapies for neurological disorders is the development of novel specific SYK inhibitors that are designed to cross the BBB well and achieve an optimal target engagement in the CNS.



7 Publication bibliography

Acarin, L.; Gonzalez, B.; Castellano, B. (2000): Neuronal, astroglial and microglial cytokine expression after an excitotoxic lesion in the immature rat brain. In *The European journal of neuroscience* 12 (10), pp. 3505–3520.

Alirezaei, Mehrdad; Kiosses, William B.; Flynn, Claudia T.; Brady, Nathan R.; Fox, Howard S. (2008): Disruption of neuronal autophagy by infected microglia results in neurodegeneration. In *PloS one* 3 (8), e2906. DOI: 10.1371/journal.pone.0002906.

Alois Alzheimer (1907): Über eine eigenartige Erkrankung der Hirnrinde. In *Allgemeine Zeitschrift fur Psychiatrie und Psychisch-gerichtliche Medizin* 64, pp. 146–148.

Alzheimer's disease facts and figures (2018). In *Alzheimer's & Dementia* 14 (3), pp. 367–429.

Andreadis, Athena (2006): Misregulation of tau alternative splicing in neurodegeneration and dementia. In *Progress in molecular and subcellular biology* 44, pp. 89–107.

Angibaud, Julie; Louveau, Antoine; Baudouin, Stephane J.; Nerriere-Daguin, Veronique; Evain, Sarah; Bonnamain, Virginie et al. (2011): The immune molecule CD3zeta and its downstream effectors ZAP-70/Syk mediate ephrin signaling in neurons to regulate early neuritogenesis. In *Journal of neurochemistry* 119 (4), pp. 708–722. DOI: 10.1111/j.1471-4159.2011.07469.x.

Aouar, Besma; Kovarova, Denisa; Letard, Sebastien; Font-Haro, Albert; Florentin, Jonathan; Weber, Jan et al. (2016): Dual Role of the Tyrosine Kinase Syk in Regulation of Toll-Like Receptor Signaling in Plasmacytoid Dendritic Cells. In *PloS one* 11 (6), e0156063. DOI: 10.1371/journal.pone.0156063.

Arendash, G. W.; King, D. L.; Gordon, M. N.; Morgan, D.; Hatcher, J. M.; Hope, C. E.; Diamond, D. M. (2001): Progressive, age-related behavioral impairments in transgenic mice carrying both mutant amyloid precursor protein and presenilin-1 transgenes. In *Brain research* 891 (1-2), pp. 42–53.

Asai, Hirohide; Ikezu, Seiko; Tsunoda, Satoshi; Medalla, Maria; Luebke, Jennifer; Haydar, Tarik et al. (2015): Depletion of microglia and inhibition of exosome synthesis halt tau propagation. In *Nature neuroscience* 18 (11), p. 1584. DOI: 10.1038/nn.4132.

Atagi, Yuka; Liu, Chia-Chen; Painter, Meghan M.; Chen, Xiao-Fen; Verbeeck, Christophe; Zheng, Honghua et al. (2015): Apolipoprotein E Is a Ligand for Triggering Receptor Expressed on Myeloid Cells 2 (TREM2). In *The Journal of biological chemistry* 290 (43), pp. 26043–26050. DOI: 10.1074/jbc.M115.679043.

Azoulay-Alfaguter, I.; Elya, R.; Avrahami, L.; Katz, A.; Eldar-Finkelman, H. (2015): Combined regulation of mTORC1 and lysosomal acidification by GSK-3 suppresses autophagy and contributes to cancer cell growth. In *Oncogene* 34 (35), pp. 4613–4623. DOI: 10.1038/onc.2014.390.

Bachmeier, Corbin; Beaulieu-Abdelahad, David; Mullan, Michael; Paris, Daniel (2011): Selective dihydropyiridine compounds facilitate the clearance of beta-amyloid across the blood-brain barrier. In *European journal of pharmacology* 659 (2-3), pp. 124–129. DOI: 10.1016/j.ejphar.2011.03.048.

Bai, Xiaochun; Ma, Dongzhu; Liu, Anling; Shen, Xiaoyun; Wang, Qiming J.; Liu, Yongjian; Jiang, Yu (2007): Rheb activates mTOR by antagonizing its endogenous inhibitor, FKBP38. In *Science (New York, N.Y.)* 318 (5852), pp. 977–980. DOI: 10.1126/science.1147379.

Bailey, Charles C.; DeVaux, Lindsey B.; Farzan, Michael (2015): The Triggering Receptor Expressed on Myeloid Cells 2 Binds Apolipoprotein E. In *The Journal of biological chemistry* 290 (43), pp. 26033–26042. DOI: 10.1074/jbc.M115.677286.

Bain, Hamish Dc; Davidson, Yvonne S.; Robinson, Andrew C.; Ryan, Sarah; Rollinson, Sara; Richardson, Anna et al. (2018): The role of lysosomes and autophagosomes in Frontotemporal Lobar Degeneration. In *Neuropathology and applied neurobiology*. DOI: 10.1111/nan.12500.

Barber, Robert C. (2012): The genetics of Alzheimer's disease. In *Scientifica* 2012, p. 246210. DOI: 10.6064/2012/246210.

Bartaula-Brevik, Sushma; Lindstad Brattås, Marte Karen; Tvedt, Tor Henrik Anderson; Reikvam, Håkon; Bruserud, Øystein (2018): Splenic tyrosine kinase (SYK) inhibitors and their possible use in acute myeloid leukemia. In *Expert opinion on investigational drugs* 27 (4), pp. 377–387. DOI: 10.1080/13543784.2018.1459562.

Bartfai, T.; Schultzberg, M. (1993): Cytokines in neuronal cell types. In *Neurochemistry international* 22 (5), pp. 435–444.

Béïque, Jean-Claude; Andrade, Rodrigo (2003): PSD-95 regulates synaptic transmission and plasticity in rat cerebral cortex. In *The Journal of Physiology* 546 (Pt 3), pp. 859–867. DOI: 10.1113/jphysiol.2002.031369.

Bejanin, Alexandre; Schonhaut, Daniel R.; La Joie, Renaud; Kramer, Joel H.; Baker, Suzanne L.; Sosa, Natasha et al. (2017): Tau pathology and neurodegeneration contribute to cognitive impairment in Alzheimer's disease. In *Brain* 140 (12), pp. 3286–3300. DOI: 10.1093/brain/awx243.

Bellucci, Arianna; Westwood, Andrew J.; Ingram, Esther; Casamenti, Fiorella; Goedert, Michel; Spillantini, Maria Grazia (2004): Induction of inflammatory mediators and microglial activation in mice transgenic for mutant human P301S tau protein. In *The American journal of pathology* 165 (5), pp. 1643–1652. DOI: 10.1016/S0002-9440(10)63421-9.

Bemiller, Shane M.; McCray, Tyler J.; Allan, Kevin; Formica, Shane V.; Xu, Guixiang; Wilson, Gina et al. (2017): TREM2 deficiency exacerbates tau pathology through dysregulated kinase signaling in a mouse model of tauopathy. In *Molecular neurodegeneration* 12 (1), p. 74. DOI: 10.1186/s13024-017-0216-6.

Benitez, Bruno A.; Cruchaga C, Carlos (2013): TREM2 and Parkinson's Disease. In *The New England journal of medicine* 369 (16), pp. 1567–1568. DOI: 10.1056/NEJMc1306509#SA4.

Bergen, M. von; Biernat, J.; Mandelkow, E.-M.; Mandelkow, Eckhard (2001): A Hexapeptide Motif (306VQIVYK311)-forming β Structure Induces the Aggregation of Tau Protein to Paired Helical Filaments. In K. Iqbal, Sangram S. Sisodia, Bengt Winblad (Eds.): Alzheimer's disease. Advances in etiology, pathogenesis and therapeutics / edited by Khalid Iqbal, Sangram S.Sisodia, Bengt Winblad. Chichester: Wiley, pp. 631–640.

Bergen, M. von; Friedhoff, P.; Biernat, J.; Heberle, J.; Mandelkow, E. M.; Mandelkow, E. (2000): Assembly of tau protein into Alzheimer paired helical filaments depends on a local

sequence motif ((306)VQIVYK(311)) forming beta structure. In *Proceedings of the National Academy of Sciences of the United States of America* 97 (10), pp. 5129–5134.

Bernhardi, Rommy von; Tichauer, Juan E.; Eugenín, Jaime (2010): Aging-dependent changes of microglial cells and their relevance for neurodegenerative disorders. In *Journal of neurochemistry* 112 (5), pp. 1099–1114. DOI: 10.1111/j.1471-4159.2009.06537.x.

Blasko, I.; Veerhuis, R.; Stampfer-Kountchev, M.; Saurwein-Teissl, M.; Eikelenboom, P.; Grubeck-Loebenstein, B. (2000): Costimulatory effects of interferon-gamma and interleukin-1beta or tumor necrosis factor alpha on the synthesis of Abeta1-40 and Abeta1-42 by human astrocytes. In *Neurobiology of disease* 7 (6 Pt B), pp. 682–689. DOI: 10.1006/nbdi.2000.0321.

Blunt, Matthew D.; Parnell, Jack; Larrayoz, Marta; Smith, Lindsay; Dobson, Rachel; Strefford, Jonathan C. et al. (2015): The Syk\Jak Inhibitor Cerdulatinib (PRT062070) Shows Promising Preclinical Activity in Chronic Lymphocytic Leukemia By Antagonising B Cell Receptor and Microenvironmental Signalling. In *Blood* 126 (23), p. 1716.

Bolmont, Tristan; Haiss, Florent; Eicke, Daniel; Radde, Rebecca; Mathis, Chester A.; Klunk, William E. et al. (2008): Dynamics of the microglial/amyloid interaction indicate a role in plaque maintenance. In *The Journal of neuroscience : the official journal of the Society for Neuroscience* 28 (16), pp. 4283–4292. DOI: 10.1523/JNEUROSCI.4814-07.2008.

Bolos, Marta; Llorens-Martin, Maria; Jurado-Arjona, Jeronimo; Hernandez, Felix; Rabano, Alberto; Avila, Jesus (2015): Direct Evidence of Internalization of Tau by Microglia In Vitro and In Vivo. In *Journal of Alzheimer's disease : JAD* 50 (1), pp. 77–87. DOI: 10.3233/JAD-150704.

Bolós, Marta; Llorens-Martín, María; Perea, Juan Ramón; Jurado-Arjona, Jerónimo; Rábano, Alberto; Hernández, Félix; Avila, Jesús (2017): Absence of CX3CR1 impairs the internalization of Tau by microglia. In *Molecular neurodegeneration* 12 (1), p. 59. DOI: 10.1186/s13024-017-0200-1.

Borchelt, D. R.; Thinakaran, G.; Eckman, C. B.; Lee, M. K.; Davenport, F.; Ratovitsky, T. et al. (1996): Familial Alzheimer's disease-linked presenilin 1 variants elevate Abeta1-42/1-40 ratio in vitro and in vivo. In *Neuron* 17 (5), pp. 1005–1013.

Borroni, Barbara; Ferrari, Francesca; Galimberti, Daniela; Nacmias, Benedetta; Barone, Cinzia; Bagnoli, Silvia et al. (2014): Heterozygous TREM2 mutations in frontotemporal dementia. In *Neurobiology of aging* 35 (4), 934.e7-10. DOI: 10.1016/j.neurobiolaging.2013.09.017.

Boucher, Jérémie; Kleinridders, André; Kahn, C. Ronald (2014): Insulin Receptor Signaling in Normal and Insulin-Resistant States. In *Cold Spring Harbor perspectives in biology* 6 (1). DOI: 10.1101/cshperspect.a009191.

Braak, H.; Braak, E. (1991): Neuropathological stageing of Alzheimer-related changes. In *Acta neuropathologica* 82 (4), pp. 239–259. DOI: 10.1007/BF00308809.

Braak, Heiko; Del Tredici, Kelly (2011): Alzheimer's pathogenesis: is there neuron-to-neuron propagation? In *Acta neuropathologica* 121 (5), pp. 589–595. DOI: 10.1007/s00401-011-0825-z.

Brown, Guy C. (2010): Nitric oxide and neuronal death. In *Nitric oxide : biology and chemistry* 23 (3), pp. 153–165. DOI: 10.1016/j.niox.2010.06.001.

Bugiani, O.; Murrell, J. R.; Giaccone, G.; Hasegawa, M.; Ghigo, G.; Tabaton, M. et al. (1999): Frontotemporal dementia and corticobasal degeneration in a family with a

P301S mutation in tau. In *Journal of neuropathology and experimental neurology* 58 (6), pp. 667–677.

Cabezas, Ricardo; Ávila, Marcos; Gonzalez, Janneth; El-Bachá, Ramon Santos; Báez, Eliana; García-Segura, Luis Miguel et al. (2014): Astrocytic modulation of blood brain barrier: perspectives on Parkinson's disease. In *Frontiers in cellular neuroscience* 8. DOI: 10.3389/fncel.2014.00211.

Caccamo, Antonella; Magrì, Andrea; Medina, David X.; Wisely, Elena V.; López-Aranda, Manuel F.; Silva, Alcino J.; Oddo, Salvatore (2013): mTOR regulates tau phosphorylation and degradation: implications for Alzheimer's disease and other tauopathies. In *Aging cell* 12 (3), pp. 370–380. DOI: 10.1111/acel.12057.

Caccamo, Antonella; Oddo, Salvatore; Tran, Lana X.; Laferla, Frank M. (2007): Lithium Reduces Tau Phosphorylation but Not Aβ or Working Memory Deficits in a Transgenic Model with Both Plaques and Tangles. In *The American Journal of Pathology* 170 (5), pp. 1669–1675. DOI: 10.2353/ajpath.2007.061178.

Cai, Yan; An, Seong Soo A.; Kim, SangYun (2015): Mutations in presenilin 2 and its implications in Alzheimer's disease and other dementia-associated disorders. In *Clinical Interventions in Aging* 10, pp. 1163–1172. DOI: 10.2147/CIA.S85808.

Cai, Yan; Zhang, Xue-Mei; Macklin, Lauren N.; Cai, Huaibin; Luo, Xue-Gang; Oddo, Salvatore et al. (2012): BACE1 elevation is involved in amyloid plaque development in the triple transgenic model of Alzheimer's disease: differential Abeta antibody labeling of early-onset axon terminal pathology. In *Neurotoxicity research* 21 (2), pp. 160–174. DOI: 10.1007/s12640-011-9256-9.

Carnevale, J.; Ross, L.; Puissant, A.; Banerji, V.; Stone, R. M.; DeAngelo, D. J. et al. (2013): SYK regulates mTOR signaling in AML. In *Leukemia* 27 (11), pp. 2118–2128. DOI: 10.1038/leu.2013.89.

Carson, Monica J.; Thrash, J. Cameron; Walter, Barbara (2006): The cellular response in neuroinflammation: The role of leukocytes, microglia and astrocytes in neuronal death and survival. In *Clinical neuroscience research* 6 (5), pp. 237–245. DOI: 10.1016/j.cnr.2006.09.004.

Cavaillon, J. M. (2001): Pro- versus anti-inflammatory cytokines: myth or reality. In *Cellular and molecular biology (Noisy-le-Grand, France)* 47 (4), pp. 695–702.

Chakrabarty, Paramita; Tianbai, Li; Herring, Amanda; Ceballos-Diaz, Carolina; Das, Pritam; Golde, Todd E. (2012): Hippocampal expression of murine IL-4 results in exacerbation of amyloid deposition. In *Molecular neurodegeneration* 7, p. 36. DOI: 10.1186/1750-1326-7-36.

Chaudhary, Anu; Fresquez, Theresa M.; Naranjo, Michele J. (2007): Tyrosine kinase Syk associates with toll-like receptor 4 and regulates signaling in human monocytic cells. In *Immunology and cell biology* 85 (3), pp. 249–256. DOI: 10.1038/sj.icb7100030.

Chen, Xiaobing; Nelson, Christopher D.; Li, Xiang; Winters, Christine A.; Azzam, Rita; Sousa, Alioscka A. et al. (2011): PSD-95 is required to sustain the molecular organization of the postsynaptic density. In *The Journal of neuroscience : the official journal of the Society for Neuroscience* 31 (17), pp. 6329–6338. DOI: 10.1523/JNEUROSCI.5968-10.2011.

Chen, Zhihong; Trapp, Bruce D. (2016): Microglia and neuroprotection. In *Journal of neurochemistry* 136 Suppl 1, pp. 10–17. DOI: 10.1111/jnc.13062.

Cherry, Jonathan D.; Olschowka, John A.; O'Banion, M. Kerry (2014): Neuroinflammation and M2 microglia: the good, the bad, and the inflamed. In *Journal of neuroinflammation* 11 (1), p. 98. DOI: 10.1186/1742-2094-11-98.

Chesser, Adrianne S.; Pritchard, Susanne M.; Johnson, Gail V. W. (2013): Tau clearance mechanisms and their possible role in the pathogenesis of Alzheimer disease. In *Frontiers in neurology* 4, p. 122. DOI: 10.3389/fneur.2013.00122.

Chiang, Gary G.; Abraham, Robert T. (2005): Phosphorylation of mammalian target of rapamycin (mTOR) at Ser-2448 is mediated by p70S6 kinase. In *The Journal of biological chemistry* 280 (27), pp. 25485–25490. DOI: 10.1074/jbc.M501707200.

Chiarini, Anna; Armato, Ubaldo; Gardenal, Emanuela; Gui, Li; Dal Prà, Ilaria (2017): Amyloid β-Exposed Human Astrocytes Overproduce Phospho-Tau and Overrelease It within Exosomes, Effects Suppressed by Calcilytic NPS 2143—Further Implications for Alzheimer's Therapy. In *Front. Neurosci.* 11, p. 217. DOI: 10.3389/fnins.2017.00217.

Choi, Soo-Ho; Gonen, Ayelet; Diehl, Cody J.; Kim, Jungsu; Almazan, Felicidad; Witztum, Joseph L.; Miller, Yury I. (2015): SYK regulates macrophage MHC-II expression via activation of autophagy in response to oxidized LDL. In *Autophagy* 11 (5), pp. 785–795. DOI: 10.1080/15548627.2015.1037061.

Citron, Martin; Westaway, David; Xia, Weiming; Carlson, George; Diehl, Thekla; Levesque, Georges et al. (1997): Mutant presenilins of Alzheimer's disease increase production of 42-residue amyloid β-protein in both transfected cells and transgenic mice. In *Nature medicine* 3 (1), p. 67. DOI: 10.1038/nm0197-67.

Clavaguera, Florence; Bolmont, Tristan; Crowther, R. Anthony; Abramowski, Dorothee; Frank, Stephan; Probst, Alphonse et al. (2009): Transmission and spreading of tauopathy in transgenic mouse brain. In *Nature cell biology* 11 (7), pp. 909–913. DOI: 10.1038/ncb1901.

Cojocaru, Inimioara Mihaela; Cojocaru, M.; Miu, Gabriela; Sapira, Violeta (2011): Study of interleukin-6 production in Alzheimer's disease. In *Romanian journal of internal medicine = Revue roumaine de medecine interne* 49 (1), pp. 55–58.

Combs, C. K.; Johnson, D. E.; Cannady, S. B.; Lehman, T. M.; Landreth, G. E. (1999): Identification of microglial signal transduction pathways mediating a neurotoxic response to amyloidogenic fragments of beta-amyloid and prion proteins. In *The Journal of neuroscience : the official journal of the Society for Neuroscience* 19 (3), pp. 928–939.

Combs, C. K.; Karlo, J. C.; Kao, S. C.; Landreth, G. E. (2001): beta-Amyloid stimulation of microglia and monocytes results in TNFalpha-dependent expression of inducible nitric oxide synthase and neuronal apoptosis. In *The Journal of neuroscience : the official journal of the Society for Neuroscience* 21 (4), pp. 1179–1188.

Corder, E. H.; Saunders, A. M.; Risch, N. J.; Strittmatter, W. J.; Schmechel, D. E.; Gaskell, P. C., JR et al. (1994): Protective effect of apolipoprotein E type 2 allele for late onset Alzheimer disease. In *Nature genetics* 7 (2), pp. 180–184. DOI: 10.1038/ng0694-180.

Corder, E. H.; Saunders, A. M.; Strittmatter, W. J.; Schmechel, D. E.; Gaskell, P. C.; Small, G. W. et al. (1993): Gene dose of apolipoprotein E type 4 allele and the risk of Alzheimer's disease in late onset families. In *Science (New York, N.Y.)* 261 (5123), pp. 921–923.

Correas, I.; Padilla, R.; Avila, J. (1990): The tubulin-binding sequence of brain microtubule-associated proteins, tau and MAP-2, is also involved in actin binding. In *Biochemical Journal* 269 (1), pp. 61–64.

Cuervo, Ana Maria (2008): Autophagy and aging: keeping that old broom working. In *Trends in genetics : TIG* 24 (12), pp. 604–612. DOI: 10.1016/j.tig.2008.10.002.

Cummings, Jeffrey; Lee, Garam; Ritter, Aaron; Zhong, Kate (2018): Alzheimer's disease drug development pipeline: 2018. In *Alzheimer's & dementia (New York, N. Y.)* 4, pp. 195–214. DOI: 10.1016/j.trci.2018.03.009.

Dantzer, Robert; O'Connor, Jason C.; Freund, Gregory G.; Johnson, Rodney W.; Kelley, Keith W. (2008): From inflammation to sickness and depression: when the immune system subjugates the brain. In *Nature reviews. Neuroscience* 9 (1), pp. 46–56. DOI: 10.1038/nrn2297.

Dardiotis, Efthimios; Siokas, Vasileios; Pantazi, Eva; Dardioti, Maria; Rikos, Dimitrios; Xiromerisiou, Georgia et al. (2017): A novel mutation in TREM2 gene causing Nasu-Hakola disease and review of the literature. In *Neurobiology of aging* 53, 194.e13-194.e22. DOI: 10.1016/j.neurobiolaging.2017.01.015.

Das, Utpal; Scott, David A.; Ganguly, Archan; Koo, Edward H.; Tang, Yong; Roy, Subhojit (2013): Activity-Induced Convergence of APP and BACE-1 in Acidic Microdomains via an Endocytosis-Dependent Pathway. In *Neuron* 79 (3), pp. 447–460. DOI: 10.1016/j.neuron.2013.05.035.

Deane, Rashid; Sagare, Abhay; Hamm, Katie; Parisi, Margaret; Lane, Steven; Finn, Mary Beth et al. (2008): apoE isoform-specific disruption of amyloid beta peptide clearance from mouse brain. In *The Journal of clinical investigation* 118 (12), pp. 4002–4013. DOI: 10.1172/JCI36663.

Dennehy, Kevin M.; Ferwerda, Gerben; Faro-Trindade, Inês; Pyż, Elwira; Willment, Janet A.; Taylor, Philip R. et al. (2008): Syk kinase is required for collaborative cytokine production induced through Dectin-1 and Toll-like receptors. In *European Journal of Immunology* 38 (2), pp. 500–506. DOI: 10.1002/eji.200737741.

Derkinderen, Pascal; Scales, Timothy M. E.; Hanger, Diane P.; Leung, Kit-Yi; Byers, Helen L.; Ward, Malcolm A. et al. (2005a): Tyrosine 394 Is Phosphorylated in Alzheimer's Paired Helical Filament Tau and in Fetal Tau with c-Abl as the Candidate Tyrosine Kinase. In *J. Neurosci.* 25 (28), pp. 6584–6593. DOI: 10.1523/JNEUROSCI.1487-05.2005.

Derkinderen, Pascal; Scales, Timothy M. E.; Hanger, Diane P.; Leung, Kit-Yi; Byers, Helen L.; Ward, Malcolm A. et al. (2005b): Tyrosine 394 Is Phosphorylated in Alzheimer's Paired Helical Filament Tau and in Fetal Tau with c-Abl as the Candidate Tyrosine Kinase. In *J. Neurosci.* 25 (28), pp. 6584–6593. DOI: 10.1523/JNEUROSCI.1487-05.2005.

Desikan, R. S.; Schork, A. J.; Wang, Y.; Witoelar, A.; Sharma, M.; McEvoy, L. K. et al. (2015): Genetic overlap between Alzheimer's disease and Parkinson's disease at the MAPT locus. In *Molecular psychiatry* 20 (12), pp. 1588–1595. DOI: 10.1038/mp.2015.6.

DeVos, Sarah L.; Goncharoff, Dustin K.; Chen, Guo; Kebodeaux, Carey S.; Yamada, Kaoru; Stewart, Floy R. et al. (2013): Antisense reduction of tau in adult mice protects against seizures. In *The Journal of neuroscience : the official journal of the Society for Neuroscience* 33 (31), pp. 12887–12897. DOI: 10.1523/JNEUROSCI.2107-13.2013.

DeVos, Sarah L.; Miller, Rebecca L.; Schoch, Kathleen M.; Holmes, Brandon B.; Kebodeaux, Carey S.; Wegener, Amy J. et al. (2017): Tau reduction prevents neuronal loss and reverses pathological tau deposition and seeding in mice with tauopathy. In *Science translational medicine* 9 (374). DOI: 10.1126/scitranslmed.aag0481.

Dixit, Ram; Ross, Jennifer L.; Goldman, Yale E.; Holzbaur, Erika L. F. (2008): Differential regulation of dynein and kinesin motor proteins by tau. In *Science (New York, N.Y.)* 319 (5866), pp. 1086–1089. DOI: 10.1126/science.1152993.

Doens, Deborah; Fernández, Patricia L. (2014): Microglia receptors and their implications in the response to amyloid β for Alzheimer's disease pathogenesis. In *Journal of neuroinflammation* 11, p. 48. DOI: 10.1186/1742-2094-11-48.

Domingues, Catarina; Cruz e Silva, Odete A.B.; Henriques, Ana Gabriela (2017): Impact of Cytokines and Chemokines on Alzheimer's Disease Neuro-pathological Hallmarks. In *Current Alzheimer Research* 14 (8), pp. 870–882. DOI: 10.2174/1567205014666170317113606.

Doody, Rachelle S.; Thomas, Ronald G.; Farlow, Martin; Iwatsubo, Takeshi; Vellas, Bruno; Joffe, Steven et al. (2014): Phase 3 trials of solanezumab for mild-to-moderate Alzheimer's disease. In *The New England journal of medicine* 370 (4), pp. 311–321. DOI: 10.1056/NEJMoa1312889.

Drewes, G.; Trinczek, B.; Illenberger, S.; Biernat, J.; Schmitt-Ulms, G.; Meyer, H. E. et al. (1995): Microtubule-associated protein/microtubule affinity-regulating kinase (p110mark). A novel protein kinase that regulates tau-microtubule interactions and dynamic instability by phosphorylation at the Alzheimer-specific site serine 262. In *The Journal of biological chemistry* 270 (13), pp. 7679–7688.

Du, Dongshu; Hu, Li; Wu, Jiaxiang; Wu, Qin; Cheng, Wenjing; Guo, Yuhong et al. (2017): Neuroinflammation contributes to autophagy flux blockage in the neurons of rostral ventrolateral medulla in stress-induced hypertension rats. In *Journal of neuroinflammation* 14 (1), p. 169. DOI: 10.1186/s12974-017-0942-2.

Duff, K.; Eckman, C.; Zehr, C.; Yu, X.; Prada, C. M.; Perez-tur, J. et al. (1996): Increased amyloid-beta42(43) in brains of mice expressing mutant presenilin 1. In *Nature* 383 (6602), pp. 710–713. DOI: 10.1038/383710a0.

Easley, Charles A.; Ben-Yehudah, Ahmi; Redinger, Carrie J.; Oliver, Stacie L.; Varum, Sandra T.; Eisinger, Vonya M. et al. (2010): mTOR-Mediated Activation of p70 S6K Induces Differentiation of Pluripotent Human Embryonic Stem Cells. In *Cellular Reprogramming* 12 (3), pp. 263–273. DOI: 10.1089/cell.2010.0011.

Efeyan, Alejo; Sabatini, David M. (2013): Nutrients versus growth factors in mTORC1 activation. In *Biochemical Society transactions* 41 (4). DOI: 10.1042/BST20130063.

Eidenmuller, J.; Fath, T.; Maas, T.; Pool, M.; Sontag, E.; Brandt, R. (2001): Phosphorylation-mimicking glutamate clusters in the proline-rich region are sufficient to simulate the functional

deficiencies of hyperphosphorylated tau protein. In *The Biochemical journal* 357 (Pt 3), pp. 759–767.

Eskelinen, Eeva-Liisa; Saftig, Paul (2009): Autophagy: a lysosomal degradation pathway with a central role in health and disease. In *Biochimica et biophysica acta* 1793 (4), pp. 664–673. DOI: 10.1016/j.bbamcr.2008.07.014.

Espinoza, Marisol; Silva, Rohan de; Dickson, Dennis W.; Davies, Peter (2008): Differential Incorporation of Tau Isoforms in Alzheimer's Disease. In *Journal of Alzheimer's disease : JAD* 14 (1), pp. 1–16.

Esposito, Giuseppe; Scuderi, Caterina; Lu, Jie; Savani, Claudia; Filippis, Daniele de; Iuvone, Teresa et al. (2008): S100B induces tau protein hyperphosphorylation via Dickopff-1 up-regulation and disrupts the Wnt pathway in human neural stem cells. In *Journal of cellular and molecular medicine* 12 (3), pp. 914–927. DOI: 10.1111/j.1582-4934.2008.00159.x.

Fahrenhold, Marie; Rakic, Sonja; Classey, John; Brayne, Carol; Ince, Paul G.; Nicoll, James A. R.; Boche, Delphine (2017): TREM2 expression in the human brain: a marker of monocyte recruitment? In *Brain pathology (Zurich, Switzerland)*. DOI: 10.1111/bpa.12564.

Faris, M.; Gaskin, F.; Parsons, J. T.; Fu, S. M. (1994): CD40 signaling pathway: anti-CD40 monoclonal antibody induces rapid dephosphorylation and phosphorylation of tyrosine-phosphorylated proteins including protein tyrosine kinase Lyn, Fyn, and Syk and the appearance of a 28-kD tyrosine phosphorylated protein. In *The Journal of experimental medicine* 179 (6), pp. 1923–1931.

Faruki, S.; Geahlen, R. L.; Asai, D. J. (2000): Syk-dependent phosphorylation of microtubules in activated B-lymphocytes. In *Journal of cell science* 113 (Pt 14), pp. 2557–2565.

Fatouros, Chronis; Pir, Ghulam Jeelani; Biernat, Jacek; Koushika, Sandhya Padmanabhan; Mandelkow, Eckhard; Mandelkow, Eva-Maria et al. (2012): Inhibition of tau aggregation in a novel Caenorhabditis elegans model of tauopathy mitigates proteotoxicity. In *Human molecular genetics* 21 (16), pp. 3587–3603. DOI: 10.1093/hmg/dds190.

Feldman, A. L.; Sun, D. X.; Law, M. E.; Novak, A. J.; Attygalle, A. D.; Thorland, E. C. et al. (2008): Overexpression of Syk tyrosine kinase in peripheral T-cell lymphomas. In *Leukemia : official journal of the Leukemia Society of America, Leukemia Research Fund, U.K* 22 (6), pp. 1139–1143. DOI: 10.1038/leu.2008.77.

Feng, Yuchen; He, Ding; Yao, Zhiyuan; Klionsky, Daniel J. (2014): The machinery of macroautophagy. In *Cell Research* 24 (1), p. 24. DOI: 10.1038/cr.2013.168.

Fernández-Nogales, Marta; Cabrera, Jorge R.; Santos-Galindo, María; Hoozemans, Jeroen J. M.; Ferrer, Isidro; Rozemuller, Annemieke J. M. et al. (2014): Huntington's disease is a four-repeat tauopathy with tau nuclear rods. In *Nature medicine* 20 (8), pp. 881–885. DOI: 10.1038/nm.3617.

Filipello, Fabia; Morini, Raffaella; Corradini, Irene; Zerbi, Valerio; Canzi, Alice; Michalski, Bernadeta et al. (2018): The Microglial Innate Immune Receptor TREM2 Is Required for Synapse Elimination and Normal Brain Connectivity. In *Immunity* 48 (5), 979-991.e8. DOI: 10.1016/j.immuni.2018.04.016.

Finelli, Deana; Rollinson, Sara; Harris, Jenny; Jones, Matthew; Richardson, Anna; Gerhard, Alex et al. (2015): TREM2 analysis and increased risk of Alzheimer's disease. In *Neurobiology of aging* 36 (1), 546.e9-13. DOI: 10.1016/j.neurobiolaging.2014.08.001.

Forlenza, Orestes V.; Diniz, Breno S.; Radanovic, Márcia; Santos, Franklin S.; Talib, Leda L.; Gattaz, Wagner F. (2011): Disease-modifying properties of long-term lithium treatment for amnestic mild cognitive impairment: randomised controlled trial. In *The British journal of psychiatry : the journal of mental science* 198 (5), pp. 351–356. DOI: 10.1192/bjp.bp.110.080044.

Frackowiak, J.; Wisniewski, H. M.; Wegiel, J.; Merz, G. S.; Iqbal, K.; Wang, K. C. (1992): Ultrastructure of the microglia that phagocytose amyloid and the microglia that produce beta-amyloid fibrils. In *Acta neuropathologica* 84 (3), pp. 225–233.

Frank, Stefanie; Burbach, Guido J.; Bonin, Michael; Walter, Michael; Streit, Wolfgang; Bechmann, Ingo; Deller, Thomas (2008): TREM2 is upregulated in amyloid plaque-associated microglia in aged APP23 transgenic mice. In *Glia* 56 (13), pp. 1438–1447. DOI: 10.1002/glia.20710.

Frautschy, S. A.; Yang, F.; Irrizarry, M.; Hyman, B.; Saido, T. C.; Hsiao, K.; Cole, G. M. (1998): Microglial response to amyloid plaques in APPsw transgenic mice. In *The American journal of pathology* 152 (1), pp. 307–317.

Fruchon, S.; Kheirallah, S.; Al Saati, T.; Ysebaert, L.; Laurent, C.; Leseux, L. et al. (2012): Involvement of the Syk-mTOR pathway in follicular lymphoma cell invasion and angiogenesis. In *Leukemia* 26 (4), pp. 795–805. DOI: 10.1038/leu.2011.248.

Funderburk, Sarah F.; Marcellino, Bridget K.; Yue, Zhenyu (2010): Cell "self-eating" (autophagy) mechanism in Alzheimer's disease. In *The Mount Sinai journal of medicine, New York* 77 (1), pp. 59–68. DOI: 10.1002/msj.20161.

Furlong, Michael T.; Mahrenholz, Alan M.; Kim, Ki-Han; Ashendel, Curtis L.; Harrison, Marietta L.; Geahlen, Robert L. (1997): Identification of the major sites of autophosphorylation of the murine protein-tyrosine kinase Syk. In *Biochimica et Biophysica Acta (BBA) - Molecular Cell Research* 1355 (2), pp. 177–190. DOI: 10.1016/S0167-4889(96)00131-0.

Furuichi, Y.; Takakura, S.; Satoh, H.; Mori, J.; Kohsaka, M. (1992): The effect of nilvadipine, a dihydropyridine type calcium channel blocker, on local cerebral blood flow in rats. In *Japanese journal of pharmacology* 58 (4), pp. 457–460.

Fuster-Matanzo, A.; Llorens-Martín, M.; Hernández, F.; Avila, J. (2013): Role of Neuroinflammation in Adult Neurogenesis and Alzheimer Disease: Therapeutic Approaches. In *Mediators of inflammation* 2013. DOI: 10.1155/2013/260925.

Futterer, K.; Wong, J.; Grucza, R. A.; Chan, A. C.; Waksman, G. (1998): Structural basis for Syk tyrosine kinase ubiquity in signal transduction pathways revealed by the crystal structure of its regulatory SH2 domains bound to a dually phosphorylated ITAM peptide. In *Journal of molecular biology* 281 (3), pp. 523–537. DOI: 10.1006/jmbi.1998.1964.

Gao, Pan; Qiao, Xianghe; Sun, Haibin; Huang, Yi; Lin, Jie; Li, Longjiang et al. (2017): Activated spleen tyrosine kinase promotes malignant progression of oral squamous cell carcinoma via mTOR/S6 signaling pathway in an ERK1/2-independent manner. In *Oncotarget* 8 (48), pp. 83900–83912. DOI: 10.18632/oncotarget.19911.

Gauthier, Serge; Feldman, Howard H.; Schneider, Lon S.; Wilcock, Gordon K.; Frisoni, Giovanni B.; Hardlund, Jiri H. et al. (2016): Efficacy and safety of tau-aggregation inhibitor therapy in patients with mild or moderate Alzheimer's disease. A randomised, controlled, double-blind, parallel-arm, phase 3 trial. In *The Lancet* 388 (10062), pp. 2873–2884. DOI: 10.1016/S0140-6736(16)31275-2.

Ge, L.; Zhang, M.; Schekman, R. (2014): Phosphatidylinositol 3-kinase and COPII generate LC3 lipidation vesicles from the ER-Golgi intermediate compartment. In *eLife* 3, pp. e04135. DOI: 10.7554/eLife.04135.

Geahlen, Robert L. (2014): Getting Syk: spleen tyrosine kinase as a therapeutic target. In *Trends in pharmacological sciences* 35 (8), pp. 414–422. DOI: 10.1016/j.tips.2014.05.007.

Getz, Godfrey S.; Reardon, Catherine A. (2009): Apoprotein E as a lipid transport and signaling protein in the blood, liver, and artery wall. In *Journal of Lipid Research* 50 (Suppl), S156-61. DOI: 10.1194/jlr.R800058-JLR200.

Ghavami, Saeid; Shojaei, Shahla; Yeganeh, Behzad; Ande, Sudharsana R.; Jangamreddy, Jaganmohan R.; Mehrpour, Maryam et al. (2014): Autophagy and apoptosis dysfunction in neurodegenerative disorders. In *Progress in neurobiology* 112, pp. 24–49. DOI: 10.1016/j.pneurobio.2013.10.004.

Ghezzi, Laura; Carandini, Tiziana; Arighi, Andrea; Fenoglio, Chiara; Arcaro, Marina; Riz, Milena de et al. (2017): Evidence of CNS beta-amyloid deposition in Nasu-Hakola disease due to the TREM2 Q33X mutation. In *Neurology* 89 (24), pp. 2503–2505. DOI: 10.1212/WNL.0000000000004747.

Ghosh, Soumitra; Geahlen, Robert L. (2015): Stress Granules Modulate SYK to Cause Microglial Cell Dysfunction in Alzheimer's Disease. In *EBioMedicine* 2 (11), pp. 1785–1798. DOI: 10.1016/j.ebiom.2015.09.053.

Glenner, G. G.; Wong, C. W. (1984a): Alzheimer's disease and Down's syndrome: sharing of a unique cerebrovascular amyloid fibril protein. In *Biochemical and biophysical research communications* 122 (3), pp. 1131–1135.

Glenner, G. G.; Wong, C. W. (1984b): Alzheimer's disease: initial report of the purification and characterization of a novel cerebrovascular amyloid protein. In *Biochemical and biophysical research communications* 120 (3), pp. 885–890.

Goate, A.; Chartier-Harlin, M. C.; Mullan, M.; Brown, J.; Crawford, F.; Fidani, L. et al. (1991): Segregation of a missense mutation in the amyloid precursor protein gene with familial Alzheimer's disease. In *Nature* 349 (6311), pp. 704–706. DOI: 10.1038/349704a0.

Goedert, M.; Jakes, R. (1990): Expression of separate isoforms of human tau protein: correlation with the tau pattern in brain and effects on tubulin polymerization. In *The EMBO journal* 9 (13), pp. 4225–4230.

Goedert, M.; Spillantini, M. G.; Jakes, R.; Rutherford, D.; Crowther, R. A. (1989): Multiple isoforms of human microtubule-associated protein tau: sequences and localization in neurofibrillary tangles of Alzheimer's disease. In *Neuron* 3 (4), pp. 519–526. DOI: 10.1016/0896-6273(89)90210-9.

Goldgaber, D.; Lerman, M. I.; McBride, O. W.; Saffiotti, U.; Gajdusek, D. C. (1987): Characterization and chromosomal localization of a cDNA encoding brain amyloid of Alzheimer's disease. In *Science (New York, N.Y.)* 235 (4791), pp. 877–880.

Gong, Cheng-Xin; Lidsky, Theodore; Wegiel, Jerzy; Zuck, Lorinda; Grundke-Iqbal, Inge; Iqbal, Khalid (2000): Phosphorylation of Microtubule-associated Protein Tau Is Regulated by Protein Phosphatase 2A in Mammalian Brain IMPLICATIONS FOR NEUROFIBRILLARY DEGENERATION IN ALZHEIMER'S DISEASE. In *J. Biol. Chem.* 275 (8), pp. 5535–5544. DOI: 10.1074/jbc.275.8.5535.

Gonzalez-Reyes, Rodrigo E.; Rubiano, Maria G. (2018): Astrocyte s RAGE: More Than Just a Question of Mood. In *Central nervous system agents in medicinal chemistry* 18 (1), pp. 39–48. DOI: 10.2174/1871524916999160505105121.

Gordon, M. N.; La Holcomb; Jantzen, P. T.; DiCarlo, G.; Wilcock, D.; Boyett, K. W. et al. (2002): Time course of the development of Alzheimer-like pathology in the doubly transgenic PS1+APP mouse. In *Experimental neurology* 173 (2), pp. 183–195. DOI: 10.1006/exnr.2001.7754.

Götz, J.; Chen, F.; van Dorpe, J.; Nitsch, R. M. (2001): Formation of Neurofibrillary Tangles in P301L Tau Transgenic Mice Induced by Aβ42 Fibrils. In *Science* 293 (5534), pp. 1491–1495. DOI: 10.1126/science.1062097.

Grathwohl, Stefan A.; Kalin, Roland E.; Bolmont, Tristan; Prokop, Stefan; Winkelmann, Georg; Kaeser, Stephan A. et al. (2009): Formation and maintenance of Alzheimer's disease beta-amyloid plaques in the absence of microglia. In *Nature neuroscience* 12 (11), pp. 1361–1363. DOI: 10.1038/nn.2432.

Griffin, W. S.; Stanley, L. C.; Ling, C.; White, L.; MacLeod, V.; Perrot, L. J. et al. (1989): Brain interleukin 1 and S-100 immunoreactivity are elevated in Down syndrome and Alzheimer disease. In *Proceedings of the National Academy of Sciences of the United States of America* 86 (19), pp. 7611–7615.

Guillot-Sestier, Marie-Victoire; Doty, Kevin R.; Gate, David; Rodriguez, Javier, JR; Leung, Brian P.; Rezai-Zadeh, Kavon; Town, Terrence (2015): Il10 deficiency rebalances innate immunity to mitigate Alzheimer-like pathology. In *Neuron* 85 (3), pp. 534–548. DOI: 10.1016/j.neuron.2014.12.068.

Guo, Tong; Noble, Wendy; Hanger, Diane P. (2017): Roles of tau protein in health and disease. In *Acta neuropathologica* 133 (5), pp. 665–704. DOI: 10.1007/s00401-017-1707-9.

Hadas, Smadar; Spira, Maya; Hanisch, Uwe-Karsten; Reichert, Fanny; Rotshenker, Shlomo (2012): Complement receptor-3 negatively regulates the phagocytosis of degenerated myelin through tyrosine kinase Syk and cofilin. In *Journal of neuroinflammation* 9 (1), p. 166. DOI: 10.1186/1742-2094-9-166.

Hamano, Tadanori; Gendron, Tania F.; Causevic, Ena; Yen, Shu-Hui; Lin, Wen-Lang; Isidoro, Ciro et al. (2008): Autophagic-lysosomal perturbation enhances tau aggregation in transfectants with induced wild-type tau expression. In *European Journal of Neuroscience* 27 (5), pp. 1119–1130. DOI: 10.1111/j.1460-9568.2008.06084.x.

Han, Chaofeng; Jin, Jing; Xu, Sheng; Liu, Haibo; Li, Nan; Cao, Xuetao (2010): Integrin CD11b negatively regulates TLR-triggered inflammatory responses by activating

Syk and promoting degradation of MyD88 and TRIF via Cbl-b. In *Nature immunology* 11 (8), pp. 734–742. DOI: 10.1038/ni.1908.

Hanger, Diane P.; Anderton, Brian H.; Noble, Wendy (2009): Tau phosphorylation: the therapeutic challenge for neurodegenerative disease. In *Trends in molecular medicine* 15 (3), pp. 112–119. DOI: 10.1016/j.molmed.2009.01.003.

Hanisch, Uwe-Karsten (2002): Microglia as a source and target of cytokines. In *Glia* 40 (2), pp. 140–155. DOI: 10.1002/glia.10161.

Hanyu, Haruo; Hirao, Kentaro; Shimizu, Soichiro; Sato, Tomohiko; Kiuchi, Akihiro; Iwamoto, Toshihiko (2007): Nilvadipine prevents cognitive decline of patients with mild cognitive impairment. In *International Journal of Geriatric Psychiatry* 22 (12), pp. 1264–1266. DOI: 10.1002/gps.1851.

Hardy, J. A.; Higgins, G. A. (1992): Alzheimer's disease: the amyloid cascade hypothesis. In *Science (New York, N.Y.)* 256 (5054), pp. 184–185.

Hardy, John; Selkoe, Dennis J. (2002): The Amyloid Hypothesis of Alzheimer's Disease: Progress and Problems on the Road to Therapeutics. In *Science* 297 (5580), pp. 353–356. DOI: 10.1126/science.1072994.

Hayden, Eric Y.; Teplow, David B. (2013): Amyloid β-protein oligomers and Alzheimer's disease. In *Alzheimer's research & therapy* 5 (6), p. 60. DOI: 10.1186/alzrt226.

Hemmings, Brian A.; Restuccia, David F. (2012): PI3K-PKB/Akt Pathway. In *Cold Spring Harbor perspectives in biology* 4 (9). DOI: 10.1101/cshperspect.a011189.

Hermida, Miguel A.; Dinesh Kumar, J.; Leslie, Nick R. (2017): GSK3 and its interactions with the PI3K/AKT/mTOR signalling network. In *Advances in biological regulation* 65, pp. 5–15. DOI: 10.1016/j.jbior.2017.06.003.

Hickman, Suzanne E.; Allison, Elizabeth K.; El Khoury, Joseph (2008): Microglial dysfunction and defective beta-amyloid clearance pathways in aging Alzheimer's disease mice. In *The Journal of neuroscience : the official journal of the Society for Neuroscience* 28 (33), pp. 8354–8360. DOI: 10.1523/JNEUROSCI.0616-08.2008.

Holcomb, L.; Gordon, M. N.; Jantzen, P.; Hsiao, K.; Duff, K.; Morgan, D. (1999): Behavioral changes in transgenic mice expressing both amyloid precursor protein and presenilin-1 mutations: lack of association with amyloid deposits. In *Behavior genetics* 29 (3), pp. 177–185.

Holcomb, L.; Gordon, M. N.; McGowan, E.; Yu, X.; Benkovic, S.; Jantzen, P. et al. (1998): Accelerated Alzheimer-type phenotype in transgenic mice carrying both mutant amyloid precursor protein and presenilin 1 transgenes. In *Nature medicine* 4 (1), pp. 97–100.

Honig, Lawrence S.; Vellas, Bruno; Woodward, Michael; Boada, Merce; Bullock, Roger; Borrie, Michael et al. (2018): Trial of Solanezumab for Mild Dementia Due to Alzheimer's Disease. In *The New England journal of medicine* 378 (4), pp. 321–330. DOI: 10.1056/NEJMoa1705971.

Hooper, C.; Killick, R.; Lovestone, S. (2008): The GSK3 hypothesis of Alzheimer's disease. In *Journal of neurochemistry* 104 (6), pp. 1433–1439. DOI: 10.1111/j.1471-4159.2007.05194.x.

Hoover, Brian R.; Reed, Miranda N.; Su, Jianjun; Penrod, Rachel D.; Kotilinek, Linda A.; Grant, Marianne K. et al. (2010): Tau mislocalization to dendritic spines mediates synaptic dysfunction

independently of neurodegeneration. In *Neuron* 68 (6), pp. 1067–1081. DOI: 10.1016/j.neuron.2010.11.030.

Hsiao, K.; Chapman, P.; Nilsen, S.; Eckman, C.; Harigaya, Y.; Younkin, S. et al. (1996): Correlative memory deficits, Abeta elevation, and amyloid plaques in transgenic mice. In *Science (New York, N.Y.)* 274 (5284), pp. 99–102.

http://www.molgen.ua.ac.be/ADMutations/.

Huang, D. Y.; Weisgraber, K. H.; Goedert, M.; Saunders, A. M.; Roses, A. D.; Strittmatter, W. J. (1995): ApoE3 binding to tau tandem repeat I is abolished by tau serine262 phosphorylation. In *Neuroscience letters* 192 (3), pp. 209–212.

Hull, M.; Berger, M.; Volk, B.; Bauer, J. (1996): Occurrence of interleukin-6 in cortical plaques of Alzheimer's disease patients may precede transformation of diffuse into neuritic plaques. In *Annals of the New York Academy of Sciences* 777, pp. 205–212.

Hutton, Mike; Lendon, Corinne L.; Rizzu, Patrizia; Baker, Matt; Froelich, Susanne; Houlden, Henry et al. (1998): Association of missense and 5′-splice-site mutations in *tau* with the inherited dementia FTDP-17. In *Nature* 393 (6686), p. 702. DOI: 10.1038/31508.

Hynd, Matthew R.; Scott, Heather L.; Dodd, Peter R. (2004): Glutamate-mediated excitotoxicity and neurodegeneration in Alzheimer's disease. In *Neurochemistry international* 45 (5), pp. 583–595. DOI: 10.1016/j.neuint.2004.03.007.

Inoki, Ken; Li, Yong; Xu, Tian; Guan, Kun-Liang (2003a): Rheb GTPase is a direct target of TSC2 GAP activity and regulates mTOR signaling. In *Genes & development* 17 (15), pp. 1829–1834. DOI: 10.1101/gad.1110003.

Inoki, Ken; Li, Yong; Zhu, Tianquan; Wu, Jun; Guan, Kun-Liang (2002): TSC2 is phosphorylated and inhibited by Akt and suppresses mTOR signalling. In *Nature cell biology* 4 (9), pp. 648–657. DOI: 10.1038/ncb839.

Inoki, Ken; Ouyang, Hongjiao; Zhu, Tianqing; Lindvall, Charlotta; Wang, Yian; Zhang, Xiaojie et al. (2006): TSC2 Integrates Wnt and Energy Signals via a Coordinated Phosphorylation by AMPK and GSK3 to Regulate Cell Growth. In *Cell* 126 (5), pp. 955–968. DOI: 10.1016/j.cell.2006.06.055.

Inoki, Ken; Zhu, Tianqing; Guan, Kun-Liang (2003b): TSC2 mediates cellular energy response to control cell growth and survival. In *Cell* 115 (5), pp. 577–590.

Inoue, Keiichi; Rispoli, Joanne; Kaphzan, Hanoch; Klann, Eric; Chen, Emily I.; Kim, Jongpil et al. (2012): Macroautophagy deficiency mediates age-dependent neurodegeneration through a phospho-tau pathway. In *Molecular neurodegeneration* 7 (1), p. 48. DOI: 10.1186/1750-1326-7-48.

Insel, Philip S.; Ossenkoppele, Rik; Gessert, Devon; Jagust, William; Landau, Susan; Hansson, Oskar et al. (2017): Time to Amyloid Positivity and Preclinical Changes in Brain Metabolism, Atrophy, and Cognition: Evidence for Emerging Amyloid Pathology in Alzheimer's Disease. In *Frontiers in neuroscience* 11. DOI: 10.3389/fnins.2017.00281.

Iqbal, Khalid; Gong, Cheng-Xin; Liu, Fei (2013): Hyperphosphorylation-Induced Tau Oligomers. In *Frontiers in neurology* 4. DOI: 10.3389/fneur.2013.00112.

Irizarry, M. C.; McNamara, M.; Fedorchak, K.; Hsiao, K.; Hyman, B. T. (1997): APPSw transgenic mice develop age-related A beta deposits and neuropil abnormalities, but no neuronal loss in CA1. In *Journal of neuropathology and experimental neurology* 56 (9), pp. 965–973.

Jack, Clifford R.; Knopman, David S.; Jagust, William J.; Petersen, Ronald C.; Weiner, Michael W.; Aisen, Paul S. et al. (2013): Update on hypothetical model of Alzheimer's disease biomarkers. In *Lancet neurology* 12 (2), pp. 207–216. DOI: 10.1016/S1474-4422(12)70291-0.

Jakus, Zoltan; Fodor, Szabina; Abram, Clare L.; Lowell, Clifford A.; Mocsai, Attila (2007): Immunoreceptor-like signaling by beta 2 and beta 3 integrins. In *Trends in cell biology* 17 (10), pp. 493–501. DOI: 10.1016/j.tcb.2007.09.001.

Jana, Malabendu; Anderson, Jamar A.; Saha, Ramendra N.; Liu, Xiaojuan; Pahan, Kalipada (2005): Regulation of inducible nitric oxide synthase in proinflammatory cytokine-stimulated human primary astrocytes. In *Free radical biology & medicine* 38 (5), pp. 655–664. DOI: 10.1016/j.freeradbiomed.2004.11.021.

Jay, Taylor R.; Miller, Crystal M.; Cheng, Paul J.; Graham, Leah C.; Bemiller, Shane; Broihier, Margaret L. et al. (2015): TREM2 deficiency eliminates TREM2+ inflammatory macrophages and ameliorates pathology in Alzheimer's disease mouse models. In *The Journal of experimental medicine* 212 (3), pp. 287–295. DOI: 10.1084/jem.20142322.

Jensen, Poul Henning; Hager, Henrik; Nielsen, Morten S.; Højrup, Peter; Gliemann, Jørgen; Jakes, Ross (1999): α-Synuclein Binds to Tau and Stimulates the Protein Kinase A-catalyzed Tau Phosphorylation of Serine Residues 262 and 356. In *J. Biol. Chem.* 274 (36), pp. 25481–25489. DOI: 10.1074/jbc.274.36.25481.

Jiang, Teng; Tan, Lan; Zhu, Xi-Chen; Zhang, Qiao-Quan; Cao, Lei; Tan, Meng-Shan et al. (2014a): Upregulation of TREM2 ameliorates neuropathology and rescues spatial cognitive impairment in a transgenic mouse model of Alzheimer's disease. In *Neuropsychopharmacology : official publication of the American College of Neuropsychopharmacology* 39 (13), pp. 2949–2962. DOI: 10.1038/npp.2014.164.

Jiang, Teng; Tan, Lan; Zhu, Xi-Chen; Zhou, Jun-Shan; Cao, Lei; Tan, Meng-Shan et al. (2015): Silencing of TREM2 exacerbates tau pathology, neurodegenerative changes, and spatial learning deficits in P301S tau transgenic mice. In *Neurobiology of aging* 36 (12), pp. 3176–3186. DOI: 10.1016/j.neurobiolaging.2015.08.019.

Jiang, Teng; Yu, Jin-Tai; Zhu, Xi-Chen; Zhang, Qiao-Quan; Cao, Lei; Wang, Hui-Fu et al. (2014b): Temsirolimus attenuates tauopathy in vitro and in vivo by targeting tau hyperphosphorylation and autophagic clearance. In *Neuropharmacology* 85, pp. 121–130. DOI: 10.1016/j.neuropharm.2014.05.032.

Jiang, Teng; Zhang, Ying-Dong; Chen, Qi; Gao, Qing; Zhu, Xi-Chen; Zhou, Jun-Shan et al. (2016): TREM2 modifies microglial phenotype and provides neuroprotection in P301S tau transgenic mice. In *Neuropharmacology* 105, pp. 196–206. DOI: 10.1016/j.neuropharm.2016.01.028.

Jonsson, Thorlakur; Atwal, Jasvinder K.; Steinberg, Stacy; Snaedal, Jon; Jonsson, Palmi V.; Bjornsson, Sigurbjorn et al. (2012): A mutation in APP protects against Alzheimer's disease and age-related cognitive decline. In *Nature* 488 (7409), pp. 96–99. DOI: 10.1038/nature11283.

Jung, Chang Hwa; Ro, Seung-Hyun; Cao, Jing; Otto, Neil Michael; Kim, Do-Hyung (2010): mTOR regulation of autophagy. In *FEBS letters* 584 (7), pp. 1287–1295. DOI: 10.1016/j.febslet.2010.01.017.

Kabeya, Y.; Mizushima, N.; Ueno, T.; Yamamoto, A.; Kirisako, T.; Noda, T. et al. (2000): LC3, a mammalian homologue of yeast Apg8p, is localized in autophagosome membranes after processing. In *The EMBO journal* 19 (21), pp. 5720–5728. DOI: 10.1093/emboj/19.21.5720.

Kagawa, H.; Nomura, S.; Ozaki, Y.; Nagahama, M.; Fukuhara, S. (1999): Effects of nilvadipine on cytokine-levels and soluble factors in collagen disease complicated with essential hypertension. In *Clinical and experimental hypertension (New York, N.Y. : 1993)* 21 (7), pp. 1177–1188.

Kametani, Fuyuki; Hasegawa, Masato (2018): Reconsideration of Amyloid Hypothesis and Tau Hypothesis in Alzheimer's Disease. In *Front. Neurosci.* 12, p. 1517. DOI: 10.3389/fnins.2018.00025.

Kandalepas, Patty C.; Sadleir, Katherine R.; Eimer, William A.; Zhao, Jie; Nicholson, Daniel A.; Vassar, Robert (2013): The Alzheimer's beta-secretase BACE1 localizes to normal presynaptic terminals and to dystrophic presynaptic terminals surrounding amyloid plaques. In *Acta neuropathologica* 126 (3), pp. 329–352. DOI: 10.1007/s00401-013-1152-3.

Kang, J.; Lemaire, H. G.; Unterbeck, A.; Salbaum, J. M.; Masters, C. L.; Grzeschik, K. H. et al. (1987): The precursor of Alzheimer's disease amyloid A4 protein resembles a cell-surface receptor. In *Nature* 325 (6106), pp. 733–736. DOI: 10.1038/325733a0.

Kaur, Maninder; Singh, Manjinder; Silakari, Om (2013): Inhibitors of switch kinase 'spleen tyrosine kinase' in inflammation and immune-mediated disorders: a review. In *European journal of medicinal chemistry* 67, pp. 434–446. DOI: 10.1016/j.ejmech.2013.04.070.

Khachaturian, Ara S.; Zandi, Peter P.; Lyketsos, Constantine G.; Hayden, Kathleen M.; Skoog, Ingmar; Norton, Maria C. et al. (2006): Antihypertensive medication use and incident Alzheimer disease: the Cache County Study. In *Archives of neurology* 63 (5), pp. 686–692. DOI: 10.1001/archneur.63.5.noc60013.

Kidd, M. (1963): Paired helical filaments in electron microscopy of Alzheimer's disease. In *Nature* 197, pp. 192–193.

Kim, Su-Man; Mun, Bo-Ram; Lee, Sun-Jun; Joh, Yechan; Lee, Hwa-Youn; Ji, Kon-Young et al. (2017): TREM2 promotes Aβ phagocytosis by upregulating C/EBPα-dependent CD36 expression in microglia. In *Scientific reports* 7 (1), p. 11118. DOI: 10.1038/s41598-017-11634-x.

Kimura, Tetsuya; Fukuda, Tetsuya; Sahara, Naruhiko; Yamashita, Shunji; Murayama, Miyuki; Mizoroki, Tatsuya et al. (2010): Aggregation of detergent-insoluble tau is involved in neuronal loss but not in synaptic loss. In *The Journal of biological chemistry* 285 (49), pp. 38692–38699. DOI: 10.1074/jbc.M110.136630.

King, Eleanor; O'Brien, John Tiernan; Donaghy, Paul; Morris, Christopher; Barnett, Nicola; Olsen, Kirsty et al. (2018): Peripheral inflammation in prodromal Alzheimer's and Lewy body dementias. In *J Neurol Neurosurg Psychiatry* 89 (4), pp. 339–345. DOI: 10.1136/jnnp-2017-317134.

Kitazawa, Masashi; Oddo, Salvatore; Yamasaki, Tritia R.; Green, Kim N.; Laferla, Frank M. (2005): Lipopolysaccharide-induced inflammation exacerbates tau pathology by a cyclin-dependent kinase 5-mediated pathway in a transgenic model of Alzheimer's disease. In *The Journal of neuroscience : the official journal of the Society for Neuroscience* 25 (39), pp. 8843–8853. DOI: 10.1523/JNEUROSCI.2868-05.2005.

Kiyota, Tomomi; Okuyama, Satoshi; Swan, Russell J.; Jacobsen, Michael T.; Gendelman, Howard E.; Ikezu, Tsuneya (2010): CNS expression of anti-inflammatory cytokine interleukin-4 attenuates Alzheimer's disease-like pathogenesis in APP+PS1 bigenic mice. In *The FASEB Journal* 24 (8), pp. 3093–3102. DOI: 10.1096/fj.10-155317.

Kober, Daniel L.; Alexander-Brett, Jennifer M.; Karch, Celeste M.; Cruchaga, Carlos; Colonna, Marco; Holtzman, Michael J.; Brett, Thomas J. (2016): Neurodegenerative disease mutations in TREM2 reveal a functional surface and distinct loss-of-function mechanisms. In *eLife* 5. DOI: 10.7554/eLife.20391.

Kober, Daniel L.; Brett, Tom J. (2017): TREM2-Ligand Interactions in Health and Disease. In *Journal of molecular biology* 429 (11), pp. 1607–1629. DOI: 10.1016/j.jmb.2017.04.004.

Koenigsknecht-Talboo, Jessica; Landreth, Gary E. (2005): Microglial phagocytosis induced by fibrillar beta-amyloid and IgGs are differentially regulated by proinflammatory cytokines. In *The Journal of neuroscience : the official journal of the Society for Neuroscience* 25 (36), pp. 8240–8249. DOI: 10.1523/JNEUROSCI.1808-05.2005.

Kontsekova, Eva; Zilka, Norbert; Kovacech, Branislav; Novak, Petr; Novak, Michal (2014): First-in-man tau vaccine targeting structural determinants essential for pathological tau-tau interaction reduces tau oligomerisation and neurofibrillary degeneration in an Alzheimer's disease model. In *Alzheimer's research & therapy* 6 (4), p. 44. DOI: 10.1186/alzrt278.

Korzhevskii, D. E.; Kirik, O. V. (2016): Brain Microglia and Microglial Markers. In *Neuroscience and Behavioral Physiology* 46 (3), pp. 284–290. DOI: 10.1007/s11055-016-0231-z.

Kosik, Kenneth S.; Orecchio, Lisa D.; Bakalis, Shelley; Neve, Rachael L. (1989): Developmentally regulated expression of specific tau sequences. In *Neuron* 2 (4), pp. 1389–1397. DOI: 10.1016/0896-6273(89)90077-9.

Kovac, Andrej; Zilka, Norbert; Kazmerova, Zuzana; Cente, Martin; Zilkova, Monika; Novak, Michal (2011): Misfolded Truncated Protein τ Induces Innate Immune Response via MAPK Pathway. In *The Journal of Immunology* 187 (5), pp. 2732–2739. DOI: 10.4049/jimmunol.1100216.

Kragh, Christine Lund; Ubhi, Kiren; Wyss-Corey, Tony; Masliah, Eliezer (2012): Autophagy in Dementias. In *Brain pathology (Zurich, Switzerland)* 22 (1), pp. 99–109. DOI: 10.1111/j.1750-3639.2011.00545.x.

Kreft, Marko; Bak, Lasse K.; Waagepetersen, Helle S.; Schousboe, Arne (2012): Aspects of astrocyte energy metabolism, amino acid neurotransmitter homoeostasis and metabolic compartmentation. In *ASN NEURO* 4 (3). DOI: 10.1042/AN20120007.

Krisenko, Mariya O.; Higgins, Renee L.; Ghosh, Soumitra; Zhou, Qing; Trybula, Joy S.; Wang, Wen-Horng; Geahlen, Robert L. (2015): Syk Is Recruited to Stress Granules and Promotes Their

Clearance through Autophagy. In *The Journal of biological chemistry* 290 (46), pp. 27803–27815. DOI: 10.1074/jbc.M115.642900.

Kurosaki, T.; Takata, M.; Yamanashi, Y.; Inazu, T.; Taniguchi, T.; Yamamoto, T.; Yamamura, H. (1994): Syk activation by the Src-family tyrosine kinase in the B cell receptor signaling. In *The Journal of experimental medicine* 179 (5), pp. 1725–1729.

Kurt, M. A.; Davies, D. C.; Kidd, M.; Duff, K.; Howlett (2003): Hyperphosphorylated tau and paired helical filament-like structures in the brains of mice carrying mutant amyloid precursor protein and mutant presenilin-1 transgenes. In *Neurobiology of disease* 14 (1), pp. 89–97.

Lanier, Lewis L.; Bakker, Alexander B.H (2000): The ITAM-bearing transmembrane adaptor DAP12 in lymphoid and myeloid cell function. In *Immunology Today* 21 (12), pp. 611–614. DOI: 10.1016/S0167-5699(00)01745-X.

Lanz, T. A.; Carter, D. B.; Merchant, K. M. (2003): Dendritic spine loss in the hippocampus of young PDAPP and Tg2576 mice and its prevention by the ApoE2 genotype. In *Neurobiology of disease* 13 (3), pp. 246–253.

Laporte, Vincent; Ait-Ghezala, Ghania; Volmar, Claude-Henry; Mullan, Michael (2006): CD40 deficiency mitigates Alzheimer's disease pathology in transgenic mouse models. In *Journal of neuroinflammation* 3, p. 3. DOI: 10.1186/1742-2094-3-3.

Lasagna-Reeves, Cristian A.; Castillo-Carranza, Diana L.; Sengupta, Urmi; Clos, Audra L.; Jackson, George R.; Kayed, Rakez (2011): Tau oligomers impair memory and induce synaptic and mitochondrial dysfunction in wild-type mice. In *Molecular neurodegeneration* 6 (1), p. 39. DOI: 10.1186/1750-1326-6-39.

Lasagna-Reeves, Cristian A.; Haro, Maria de; Hao, Shuang; Park, Jeehye; Rousseaux, Maxime W. C.; Al-Ramahi, Ismael et al. (2016): Reduction of Nuak1 Decreases Tau and Reverses Phenotypes in a Tauopathy Mouse Model. In *Neuron* 92 (2), pp. 407–418. DOI: 10.1016/j.neuron.2016.09.022.

Latour, S.; Fournel, M.; Veillette, A. (1997): Regulation of T-cell antigen receptor signalling by Syk tyrosine protein kinase. In *Molecular and Cellular Biology* 17 (8), pp. 4434–4441.

Lauritzen, Inger; Pardossi-Piquard, Raphaelle; Bourgeois, Alexandre; Pagnotta, Sophie; Biferi, Maria-Grazia; Barkats, Martine et al. (2016): Intraneuronal aggregation of the beta-CTF fragment of APP (C99) induces Abeta-independent lysosomal-autophagic pathology. In *Acta neuropathologica*. DOI: 10.1007/s00401-016-1577-6.

Le Couteur, David G.; Hunter, Sally; Brayne, Carol (2016): Solanezumab and the amyloid hypothesis for Alzheimer's disease. In *BMJ (Clinical research ed.)* 355, i6771. DOI: 10.1136/bmj.i6771.

Lebouvier, T.; Scales, T. M.; Williamson, R.; Noble, W.; Duyckaerts, C.; Hanger, D. P. et al. (2009): The microtubule-associated protein tau is also phosphorylated on tyrosine. In *Journal of Alzheimer's disease : JAD* 18 (1), pp. 1–9. DOI: 10.3233/JAD-2009-1116.

Lebouvier, Thibaud; Scales, Timothy M. E.; Hanger, Diane P.; Geahlen, Robert L.; Lardeux, Bernard; Reynolds, C. Hugh et al. (2008): The microtubule-associated protein tau is phosphorylated by Syk. In *Biochimica et biophysica acta* 1783 (2), pp. 188–192. DOI: 10.1016/j.bbamcr.2007.11.005.

Lee, Ju-Hyun; Yu, W. Haung; Kumar, Asok; Lee, Sooyeon; Mohan, Panaiyur S.; Peterhoff, Corrinne M. et al. (2010): Lysosomal proteolysis and autophagy require presenilin 1 and are disrupted by Alzheimer-related PS1 mutations. In *Cell* 141 (7), pp. 1146–1158. DOI: 10.1016/j.cell.2010.05.008.

Lee, Seung-Hye; Le Pichon, Claire E.; Adolfsson, Oskar; Gafner, Valérie; Pihlgren, Maria; Lin, Han et al. (2016): Antibody-Mediated Targeting of Tau In Vivo Does Not Require Effector Function and Microglial Engagement. In *Cell Reports* 16 (6), pp. 1690–1700. DOI: 10.1016/j.celrep.2016.06.099.

Lee, Sooyeon; Sato, Yutaka; Nixon, Ralph A. (2011): Lysosomal proteolysis inhibition selectively disrupts axonal transport of degradative organelles and causes an Alzheimer's-like axonal dystrophy. In *The Journal of neuroscience : the official journal of the Society for Neuroscience* 31 (21), pp. 7817–7830. DOI: 10.1523/JNEUROSCI.6412-10.2011.

Lee, Yun-Il; Seo, MiRan; Kim, Yeni; Kim, So-Young; Kang, Ung Gu; Kim, Yong-Sik; Juhnn, Yong-Sung (2005): Membrane Depolarization Induces the Undulating Phosphorylation/Dephosphorylation of Glycogen Synthase Kinase 3β, and This Dephosphorylation Involves Protein Phosphatases 2A and 2B in SH-SY5Y Human Neuroblastoma Cells. In *J. Biol. Chem.* 280 (23), pp. 22044–22052. DOI: 10.1074/jbc.M413987200.

Leroy, Karelle; Ando, Kunie; Héraud, Céline; Yilmaz, Zehra; Authelet, Michèle; Boeynaems, Jean-Marie et al. (2010): Lithium Treatment Arrests the Development of Neurofibrillary Tangles in Mutant Tau Transgenic Mice with Advanced Neurofibrillary Pathology. In *Journal of Alzheimer's Disease* 19 (2), pp. 705–719. DOI: 10.3233/JAD-2010-1276.

Leroy, Karelle; Boutajangout, Allal; Authelet, M.; Woodgett, James R.; Anderton, Brian H.; Brion, Jean-Pierre (2002): The active form of glycogen synthase kinase-3β is associated with granulovacuolar degeneration in neurons in Alzheimer's disease. In *Acta neuropathologica* 103 (2), pp. 91–99. DOI: 10.1007/s004010100435.

Leseux, Ludivine; Hamdi, Safouane M.; Al Saati, Talal; Capilla, Florence; Recher, Christian; Laurent, Guy; Bezombes, Christine (2006): Syk-dependent mTOR activation in follicular lymphoma cells. In *Blood* 108 (13), pp. 4156–4162. DOI: 10.1182/blood-2006-05-026203.

Leung, Rufina; Proitsi, Petroula; Simmons, Andrew; Lunnon, Katie; Güntert, Andreas; Kronenberg, Deborah et al. (2013): Inflammatory Proteins in Plasma Are Associated with Severity of Alzheimer's Disease. In *PLOS ONE* 8 (6), e64971. DOI: 10.1371/journal.pone.0064971.

Lewis, Jada; Dickson, Dennis W.; Lin, Wen-Lang; Chisholm, Louise; Corral, Anthony; Jones, Graham et al. (2001): Enhanced Neurofibrillary Degeneration in Transgenic Mice Expressing Mutant Tau and APP. In *Science* 293 (5534), pp. 1487–1491. DOI: 10.1126/science.1058189.

Leyns, Cheryl E. G.; Ulrich, Jason D.; Finn, Mary B.; Stewart, Floy R.; Koscal, Lauren J.; Remolina Serrano, Javier et al. (2017): TREM2 deficiency attenuates neuroinflammation and protects against neurodegeneration in a mouse model of tauopathy. In *Proceedings of the National Academy of Sciences of the United States of America* 114 (43), pp. 11524–11529. DOI: 10.1073/pnas.1710311114.

Liddelow, Shane A.; Guttenplan, Kevin A.; Clarke, Laura E.; Bennett, Frederick C.; Bohlen, Christopher J.; Schirmer, Lucas et al. (2017): Neurotoxic reactive astrocytes are induced by activated microglia. In *Nature* 541 (7638), pp. 481–487. DOI: 10.1038/nature21029.

Lin, Kai-Chun; Huang, Duen-Yi; Huang, De-Wei; Tzeng, Shiang-Jong; Lin, Wan-Wan (2016): Inhibition of AMPK through Lyn-Syk-Akt enhances FcepsilonRI signal pathways for allergic response. In *Journal of molecular medicine (Berlin, Germany)* 94 (2), pp. 183–194. DOI: 10.1007/s00109-015-1339-2.

Lin, Wen-Lang; Lewis, Jada; Yen, Shu-Hui; Hutton, Michael; Dickson, Dennis W. (2003): Ultrastructural neuronal pathology in transgenic mice expressing mutant (P301L) human tau. In *Journal of neurocytology* 32 (9), pp. 1091–1105. DOI: 10.1023/B:NEUR.0000021904.61387.95.

Liu, Delong; Mamorska-Dyga, Aleksandra (2017): Syk inhibitors in clinical development for hematological malignancies. In *Journal of hematology & oncology* 10 (1), p. 145. DOI: 10.1186/s13045-017-0512-1.

Liu, Fei; Grundke-Iqbal, Inge; Iqbal, Khalid; Gong, Cheng-Xin (2005): Contributions of protein phosphatases PP1, PP2A, PP2B and PP5 to the regulation of tau phosphorylation. In *European Journal of Neuroscience* 22 (8), pp. 1942–1950. DOI: 10.1111/j.1460-9568.2005.04391.x.

Liu, Fei; Li, Bin; Tung, E-Jan; Grundke-Iqbal, Inge; Iqbal, Khalid; Gong, Cheng-Xin (2007): Site-specific effects of tau phosphorylation on its microtubule assembly activity and self-aggregation. In *European Journal of Neuroscience* 26 (12), pp. 3429–3436. DOI: 10.1111/j.1460-9568.2007.05955.x.

Lossos, Alexander; Reches, Avinoam; Gal, Aya; Newman, Joel P.; Soffer, Dov; Gomori, John Moshe et al. (2003): Frontotemporal dementia and parkinsonism with the P301S tau gene mutation in a Jewish family. In *Journal of neurology* 250 (6), pp. 733–740. DOI: 10.1007/s00415-003-1074-4.

Lovering, Frank; McDonald, Joseph; Whitlock, Gavin A.; Glossop, Paul A.; Phillips, Chris; Bent, Andrew et al. (2012): Identification of type-II inhibitors using kinase structures. In *Chemical biology & drug design* 80 (5), pp. 657–664. DOI: 10.1111/j.1747-0285.2012.01443.x.

Lu, Yong-Chen; Yeh, Wen-Chen; Ohashi, Pamela S. (2008): LPS/TLR4 signal transduction pathway. In *Cytokine* 42 (2), pp. 145–151. DOI: 10.1016/j.cyto.2008.01.006.

Lue, Lih-Fen; Schmitz, Christopher T.; Serrano, Geidy; Sue, Lucia I.; Beach, Thomas G.; Walker, Douglas G. (2015): TREM2 Protein Expression Changes Correlate with Alzheimer's Disease Neurodegenerative Pathologies in Post-Mortem Temporal Cortices. In *Brain pathology (Zurich, Switzerland)* 25 (4), pp. 469–480. DOI: 10.1111/bpa.12190.

Ma, Jiao; Xing, Wei; Coffey, Greg; Dresser, Karen; Lu, Kellie; Guo, Ailin et al. (2015): Cerdulatinib, a novel dual SYK/JAK kinase inhibitor, has broad anti-tumor activity in both ABC and GCB types of diffuse large B cell lymphoma. In *Oncotarget* 6 (41), pp. 43881–43896. DOI: 10.18632/oncotarget.6316.

Magalhaes, Carolina Antunes; Carvalho, Maria das Gracas; Sousa, Lirlandia Pires de; Caramelli, Paulo; Gomes, Karina Braga (2017): Alzheimer's disease and cytokine IL-10 gene polymorphisms: is there an association? In *Arquivos de neuro-psiquiatria* 75 (9), pp. 649–656. DOI: 10.1590/0004-282X20170110.

Mander, Palwinder; Brown, Guy C. (2005): Activation of microglial NADPH oxidase is synergistic with glial iNOS expression in inducing neuronal death: a dual-key mechanism of inflammatory neurodegeneration. In *Journal of neuroinflammation* 2, p. 20. DOI: 10.1186/1742-2094-2-20.

Martin, Ludovic; Latypova, Xenia; Terro, Faraj (2011): Post-translational modifications of tau protein: implications for Alzheimer's disease. In *Neurochemistry international* 58 (4), pp. 458–471. DOI: 10.1016/j.neuint.2010.12.023.

Masliah, E. (1995): Mechanisms of synaptic dysfunction in Alzheimer's disease. In *Histology and histopathology* 10 (2), pp. 509–519.

Masters, C. L.; Simms, G.; Weinman, N. A.; Multhaup, G.; McDonald, B. L.; Beyreuther, K. (1985): Amyloid plaque core protein in Alzheimer disease and Down syndrome. In *Proceedings of the National Academy of Sciences of the United States of America* 82 (12), pp. 4245–4249.

Matos, M.; Augusto, E.; Oliveira, C. R.; Agostinho, P. (2008): Amyloid-beta peptide decreases glutamate uptake in cultured astrocytes: involvement of oxidative stress and mitogen-activated protein kinase cascades. In *Neuroscience* 156 (4), pp. 898–910. DOI: 10.1016/j.neuroscience.2008.08.022.

Maximova, Olga A.; Murphy, Brian R.; Pletnev, Alexander G. (2010): High-throughput automated image analysis of neuroinflammation and neurodegeneration enables quantitative assessment of virus neurovirulence. In *Vaccine* 28 (52), pp. 8315–8326. DOI: 10.1016/j.vaccine.2010.07.070.

McDonald; Brunden, K. R.; Landreth, G. E. (1997): Amyloid fibrils activate tyrosine kinase-dependent signaling and superoxide production in microglia. In *The Journal of neuroscience : the official journal of the Society for Neuroscience* 17 (7), pp. 2284–2294.

McGeer, Patrick L.; McGeer, Edith G. (2013): The amyloid cascade-inflammatory hypothesis of Alzheimer disease. Implications for therapy. In *Acta neuropathologica* 126 (4), pp. 479–497. DOI: 10.1007/s00401-013-1177-7.

Mehta, Dev; Jackson, Robert; Paul, Gaurav; Shi, Jiong; Sabbagh, Marwan (2017): Why do trials for Alzheimer's disease drugs keep failing? A discontinued drug perspective for 2010-2015. In *Expert opinion on investigational drugs* 26 (6), pp. 735–739. DOI: 10.1080/13543784.2017.1323868.

Mejia-Garcia, T. A.; Paes-de-Carvalho, R. (2007): Nitric oxide regulates cell survival in purified cultures of avian retinal neurons: involvement of multiple transduction pathways. In *Journal of neurochemistry* 100 (2), pp. 382–394. DOI: 10.1111/j.1471-4159.2006.04244.x.

Menzies, Fiona M.; Fleming, Angeleen; Rubinsztein, David C. (2015): Compromised autophagy and neurodegenerative diseases. In *Nature reviews. Neuroscience* 16 (6), pp. 345–357. DOI: 10.1038/nrn3961.

Meske, Volker; Albert, Frank; Ohm, Thomas Georg (2008): Coupling of Mammalian Target of Rapamycin with Phosphoinositide 3-Kinase Signaling Pathway Regulates Protein Phosphatase 2A- and Glycogen Synthase Kinase-3β-dependent Phosphorylation of Tau. In *J. Biol. Chem.* 283 (1), pp. 100–109. DOI: 10.1074/jbc.M704292200.

Millecamps, Stéphanie; Julien, Jean-Pierre (2013): Axonal transport deficits and neurodegenerative diseases. In *Nature Reviews Neuroscience* 14 (3), p. 161. DOI: 10.1038/nrn3380.

Mizushima, Noboru; Yoshimori, Tamotsu (2007): How to Interpret LC3 Immunoblotting. In *Autophagy* 3 (6), pp. 542–545. DOI: 10.4161/auto.4600.

Mócsai, Attila; Ruland, Jürgen; Tybulewicz, Victor L. J. (2010): The SYK tyrosine kinase: a crucial player in diverse biological functions. In *Nature reviews. Immunology* 10 (6), pp. 387–402. DOI: 10.1038/nri2765.

Morales, Inelia; Jimenez, Jose M.; Mancilla, Marcela; Maccioni, Ricardo B. (2013): Tau oligomers and fibrils induce activation of microglial cells. In *Journal of Alzheimer's disease : JAD* 37 (4), pp. 849–856. DOI: 10.3233/JAD-131843.

Morfini, Gerardo; Szebenyi, Györgyi; Elluru, Ravindhra; Ratner, Nancy; Brady, Scott T. (2002): Glycogen synthase kinase 3 phosphorylates kinesin light chains and negatively regulates kinesin-based motility. In *The EMBO journal* 21 (3), pp. 281–293. DOI: 10.1093/emboj/21.3.281.

Morris, Meaghan; Knudsen, Giselle M.; Maeda, Sumihiro; Trinidad, Jonathan C.; Ioanoviciu, Alexandra; Burlingame, Alma L.; Mucke, Lennart (2015): Tau post-translational modifications in wild-type and human amyloid precursor protein transgenic mice. In *Nature neuroscience* 18 (8), p. 1183. DOI: 10.1038/nn.4067.

Morris, Meaghan; Maeda, Sumihiro; Vossel, Keith; Mucke, Lennart (2011): The many faces of tau. In *Neuron* 70 (3), pp. 410–426. DOI: 10.1016/j.neuron.2011.04.009.

Motta, M.; Imbesi, R.; Di Rosa, M.; Stivala, F.; Malaguarnera, L. (2007): Altered plasma cytokine levels in Alzheimer's disease: correlation with the disease progression. In *Immunology letters* 114 (1), pp. 46–51. DOI: 10.1016/j.imlet.2007.09.002.

Mullan, M.; Crawford, F.; Axelman, K.; Houlden, H.; Lilius, L.; Winblad, B.; Lannfelt, L. (1992): A pathogenic mutation for probable Alzheimer's disease in the APP gene at the N-terminus of beta-amyloid. In *Nature genetics* 1 (5), pp. 345–347. DOI: 10.1038/ng0892-345.

Mullard, Asher (2018): BACE failures lower AD expectations, again. In *Nature reviews. Drug discovery* 17 (6), p. 385. DOI: 10.1038/nrd.2018.94.

Mullen, R. J.; Buck, C. R.; Smith, A. M. (1992): NeuN, a neuronal specific nuclear protein in vertebrates. In *Development (Cambridge, England)* 116 (1), pp. 201–211.

Munson, M. J.; Ganley, I. G. (2015): MTOR, PIK3C3, and autophagy: Signaling the beginning from the end. In *Autophagy* 11 (12), pp. 2375–2376. DOI: 10.1080/15548627.2015.1106668.

Nathan, Carl; Calingasan, Noel; Nezezon, Jon; Ding, Aihao; Lucia, M. Scott; La Perle, Krista et al. (2005): Protection from Alzheimer's-like disease in the mouse by genetic ablation of inducible nitric oxide synthase. In *The Journal of experimental medicine* 202 (9), pp. 1163–1169. DOI: 10.1084/jem.20051529.

Nelson, Peter T.; Alafuzoff, Irina; Bigio, Eileen H.; Bouras, Constantin; Braak, Heiko; Cairns, Nigel J. et al. (2012): Correlation of Alzheimer Disease Neuropathologic Changes With Cognitive Status: A Review of the Literature. In *Journal of neuropathology and experimental neurology* 71 (5), pp. 362–381. DOI: 10.1097/NEN.0b013e31825018f7.

Nilsson, Per; Loganathan, Krishnapriya; Sekiguchi, Misaki; Matsuba, Yukio; Hui, Kelvin; Tsubuki, Satoshi et al. (2013): Abeta secretion and plaque formation depend on autophagy. In *Cell reports* 5 (1), pp. 61–69. DOI: 10.1016/j.celrep.2013.08.042.

Nixon, R. A.; Wegiel, J.; Kumar, A.; Yu, W. H.; Peterhoff, C.; Cataldo, A.; Am Cuervo (2005): Extensive involvement of autophagy in Alzheimer disease: an immuno-electron microscopy study. In *Journal of neuropathology and experimental neurology* 64 (2), pp. 113–122.

Nixon, Ralph A. (2007): Autophagy, amyloidogenesis and Alzheimer disease. In *Journal of cell science* 120 (Pt 23), pp. 4081–4091. DOI: 10.1242/jcs.019265.

Nixon, Ralph A.; Yang, Dun-Sheng (2011): Autophagy failure in Alzheimer's disease--locating the primary defect. In *Neurobiology of disease* 43 (1), pp. 38–45. DOI: 10.1016/j.nbd.2011.01.021.

Noraz, Nelly; Jaaoini, Iness; Charoy, Camille; Watrin, Chantal; Chounlamountri, Naura; Benon, Aurelien et al. (2016): Syk kinases are required for spinal commissural axon repulsion at the midline via ephrin/Eph pathway. In *Development (Cambridge, England)*. DOI: 10.1242/dev.128629.

Nygaard, Haakon B.; van Dyck, Christopher H.; Strittmatter, Stephen M. (2014): Fyn kinase inhibition as a novel therapy for Alzheimer's disease. In *Alzheimer's research & therapy* 6 (1), p. 8. DOI: 10.1186/alzrt238.

Ogasawara, K.; Noda, A.; Yasuda, S.; Kobayashi, M.; Yukawa, H.; Ogawa, A. (2003): Effect of calcium antagonist on cerebral blood flow and oxygen metabolism in patients with hypertension and chronic major cerebral artery occlusion: a positron emission tomography study. In *Nuclear medicine communications* 24 (1), pp. 71–76. DOI: 10.1097/01.mnm.0000051634.18733.46.

Ossenkoppele, Rik; van Berckel, Bart Nm; Prins, Niels D. (2011): Amyloid imaging in prodromal Alzheimer's disease. In *Alzheimer's research & therapy* 3 (5), p. 26. DOI: 10.1186/alzrt88.

Ozcelik, Sefika; Fraser, Graham; Castets, Perrine; Schaeffer, Véronique; Skachokova, Zhiva; Breu, Karin et al. (2013): Rapamycin attenuates the progression of tau pathology in P301S tau transgenic mice. In *PloS one* 8 (5), e62459. DOI: 10.1371/journal.pone.0062459.

Paholikova, Kristina; Salingova, Barbara; Opattova, Alena; Skrabana, Rostislav; Majerova, Petra; Zilka, Norbert et al. (2015): N-terminal truncation of microtubule associated protein tau dysregulates its cellular localization. In *Journal of Alzheimer's disease : JAD* 43 (3), pp. 915–926. DOI: 10.3233/JAD-140996.

Paloneva, J.; Autti, T.; Raininko, R.; Partanen, J.; Salonen, O.; Puranen, M. et al. (2001): CNS manifestations of Nasu-Hakola disease: a frontal dementia with bone cysts. In *Neurology* 56 (11), pp. 1552–1558.

Paloneva, Juha; Manninen, Tuula; Christman, Grant; Hovanes, Karine; Mandelin, Jami; Adolfsson, Rolf et al. (2002): Mutations in two genes encoding different subunits of a receptor signaling complex result in an identical disease phenotype. In *American journal of human genetics* 71 (3), pp. 656–662. DOI: 10.1086/342259.

Paolicelli, Rosa C.; Bolasco, Giulia; Pagani, Francesca; Maggi, Laura; Scianni, Maria; Panzanelli, Patrizia et al. (2011): Synaptic Pruning by Microglia Is Necessary for Normal Brain Development. In *Science* 333 (6048), pp. 1456–1458. DOI: 10.1126/science.1202529.

Papageorgiou, Ismini E.; Lewen, Andrea; Galow, Lukas V.; Cesetti, Tiziana; Scheffel, Jörg; Regen, Tommy et al. (2016): TLR4-activated microglia require IFN-γ to induce severe neuronal dysfunction and death in situ. In *Proceedings of the National Academy of Sciences of the United States of America* 113 (1), pp. 212–217. DOI: 10.1073/pnas.1513853113.

Paris, Daniel; Ait-Ghezala, Ghania; Bachmeier, Corbin; Laco, Gary; Beaulieu-Abdelahad, David; Lin, Yong et al. (2014): The spleen tyrosine kinase (Syk) regulates Alzheimer amyloid-beta production and Tau hyperphosphorylation. In *The Journal of biological chemistry* 289 (49), pp. 33927–33944. DOI: 10.1074/jbc.M114.608091.

Paris, Daniel; Bachmeier, Corbin; Patel, Nikunj; Quadros, Amita; Volmar, Claude-Henry; Laporte, Vincent et al. (2011): Selective antihypertensive dihydropyridines lower Abeta accumulation by targeting both the production and the clearance of Abeta across the blood-brain barrier. In *Molecular medicine (Cambridge, Mass.)* 17 (3-4), pp. 149–162. DOI: 10.2119/molmed.2010.00180.

Paris, Daniel; Quadros, Amita; Humphrey, James; Patel, Nikunj; Crescentini, Robert; Crawford, Fiona; Mullan, Michael (2004): Nilvadipine antagonizes both Abeta vasoactivity in isolated arteries, and the reduced cerebral blood flow in APPsw transgenic mice. In *Brain research* 999 (1), pp. 53–61.

Parr, Callum; Carzaniga, Raffaela; Gentleman, Steve M.; van Leuven, Fred; Walter, Jochen; Sastre, Magdalena (2012): Glycogen Synthase Kinase 3 Inhibition Promotes Lysosomal Biogenesis and Autophagic Degradation of the Amyloid-β Precursor Protein. In *Molecular and Cellular Biology* 32 (21), pp. 4410–4418. DOI: 10.1128/MCB.00930-12.

Peacock, M. L.; Warren, J. T.; Roses, A. D.; Fink, J. K. (1993): Novel polymorphism in the A4 region of the amyloid precursor protein gene in a patient without Alzheimer's disease. In *Neurology* 43 (6), pp. 1254–1256.

Pei, J. J.; Tanaka, T.; Tung, Y. C.; Braak, E.; Iqbal, K.; Grundke-Iqbal, I. (1997): Distribution, levels, and activity of glycogen synthase kinase-3 in the Alzheimer disease brain. In *Journal of neuropathology and experimental neurology* 56 (1), pp. 70–78.

Pei, Jin-Jing; An, Wen-Lin; Zhou, Xin-Wen; Nishimura, Takeshi; Norberg, Jan; Benedikz, Eirikur et al. (2006): P70 S6 kinase mediates tau phosphorylation and synthesis. In *FEBS letters* 580 (1), pp. 107–114. DOI: 10.1016/j.febslet.2005.11.059.

Perea, Juan R.; Llorens-Martín, María; Ávila, Jesús; Bolós, Marta (2018): The Role of Microglia in the Spread of Tau: Relevance for Tauopathies. In *Front. Cell. Neurosci.* 12, p. 172. DOI: 10.3389/fncel.2018.00172.

Perlmutter, L. S.; Barron, E.; Chui, H. C. (1990): Morphologic association between microglia and senile plaque amyloid in Alzheimer's disease. In *Neuroscience letters* 119 (1), pp. 32–36.

Peruzzi, G.; Molfetta, R.; Gasparrini, F.; Vian, L.; Morrone, S.; Piccoli, M. et al. (2007): The Adaptor Molecule CIN85 Regulates Syk Tyrosine Kinase Level by Activating the Ubiquitin-Proteasome Degradation Pathway. In *The Journal of Immunology* 179 (4), pp. 2089–2096. DOI: 10.4049/jimmunol.179.4.2089.

Piras, Antonio; Collin, Ludovic; Gruninger, Fiona; Graff, Caroline; Ronnback, Annica (2016): Autophagic and lysosomal defects in human tauopathies: analysis of post-mortem brain from patients with familial Alzheimer disease, corticobasal degeneration and progressive supranuclear palsy. In *Acta neuropathologica communications* 4, p. 22. DOI: 10.1186/s40478-016-0292-9.

Prasad, Hari; Rao, Rajini (2015): The Na+/H+ Exchanger NHE6 Modulates Endosomal pH to Control Processing of Amyloid Precursor Protein in a Cell Culture Model of Alzheimer Disease. In *J. Biol. Chem.* 290 (9), pp. 5311–5327. DOI: 10.1074/jbc.M114.602219.

Prokop, Stefan; Miller, Kelly R.; Heppner, Frank L. (2013): Microglia actions in Alzheimer's disease. In *Acta Neuropathol* 126 (4), pp. 461–477. DOI: 10.1007/s00401-013-1182-x.

Puertollano, R. (2014): mTOR and lysosome regulation. In *F1000Prime Reports* 6. DOI: 10.12703/P6-52.

Pugsley, Haley R. (2017): Assessing Autophagic Flux by Measuring LC3, p62, and LAMP1 Co-localization Using Multispectral Imaging Flow Cytometry. In *Journal of visualized experiments : JoVE* (125). DOI: 10.3791/55637.

Qian, Jing; Wolters, Frank J.; Beiser, Alexa; Haan, Mary; Ikram, M. Arfan; Karlawish, Jason et al. (2017): APOE-related risk of mild cognitive impairment and dementia for prevention trials: An analysis of four cohorts. In *PLoS Med* 14 (3), e1002254. DOI: 10.1371/journal.pmed.1002254.

Quintanilla, Rodrigo A.; Orellana, Daniel I.; Gonzalez-Billault, Christian; Maccioni, Ricardo B. (2004): Interleukin-6 induces Alzheimer-type phosphorylation of tau protein by deregulating the cdk5/p35 pathway. In *Experimental cell research* 295 (1), pp. 245–257. DOI: 10.1016/j.yexcr.2004.01.002.

Ramirez, A. E.; Pacheco, C. R.; Aguayo, L. G.; Opazo, C. M. (2014): Rapamycin protects against Abeta-induced synaptotoxicity by increasing presynaptic activity in hippocampal neurons. In *Biochimica et biophysica acta* 1842 (9), pp. 1495–1501. DOI: 10.1016/j.bbadis.2014.04.019.

Ren, F.; Zhang, L.; Zhang, X.; Shi, H.; Wen, T.; Bai, L. et al. (2016): Inhibition of glycogen synthase kinase 3β promotes autophagy to protect mice from acute liver failure mediated by peroxisome proliferator-activated receptor α. In *Cell death & disease* 7 (3), e2151. DOI: 10.1038/cddis.2016.56.

Richards, G. R.; Smith, A. J.; Cuddon, P.; Ma, Q. P.; Leveridge, M.; Kerby, J. et al. (2006): The JAK3 inhibitor WHI-P154 prevents PDGF-evoked process outgrowth in human neural precursor cells. In *Journal of neurochemistry* 97 (1), pp. 201–210. DOI: 10.1111/j.1471-4159.2006.03723.x.

Robakis, N. K.; Ramakrishna, N.; Wolfe, G.; Wisniewski, H. M. (1987): Molecular cloning and characterization of a cDNA encoding the cerebrovascular and the neuritic plaque amyloid peptides. In *Proceedings of the National Academy of Sciences of the United States of America* 84 (12), pp. 4190–4194.

Rogers, J.; Strohmeyer, R.; Kovelowski, C. J.; Li, R. (2002): Microglia and inflammatory mechanisms in the clearance of amyloid beta peptide. In *Glia* 40 (2), pp. 260–269. DOI: 10.1002/glia.10153.

Rosenblum, William I. (2014): Why Alzheimer trials fail. Removing soluble oligomeric beta amyloid is essential, inconsistent, and difficult. In *Neurobiology of aging* 35 (5), pp. 969–974. DOI: 10.1016/j.neurobiolaging.2013.10.085.

Rosenthal, J. (1994): Nilvadipine: profile of a new calcium antagonist. An overview. In *Journal of cardiovascular pharmacology* 24 Suppl 2, S92-107.

Sada, Kiyonao; Takano, Tomoko; Yanagi, Shigeru; Yamamura, Hirohei (2001): Structure and Function of Syk Protein-Tyrosine Kinase. In *J Biochem* 130 (2), pp. 177–186. Available online at http://jb.oxfordjournals.org/content/130/2/177.full.pdf.

Sadleir, Katherine R.; Kandalepas, Patty C.; Buggia-Prevot, Virginie; Nicholson, Daniel A.; Thinakaran, Gopal; Vassar, Robert (2016): Presynaptic dystrophic neurites surrounding amyloid plaques are sites of microtubule disruption, BACE1 elevation, and increased Abeta generation in Alzheimer's disease. In *Acta neuropathologica*. DOI: 10.1007/s00401-016-1558-9.

Saha, Ramendra N.; Pahan, Kalipada (2006): Signals for the induction of nitric oxide synthase in astrocytes. In *Neurochemistry international* 49 (2), pp. 154–163. DOI: 10.1016/j.neuint.2006.04.007.

Sanan, D. A.; Weisgraber, K. H.; Russell, S. J.; Mahley, R. W.; Huang, D.; Saunders, A. et al. (1994): Apolipoprotein E associates with beta amyloid peptide of Alzheimer's disease to form novel monofibrils. Isoform apoE4 associates more efficiently than apoE3. In *The Journal of clinical investigation* 94 (2), pp. 860–869. DOI: 10.1172/JCI117407.

Sanchez-Varo, Raquel; Trujillo-Estrada, Laura; Sanchez-Mejias, Elisabeth; Torres, Manuel; Baglietto-Vargas, David; Moreno-Gonzalez, Ines et al. (2012): Abnormal accumulation of autophagic vesicles correlates with axonal and synaptic pathology in young Alzheimer's mice hippocampus. In *Acta neuropathologica* 123 (1), pp. 53–70. DOI: 10.1007/s00401-011-0896-x.

Sanchez-Wandelmer, J.; Reggiori, F. (2013): Amphisomes: out of the autophagosome shadow? In *The EMBO journal* 32 (24), pp. 3116–3118. DOI: 10.1038/emboj.2013.246.

Sarkar, Sovan (2013): Regulation of autophagy by mTOR-dependent and mTOR-independent pathways: autophagy dysfunction in neurodegenerative diseases and therapeutic application of autophagy enhancers. In *Biochemical Society transactions* 41 (5), pp. 1103–1130. DOI: 10.1042/BST20130134.

Satoh, Jun-Ichi; Kino, Yoshihiro; Yanaizu, Motoaki; Saito, Yuko (2018): Alzheimer's disease pathology in Nasu-Hakola disease brains. In *Intractable & Rare Diseases Research* 7 (1), pp. 32–36. DOI: 10.5582/irdr.2017.01088.

Satoh, Jun-Ichi; Tabunoki, Hiroko; Ishida, Tsuyoshi; Yagishita, Saburo; Jinnai, Kenji; Futamura, Naonobu et al. (2012): Phosphorylated Syk expression is enhanced in Nasu-Hakola disease brains. In *Neuropathology : official journal of the Japanese Society of Neuropathology* 32 (2), pp. 149–157. DOI: 10.1111/j.1440-1789.2011.01256.x.

Scales, Timothy M. E.; Derkinderen, Pascal; Leung, Kit-Yi; Byers, Helen L.; Ward, Malcolm A.; Price, Caroline et al. (2011): Tyrosine Phosphorylation of Tau by the Src Family Kinases Lck and Fyn. In *Molecular neurodegeneration* 6, p. 12. DOI: 10.1186/1750-1326-6-12.

Schaeffer, Véronique; Lavenir, Isabelle; Ozcelik, Sefika; Tolnay, Markus; Winkler, David T.; Goedert, Michel (2012): Stimulation of autophagy reduces neurodegeneration in a mouse model

of human tauopathy. In *Brain : a journal of neurology* 135 (Pt 7), pp. 2169–2177. DOI: 10.1093/brain/aws143.

Scheib, Jami L.; Sullivan, Chelsea S.; Carter, Bruce D. (2012): Jedi-1 and MEGF10 signal engulfment of apoptotic neurons through the tyrosine kinase Syk. In *The Journal of neuroscience : the official journal of the Society for Neuroscience* 32 (38), pp. 13022–13031. DOI: 10.1523/JNEUROSCI.6350-11.2012.

Schenk, D.; Barbour, R.; Dunn, W.; Gordon, G.; Grajeda, H.; Guido, T. et al. (1999): Immunization with amyloid-beta attenuates Alzheimer-disease-like pathology in the PDAPP mouse. In *Nature* 400 (6740), pp. 173–177. DOI: 10.1038/22124.

Schindelin, Johannes; Arganda-Carreras, Ignacio; Frise, Erwin; Kaynig, Verena; Longair, Mark; Pietzsch, Tobias et al. (2012): Fiji. An open-source platform for biological-image analysis. In *Nature methods* 9 (7), pp. 676–682. DOI: 10.1038/nmeth.2019.

Schmidt, Enrico K.; Clavarino, Giovanna; Ceppi, Maurizio; Pierre, Philippe (2009): SUnSET, a nonradioactive method to monitor protein synthesis. In *Nature methods* 6 (4), pp. 275–277. DOI: 10.1038/nmeth.1314.

Schmidt, M. L.; DiDario, A. G.; Lee, V. M.; Trojanowski, J. Q. (1994): An extensive network of PHF tau-rich dystrophic neurites permeates neocortex and nearly all neuritic and diffuse amyloid plaques in Alzheimer disease. In *FEBS letters* 344 (1), pp. 69–73.

Schweig, Jonas Elias; Yao, Hailan; Beaulieu-Abdelahad, David; Ait-Ghezala, Ghania; Mouzon, Benoit; Crawford, Fiona et al. (2017): Alzheimer's disease pathological lesions activate the spleen tyrosine kinase. In *Acta neuropathologica communications* 5 (1), p. 69. DOI: 10.1186/s40478-017-0472-2.

Sei, Y.; Vitković, L.; Yokoyama, M. M. (1995): Cytokines in the central nervous system: regulatory roles in neuronal function, cell death and repair. In *Neuroimmunomodulation* 2 (3), pp. 121–133. DOI: 10.1159/000096881.

Selkoe, D. J. (1991): The molecular pathology of Alzheimer's disease. In *Neuron* 6 (4), pp. 487–498.

Selkoe, Dennis J.; Hardy, John (2016): The amyloid hypothesis of Alzheimer's disease at 25 years. In *EMBO molecular medicine* 8 (6), pp. 595–608. DOI: 10.15252/emmm.201606210.

Sengupta, A.; Kabat, J.; Novak, M.; Wu, Q.; Grundke-Iqbal, I.; Iqbal, K. (1998): Phosphorylation of tau at both Thr 231 and Ser 262 is required for maximal inhibition of its binding to microtubules. In *Archives of Biochemistry and Biophysics* 357 (2), pp. 299–309. DOI: 10.1006/abbi.1998.0813.

Serenó, L.; Coma, M.; Rodríguez, M.; Sánchez-Ferrer, P.; Sánchez, M. B.; Gich, I. et al. (2009): A novel GSK-3β inhibitor reduces Alzheimer's pathology and rescues neuronal loss in vivo. In *Neurobiology of disease* 35 (3), pp. 359–367. DOI: 10.1016/j.nbd.2009.05.025.

Sevigny, Jeff; Chiao, Ping; Bussiere, Thierry; Weinreb, Paul H.; Williams, Leslie; Maier, Marcel et al. (2016): The antibody aducanumab reduces Abeta plaques in Alzheimer's disease. In *Nature* 537 (7618), pp. 50–56. DOI: 10.1038/nature19323.

Sharman, Jeff; Hawkins, Michael; Kolibaba, Kathryn; Boxer, Michael; Klein, Leonard; Wu, Meihua et al. (2015): An open-label phase 2 trial of entospletinib (GS-

9973), a selective spleen tyrosine kinase inhibitor, in chronic lymphocytic leukemia. In *Blood* 125 (15), pp. 2336–2343. DOI: 10.1182/blood-2014-08-595934.

Sherrington, R.; Froelich, S.; Sorbi, S.; Campion, D.; Chi, H.; Rogaeva, E. A. et al. (1996): Alzheimer's disease associated with mutations in presenilin 2 is rare and variably penetrant. In *Human molecular genetics* 5 (7), pp. 985–988.

Sherrington, R.; Rogaev, E. I.; Liang, Y.; Rogaeva, E. A.; Levesque, G.; Ikeda, M. et al. (1995): Cloning of a gene bearing missense mutations in early-onset familial Alzheimer's disease. In *Nature* 375 (6534), pp. 754–760. DOI: 10.1038/375754a0.

Shi, Yang; Yamada, Kaoru; Liddelow, Shane Antony; Smith, Scott T.; Zhao, Lingzhi; Luo, Wenjie et al. (2017): ApoE4 markedly exacerbates tau-mediated neurodegeneration in a mouse model of tauopathy. In *Nature* 549 (7673), p. 523. DOI: 10.1038/nature24016.

Sidoryk-Wegrzynowicz, Marta; Gerber, Yannick N.; Ries, Miriam; Sastre, Magdalena; Tolkovsky, Aviva M.; Spillantini, Maria Grazia (2017): Astrocytes in mouse models of tauopathies acquire early deficits and lose neurosupportive functions. In *Acta neuropathologica communications* 5 (1), p. 89. DOI: 10.1186/s40478-017-0478-9.

Siemers, Eric R.; Sundell, Karen L.; Carlson, Christopher; Case, Michael; Sethuraman, Gopalan; Liu-Seifert, Hong et al. (2016): Phase 3 solanezumab trials. Secondary outcomes in mild Alzheimer's disease patients. In *Alzheimer's & dementia : the journal of the Alzheimer's Association* 12 (2), pp. 110–120. DOI: 10.1016/j.jalz.2015.06.1893.

Sierra, Ana; Navascués, Julio; Cuadros, Miguel A.; Calvente, Ruth; Martín-Oliva, David; Ferrer-Martín, Rosa M. et al. (2014): Expression of Inducible Nitric Oxide Synthase (iNOS) in Microglia of the Developing Quail Retina. In *PloS one* 9 (8). DOI: 10.1371/journal.pone.0106048.

Silva, Rohan de; Lashley, Tammaryn; Strand, Catherine; Shiarli, Anna-Maria; Shi, Jing; Tian, Jinzhou et al. (2006): An immunohistochemical study of cases of sporadic and inherited frontotemporal lobar degeneration using 3R- and 4R-specific tau monoclonal antibodies. In *Acta neuropathologica* 111 (4), pp. 329–340. DOI: 10.1007/s00401-006-0048-x.

Siman, Robert; Cocca, Ryan; Dong, Yina (2015): The mTOR Inhibitor Rapamycin Mitigates Perforant Pathway Neurodegeneration and Synapse Loss in a Mouse Model of Early-Stage Alzheimer-Type Tauopathy. In *PloS one* 10 (11), pp. e0142340. DOI: 10.1371/journal.pone.0142340.

Šimić, Goran; Babić Leko, Mirjana; Wray, Selina; Harrington, Charles; Delalle, Ivana; Jovanov-Milošević, Nataša et al. (2016): Tau Protein Hyperphosphorylation and Aggregation in Alzheimer's Disease and Other Tauopathies, and Possible Neuroprotective Strategies. In *Biomolecules* 6 (1). DOI: 10.3390/biom6010006.

Simonovitch, Shira; Schmukler, Eran; Bespalko, Alina; Iram, Tal; Frenkel, Dan; Holtzman, David M. et al. (2016): Impaired Autophagy in APOE4 Astrocytes. In *Journal of Alzheimer's disease : JAD* 51 (3), pp. 915–927. DOI: 10.3233/JAD-151101.

Sofroniew, Michael V.; Vinters, Harry V. (2010): Astrocytes: biology and pathology. In *Acta neuropathologica* 119 (1), pp. 7–35. DOI: 10.1007/s00401-009-0619-8.

Sollvander, Sofia; Nikitidou, Elisabeth; Brolin, Robin; Soderberg, Linda; Sehlin, Dag; Lannfelt, Lars; Erlandsson, Anna (2016): Accumulation of amyloid-beta by astrocytes result in enlarged endosomes and microvesicle-induced apoptosis of neurons. In *Molecular neurodegeneration* 11 (1), p. 38. DOI: 10.1186/s13024-016-0098-z.

Sondag, Cindy M.; Combs, Colin K. (2004): Amyloid precursor protein mediates proinflammatory activation of monocytic lineage cells. In *The Journal of biological chemistry* 279 (14), pp. 14456–14463. DOI: 10.1074/jbc.M313747200.

Sondag, Cindy M.; Dhawan, Gunjan; Combs, Colin K. (2009): Beta amyloid oligomers and fibrils stimulate differential activation of primary microglia. In *Journal of neuroinflammation* 6, p. 1. DOI: 10.1186/1742-2094-6-1.

Sonoda, Y.; Tooyama, I.; Mukai, H.; Maeda, K.; Akiyama, H.; Kawamata, T. (2016): S6 kinase phosphorylated at T229 is involved in tau and actin pathologies in Alzheimer's disease. In *Neuropathology : official journal of the Japanese Society of Neuropathology* 36 (4), pp. 325–332. DOI: 10.1111/neup.12275.

Speich, Henry E.; Grgurevich, Svetozar; Kueter, Teddi J.; Earhart, Angela D.; Slack, Steven M.; Jennings, Lisa K. (2008): Platelets undergo phosphorylation of Syk at Y525/526 and Y352 in response to pathophysiological shear stress. In *American journal of physiology. Cell physiology* 295 (4), C1045-54. DOI: 10.1152/ajpcell.90644.2007.

Sperfeld, A. D.; Collatz, M. B.; Baier, H.; Palmbach, M.; Storch, A.; Schwarz, J. et al. (1999): FTDP-17: an early-onset phenotype with parkinsonism and epileptic seizures caused by a novel mutation. In *Annals of neurology* 46 (5), pp. 708–715.

Sperling, Reisa A.; Jack, Clifford R.; Aisen, Paul S. (2011): Testing the right target and right drug at the right stage. In *Science translational medicine* 3 (111), 111cm33. DOI: 10.1126/scitranslmed.3002609.

Spires-Jones, Tara L.; Kopeikina, Katherine J.; Koffie, Robert M.; Calignon, Alix de; Hyman, Bradley T. (2011): Are Tangles as Toxic as They Look? In *Journal of Molecular Neuroscience* 45 (3), pp. 438–444. DOI: 10.1007/s12031-011-9566-7.

Srivastava, Isha N.; Shperdheja, Jona; Baybis, Marianna; Ferguson, Tanya; Crino, Peter B. (2016): mTOR pathway inhibition prevents neuroinflammation and neuronal death in a mouse model of cerebral palsy. In *Neurobiology of disease* 85, pp. 144–154. DOI: 10.1016/j.nbd.2015.10.001.

St-Amour, Isabelle; Cicchetti, Francesca; Calon, Frederic (2016): Immunotherapies in Alzheimer's disease. Too much, too little, too late or off-target? In *Acta neuropathologica* 131 (4), pp. 481–504. DOI: 10.1007/s00401-015-1518-9.

Stretton, Clare; Hoffmann, Thorsten M.; Munson, Michael J.; Prescott, Alan; Taylor, Peter M.; Ganley, Ian G.; Hundal, Harinder S. (2015): GSK3-mediated raptor phosphorylation supports amino-acid-dependent mTORC1-directed signalling. In *The Biochemical journal* 470 (2), pp. 207–221. DOI: 10.1042/BJ20150404.

Strooper, B. de; Saftig, P.; Craessaerts, K.; Vanderstichele, H.; Guhde, G.; Annaert, W. et al. (1998): Deficiency of presenilin-1 inhibits the normal cleavage of amyloid precursor protein. In *Nature* 391 (6665), pp. 387–390. DOI: 10.1038/34910.

Su, Fan; Bai, Feng; Zhang, Zhijun (2016): Inflammatory Cytokines and Alzheimer's Disease: A Review from the Perspective of Genetic Polymorphisms. In *Neuroscience bulletin* 32 (5), pp. 469–480. DOI: 10.1007/s12264-016-0055-4.

Su, J. H.; Cummings, B. J.; Cotman, C. W. (1993): Identification and distribution of axonal dystrophic neurites in Alzheimer's disease. In *Brain research* 625 (2), pp. 228–237.

Taft, Christine E.; Turrigiano, Gina G. (2014): PSD-95 promotes the stabilization of young synaptic contacts. In *Philosophical transactions of the Royal Society of London. Series B, Biological sciences* 369 (1633), p. 20130134. DOI: 10.1098/rstb.2013.0134.

Tahara, Kazuki; Kim, Hong-Duck; Jin, Jing-Ji; Maxwell, J. Adam; Li, Ling; Fukuchi, Ken-ichiro (2006): Role of toll-like receptor signalling in Abeta uptake and clearance. In *Brain : a journal of neurology* 129 (Pt 11), pp. 3006–3019. DOI: 10.1093/brain/awl249.

Takada, Yasunari; Aggarwal, Bharat B. (2004): TNF activates Syk protein tyrosine kinase leading to TNF-induced MAPK activation, NF-kappaB activation, and apoptosis. In *Journal of immunology (Baltimore, Md. : 1950)* 173 (2), pp. 1066–1077.

Takashima, A.; Murayama, M.; Murayama, O.; Kohno, T.; Honda, T.; Yasutake, K. et al. (1998): Presenilin 1 associates with glycogen synthase kinase-3 and its substrate tau. In *Neuroscience letters* 95 (16), pp. 9637–9641. DOI: 10.1073/pnas.95.16.9637.

Takeshi Yura, Arnel B. Concepcion, Gyoonhee Han, Makiko Marumo, Hiroko Katsumata, Norihiro Kawamura, Toshio Kokubo, Hiroshi Komura, Yingfu Li, Timothy B. Lowinger, Muneto Mogi, Noriyuki Yamamoto, Nagahiro Yoshida, Scott Miller, Margaret A. Popp, Aniko M. Redmann, Martha E. Rodriguez, William J. Scott, Ming Wang (2001): Imidazopyrimidine derivatives and triazolopyrimidine derivatives. Patent no. WO2001083485.

Takeuchi, Hiroki; Iba, Michiyo; Inoue, Haruhisa; Higuchi, Makoto; Takao, Keizo; Tsukita, Kayoko et al. (2011): P301S mutant human tau transgenic mice manifest early symptoms of human tauopathies with dementia and altered sensorimotor gating. In *PloS one* 6 (6), pp. e21050. DOI: 10.1371/journal.pone.0021050.

Talantova, Maria; Sanz-Blasco, Sara; Zhang, Xiaofei; Xia, Peng; Akhtar, Mohd Waseem; Okamoto, Shu-ichi et al. (2013): Aβ induces astrocytic glutamate release, extrasynaptic NMDA receptor activation, and synaptic loss. In *Proceedings of the National Academy of Sciences of the United States of America* 110 (27), E2518-27. DOI: 10.1073/pnas.1306832110.

Tammineni, Prasad; Ye, Xuan; Feng, Tuancheng; Aikal, Daniyal; Cai, Qian (2017): Impaired retrograde transport of axonal autophagosomes contributes to autophagic stress in Alzheimer's disease neurons. In *eLife* 6. DOI: 10.7554/eLife.21776.

Tan, J.; Town, T.; Paris, D.; Mori, T.; Suo, Z.; Crawford, F. et al. (1999): Microglial activation resulting from CD40-CD40L interaction after beta-amyloid stimulation. In *Science (New York, N.Y.)* 286 (5448), pp. 2352–2355.

Tang, Zhi; Bereczki, Erika; Zhang, Haiyan; Wang, Shan; Li, Chunxia; Ji, Xinying et al. (2013): Mammalian target of rapamycin (mTor) mediates tau protein dyshomeostasis: implication for Alzheimer disease. In *The Journal of biological chemistry* 288 (22), pp. 15556–15570. DOI: 10.1074/jbc.M112.435123.

Tang, Zhi; Ioja, Eniko; Bereczki, Erika; Hultenby, Kjell; Li, Chunxia; Guan, Zhizhong et al. (2015): mTor mediates tau localization and secretion: Implication for Alzheimer's disease. In *Biochimica et biophysica acta* 1853 (7), pp. 1646–1657. DOI: 10.1016/j.bbamcr.2015.03.003.

Tanida, I.; Ueno, T.; Kominami, E. (2008): LC3 and Autophagy. In *Methods in molecular biology (Clifton, N.J.)* 445, pp. 77–88. DOI: 10.1007/978-1-59745-157-4_4.

Tanzi, R. E.; Gusella, J. F.; Watkins, P. C.; Bruns, G. A.; St George-Hyslop, P.; van Keuren, M. L. et al. (1987): Amyloid beta protein gene: cDNA, mRNA distribution, and genetic linkage near the Alzheimer locus. In *Science (New York, N.Y.)* 235 (4791), pp. 880–884.

Terry, R. D. (1963): The fine structure of neurofibrillary tangles in Alzheimer's disease. In *Journal of neuropathology and experimental neurology* 22, pp. 629–642.

Thal, Dietmar Rudolf (2012): The role of astrocytes in amyloid beta-protein toxicity and clearance. In *Experimental neurology* 236 (1), pp. 1–5. DOI: 10.1016/j.expneurol.2012.04.021.

Tomidokoro, Y.; Harigaya, Y.; Matsubara, E.; Ikeda, M.; Kawarabayashi, T.; Shirao, T. et al. (2001): Brain Abeta amyloidosis in APPsw mice induces accumulation of presenilin-1 and tau. In *The Journal of pathology* 194 (4), pp. 500–506.

Tramutola, Antonella; Triplett, Judy C.; Di Domenico, Fabio; Niedowicz, Dana M.; Murphy, Michael P.; Coccia, Raffaella et al. (2015): Alteration of mTOR signaling occurs early in the progression of Alzheimer disease (AD): analysis of brain from subjects with pre-clinical AD, amnestic mild cognitive impairment and late-stage AD. In *Journal of neurochemistry* 133 (5), pp. 739–749. DOI: 10.1111/jnc.13037.

Tsang, Emily; Giannetti, Anthony M.; Shaw, David; Dinh, Marie; Tse, Joyce K. Y.; Gandhi, Shaan et al. (2008): Molecular Mechanism of the Syk Activation Switch. In *J. Biol. Chem.* 283 (47), pp. 32650–32659. DOI: 10.1074/jbc.M806340200.

Tsujimura, Toshiaki; Yanagi, Shigeru; Inatome, Ryoko; Takano, Tomoko; Ishihara, Itsuko; Mitsui, Norihiro et al. (2001): Syk protein-tyrosine kinase is involved in neuron-like differentiation of embryonal carcinoma P19 cells. In *FEBS letters* 489 (2-3), pp. 129–133. DOI: 10.1016/S0014-5793(01)02097-X.

Turnbull, Isaiah R.; Gilfillan, Susan; Cella, Marina; Aoshi, Taiki; Miller, Mark; Piccio, Laura et al. (2006): Cutting edge: TREM-2 attenuates macrophage activation. In *Journal of immunology (Baltimore, Md. : 1950)* 177 (6), pp. 3520–3524.

Ulrich, Jason D.; Finn, Mary Beth; Wang, Yaming; Shen, Alice; Mahan, Thomas E.; Jiang, Hong et al. (2014): Altered microglial response to Abeta plaques in APPPS1-21 mice heterozygous for TREM2. In *Molecular neurodegeneration* 9, p. 20. DOI: 10.1186/1750-1326-9-20.

Ulrich, Jason D.; Holtzman, David M. (2016): TREM2 Function in Alzheimer's Disease and Neurodegeneration. In *ACS chemical neuroscience* 7 (4), pp. 420–427. DOI: 10.1021/acschemneuro.5b00313.

Ulrich, Jason D.; Ulland, Tyler K.; Colonna, Marco; Holtzman, David M. (2017): Elucidating the Role of TREM2 in Alzheimer's Disease. In *Neuron* 94 (2), pp. 237–248. DOI: 10.1016/j.neuron.2017.02.042.

Vega, Irving E.; Cui, Li; Propst, Josh A.; Hutton, Michael L.; Lee, Gloria; Yen, Shu-Hui (2005): Increase in tau tyrosine phosphorylation correlates with the formation of tau

aggregates. In *Molecular Brain Research* 138 (2), pp. 135–144. DOI: 10.1016/j.molbrainres.2005.04.015.

Verghese, Philip B.; Castellano, Joseph M.; Garai, Kanchan; Wang, Yinong; Jiang, Hong; Shah, Aarti et al. (2013): ApoE influences amyloid-β (Aβ) clearance despite minimal apoE/Aβ association in physiological conditions. In *Proceedings of the National Academy of Sciences of the United States of America* 110 (19), E1807-16. DOI: 10.1073/pnas.1220484110.

Vershinin, Michael; Xu, Jing; Razafsky, David S.; King, Stephen J.; Gross, Steven P. (2008): Tuning microtubule-based transport via filamentous MAPs: the problem of dynein. In *Traffic (Copenhagen, Denmark)* 9 (6), pp. 882–892. DOI: 10.1111/j.1600-0854.2008.00741.x.

Vos, Kurt J. de; Grierson, Andrew J.; Ackerley, Steven; Miller, Christopher C. J. (2008): Role of axonal transport in neurodegenerative diseases. In *Annual review of neuroscience* 31, pp. 151–173. DOI: 10.1146/annurev.neuro.31.061307.090711.

Wang, Hongjie; Wang, Ruizhi; Carrera, Ivan; Xu, Shaohua; Lakshmana, Madepalli K. (2016): TFEB Overexpression in the P301S Model of Tauopathy Mitigates Increased PHF1 Levels and Lipofuscin Puncta and Rescues Memory Deficits. In *eNeuro* 3 (2). DOI: 10.1523/ENEURO.0042-16.2016.

Wang, I-Fang; Guo, Bo-Shen; Liu, Yu-Chih; Wu, Cheng-Chun; Yang, Chun-Hung; Tsai, Kuen-Jer; Shen, Che-Kun James (2012): Autophagy activators rescue and alleviate pathogenesis of a mouse model with proteinopathies of the TAR DNA-binding protein 43. In *Proceedings of the National Academy of Sciences of the United States of America* 109 (37), pp. 15024–15029. DOI: 10.1073/pnas.1206362109.

Wang, Wen-Ying; Tan, Meng-Shan; Yu, Jin-Tai; Tan, Lan (2015a): Role of pro-inflammatory cytokines released from microglia in Alzheimer's disease. In *Annals of Translational Medicine* 3 (10). DOI: 10.3978/j.issn.2305-5839.2015.03.49.

Wang, Yaming; Cella, Marina; Mallinson, Kaitlin; Ulrich, Jason D.; Young, Katherine L.; Robinette, Michelle L. et al. (2015b): TREM2 lipid sensing sustains the microglial response in an Alzheimer's disease model. In *Cell* 160 (6), pp. 1061–1071. DOI: 10.1016/j.cell.2015.01.049.

Wang, Yipeng; Mandelkow, Eckhard (2016): Tau in physiology and pathology. In *Nature Reviews Neuroscience* 17 (1), p. 22. DOI: 10.1038/nrn.2015.1.

Watt, Andrew D.; Crespi, Gabriela A. N.; Down, Russell A.; Ascher, David B.; Gunn, Adam; Perez, Keyla A. et al. (2014): Do current therapeutic anti-Abeta antibodies for Alzheimer's disease engage the target? In *Acta neuropathologica* 127 (6), pp. 803–810. DOI: 10.1007/s00401-014-1290-2.

Webb, Robin L.; Murphy, M. Paul (2012): β -Secretases, Alzheimer's Disease, and Down Syndrome. In *Current Gerontology and Geriatrics Research* 2012 (11), pp. 1–8. DOI: 10.1155/2012/362839.

Wegiel, J.; Wang, K. C.; Imaki, H.; Rubenstein, R.; Wronska, A.; Osuchowski, M. et al. (2001): The role of microglial cells and astrocytes in fibrillar plaque evolution in transgenic APP(SW) mice. In *Neurobiology of aging* 22 (1), pp. 49–61.

Wegiel, Jerzy; Imaki, Humi; Wang, Kuo-Chiang; Wegiel, Jarek; Rubenstein, Richard (2004): Cells of monocyte/microglial lineage are involved in both microvessel amyloidosis and fibrillar

plaque formation in APPsw tg mice. In *Brain research* 1022 (1-2), pp. 19–29. DOI: 10.1016/j.brainres.2004.06.058.

Weikel, Karen A.; Cacicedo, José M.; Ruderman, Neil B.; Ido, Yasuo (2016): Knockdown of GSK3β increases basal autophagy and AMPK signalling in nutrient-laden human aortic endothelial cells. In *Bioscience Reports* 36 (5). DOI: 10.1042/BSR20160174.

Wennström, Malin; Hall, Sara; Nägga, Katarina; Londos, Elisabet; Minthon, Lennart; Hansson, Oskar (2015): Cerebrospinal fluid levels of IL-6 are decreased and correlate with cognitive status in DLB patients. In *Alzheimer's research & therapy* 7 (1), p. 63. DOI: 10.1186/s13195-015-0145-y.

Wisniewski, T.; Castano, E. M.; Golabek, A.; Vogel, T.; Frangione, B. (1994): Acceleration of Alzheimer's fibril formation by apolipoprotein E in vitro. In *The American journal of pathology* 145 (5), pp. 1030–1035.

Wolf, H. K.; Buslei, R.; Schmidt-Kastner, R.; Schmidt-Kastner, P. K.; Pietsch, T.; Wiestler, O. D.; Blümcke, I. (1996): NeuN: a useful neuronal marker for diagnostic histopathology. In *J Histochem Cytochem.* 44 (10), pp. 1167–1171. DOI: 10.1177/44.10.8813082.

Wolfe, M. S.; Xia, W.; Ostaszewski, B. L.; Diehl, T. S.; Kimberly, W. T.; Selkoe, D. J. (1999): Two transmembrane aspartates in presenilin-1 required for presenilin endoproteolysis and gamma-secretase activity. In *Nature* 398 (6727), pp. 513–517. DOI: 10.1038/19077.

Wu, Chang-Chih; Hou, Shirui; Orr, Brent A.; Kuo, Bryan R.; Youn, Yong Ha; Ong, Taren et al. (2017): mTORC1-Mediated Inhibition of 4EBP1 Is Essential for Hedgehog Signaling-Driven Translation and Medulloblastoma. In *Developmental cell* 43 (6), 673-688.e5. DOI: 10.1016/j.devcel.2017.10.011.

Xia, MengQi; Hyman, Bradley T. (2002): GROalpha/KC, a chemokine receptor CXCR2 ligand, can be a potent trigger for neuronal ERK1/2 and PI-3 kinase pathways and for tau hyperphosphorylation-a role in Alzheimer's disease? In *Journal of neuroimmunology* 122 (1-2), pp. 55–64.

Xu, Ning; Tang, Xiao-Hui; Pan, Wei; Xie, Ze-Min; Zhang, Guang-Fen; Ji, Mu-Huo et al. (2017): Spared Nerve Injury Increases the Expression of Microglia M1 Markers in the Prefrontal Cortex of Rats and Provokes Depression-Like Behaviors. In *Front. Neurosci.* 11, p. 209. DOI: 10.3389/fnins.2017.00209.

Yamada, Kaoru (2017): Extracellular Tau and Its Potential Role in the Propagation of Tau Pathology. In *Frontiers in neuroscience* 11. DOI: 10.3389/fnins.2017.00667.

Yamamoto, Noriyuki; Takeshita, Keisuke; Shichijo, Michitaka; Kokubo, Toshio; Sato, Masako; Nakashima, Kosuke et al. (2003): The orally available spleen tyrosine kinase inhibitor 2-7-(3,4-dimethoxyphenyl)-imidazo1,2-cpyrimidin-5-ylaminonicotinamide dihydrochloride (BAY 61-3606) blocks antigen-induced airway inflammation in rodents. In *The Journal of pharmacology and experimental therapeutics* 306 (3), pp. 1174–1181. DOI: 10.1124/jpet.103.052316.

Yamazaki, Tsuneo; Koo, Edward H.; Selkoe, Dennis J. (1997): Cell Surface Amyloid β-Protein Precursor Colocalizes with β1 Integrins at Substrate Contact Sites in Neural Cells. In *J. Neurosci.* 17 (3), pp. 1004–1010. DOI: 10.1523/JNEUROSCI.17-03-01004.1997.

Yanamandra, Kiran; Jiang, Hong; Mahan, Thomas E.; Maloney, Susan E.; Wozniak, David F.; Diamond, Marc I.; Holtzman, David M. (2015): Anti-tau antibody reduces insoluble tau and decreases brain atrophy. In *Annals of clinical and translational neurology* 2 (3), pp. 278–288. DOI: 10.1002/acn3.176.

Yang, Yi; Chen, Sicong; Zhang, Jiafeng; Li, Chentan; Sun, Yonghong; Zhang, Lihui; Zheng, Xiaoxiang (2014): Stimulation of autophagy prevents amyloid-beta peptide-induced neuritic degeneration in PC12 cells. In *Journal of Alzheimer's disease : JAD* 40 (4), pp. 929–939. DOI: 10.3233/JAD-132270.

Yao, Xiu-Qing; Zhang, Xiao-Xue; Yin, Yang-Yang; Liu, Bin; Luo, Dan-Ju; Liu, Dan et al. (2011): Glycogen synthase kinase-3β regulates Tyr307 phosphorylation of protein phosphatase-2A via protein tyrosine phosphatase 1B but not Src. In *Biochemical Journal* 437 (2), pp. 335–344. DOI: 10.1042/BJ20110347.

Yao, Yinan; Li, Hequan; Chen, Junjun; Xu, Weiyi; Yang, Guangdie; Bao, Zhang et al. (2016): TREM-2 serves as a negative immune regulator through Syk pathway in an IL-10 dependent manner in lung cancer. In *Oncotarget*. DOI: 10.18632/oncotarget.8813.

Ying, Haiyan; Li, Zhenping; Yang, Lifen; Zhang, Jian (2011): Syk mediates BCR- and CD40-signaling integration during B cell activation. In *Immunobiology* 216 (5), pp. 566–570. DOI: 10.1016/j.imbio.2010.09.016.

Yoon, S. S.; Jo, S. A. (2012): Mechanisms of Amyloid-β Peptide Clearance: Potential Therapeutic Targets for Alzheimer's Disease. In *Biomolecules & Therapeutics* 20 (3), pp. 245–255. DOI: 10.4062/biomolther.2012.20.3.245.

Yoshiyama, Yasumasa; Higuchi, Makoto; Zhang, Bin; Huang, Shu-Ming; Iwata, Nobuhisa; Saido, Takaomi C. et al. (2007): Synapse loss and microglial activation precede tangles in a P301S tauopathy mouse model. In *Neuron* 53 (3), pp. 337–351. DOI: 10.1016/j.neuron.2007.01.010.

Youssef, Lama A.; Wilson, Bridget S.; Oliver, Janet M. (2002): Proteasome-dependent regulation of Syk tyrosine kinase levels in human basophils. In *Journal of Allergy and Clinical Immunology* 110 (3), pp. 366–373. DOI: 10.1067/mai.2002.127562.

Yu, Yu; Gaillard, Stephanie; Phillip, Jude M.; Huang, Tai-Chung; Pinto, Sneha M.; Tessarollo, Nayara G. et al. (2015): Inhibition of Spleen Tyrosine Kinase Potentiates Paclitaxel-Induced Cytotoxicity in Ovarian Cancer Cells by Stabilizing Microtubules. In *Cancer cell* 28 (1), pp. 82–96. DOI: 10.1016/j.ccell.2015.05.009.

Yuan, Peng; Condello, Carlo; Keene, C. Dirk; Wang, Yaming; Bird, Thomas D.; Paul, Steven M. et al. (2016): TREM2 Haplodeficiency in Mice and Humans Impairs the Microglia Barrier Function Leading to Decreased Amyloid Compaction and Severe Axonal Dystrophy. In *Neuron* 90 (4), pp. 724–739. DOI: 10.1016/j.neuron.2016.05.003.

Zare-Shahabadi, Ameneh; Masliah, Eliezer; Johnson, Gail V. W.; Rezaei, Nima (2015): Autophagy in Alzheimer's disease. In *Reviews in the neurosciences* 26 (4), pp. 385–395. DOI: 10.1515/revneuro-2014-0076.

Zhang, J.; Billingsley, M. L.; Kincaid, R. L.; Siraganian, R. P. (2000): Phosphorylation of Syk activation loop tyrosines is essential for Syk function. An in vivo study using a specific anti-Syk

activation loop phosphotyrosine antibody. In *The Journal of biological chemistry* 275 (45), pp. 35442–35447. DOI: 10.1074/jbc.M004549200.

Zhang, Jin; Gao, Zhanguo; Yin, Jun; Quon, Michael J.; Ye, Jianping (2008): S6K Directly Phosphorylates IRS-1 on Ser-270 to Promote Insulin Resistance in Response to TNF-α Signaling through IKK2*S. In *The Journal of biological chemistry* 283 (51), pp. 35375–35382. DOI: 10.1074/jbc.M806480200.

Zhang, Xue-Mei; Cai, Yan; Xiong, Kun; Cai, Huaibin; Luo, Xue-Gang; Feng, Jia-Chun et al. (2009): Beta-secretase-1 elevation in transgenic mouse models of Alzheimer's disease is associated with synaptic/axonal pathology and amyloidogenesis: implications for neuritic plaque development. In *The European journal of neuroscience* 30 (12), pp. 2271–2283. DOI: 10.1111/j.1460-9568.2009.07017.x.

Zhao, Jie; O'Connor, Tracy; Vassar, Robert (2011): The contribution of activated astrocytes to Abeta production: implications for Alzheimer's disease pathogenesis. In *Journal of neuroinflammation* 8, p. 150. DOI: 10.1186/1742-2094-8-150.

Zhao, Ruohe; Hu, Wanling; Tsai, Julia; Li, Wei; Gan, Wen-Biao (2017): Microglia limit the expansion of β-amyloid plaques in a mouse model of Alzheimer's disease. In *Molecular neurodegeneration* 12 (1), p. 47. DOI: 10.1186/s13024-017-0188-6.

Zhao, Yingjun; Wu, Xilin; Li, Xiaoguang; Jiang, Lu-Lin; Gui, Xun; Liu, Yan et al. (2018): TREM2 Is a Receptor for beta-Amyloid that Mediates Microglial Function. In *Neuron* 97 (5), 1023-1031.e7. DOI: 10.1016/j.neuron.2018.01.031.

Zheng, Hui-fen; Yang, Ya-ping; Hu, Li-fang; Wang, Mei-Xia; Wang, Fen; Cao, Li-Dan et al. (2013): Autophagic impairment contributes to systemic inflammation-induced dopaminergic neuron loss in the midbrain. In *PloS one* 8 (8), e70472. DOI: 10.1371/journal.pone.0070472.

Zhou, Xiaogang; Zhou, Jian; Li, Xilei; Guo, Chang'an; Fang, Taolin; Chen, Zhengrong (2011): GSK-3β inhibitors suppressed neuroinflammation in rat cortex by activating autophagy in ischemic brain injury. In *Biochemical and biophysical research communications* 411 (2), pp. 271–275. DOI: 10.1016/j.bbrc.2011.06.117.

Zyss, Deborah; Montcourrier, Philippe; Vidal, Benjamin; Anguille, Christelle; Merezegue, Fabrice; Sahuquet, Alain et al. (2005): The Syk tyrosine kinase localizes to the centrosomes and negatively affects mitotic progression. In *Cancer research* 65 (23), pp. 10872–10880. DOI: 10.1158/0008-5472.CAN-05-1270.

8 Appendix: Published Research Articles

Schweig et al. Acta Neuropathologica Communications (2017) 5:69
DOI 10.1186/s40478-017-0472-2

Acta Neuropathologica Communications

RESEARCH Open Access

Alzheimer's disease pathological lesions activate the spleen tyrosine kinase

Jonas Elias Schweig[1,2*], Hailan Yao[1,3], David Beaulieu-Abdelahad[1], Ghania Ait-Ghezala[1,3], Benoit Mouzon[1,2,3], Fiona Crawford[1,2,3], Michael Mullan[1,2] and Daniel Paris[1,2,3]

Abstract

The pathology of Alzheimer's disease (AD) is characterized by dystrophic neurites (DNs) surrounding extracellular Aβ-plaques, microgliosis, astrogliosis, intraneuronal tau hyperphosphorylation and aggregation. We have previously shown that inhibition of the spleen tyrosine kinase (Syk) lowers Aβ production and tau hyperphosphorylation in vitro and in vivo. Here, we demonstrate that Aβ-overexpressing Tg PS1/APPsw, Tg APPsw mice, and tau overexpressing Tg Tau P301S mice exhibit a pathological activation of Syk compared to wild-type littermates. Syk activation is occurring in a subset of microglia and is age-dependently increased in Aβ-plaque-associated dystrophic neurites of Tg PS1/APPsw and Tg APPsw mice. In Tg Tau P301S mice, a pure model of tauopathy, activated Syk occurs in neurons that show an accumulation of misfolded and hyperphosphorylated tau in the cortex and hippocampus. Interestingly, the tau pathology is exacerbated in neurons that display high levels of Syk activation supporting a role of Syk in the formation of tau pathological species in vivo. Importantly, human AD brain sections show both pathological Syk activation in DNs around Aβ deposits and in neurons immunopositive for pathological tau species recapitulating the data obtained in transgenic mouse models of AD. Additionally, we show that Syk overexpression leads to increased tau accumulation and promotes tau hyperphosphorylation at multiple epitopes in human neuron-like SH-SY5Y cells, further supporting a role of Syk in the formation of tau pathogenic species. Collectively, our data show that Syk activation occurs following Aβ deposition and the formation of tau pathological species. Given that we have previously shown that Syk activation also promotes Aβ formation and tau hyperphosphorylation, our data suggest that AD pathological lesions may be self-propagating via a Syk dependent mechanism highlighting Syk as an attractive therapeutic target for the treatment of AD.

Keywords: Alzheimer's disease, Spleen tyrosine Kinase, Dystrophic neurite, Aβ, sAPPβ, BACE1, Tau hyperphosphorylation, Tau oligomers, Tg PS1/APPsw, Tg APPsw, Tg Tau P301S

Introduction

Alzheimer's disease (AD) is a neurodegenerative disease that accounts for the majority of all cases of dementia. AD pathological hallmarks include extracellular aggregates of Aβ, intracellular tau hyperphosphorylation and aggregation, as well as neuroinflammation. Tau is a microtubule-associated protein (MAP) involved in many essential cellular processes including stabilization of the microtubule network, thereby providing a functional basis for intracellular transport [10]. Misfolding and pathological post-translational modifications including tau hyperphosphorylation contribute to its oligomerization and accumulation that ultimately leads to neuronal death [10]. In addition, tau mutations that cause familial forms of dementia associated with the formation of tau aggregates have been identified suggesting that pathological tau species may play a key role in AD.

Tau and Aβ have been proposed to synergistically contribute to the pathobiology of AD [25]. Through cleavage of the amyloid precursor protein (APP) by α, β and γ-secretases different variants of Aβ and soluble APP forms (α, β) are generated [41]. A variety of post-translational modifications and the nature of the Aβ variants define their susceptibility to aggregation and neurotoxicity [41, 42]. Several mutations in the *APP* and presenilin (*PSEN1/2)* genes (members of the γ-secretase

* Correspondence: jschweig@roskampinstitute.net
[1]The Roskamp Institute, 2040 Whitfield Avenue, Sarasota, FL 34243, USA
[2]The Open University, Milton Keynes MK7 6AA, UK
Full list of author information is available at the end of the article

complex) have been identified and cause familial forms of AD (FAD) [36]. These mutations either render APP more susceptible to cleavage by the β-secretase (BACE-1) or the γ-secretase resulting in increased Aβ production or lead to the production of longer forms of Aβ that are more prone to aggregation and accumulation resulting in early onset AD (EOAD). In contrast, the etiology of sporadic or late onset AD (LOAD) accounts for more than 99% of all AD cases and remains unknown [24].

Many studies have suggested the importance of neuroinflammation caused by Aβ in AD and that a therapeutic strategy can only be successful if it counteracts the neurotoxicity caused by inflammation [24, 29]. Aβ fibrils have been shown to trigger an inflammatory response in primary microglial and monocytic cells via an activation of the tyrosine kinases Lyn (**L**ck/**Y**es **n**ovel tyrosine kinase) and Syk (spleen tyrosine kinase) [3, 23]. Importantly, Syk inhibition appears to prevent Aβ-mediated neurotoxicity in vitro [3]. A subsequent study also showed that Syk is the mediator of the Aβ-induced cytokine production including tumor necrosis factor alpha (TNFα) and interleukin 1 beta (IL-1β) by activated microglia [4] suggesting that Syk is a key kinase responsible for the proinflammatory activity of Aβ.

Many different sites of tau hyperphosphorylation have been identified in AD and various kinases have been the subject of investigations regarding their possible involvement in tau pathogenesis. Syk and Src family kinases have been shown to phosphorylate tau directly at Y18 [20, 25]. Tau tyrosine phosphorylation is considered an early pathological change in AD [5, 20]. Syk has also been shown to phosphorylate microtubules which could have an effect on microtubule polymerization or the interaction of signaling molecules with the microtubule network [6]. Moreover, pharmacological Syk inhibition has been found to stabilize microtubules through dephosphorylation of microtubules and microtubule associated proteins (MAPs) [44].

We have previously shown that Syk regulates the activation of the glycogen synthase kinase-3β (GSK3β), one of the main tau kinase that phosphorylates tau at multiple sites present in neurofibrillary tangles [28]. In addition, we have shown that Syk also regulates Aβ production and proposed that Syk could be an important therapeutic target for the treatment of AD as pharmacological inhibition of Syk appears to reduce tau hyperphosphorylation and Aβ production both in vitro and in vivo [28].

Syk is a non-receptor protein-tyrosine kinase (PTK) that mediates inflammatory responses [8]. PTKs like Syk are part of receptor-mediated signal transduction cascades that require their intracellular association with integral membrane receptors including toll-like receptors (TLRs [11]) and Fc receptors (FcγR [14], FcεRI [21]). Recruitment and activation of Syk is also mediated by activation of triggering receptor expressed on myeloid cells 2 (TREM2) [18]. Interestingly, several variants of TREM2 are associated with an increased risk to develop AD and have been shown to alter AD pathology including Aβ deposition, tau hyperphosphorylation, neuroinflammation and synaptic loss in AD mouse models [17]. Syk becomes active through autophosphorylation and several Syk autophosphorylation sites have been identified in vitro: Y130, Y290, Y317, Y346, Y358, and Y525/526. The Y525/526 phosphorylation site is the main site involved in receptor-mediated Syk activation and signal propagation [30]. Although our previous work suggests that Syk could represent a therapeutic target for AD, the cellular localization and the activity pattern of Syk in the brains of transgenic mouse models of AD and AD pathological specimens remains to be determined. We therefore investigated in this study whether Syk activation occurs in the brains of different mouse models of AD and in human AD brain by monitoring the Y525/526 Syk autophosphorylation site and analyzing its association with AD pathological hallmarks.

We investigated two different AD mouse models that overexpress APP and one mouse model of pure tauopathy that overexpresses human tau with the P301S mutation. In our study, we employed transgenic APPsw (Tg 2576) mice overexpressing the Swedish mutation (KM670/671NL) of APP695 under the control of the hamster prion protein promoter [13]. These mice have elevated levels of Aβ and typically develop Aβ plaques at the age of 11 months [15]. We also analyzed transgenic PS1/APPsw mice which carry the APP KM670/671NL (Swedish) and the PSEN1 M146L mutations. In these mice, the human PSEN1 M146 L transgene is driven by the PDGF-β promoter. These double transgenic mice develop cortical and hippocampal amyloid deposits at 6 months of age; much earlier than the single transgenic APPsw (Tg2576). Additionally, the total Aβ burden is increased in these double transgenic mice compared to the single Tg 2576 transgenic mice [12]. Aβ deposits are associated with dystrophic neurites that occur at 12 months of age in Tg PS1/APPsw mice [9]. Furthermore, these mice display an increase in Aβ plaque-associated microglia and astrocytes at 6 months of age. However, increased microglial activity has been found to occur at 12 months [9]. In addition, we analyzed whether Syk activation occurs in the brain of transgenic Tau P301S PS19 mice that overexpress human tau with the P301S mutation. The P301S mutation in the tau gene on chromosome 17 has been associated with autosomal dominantly inherited frontotemporal dementia and parkinsonism (FTDP-17) [1, 22, 38]. The expression of the P301S mutated tau is fivefold higher in Tg Tau P301S mice than the endogenous mouse protein and is driven by the mouse prion protein promoter [43].

Interestingly, these mice progressively develop neurodegeneration and display intraneuronal tau hyperphosphorylation and aggregation that closely mimic neurofibrillary tangles.

In this study, we show by high-resolution confocal microscopy that Syk activation is increased in a subset of activated microglia and in dystrophic neurites around Aβ plaques of Tg APPsw and Tg PS1/APPsw mice. Interestingly, pSyk is also age-dependently increased in neurons of Tg Tau P301S mice. The degree of colocalization between Syk and tau is largely dependent on the tau epitope investigated and differs between various phospho-tau epitopes and tau oligomers/conformers. The level of Syk activation, as measured by fluorescence intensity, correlates with the amount of pathological tau species detected. In addition, we show that Syk overexpression in human neuronal like cells (SH-SY5Y) results in increased total tau and tau phosphorylation levels at multiple epitopes. Taken together, our results show that β-amyloid and tau pathological species both activate Syk in vivo and conversely, that Syk is involved in microglial activation, plays a role in the pathogenesis of dystrophic neurites (DNs) and contributes to the formation of pathological tau species therefore exacerbating AD pathological lesions. Interestingly, human AD brain sections exhibit the same pattern of Syk activation as the mouse models of β-amyloidosis and tauopathy combined. Human AD brain sections show an increase in pSyk (phosphorylated Syk at Y525/526) levels in DNs around β – amyloid plaques and in neurons immunopositive for hyperphosphorylated tau (Y18) and pathological tau conformers (MC1), whereas brain sections from non-demented controls do not show any pSyk increase. Altogether, these data suggest a crucial role of Syk in the pathobiology of AD and highlight Syk as a promising therapeutic target in AD.

Materials and methods

Animals

Tg PS1/APPsw, Tg APPsw, Tg Tau P301S and wild-type mice were generated and maintained in a C57BL/6 genetic background as previously described [28]. All mice were maintained under specific pathogen free conditions in ventilated racks in the Association for Assessment and Accreditation of Laboratory Animal Care International (AAALAC) accredited vivarium of the Roskamp Institute. All experiments involving mice were reviewed and approved by the Institutional Animal Care and Use Committee of the Roskamp Institute before implementation and were conducted in compliance with the National Institutes of Health Guidelines for the Care and Use of Laboratory Animals.

Tissue processing

All mice were humanely euthanatized and their brains were collected and fixed in 4% paraformaldehyde (PFA) for 48 h. The method of euthanasia used follow the AVMA (American Veterinary Medical Association) guidelines for the euthanasia of animals. Briefly, mice were rendered unconscious through inhalation of 5% isoflurane in oxygen using a vaporizer and a gas chamber. While under anesthesia, after verifying the absence of reflexes, mice were euthanatized by exsanguination (blood was withdrawn from cardiac puncture).

Subsequently, the hemispheres were processed in a Sakura Tissue-Tek VIP (Leica Biosystems Inc., IL, USA) vacuum infiltration processor. Brains were then embedded in paraffin with the Sakura Tissue-Tek (Leica Biosystems Inc., IL, USA) and stored at 4 °C for 2 days for subsequent cutting with a Leica RM2235 microtome (Leica Biosystems Inc., IL, USA). All brains were cut at a thickness of 12 μm. Sagittal slices were mounted on glass slides and dried for 48 h at 37 °C for subsequent immunofluorescence staining and confocal imaging.

Immunofluorescence

Paraffin sections were washed in two baths of histoclear (National Diagnostics, USA) and progressively rehydrated with ethanol gradients and phosphate buffered saline (PBS, Sigma Aldrich, MO, USA). Brain sections were subjected to antigen retrieval for 7 min in citric acid buffer (pH 6) at 100 °C. All sections were treated with 0.05% Sudan Black in 70% ethanol to quench autofluorescence. Sections were then blocked in PBS containing 10% donkey serum (Abcam, MA, USA) for 1 h. Sections were incubated in PBS containing 1% donkey serum and the respective panel of primary antibodies overnight at 4 °C. The following antibodies were used: CP13 (anti(α)-phospho-tau (pTau) S202, 1:200, Dr. Peter Davies' Lab), MC1 (α-conformational tau, 1:200, Dr. Peter Davies' Lab), TOC1 (1:200, Dr. Lester Binder's Lab), PHF-1 (α-pTau S396/404, 1:200, Dr. Peter Davies' Lab), 9G3 (α-pTau Y18, 1:200, MediMabs Inc., QC, Canada), DA9 (α-total-tau (tTau), 1:200, Dr. Peter Davies' Lab), α-BACE1 (1:200 Cell Signaling, MA, USA), α-sAPPβ with Swedish mutation (1:100 Immuno-Biological Laboratories Co, Ltd., Japan), α-Iba1 (1:300, Abcam, MA, USA), α-GFAP (1:5000, Aves Labs, OR, USA), α-pSyk (Y525/526, 1:200, Cell Signaling, MA, USA). In addition to the α-pSyk (Y525/526, 1:200, Cell Signaling, MA, USA), we used the α-pSyk (Y525/526, 1:100, Abgent, CA, USA) and obtained similar results. After three washing steps in PBS for 5 min, sections were incubated in a solution containing PBS, 1% donkey serum and the respective panel of secondary antibodies for 1 h in the dark at room temperature in a humidified chamber. The following secondary antibodies were used: donkey α-rabbit, α-goat, α-mouse conjugated to Alexa 488, 568 and 647, respectively (1:500, Life technologies). After three washing steps in PBS for 5 min, sections

were mounted in Fluoroshield with or without DAPI (Sigma Aldrich, MO, USA). All images were acquired using the confocal microscope LSM 800 (Carl Zeiss AG, Germany), the ZEN Blue 2.1 (Carl Zeiss AG, Germany) software and a 20× or 63× objective. The acquisition settings were kept the same for all genotypes within the same experiment.

For qualitative analysis of the pSyk burden in Tg PS1/APPsw and Tg APPsw mice compared to age-matched WT littermates ($n = 6$ for each genotype, equal amount of male and female), 116 ± 13.5 (avg. ± SEM) weeks of age were stained and analyzed as described above (Fig. 1).

For qualitative analysis of the pSyk burden in Tg Tau P301S mice compared to WT littermates, hippocampi and cortices of 16 male and female mice ranging from 8 to 56 weeks of age were stained and analyzed as described above.

For the quantitative analysis of the pSyk burden (Fig. 3), 140 randomly-selected microscopic fields of four non-consecutive brain slices (containing the hippocampus) from six animals per genotype (equal number of male and female) were acquired. The area covered with the pSyk immunopositive staining was quantified with Fiji [34] in microscopic fields containing Aβ plaques as well as in microscopic fields not containing Aβ deposits. The PS1/APPsw, APPsw and WT mice of the younger cohort were on average 45 ± 0.3 (avg. ± SEM) weeks old. The average age of the mice of the older cohort was 116 ± 13.5 weeks (±SEM). The pSyk burden of the transgenic mice was normalized to the level of pSyk burden quantified in wild-type littermates of the respective age-group. As a negative control, primary antibodies were omitted to determine background and autofluorescence (not shown).

For the quantitative analysis of the colocalization of pSyk and different tau epitopes (Fig. 8) between 400 and 570 cortical fields (50,000 μm^2 per field) from four male Tg Tau P301S animals (average age 47 ± 3.1 (SEM) weeks) were analyzed for each tau epitope. To quantify the percentage of the immunopositive neurons a total of 2546 microscopic fields and 21,800 neurons were counted using the Zen Blue 2.1 software (Carl Zeiss AG, Germany).

The fluorescence intensities (Figs. 9, 10, 11, 12 and 13) of 30 to 40 neurons immunopositive for pSyk, pTau or both (colocalized) were determined for each tau epitope (total of 90 neurons per epitope) using Zen Blue 2.1 (Carl Zeiss AG, Germany). The male Tg Tau P301S mice ($n = 4$) used for quantification were on average 47 ± 3.1 weeks old (avg. ± SEM).

In addition, the different immunostainings mentioned above were performed on paraffin-embedded tissue sections (10 μm, dorsolateral frontal cortex) from a 67-year-old, male patient with AD (Braak VI) and a 102-year-old, male non-demented control that were provided by Dr. Ann McKee (Boston University, MA, USA). Institutional review board approval for brain donation was obtained through the Boston University Alzheimer's Disease Center (BUADC, Boston, MA, USA).

Cell culture

SH-SY5Y cells were purchased from American Type Culture Collection (VA, USA). SH-SY5Y cells were grown in DMEM/F12 medium (Thermo Fisher Scientific, MA, USA) supplemented with 10% fetal bovine serum (Thermo Fisher Scientific, MA, USA), GlutaMAX and 1% penicillin/streptomycin/fungizone.

Generation of Syk overexpressing SH-SY5Y cells

A human cDNA ORF Clone of the human SYK gene (NM_003177, transcript variant 1) was purchased from OriGene Technologies (MD, USA). The cDNA fragment encoding human SYK was amplified by PCR using PfuUltra II Fusion HS DNA polymerase (Agilent Genomics, CA, USA) and subcloned into the p3xFLAG-Myc-CMV™-26 Expression Vector (Sigma-Aldrich, MO, USA) to generate the pCMV-SYK-Flag plasmid. The entire reading frame of the plasmid was confirmed by DNA sequencing. SH-SY5Y cells were maintained in advanced DMEM/F-12 medium supplemented with 10% fetal bovine serum, 1% GlutaMAX, 1% penicillin/streptomycin (Thermo Fisher Scientific, MA, USA) and incubated in a humidified 5% CO_2 atmosphere at 37 °C. For stable transfection, SH-SY5Y cells were grown in 6-wells cell culture plates until reaching 70-80% confluence and transfected with 3 μg of empty pCMV vector (control cells) or pCMV-SYK-Flag plasmids per well using lipofectamine 2000 (Thermo Fisher Scientific, MA, USA). After 48 h, the medium surrounding transfected cells was replaced with fresh medium containing 0.2 mg/ml of G418 for selection. After 14 days of selection, G418 resistant cells were trypsinized and expanded. The expression efficiency of SYK was analyzed by Western blot using antibodies against SYK (4D10 Syk antibody, Santa Cruz Biotechnology, TX, USA) and the Flag tag (Sigma-Aldrich, MO, USA).

Immunoblotting

SH-SY5Y cells were cultured in 24-well-plates for 24 h and subsequently lysed with mammalian protein extraction reagent (MPER, Thermo Fisher Scientific, MA, USA) containing Halt protease & phosphatase single use inhibitor/EDTA (Thermo Fisher Scientific, MA, USA) and 1 mM PMSF. Proteins of cell lysates were separated by 10% tris-glycine-SDS-PAGE using 1 mm Criterion TGX gels (Bio-Rad Laboratories, CA, USA) and electrotransferred onto 0.2 μm PVDF membranes (Bio-Rad Laboratories, CA, USA). Membranes were blocked in TBS containing 5% non-fat dried milk for 1 h and were

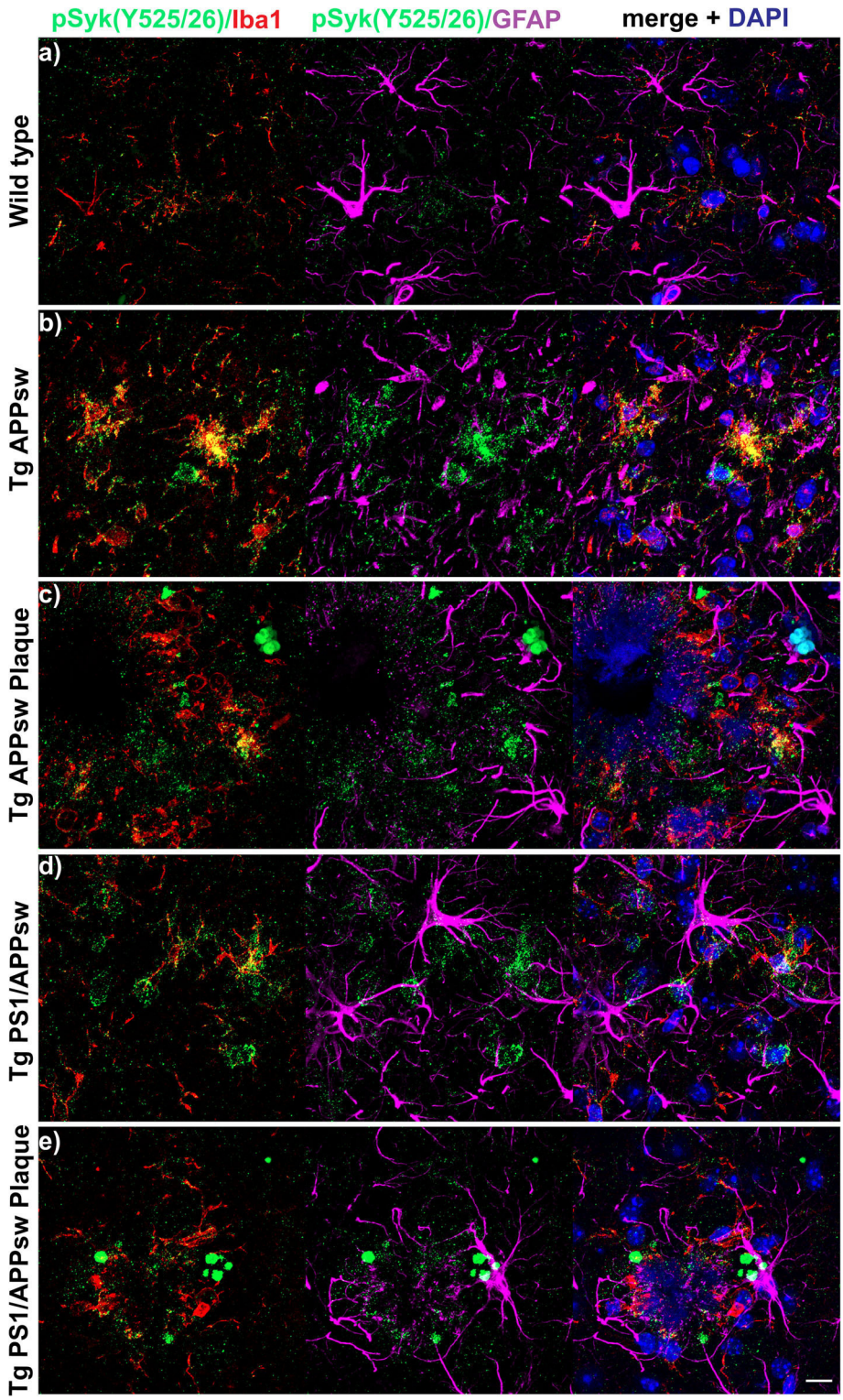

Fig. 1 (See legend on next page.)

(See figure on previous page.)
Fig. 1 pSyk is increased in activated microglia and non-glial cells associated with Aβ-plaques in Tg APPsw and Tg PS1/APPsw mice. **a** Spatial distribution and cellular localization of activated/phosphorylated Syk were investigated in the cortex of 116 ± 13.5-week-old (avg. ± SEM) wild-type mice ($n = 6$) by triple-immunostaining of pSyk (Y525/526, green), microglia (Iba1, red) and astrocytes (GFAP, purple). Nuclei were stained with DAPI (blue). **b** Syk activation in wild-type animals was compared to age-matched Tg APPsw ($n = 6$) (**b**-**c**) and Tg PS1/APPsw littermates ($n = 6$) (**d**-**e**). Plaque-associated cortical areas (**c**, **e**) were compared to non-plaque-associated areas (**b**, **d**). Qualitative image analysis of orthogonal projections and 3D-image analysis (not-shown) revealed an increased pSyk burden in transgenic (**b**-**e**) compared to wild-type mice (**a**) and a colocalization of pSyk and Iba1 but not GFAP in Aβ-overexpressing animals (**b**-**d**). Large, non-glial spherical accumulations of pSyk were observed in plaque-associated areas (**e**). The scale bar represents 10 μm

hybridized with the primary antibody (αSyk (4D10, 1:1000, Santa Cruz, TX, USA), αpTau S396/404 (PHF-1, 1:1000, Dr. Peter Davies' Lab), αtTau (DA9, 1:1000, Dr. Peter Davies' Lab), αpTau Y18 (9G3, 1:1000, MediMabs Inc., QC, Canada,) overnight at 4 °C. Subsequently, the membranes were incubated for 1 h in HRP-conjugated αmouse secondary antibody (1:1000, Cell Signaling, MA, USA). Western blots were visualized using chemiluminescence (Super Signal West Femto Maxium Sensitity Substrate, Thermo Fisher Scientific, MA, USA). Signals were quantified using ChemiDoc XRS (Bio-Rad Laboratories, CA, USA) and densitometric analyses were performed using Quantity One (Bio-Rad Laboratories, CA, USA) image analysis software.

Statistical analyses

The data were analyzed and plotted with GraphPad Prism (GraphPad Software, Inc., CA, USA). The Shapiro-Wilk test for normality was used to test for Gaussian distribution. Statistical significance was determined by either Kruskal-Wallis followed by Dunn's post-hoc test or the non-parametric Mann–Whitney test. All data are presented as mean ± the standard error of the mean (SEM) and $p < 0.05$ was considered significant.

Results

Syk activation in activated microglia and non-glial cells associated with Aβ-plaques in Tg APPsw and Tg PS1/APPsw mice

To investigate whether pathological Syk activation occurs in the brain of AD mouse models, we analyzed the brains of 116-week-old wild-type, Tg APPsw and Tg PS1/APPsw mice using high-resolution confocal microscopy and immunofluorescence. All transgenic mice (Fig. 1b-e) exhibit an increased Iba-1 and GFAP reactivity compared to wild-type littermates (Fig. 1a). Moreover,wild-type some of the activated amoeboid microglia that are observed in transgenic mice are also strongly positive for pSyk (Fig. 1b-d). By contrast, we did not detect any pSyk immunoreactivity in astrocytes (Fig. 1). In addition, we observed that pSyk immunoreactivity is upregulated near Aβ plaques but neither colocalizes with microglia nor astrocytes suggesting that it could be of neuronal origin. (Fig. 1e). We further investigated the cellular origin of these pSyk accumulations by immunofluorescence staining and confocal microscopy (Fig. 2).

pSyk is increased in dystrophic neurites of Aβ-overexpressing mice

To further characterize the cellular origin of pSyk accumulations near Aβ plaques, we tested different markers of dystrophic neurites (BACE-1 and sAPPβ) [31] and found a strong colocalization between pSyk and sAPPβ (Fig. 2a) associated with Aβ deposits. The sAPPβ staining clearly reveals dystrophic swellings of neurites (Fig. 2a) which are a known hallmark of AD. Most of the dystrophic neurites are positive for pSyk (Fig. 2a). Additionally, we found a strong colocalization between sAPPβ and BACE-1 (Fig. 2b) which are often used as markers of dystrophic neurites. Both sAPPβ and BACE-1 exhibit circular accumulations near Aβ plaques (Fig. 2b), highly reminiscent of the pattern observed for activated Syk.

In conclusion, activated Syk is not only found in microglia but also in neurons near Aβ deposits, particularly in dystrophic neurites of Tg APPsw and Tg PS1/APPsw mice supporting a possible role of Syk activation in the formation of dystrophic neurites. Dystrophic neurites are characterized by an accumulation of BACE-1 and sAPPβ [31] and our previous work [28] has shown that Syk regulates BACE-1 expression and sAPPβ levels suggesting that Syk upregulation in dystrophic neurites could contribute to the accumulation of BACE-1 and sAPPβ.

Cortical pSyk burden is age-dependently increased in Aβ-overexpressing mice, particularly in microscopic fields containing Aβ-plaques, compared to wild-type littermates

We also quantified the pSyk burden observed in the cortex of Tg APPsw, Tg PS1/APPsw and wild-type (WT) littermates (Figs. 1 and 2). Two different age-groups were investigated: younger animals, 45 weeks of age and older animals 116 weeks of age in average. In 45-week-old Tg APPsw mice, we did not observe significant β-amyloidosis (only three Aβ plaques were found in the cohort of mice analyzed) (data not shown) showing that, at that age, the Aβ pathology is almost inexistent in these mice. We differentiated between microscopic fields containing Aβ deposits and microscopic fields not

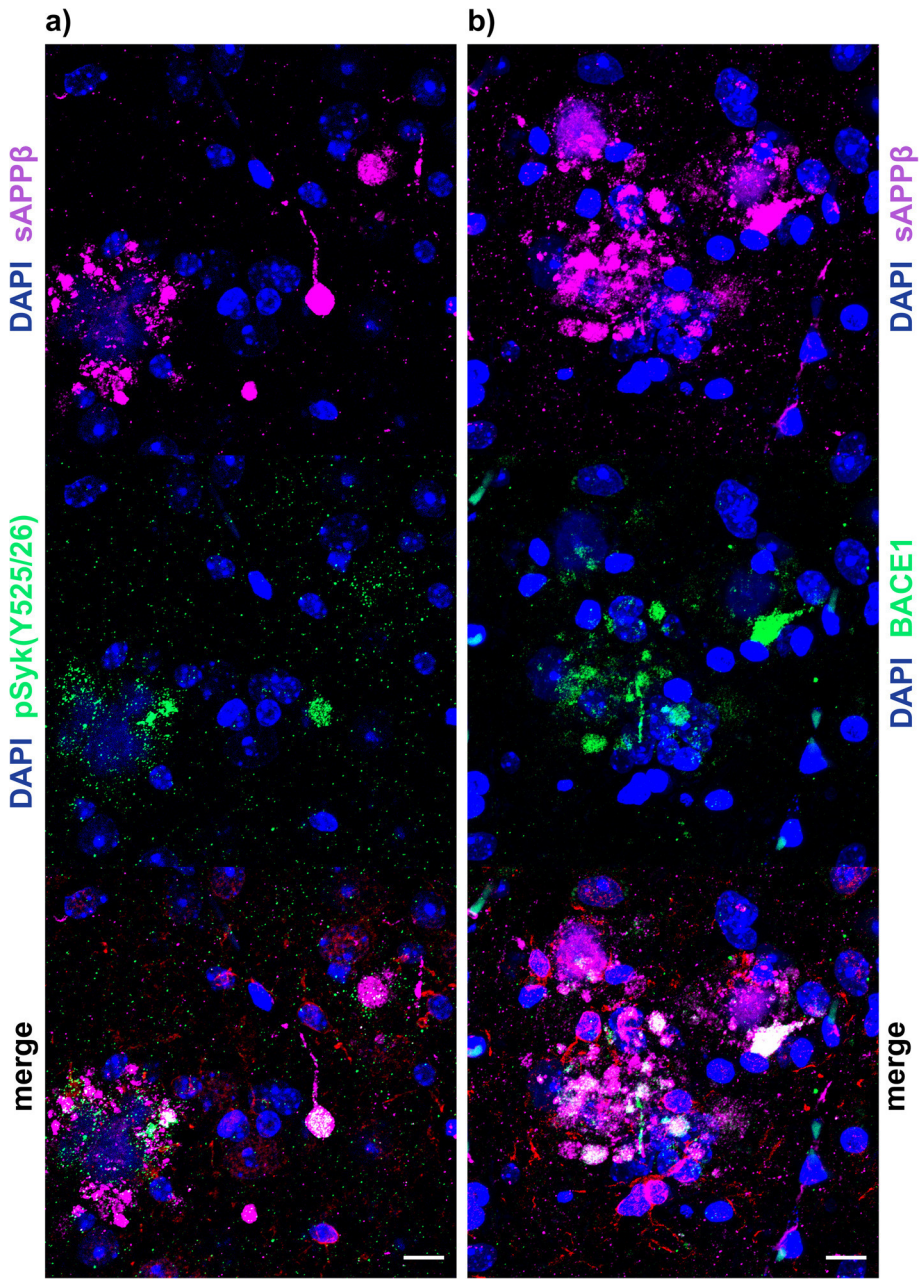

Fig. 2 pSyk is increased in dystrophic neurites of Aβ-overexpressing mice. Representative confocal image of depicting the cortex of 116.5 ± 13.5-week-old Tg PS1/APPsw mice stained for sAPPβ (*purple*), pSyk (*green*, **a**), BACE1 (*green*, **b**), Iba-1 (*red*). Nuclei were stained with DAPI (*blue*). **a** pSyk was accumulated in dystrophic neurites positive for sAPPβ (**a**) and BACE1 (**b**). The scale bars represent 10 μm

containing Aβ deposits for the quantification of the pSyk burden in Tg PS1/APPsw and older Tg APPsw mice. 45-week-old Tg APPsw and Tg PS1/APPsw mice do not show any significant difference in pSyk burden in fields without Aβ deposits compared to WT mice. The pSyk burden of 45-week-old Tg APPsw mice is identical to that of the WT mice (100 ± 6.76% compared to 80.85 ± 11.77%; Fig. 3a). The pSyk burden in fields not containing Aβ plaques in Tg PS1/APPsw mice is not statistically significantly elevated (153.48 ± 18.47%), compared to the WT littermates. As expected, 45-week-old Tg PS1/APPsw mice exhibited a significantly higher pSyk burden in fields containing Aβ plaques (410.19 ± 46.46%) compared to WT and Tg APPsw mice.

The analysis of the pSyk burden in the cortex of older animals (average age: 116 weeks) revealed large differences between genotypes. The pSyk burden of Tg APPsw (216.32 ± 45.23%) mice in microscopic fields without

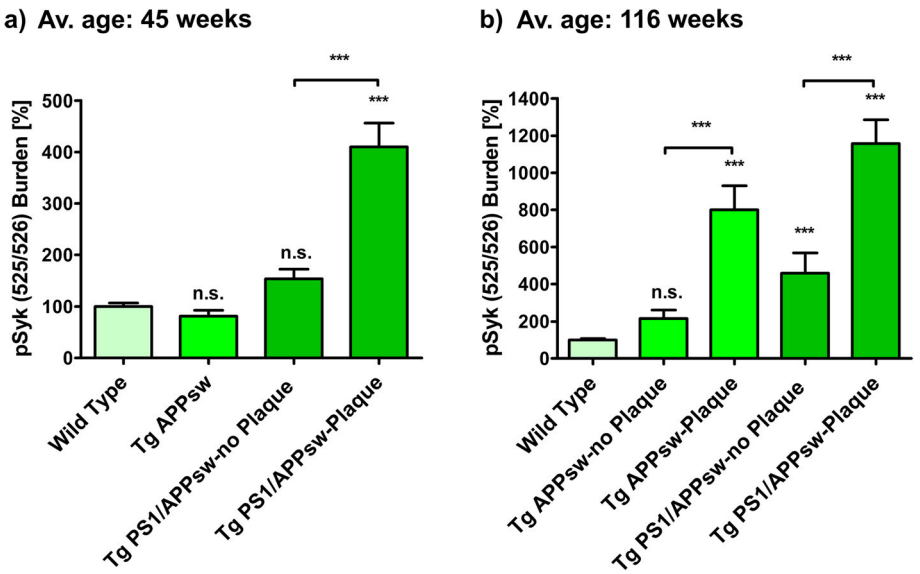

Fig. 3 Cortical pSyk burden is age-dependently increased in Aβ-overexpressing mice, particularly in microscopic fields containing Aβ deposits, compared to wild-type littermates. Cortical pSyk burden (area covered) of immunofluorescence images (Fig. 1) was quantified in 45 ± 0.3-week-old (avg. ± SEM) (**a**) and 116 ± 13.5-week-old (avg. ± SEM) (**b**) Tg APPsw ($n = 6$) and Tg PS1/APPsw mice ($n = 6$), compared and normalized to wild-type littermates ($n = 6$). Microscopic fields containing Aβ deposits were distinguished from microscopic fields not containing Aβ deposits as described in the materials and methods section. Kruskal-Wallis and post-hoc Dunn's multiple comparison test revealed a significant increase ($p < 0.001$) in pSyk in fields containing Aβ deposits in younger Tg PS1/APPsw animals compared to age-matched wild-type littermates (**a**). pSyk burden in older Tg APPsw and Tg PS1/APPsw mice was statistically significantly increased in cortical microscopic fields containing Aβ deposits compared to age-matched wild-type littermates ($p < 0.001$). Older Tg PS1/APPsw mice also exhibited a statistically significant pSyk burden increase in microscopic fields not containing Aβ deposits ($p < 0.001$), whereas the pSyk burden in Tg APPsw in microscopic fields not containing Aβ deposits was not statistically different from wild-type littermates ($P > 0.05$). Six animals per genotype were analyzed. Error bars represent SEM

plaques is not significantly increased compared to WT mice (100 ± 7.78%) (Fig. 3b). In contrast, microscopic fields of older Tg APPsw mice containing Aβ deposits exhibit a strong increase in pSyk burden (799.95 ± 130.19%) compared to age-matched WT mice. Tg PS1/APPsw mice also exhibit a statistically significant increase in pSyk burden in microscopic fields that do not contain Aβ deposits (458.1 ± 109.68) compared to age-matched WT controls. In addition, a much greater pSyk burden is found in Tg PS1/APPsw in microscopic fields containing Aβ deposits. In these fields, the pSyk burden is increased by 1157.31 ± 129.68% compared to WT littermates (Fig. 3b).

In conclusion, our data show that the pSyk burden is highly associated with Aβ plaques and increases with age in Tg PS1/APPsw and Tg APPsw mice whereas no activation of Syk is observed in the brain of WT littermates. The upregulation of Syk activation observed in the brains of Tg APPsw and Tg PS1/APPsw is mainly attributable to pSyk accumulations in dystrophic neurites that are associated with Aβ plaques and increase with age and Aβ burden.

Syk activity is increased in hippocampal and cortical neurons of Tg Tau P301S mice

Having shown that Aβ-overexpressing mouse models of AD exhibit an increased Syk activation in microglia and dystrophic neurites, we investigated whether Syk activation also occurs in Tg Tau P301S mice (a pure model of tauopathy) using immunofluorescence and confocal microscopy. Hippocampal neurons of Tg Tau P301S mice exhibit a high level of tau hyperphosphorylation (Fig. 4b) as well as an accumulation of pathogenic tau conformers (MC1, not shown) compared to WT littermates (Fig. 4a). Most importantly, pathological tau species clearly colocalize with pSyk (Y525/526) in hippocampal neurons (Fig. 4b). The pSyk burden is particularly prominent in hippocampal neurons of Tg Tau P301S mice (Fig. 4b) whereas WT littermates do not exhibit any pSyk immunoreactivity in the hippocampus (Fig. 4a).

Cortical neurons of Tg Tau P301S mice also exhibit an increased level of tau hyperphosphorylation (Fig. 5b) compared to wild-type littermates (Fig. 5a). We observed a colocalization between pSyk and pTau (S202) immunoreactivities in cortical neurons. Interestingly, we also observed neurons that are singly immunopositive for tau or for pSyk. We addressed this observation by performing additional analyses (Figs. 8, 9, 10, 11, 12, 13, 14 and 15).

We also analyzed the temporal changes of pSyk and tau levels in hippocampi and cortices of Tg Tau P301S mice between the age of 8 and 56 weeks (Figs. 6 and 7). WT mice do not exhibit any detectable tau phosphorylation

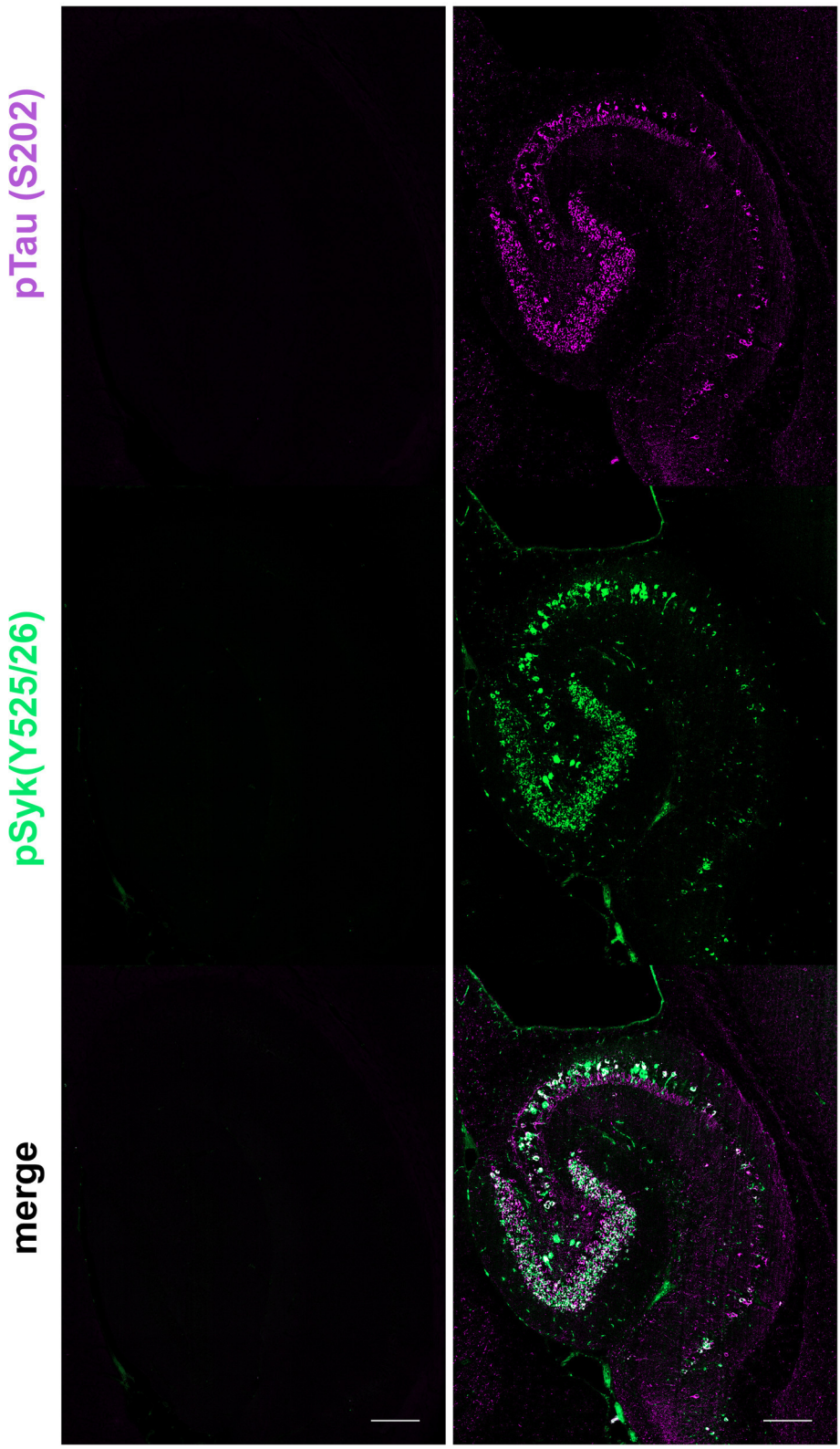

Fig. 4 (See legend on next page.)

(See figure on previous page.)
Fig. 4 pSyk is increased in hippocampal neurons of Tg Tau P301S mice compared to wild-type littermates. Representative confocal image depicting 56 week-old male Tg Tau P301S and wild-type mice stained with antibodies against pTau (S202, purple) and pSyk (Y525/526, green). **a** Wild-type mice did not exhibit any tau phosphorylation nor Syk activation in their hippocampi. **b** Tau-overexpressing Tg Tau P301S mice exhibited a prominent tau phosphorylation at S202 that colocalized with Syk activation in hippocampal neurons. The scale bars represent 200 μm

(Fig. 6f) or tau oligomerization at any age (not shown). We then focused on the dentate gyrus of the hippocampus and found an age-dependent increase of tau phosphorylation (Fig. 6, S202, left panels) in Tg Tau P301S mice. Tau phosphorylation at S202 in the dentate gyrus was already detectable in 8-week-old Tg Tau P301S mice, however, pSyk immunoreactivity was not observed. Neurons immunopositive for pSyk (Y525/526) and pTau (S202) or tau conformers (MC1, not shown) were observed in the dentate gyrus of 42-week-old Tg Tau P301S mice (Fig. 6d). The neuronal pSyk burden also increases with age in Tg Tau P301S mice and is mainly restricted to the neuronal cell body (Fig. 6). Interestingly, microglia and neurites did not exhibit activated Syk in the hippocampus of Tau P301S mice (Fig. 6). Abnormal Syk activation seems to follow tau hyperphosphorylation (S202) in the hippocampus of Tg P301S mice (Fig. 6), as well as the formation of MC1-tau pathological conformers (data not shown here but MC1 and pSyk colocalization were quantified below).

Cortical neurons of Tg Tau P301S mice also show an increase in tau hyperphosphorylation and pSyk with age (Fig. 7). Interestingly, the onset of abnormal Syk activation occurs earlier (16 weeks of age) in the cortex than in the hippocampus (Fig. 7b compared to Fig. 6d). In conclusion, both pSyk and tau pathology in Tg Tau P301S mice increase with age but the progression is different in the hippocampus and the cortex. Many cortical neurons exhibit a colocalization of pSyk and pTau (S202) (Fig. 7b-c, e) but as mentioned earlier, there are also neurons that are singly immunopositive for pSyk or pTau.

We further quantified the number of neurons that are singly pSyk immunopositive, singly immunopositive for tau pathogenic species and neurons immunopositive for both pSyk and tau pathogenic species in the cortex of 47-week-old Tg Tau P301S mice (Fig. 8). We calculated the percentages of neurons singly immunopositive for either pSyk, pathogenic tau species or neurons immunopositive for both. The sum of all cortical neurons counted was considered 100% including neurons positive for pSyk and the respective tau epitope and neurons immunopositive for both. For all the tau epitopes tested, we found that only a small fraction of the neurons is singly immunopositive for pSyk (9.7 ± 4.4% (pTau, Y18); 2.5 ± 1.2% (pTau, S202); 9.2 ± 1.6% (MC1 pathogenic tau conformers); 9.6 ± 6.3% (pTau, S396/404); 4.8 ± 2.0% (TOC1 (tau oligomers)). Interestingly, a larger percentage of neurons is immunoreactive for both pSyk and tau pathogenic species (44.7 ± 8.6% (MC1); 39.7 ± 12.4% pTau Y18; 22.5 ± 18.6% (PHF-1, pTau S396/404); 12.4 ± 8.1% (TOC1, tau oligomers) but only 5.7 ± 2.2% for pTau (S202)). The neurons singly immunopositive for tau complement these observations with relative values of 46.1 ± 8.2% (MC1), 50.6 ± 16.3% (Y18), 67.9 ± 24.9% (S396/404), 82.8 ± 10.1% (TOC1), and 91.8 ± 3.2% (S202) (Fig. 8). The differences in relative colocalization between pSyk and specific tau pathologic species suggest that specific pathogenic forms of tau may have a different impact on Syk activation or either that Syk activation may contribute to the formation of specific tau pathogenic species (Fig. 8). We therefore subsequently measured the fluorescent intensities of pSyk and of the different tau epitopes to determine whether the level of Syk activation correlates with the amount of specific tau pathogenic species. In general, we found that neurons that exhibit a high level of pSyk immunoreactivity also demonstrate a higher level of tau pathogenic species whereas neurons that are weakly immunopositive for pSyk show less tau pathology (Figs. 9, 10, 11, 12 and 13). In addition, neurons that are singly immunopositive for tau pathogenic species (including hyperphosphorylated tau and misfolded tau) show also less intense tau pathologies, as measured by fluorescent intensities, than neurons that are displaying both pSyk and tau pathology, further supporting a role of Syk in the formation of tau pathogenic species. For instance, the level of pathogenic tau conformers (MC1) is significantly increased in neurons that are also strongly immunopositive for pSyk compared to neurons that are singly immunopositive for MC1 (Fig. 9d, $p < 0.05$). Interestingly, the level of pSyk is also significantly increased in neurons that display an accumulation of MC1 pathogenic conformers compared to neurons that are singly immunopositive for pSyk (Fig. 9e, $p < 0.01$). These data suggest that pathogenic tau conformers and Syk activation may promote each other. We found that tau phosphorylation at Y18 is significantly increased in neurons that are also immunopositive for pSyk (Fig. 10d, $p < 0.05$) which is consistent with previous data showing that in vitro Syk can phosphorylates tau at Y18. We have previously shown that Syk positively regulates GSK-3β activity in vitro. It is therefore consistent with our observation that the GSK-3β-dependent phospho-tau epitope (S396/404, PHF-1) is also increased in neurons that display Syk activation (Fig. 11d, $p < 0.0001$). The pSyk level, however, is not statistically significantly increased in

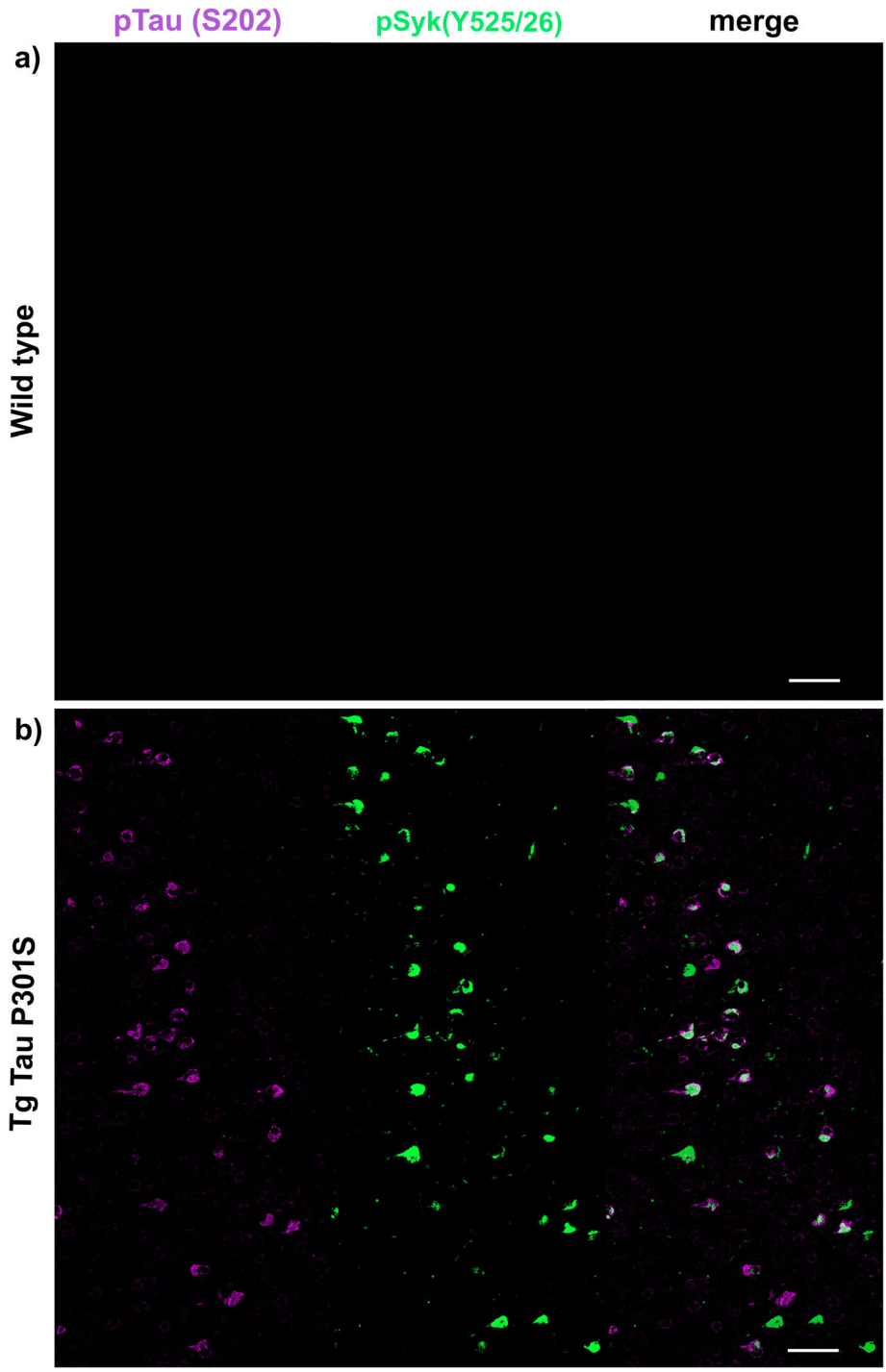

Fig. 5 pSyk is increased in cortical neurons of Tg Tau P301S mice compared to wild-type littermates. Representative confocal image depicting 56 week-old male Tg Tau P301S and wild-type mice stained with antibodies against pTau (S202, purple), pSyk (Y525/526, *green*). **a** Wild-type mice did not exhibit any tau phosphorylation nor Syk activation in their cortices. **b** Tau-overexpressing Tg Tau P301S mice exhibited a prominent tau phosphorylation at S202 that colocalized with Syk activation in cortical neurons. The scale bars represent 100 μm

neurons that are immunopositive for both PHF-1 and pSyk compared to neurons that are singly immunopositive for pSyk suggesting that PHF-1 phosphorylated tau species do not induce Syk activation (Fig. 11e). Similar observations were obtained for tau oligomers (Fig. 12, TOC1) and tau species phosphorylated at S202 (Fig. 13, CP13). Altogether, these data suggest that only certain pathogenic forms of tau (MC1, Y18) promote Syk

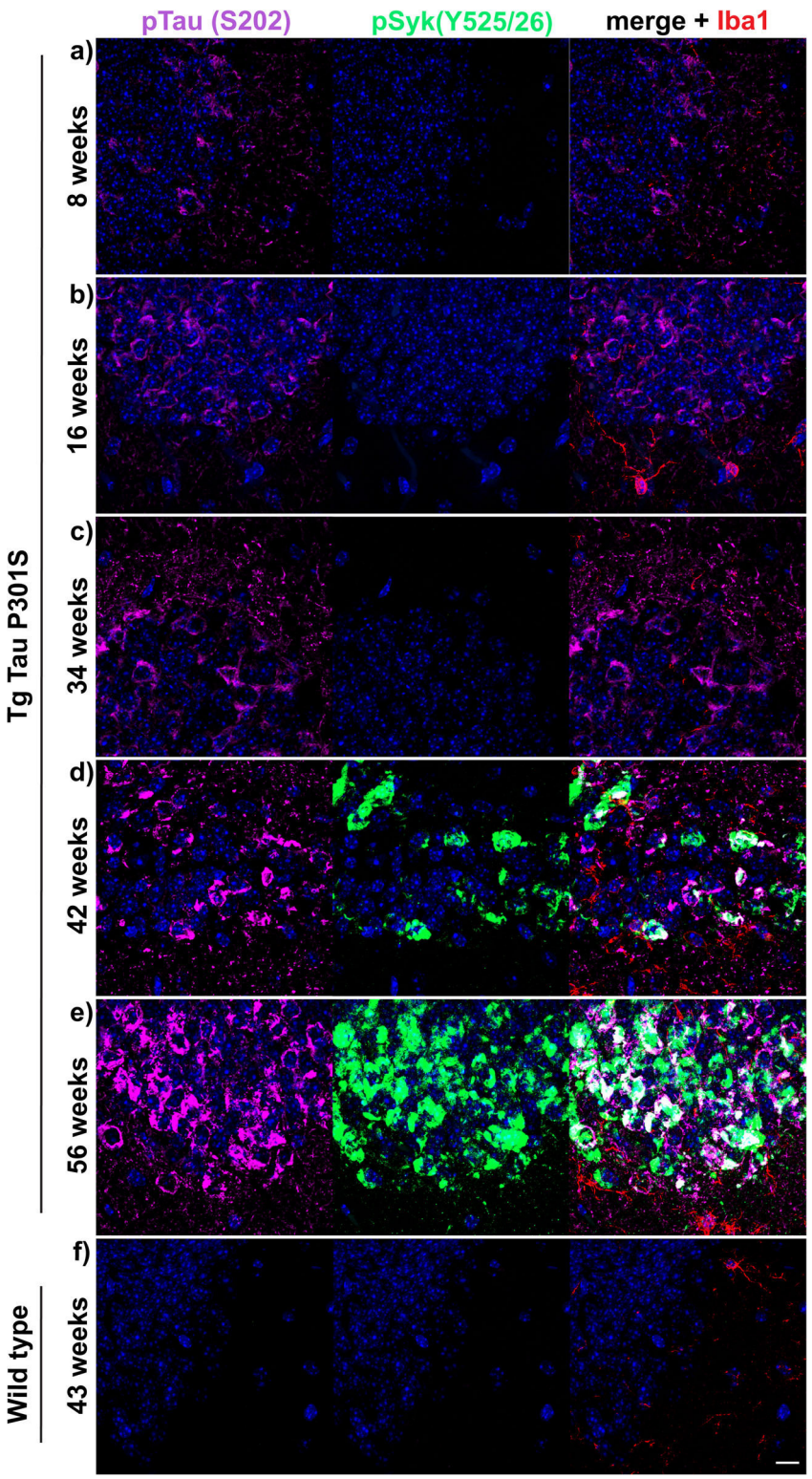

Fig. 6 pSyk is increased age-dependently in hippocampal neurons of Tg Tau P301S mice compared to wild-type littermates. Representative confocal image depicting Tg Tau P301S and wild-type mice ($n = 16$) stained with antibodies against pTau (S202, *purple*), pSyk (Y525/526, *green*) and Iba-1 (*red*). Nuclei were stained with DAPI. **a**-**e** Tau-overexpressing Tg Tau P301S mice exhibited a prominent tau phosphorylation (S202) that increased with age and colocalized with Syk activation in hippocampal neurons. **f** Wild-type mice did not exhibit any tau phosphorylation nor Syk activation in their hippocampi. The scale bar represents 10 μm

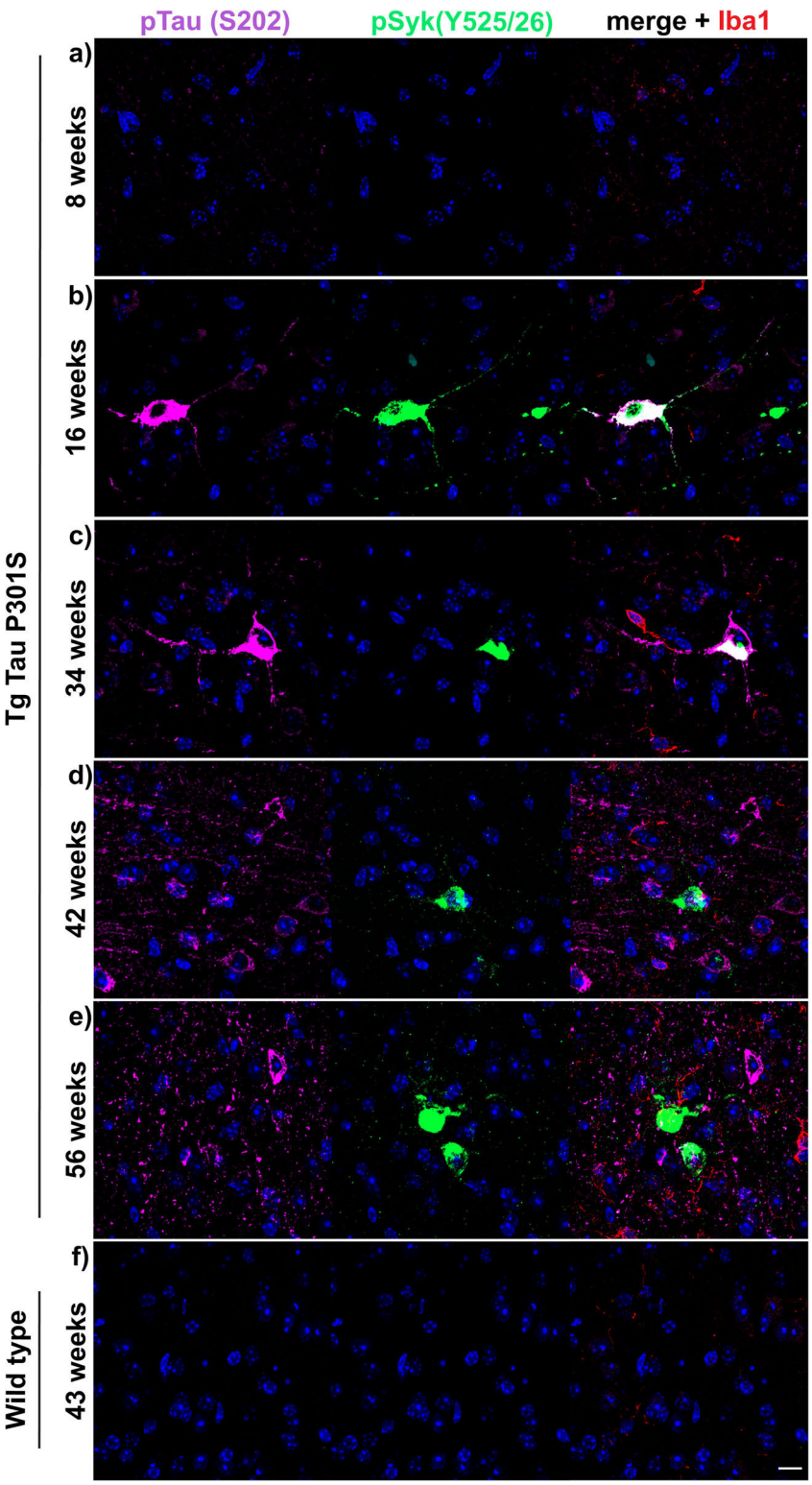

Fig. 7 pSyk is increased age-dependently in cortical neurons of Tg Tau P301S mice compared to wild-type littermates. Representative confocal image depicting Tg Tau P301S and wild-type mice ($n = 16$) stained with antibodies against pTau (S202, *purple*), pSyk (Y525/526, *green*) and Iba-1 (*red*). Nuclei were stained with DAPI. **a**-**e** Tau-overexpressing Tg Tau P301S mice exhibited a prominent tau phosphorylation (S202) that increased with age and partially colocalized with Syk activation in cortical neurons. **f** Wild-type mice did not exhibit any tau phosphorylation nor Syk activation in their cortices. The scale bar represents 10 μm

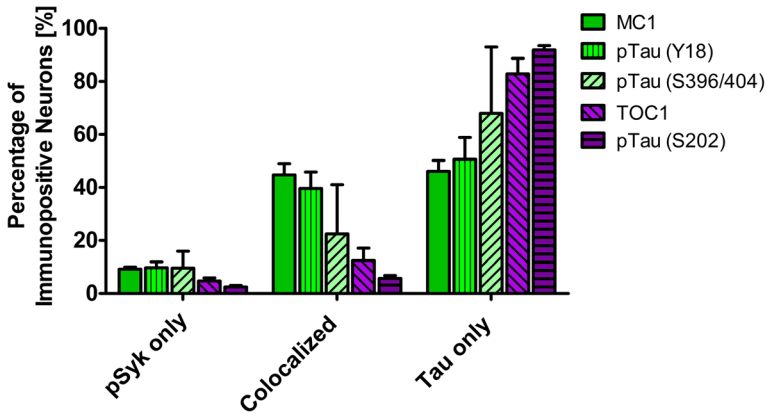

Fig. 8 The degree of colocalization of pSyk and tau differs for various tau epitopes. Sections from Tg Tau P301S mice ($n = 4$, 47 ± 3.1-week-old) were stained with antibodies against pTau (S202, S396/404, Y18), tau oligomers (TOC1) or tau conformers (MC1) and pSyk (Y525/526, *green*). The cortices were divided in ROIs (each at a size of 50,000μm^2) and neurons singly immunopositive for pSyk, singly immunoreactive for the respective tau epitope and the neurons immunopositive for both pSyk and the respective tau epitope (colocalized) were counted and the percentages of each neuronal fraction calculated using Zen *Blue* 2.1 (Zeiss) and Excel (MS Office), respectively. In average, 509 cortical fields were analyzed for each epitope (total of 21,800 neurons counted). The percentage of neurons singly immunopositive for pSyk was at a similar level for all tau epitopes investigated (pSyk only). MC1 and pTau Y18 show the highest colocalization with pSyk whereas the incidence of neurons immunopositive for both pSyk and TOC1 or pTau S202 was much lower (colocalized fraction). The error bars represent SEM

activation, whereas Syk activation appears to directly induce tau phosphorylation at Y18 and to indirectly regulate tau phosphorylation at multiple epitopes (S396/404, S202) as well as tau misfolding (MC1, TOC1).

Syk overexpression increases tau phosphorylation and total tau levels in SH-SY5Y cells

To further investigate the impact of Syk on tau, we generated human neuronal-like (SH-SY5Y) cells overexpressing Syk (Syk-OX). Syk-OX SH-SY5Y cells show an approximate 17-fold increase in Syk expression compared to control SH-SY5Y cells transfected with the empty vector (Fig. 14b, $p < 0.0001$). Interestingly, Syk upregulation in SH-SY5Y cells leads to a significant increase (1.7-fold) in phosphorylated tau at Y18 (Fig. 14c, $p < 0.01$) and at S396/404 (Fig. 14d, 3-fold, $p < 0.0001$) compared to control cells. Total tau levels are also significantly increased following Syk overexpression (Fig. 14e, 4.2-fold, $p < 0.0001$). We analyzed the possible impact of Syk overexpression on Tau mRNA levels by quantitative RT-PCR and found that Syk overexpression does not affect Tau transcription (data not shown) suggesting that Syk may regulate tau degradation or tau protein translation. In summary, these results show that the accumulation of tau pathogenic species can trigger Syk activation, as shown in Tg Tau P301S mice (Figs. 8, 9, 10, 11, 12 and 13), whereas Syk itself appears to regulate total tau levels and tau phosphorylation at multiple epitopes (Fig. 14) therefore influencing the development of the tau pathology.

Syk activity is increased in cortical neurons immunopositive for pTau (Y18), conformationally altered Tau (MC1) and in dystrophic neurites in human AD compared to non-demented control

We also performed different immunostainings against Aβ, pSyk, GFAP, Iba-1, tau pathogenic conformers (MC1) and phosphorylated tau at Y18 using brain sections from human AD and non-demented controls. We found an increase in Syk activation in DNs surrounding Aβ deposits as well as in neurons displaying an accumulation of phosphorylated Tau at Y18 and elevated levels of MC1 pathogenic tau conformers in AD brain sections whereas only weak immunoreactivity for pSyk was observed in brain sections from a non-demented control (Figs. 15, 16 and 17). As observed in the AD mouse models, astrocytes did not exhibit Syk activation in neither the AD brain section nor the control. Only a subset of microglial cells exhibited a weak pSyk signal. Most of the detected pSyk signal was of neuronal origin and either localized in somata or DNs. These data complement our observation in AD mouse models and reveal an association between Syk activation and typical AD pathological lesions in the human brain. Further studies will be required using a larger sample of AD pathological specimen to further clarify the role of Syk activation in AD brains.

Discussion

Our previous studies have shown that tau hyperphosphorylation, Aβ production and neuroinflammation are reduced following Syk inhibition [28]. These data

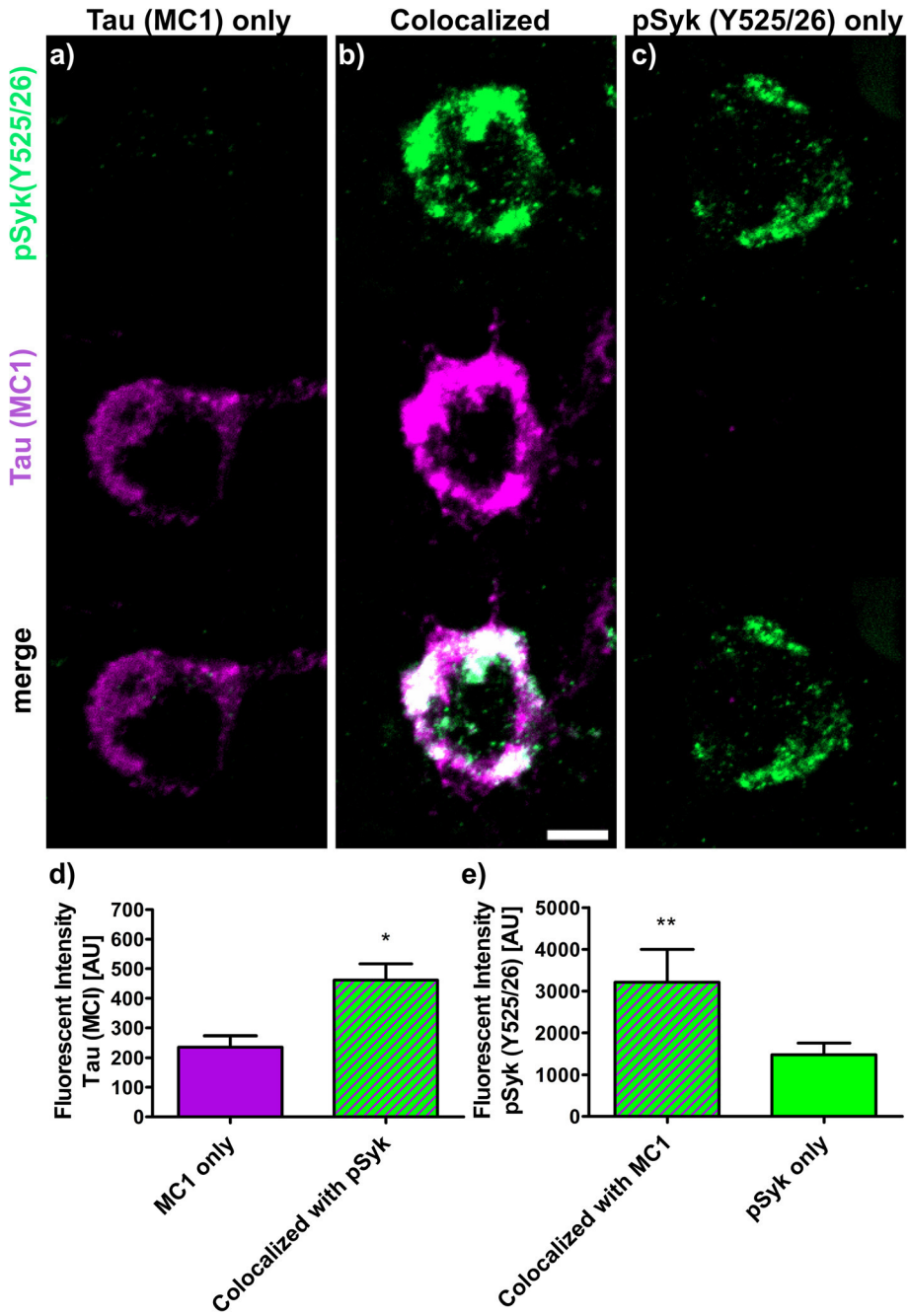

Fig. 9 The amount of MC1 tau conformers and pSyk (Y525/526) levels cross-influence each other. Sections from Tg Tau P301S ($n = 4$, 47 ± 3.1-week-old) were stained with antibodies against tau conformers (MC1, *purple*) and pSyk (Y525/526, *green*). Fluorescent intensities of MC1 and pSyk were measured using Zen Blue 2.1 (Zeiss). Three different neuronal fractions were differentiated: **a** neurons singly immunopositive for MC1, (**b**) neurons singly immunopositive for pSyk and (**c**) neurons immunopositive for both MC1 and pSyk (colocalized). **d** Fluorescent intensities of MC1 were compared between neurons singly MC1 positive (*purple*) and neurons exhibiting a colocalization of MC1 and pSyk (*purple-green-striped*). Two-tailed Mann–Whitney test revealed a significant increase ($p < 0.05$) of MC1 fluorescent intensity in neurons exhibiting a colocalization of MC1 and pSyk compared to neurons singly immunopositive for MC1. **e** Fluorescent intensities of pSyk were compared between neurons singly immunopositive for pSyk (*green*) and neurons that show an immunoreactivity for both pSyk and MC1 (*purple-green-striped*). Two-tailed Mann–Whitney test revealed a significant increase ($p < 0.01$) of pSyk fluorescent intensity in neurons immunoreactive for both pSyk and MC1 compared neurons that are singly immunopositive for pSyk. The scale bar represents 10 μm. The error bars represent SEM

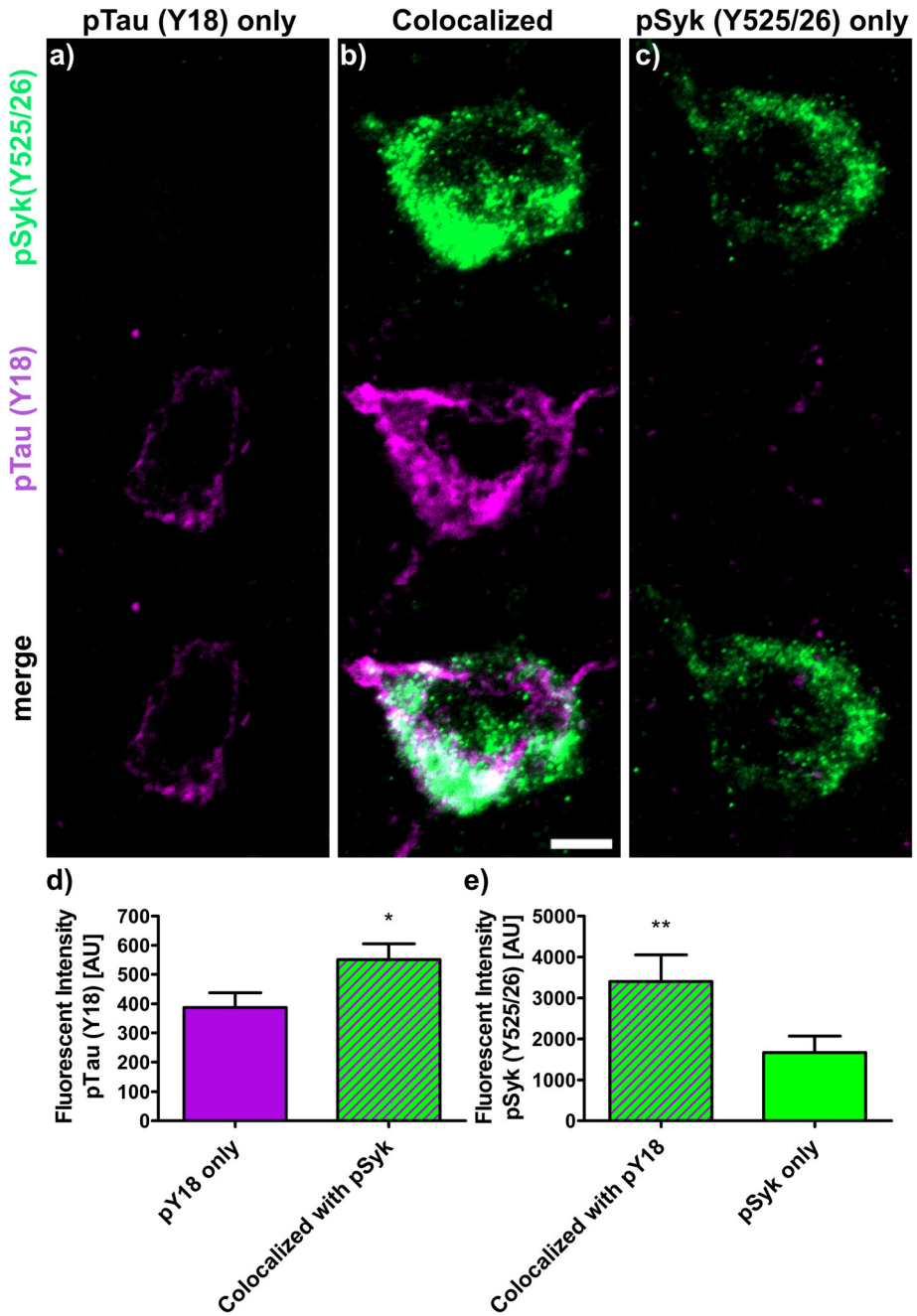

Fig. 10 Tau phosphorylation at Y18 and Syk activation (Y525/526) cross-influence each other. Sections from Tg Tau P301S ($n = 4$, 47 ± 3.1-week-old) were stained with antibodies against phosphorylated tau (Y18, *purple*) and pSyk (Y525/526, *green*). Fluorescent intensities of pTau (pY18) and pSyk were measured using Zen Blue 2.1 (Zeiss). Three different neuronal fractions were differentiated: **a** neurons singly immunopositive for pY18, (**b**) neurons singly immunopositive for pSyk and (**c**) neurons immunopositive for both (colocalized). **d** Fluorescent intensities of pY18 tau were compared between singly pY18 immunopositive and the double immunopositive neurons (colocalized, purple-green-striped). Two-tailed Mann–Whitney test revealed a significant increase ($p < 0.05$) of pY18 fluorescent intensity for neurons exhibiting a colocalization compared to the neurons singly immunopositive for pY18 tau. **e** Fluorescent intensities of pSyk were compared between singly pSyk immunopositive neurons (*green*) and double immunopositive neurons for pSyk and pY18 tau (*purple-green-striped*). Two-tailed Mann–Whitney test revealed a significant increase ($p < 0.01$) of pSyk fluorescent intensity in neurons double immunopositive for pSyk and pY18 tau compared to singly pSyk immunopositive neurons. The scale bar represents 10 μm. The error bars represent SEM

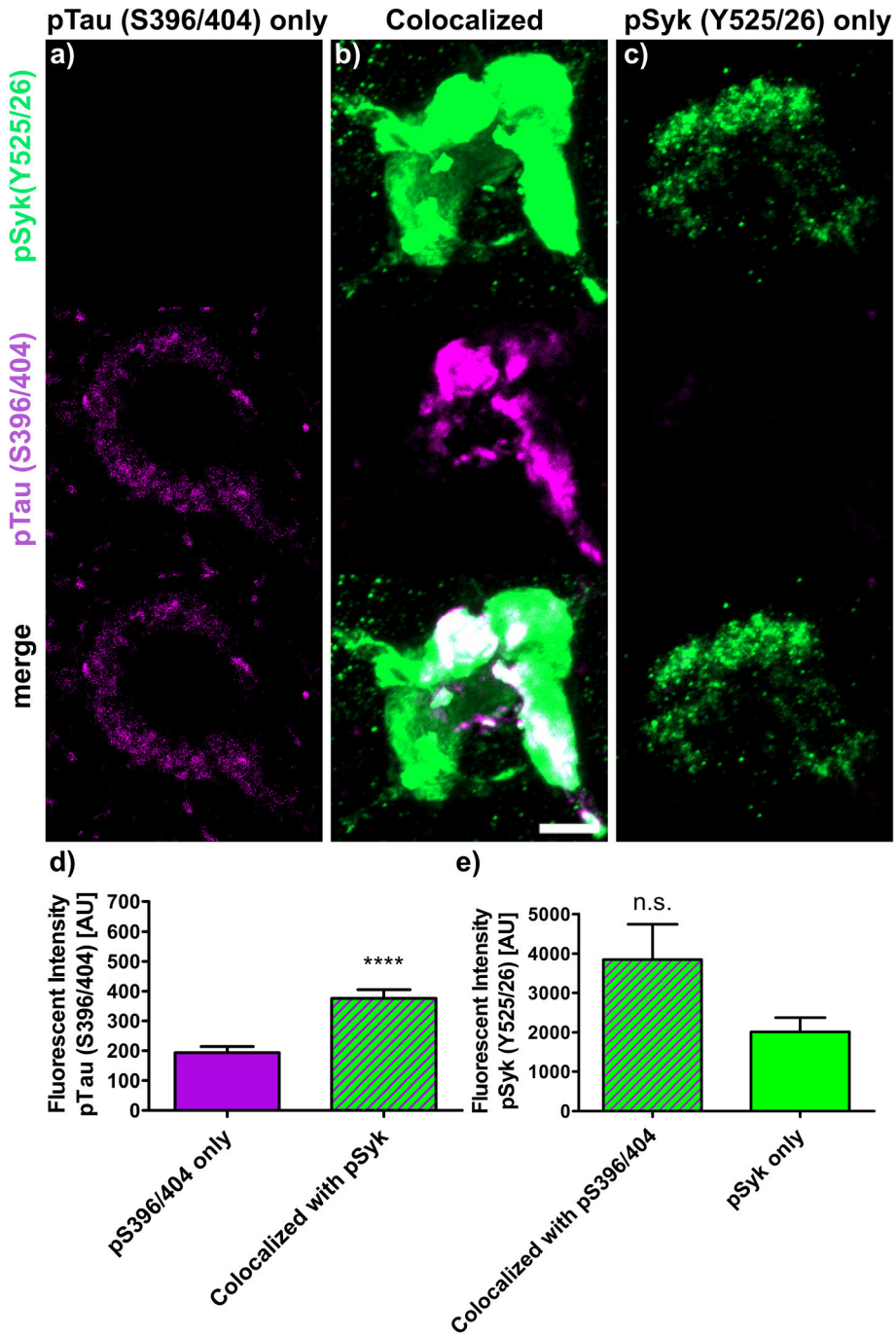

Fig. 11 Syk activation (pSyk (Y525/526) influences the level of tau phosphorylation at S396/404. Sections from Tg Tau P301S ($n = 4$, 47 ± 3.1-week-old) were stained with antibodies against phosphorylated tau (S396/404, *purple*) and pSyk (Y525/526, *green*). Fluorescent intensities of pTau (pS396/404) and pSyk were measured using Zen Blue 2.1 (Zeiss). Three different neuronal fractions were differentiated: **a** neurons singly immunopositive for pS396/404 tau, (**b**) neurons singly immunopositive for pSyk and (**c**) neurons immunopositive for both (colocalized). **d** Fluorescent intensities of pS396/404 tau were compared between neurons singly immunopositive for pS396/404 (*purple*) and the neurons exhibiting a colocalization of pS396/404 and pSyk (*purple-green-striped*). Two-tailed Mann–Whitney test revealed a significant increase ($p < 0.0001$) of pS396/404 fluorescent intensity in the neurons exhibiting a colocalization compared to neurons singly immunopositive for pS396/404 tau. **e** Fluorescent intensities of pSyk were compared between singly pSyk immunopositive neurons (*green*) and neurons exhibiting a colocalization of pSyk and pS396/404 tau (*purple-green-striped*). Two-tailed Mann–Whitney test revealed no significant change of pSyk fluorescent intensity in neurons exhibiting a colocalization compared to singly pSyk immunopositive neurons. The scale bar represents 10 μm. The error bars represent SEM

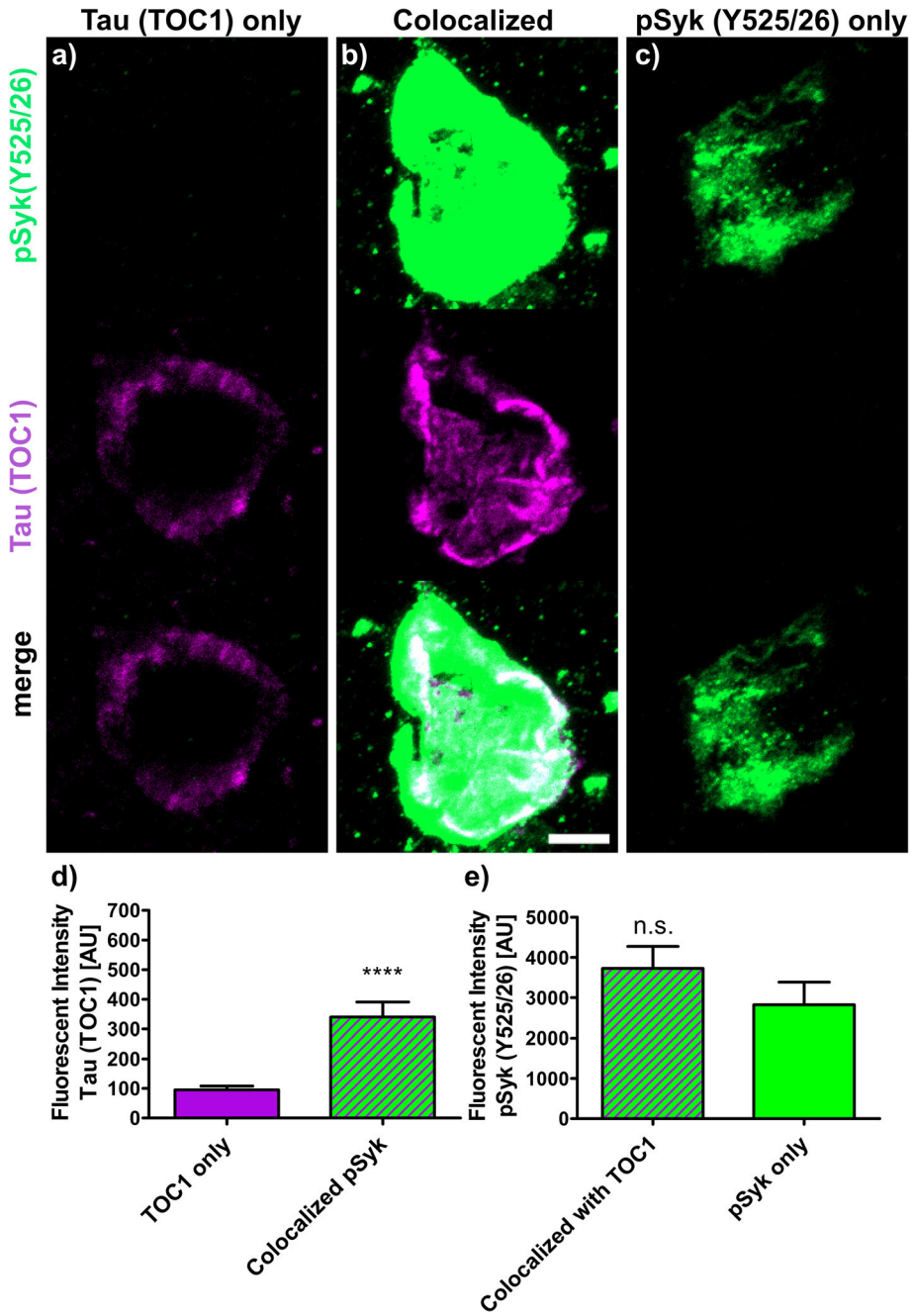

Fig. 12 Syk activation (Y525/526) influences the level of tau oligomerization (TOC1). Sections from Tg Tau P301S ($n = 4$, 47 ± 3.1-week-old) stained with antibodies against tau oligomers (TOC1, *purple*) and pSyk (Y525/526, *green*). Fluorescent intensities of oligomerized tau (TOC1) and pSyk were measured using Zen Blue 2.1 (Zeiss). Three different neuronal fractions were differentiated: **a**) neurons singly immunopositive for TOC1, (**b**) neurons singly immunopositive for pSyk and (**c**) neurons immunopositive for both (colocalized). **d** Fluorescent intensities of TOC1 were compared between neurons singly immunopositive for TOC1 (*purple*) and neurons exhibiting a colocalization of pSyk and TOC1 (*purple-green-striped*). Two-tailed Mann–Whitney test revealed a significant increase ($p < 0.0001$) of TOC1 fluorescent intensity in neurons exhibiting a colocalization with pSyk compared to singly TOC1 immunopositive neurons. **e** Fluorescent intensities of pSyk were compared between neurons singly immunopositive for pSyk (*green*) and neurons exhibiting a colocalization pf TOC1 and pSyk (*purple-green-striped*). Two-tailed Mann–Whitney test revealed no significant change of pSyk fluorescent intensity in neurons exhibiting a colocalization compared to the singly pSyk immunopositive neurons. The scale bar represents 10 μm. The error bars represent SEM

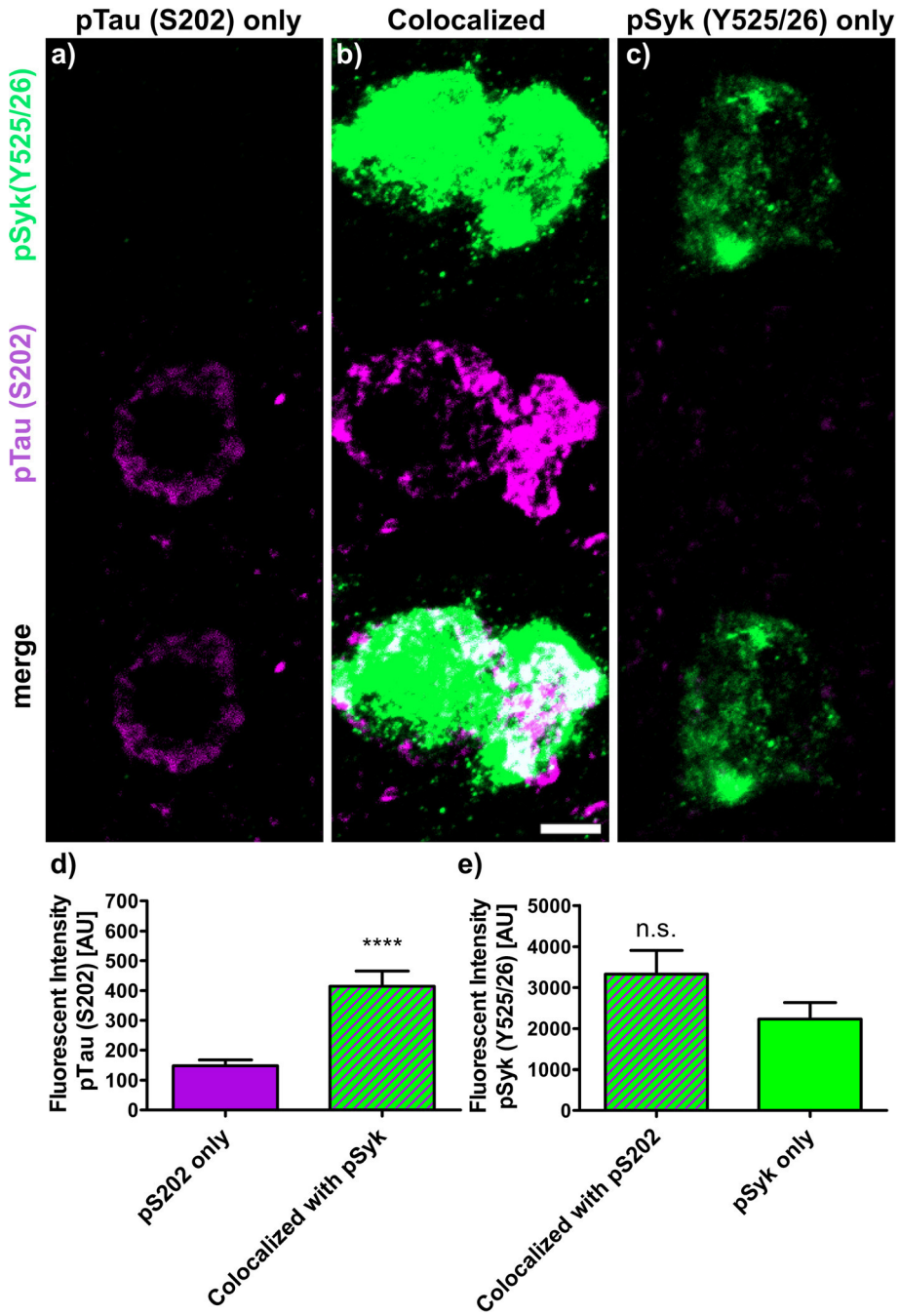

Fig. 13 Syk activation (Y525/526) influences the level of tau phosphorylation at S202. Sections from Tg Tau P301S ($n = 4$, 47 ± 3.1-week-old) stained with antibodies against phosphorylated tau (S202, *purple*) and pSyk (Y525/526, *green*). Fluorescent intensities of pTau (S202) and pSyk were measured using Zen Blue 2.1 (Zeiss). Three different neuronal fractions were differentiated: **a** neurons singly immunopositive for S202, (**b**) neurons singly immunopositive for pSyk and (**c**) neurons immunopositive for both (colocalized). **d** Fluorescent intensities of pS202 tau were compared between neurons singly pS202 immunopositive (*purple*) and neurons exhibiting a colocalization between pS202 and pSyk (*purple-green-striped*). Two-tailed Mann–Whitney test revealed a significant increase ($p < 0.0001$) of pS202 fluorescent intensity in neurons exhibiting a colocalization compared to neurons singly immunopositive for pS202. **e** Fluorescent intensities of pSyk were compared between neurons singly immunopositive for pSyk (*green*) and neurons exhibiting a colocalization of pSyk and pS202 tau (*purple-green-striped*). Two-tailed Mann–Whitney test revealed no significant change of pSyk fluorescent intensity in neurons exhibiting a colocalization compared to singly pSyk immunopositive neurons. The scale bar represents 10 μm. The error bars represent SEM

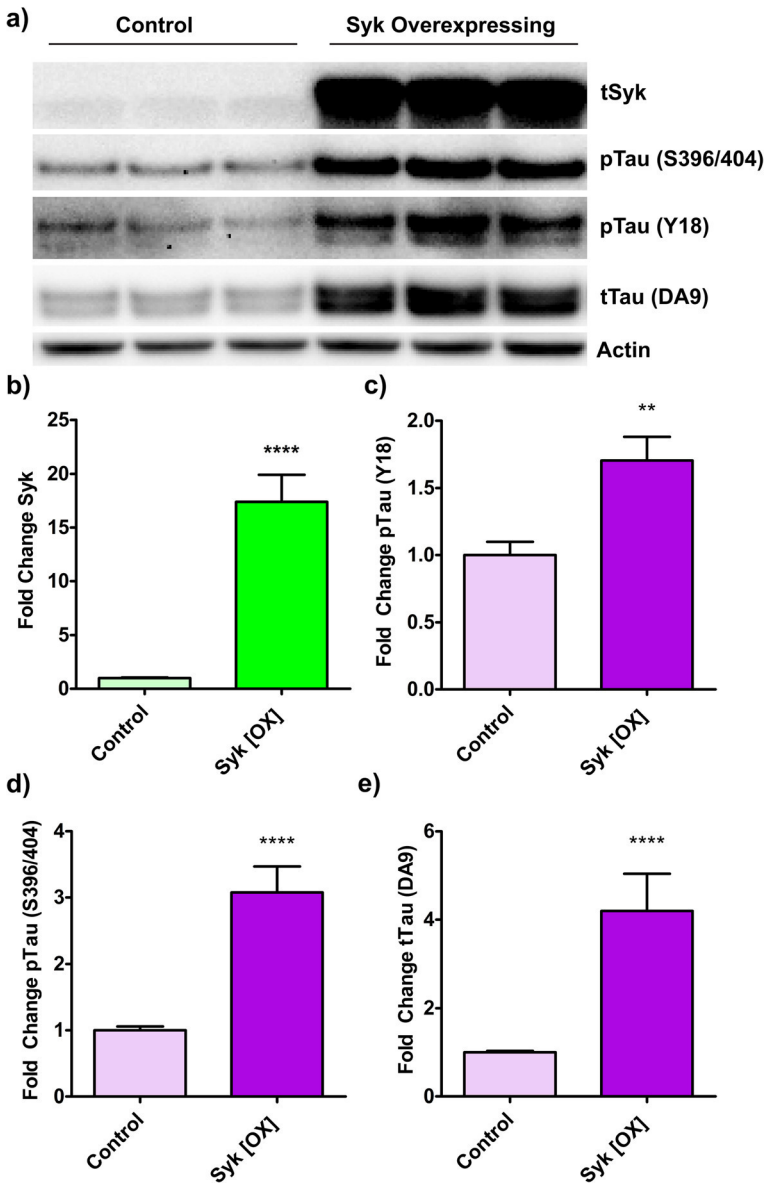

Fig. 14 Syk overexpression increases tau phosphorylation and total tau levels in SH-SY5Y cells. SH-SY5Y cells were transfected with either the empty plasmid as a control or with the same plasmid carrying the Syk sequence for overexpression (Syk OX). Proteins expressed by transfected SH-SY5Y cells were analyzed by Western-blotting. Western-blots chemiluminescent signals were quantified and results were tested for normal distribution using the Shapiro-Wilk test. A subsequent Mann–Whitney test was used to test for statistical significance. **a** Representative Western blots are shown. **b** Level of Syk overexpression is in average 17.3 times higher than in control cells ($p \leq 0.0001$, $n = 18$). **c** Level of tau phosphorylation at Y18 is 1.7 times higher in Syk overexpressing compared to control cells ($p \leq 0.01$, $n = 11$). **d** Level of tau phosphorylation at S396/404 is 3 times higher in Syk overexpressing compared to control cells ($p \leq 0.0001$, $n = 17$). **e** Level of total tau (DA9) is 4.1 times higher in Syk overexpressing compared to control cells ($p \leq 0.0001$, $n = 18$). The error bars represent SEM

prompted us to investigate the level of Syk activation in different mouse models of AD and in brain sections from a non-demented control and an AD patient. We found that Syk activation occurs in three different mouse models of AD, overexpressing Aβ or tau, showing that Syk activation is triggered by both Aβ deposits and tau pathological species. Most importantly, we made similar observations in human AD brain sections.

Recent late phase clinical trials targeting the major pathological hallmarks of AD, mainly extracellular Aβ plaques or intra-neuronal tau aggregates, have been unsuccessful so far and have failed to prevent cognitive decline and brain atrophy in AD patients [7, 19, 37, 39]. As PET scan imaging of AD patients reveals that Aβ deposits and pathological tau accumulation occur during the prodromal phase of AD [26], it has been suggested

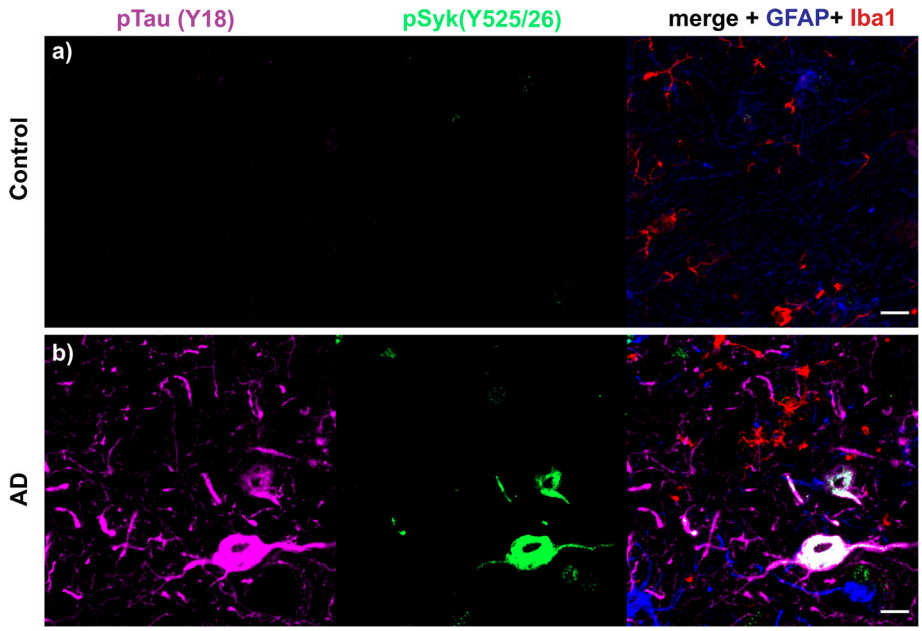

Fig. 15 pSyk is increased in cortical neurons immunopositive for pTau (Y18) of human AD compared to non-demented controls. Representative confocal images of the dorsolateral frontal cortex sections of human AD (**b**) were stained with antibodies against pTau (Y18) (*purple*), pSyk (525/526) (*green*), Iba-1 (*red*) and GFAP (*blue*) and compared to control brain sections (**a**). **a** The non-demented control (102-year-old, male) does not exhibit any tau phosphorylation nor increased Syk activation in the dorsolateral frontal cortex. **b** The AD brain (67-year-old, male) exhibits a prominent tau phosphorylation at Y18 that colocalizes with Syk activation (Y525/526) in cortical neurons. The scale bars represent 10 μm

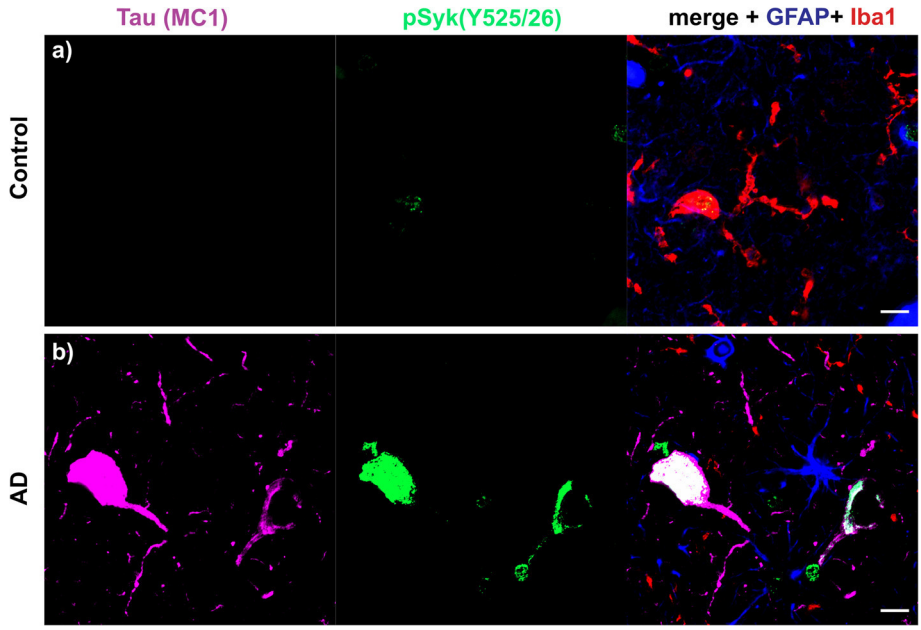

Fig. 16 pSyk is increased in cortical neurons immunopositive for MC1 pathogenic Tau conformers in AD compared to brain sections from a non-demented control. Representative confocal images of the dorsolateral frontal cortex sections of human AD (**b**) were stained with antibodies against conformationally altered tau species (MC1) (*purple*), pSyk (525/526) (*green*), Iba-1 (*red*) and GFAP (*blue*) and compared to non-demented control brain sections (**a**). **a** The non-demented control (102-year-old, male) does not exhibit any cells immunopositive for MC1 nor increased in Syk activation in the dorsolateral frontal cortex. **b** The AD brain (67-year-old, male) exhibits neurons strongly immunopositive for MC1 that colocalize with Syk activation (Y525/526) in cortical neurons. The scale bars represent 10 μm

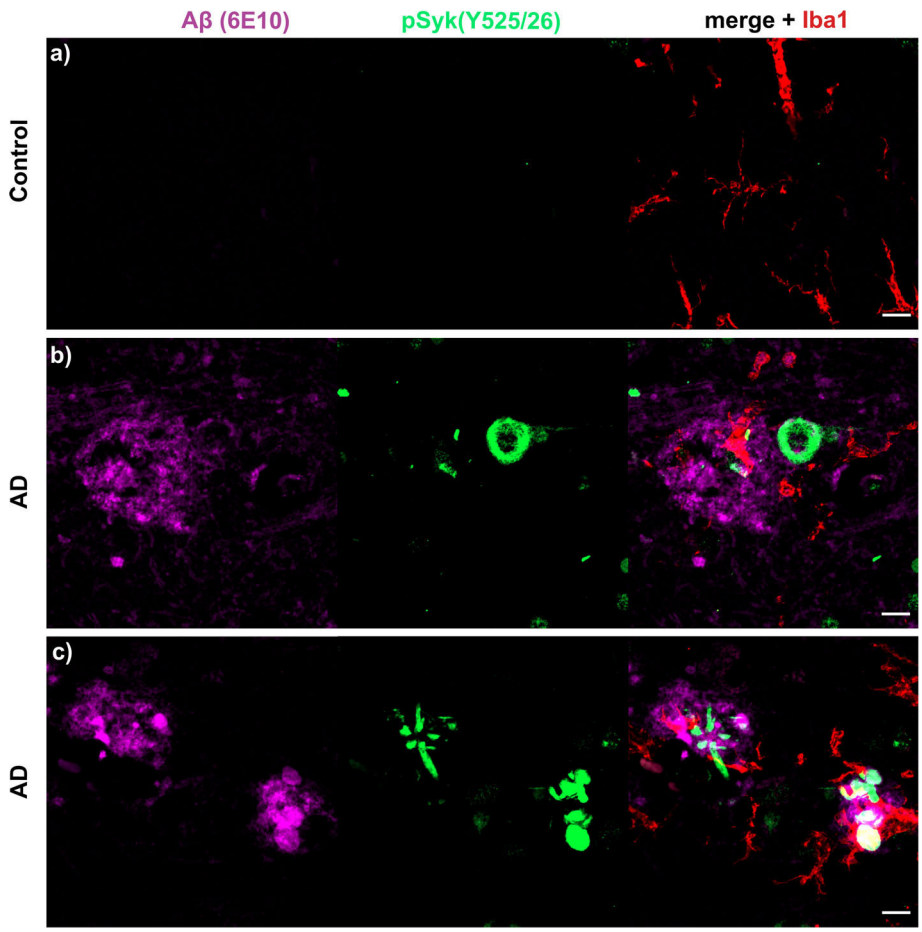

Fig. 17 pSyk is increased in dystrophic neurites associated with β-amyloid plaques of human AD patients compared to healthy controls. Representative confocal images of dorsolateral frontal cortex sections of human AD (**b**) were stained with antibodies against Aβ (6E10) (*purple*), pSyk (525/526) (*green*), Iba-1 (*red*) and compared to non-demented control brain sections (**a**). **a** The non-demented control (102-year-old, male) does not exhibit any Aβ deposits nor increased Syk activation in neurons. **b** The AD brain (67-year-old, male) exhibits neurons strongly immunopositive for pSyk (Y525/526). **c** The AD brain also exhibits dystrophic neurites immunopositive for pSyk (Y525/526) near/within Aβ deposits. The scale bars represent 10 μm

that therapies that are targeting Aβ or pathological tau accumulation must be implemented decades before the appearance of the symptoms to be successful [26]. Hence, pharmacological intervention at downstream targets of Aβ and tau may represent a more promising therapeutic strategy for AD patients. However, therapeutic targets downstream of the Aβ and tau pathological lesions remain to be identified. Our work supports the view that Syk may be such a therapeutic target as it appears to be activated in vivo in response to β-amyloidosis and the formation of pathological tau species.

In this study, we report a hyperactivation of Syk in the brains of three different AD mouse models versus wild-type/littermate controls and human AD compared to non-demented controls. In Tg PS1/APPsw, Tg APPsw mice, Syk activity is largely increased in activated microglia and in DNs around Aβ deposits. In addition, we observed an activation of Syk in DNs around Aβ deposits in an AD pathological specimen. In Tg Tau P301S mice and AD brain sections, Syk hyperactivation is colocalized with misfolded tau and hyperphosphorylated tau in neurons.

The strong increase in activated Syk observed in dystrophic neurites (DNs) surrounding Aβ deposits may suggest the involvement of Syk in the formation of these DNs that ultimately leads to the synaptic loss observed in AD [32]. DNs are characterized by an accumulation of BACE-1 and sAPPβ which implies a contribution of DNs to Aβ production and accumulation [31]. In fact, several in vivo studies have shown that BACE-1 immunopositive dystrophic neurites precede Aβ plaque formation in the brains of 3xTg-AD, 2xFAD and 5xFAD mice and therefore, represent an early pathological event in AD [2, 16, 45]. Our previous in vitro and in vivo data have shown that Syk regulates Aβ and sAPPβ production

via a modulation of BACE-1 expression [28] and therefore support a causative role of Syk activation in the accumulation of BACE-1 and sAPPβ in DNs.

The increased activation of Syk in activated microglia of Aβ-overexpressing mice further supports a role of Syk in microglial activation in vivo and suggests that Aβ accumulation can lead to an activation of Syk in microglia. Previous in vitro studies have shown that Aβ fibrils and oligomers can trigger a microglial inflammatory response mediated by Syk and leading to neurotoxicity [3, 4, 23].

Recruitment and activation of Syk can also be mediated by activation of triggering receptor expressed on myeloid cells 2 (TREM2) [18]. TREM2 is a type I transmembrane protein and part of the immunoglobulin (Ig) receptor superfamily. Since TREM2 does not have any cytoplasmic signaling motifs, an adaptor protein DNAX-activating protein of 12 kDa (DAP12, also known as TYROBP) is needed for TREM2 signal transduction. DAP12 interacts with the transmembrane domain of TREM2. The cytoplasmic domain of DAP12 contains an immunoreceptor tyrosine activation motif (ITAM) that provides docking sites for Syk activation. Interestingly, loss-of-function mutations in the DAP12 or TREM2 genes cause a rare autosomal recessive disorder called Nasu-Hakola disease (NHD) whereas heterozygous carriers of these mutations show an elevated risk to develop AD [27]. Symptoms of NDH include multifocal bone cysts and presenile dementia. Interestingly, Syk activation (pSyk, Y525/526) is increased in NHD neurons compared to controls [33] and was found to be also present in microglia and macrophages but not in astrocytes or oligodendrocytes [33] supporting a role of Syk activation in the development of NHD dementia.

Syk plays a key role in the activation of immune cells and the production of inflammatory cytokines. We have shown previously that activation of NFκB (nuclear factor kappa-light-chain-enhancer of activated B cells) which is known to play a regulatory role in neuroinflammation, is prevented following either pharmacological Syk inhibition or genetic knockdown of Syk [28]. Hence, this suggests a role of Syk in the regulation of neuroinflammation. In addition, Syk has been shown to mediate the neuroinflammation and neurotoxicity caused by Aβ [3, 23]. Furthermore, the Aβ-induced cytokine production by microglia has been found to be mediated by Syk [4], suggesting that Syk is involved in the microglial proinflammatory response.

The pathological analysis of Tg Tau P301S mice shows that Syk activation is associated with the formation of hyperphosphorylated tau and misfolded tau in the hippocampus and cortex while our previous work has shown that Syk inhibition can reduce tau phosphorylation at multiple AD relevant epitopes [28]. Interestingly, we show here that Syk upregulation in human neuronal like SH-SY5Y cells induces tau accumulation and tau phosphorylation further confirming a role of Syk in the formation of tau pathogenic species. Altogether, our data suggest that Syk activation may also promote tau hyperphosphorylation and misfolding in vivo as neurons that show higher levels of Syk activation also show more accumulation of hyperphosphorylated tau and tau pathogenic conformers. Pathological tau species accumulation clearly results in Syk activation in Tg Tau P301S mice while Syk activation appears to be a mediator of the formation of tau pathogenic species, thereby implying the existence of a positive feedback loop resulting in an enhanced progression of tau pathology. Given that Syk is also present in DNs which exhibit tau accumulation and tau phosphorylation [35, 40], this further supports a pathological role of Syk in the formation of DNs and ultimately synaptical loss.

Our previous in vivo and in vitro data show decreased tau phosphorylation at multiple epitopes (S396/404, S202, Y18) following Syk inhibition [28]. Interestingly, we show here that Syk overexpression in SH-SY5Y cells increases tau phosphorylation and total tau levels (Y18, S396/404, DA9). The increase in total tau levels following Syk upregulation is not caused by an increased transcription, as tau mRNA levels do not vary between Syk overexpressing and control cells (data not shown). Therefore, increased Syk levels may lead to an increased translation or decreased degradation of tau or a combination of both. However, the molecular mechanisms responsible for the increased tau levels following Syk overexpression or decreased tau following Syk inhibition remain to be further investigated and are currently being studied in our laboratory.

In this study, we also provide evidence for an aberrant Syk activation in dystrophic neurites around Aβ deposits and in neurons immunopositive for pathological tau species in human AD brain sections further validating the data obtained with different transgenic mouse models of AD.

Conclusions

In conclusion, our data support a pathological role of Syk in the formation of Aβ deposits and misfolded tau and suggest additionally that reduction of Syk hyperactivity through pharmacological inhibition may be a promising therapeutic approach for the treatment of AD.

Acknowledgements

Funding for these studies was provided in part by the Department of Veterans Affairs VA Merit 1I01BX002572-(FC). We are thankful to the Roskamp Foundation for providing additional funding which helped to make this study possible. We are grateful to Dr. Peter Davies (Litwin-Zucker Center for Research on Alzheimer's disease, Feinstein Institute, Manhasset, NY, USA) for kindly providing the PHF-1, CP13, DA9, RZ3 and MC1 antibodies. We are also thankful to Dr. Lester Binder (Department of Translational Science & Molecular Medicine, Michigan State University College of Human Medicine, Grand Rapids, MI, USA) for providing the

TOC1 antibody. Finally, we are grateful to Dr. Ann McKee (Boston University Alzheimer's Disease and CTE Center, Boston University School of Medicine, Boston, MA, USA) for providing tissue sections from an AD patient and a non-demented control.

Availability of data and materials
The datasets generated and/or analyzed during the current study are available from the corresponding author on reasonable request.

Authors' contributions
All authors read and approved the final manuscript.

Ethics approval
All the work involving mice was reviewed and approved by the Roskamp Institute Institutional Animal Care and Use Committee (IACUC) before implementation under the protocol R#073 and was conducted in compliance with the National Institutes of Health Guidelines for the Care and Use of Laboratory Animals.

Competing interests
The authors declare that they have no competing interests.

Publisher's Note

Author details
[1]The Roskamp Institute, 2040 Whitfield Avenue, Sarasota, FL 34243, USA. [2]The Open University, Milton Keynes MK7 6AA, UK. [3]James A. Haley Veterans' Hospital, Tampa, FL 33612, USA.

Received: 30 August 2017 Accepted: 30 August 2017
Published online: 06 September 2017

References
1. Bugiani O, Murrell JR, Giaccone G et al (1999) Frontotemporal dementia and corticobasal degeneration in a family with a P301S mutation in tau. J Neuropathol Exp Neurol 58(6):667–677
2. Cai Y, Zhang X-M, Macklin LN et al (2012) BACE1 elevation is involved in amyloid plaque development in the triple transgenic model of Alzheimer's disease: differential Abeta antibody labeling of early-onset axon terminal pathology. Neurotox Res 21(2):160–174. doi:10.1007/s12640-011-9256-9
3. Combs CK, Johnson DE, Cannady SB et al (1999) Identification of microglial signal transduction pathways mediating a neurotoxic response to amyloidogenic fragments of beta-amyloid and prion proteins. J Neurosci 19(3):928–939
4. Combs CK, Karlo JC, Kao SC et al (2001) Beta-Amyloid stimulation of microglia and monocytes results in TNFalpha-dependent expression of inducible nitric oxide synthase and neuronal apoptosis. J Neurosci 21(4):1179–1188
5. Derkinderen P, Scales TME, Hanger DP et al (2005) Tyrosine 394 is Phosphorylated in Alzheimer's paired helical filament tau and in fetal tau with c-Abl as the candidate tyrosine Kinase. J Neurosci 25(28):6584–6593. doi:10.1523/JNEUROSCI.1487-05.2005
6. Faruki S, Geahlen RL, Asai DJ (2000) Syk-dependent phosphorylation of microtubules in activated B-lymphocytes. J Cell Sci 113(Pt 14):2557–2565
7. Gauthier S, Feldman HH, Schneider LS et al (2016) Efficacy and safety of tau-aggregation inhibitor therapy in patients with mild or moderate Alzheimer's disease: a randomised, controlled, double-blind, parallel-arm, phase 3 trial. Lancet 388(10062):2873–2884. doi:10.1016/S0140-6736(16)31275-2
8. Geahlen RL (2014) Getting Syk: spleen tyrosine kinase as a therapeutic target. Trends Pharmacol Sci 35(8):414–422. doi:10.1016/j.tips.2014.05.007
9. Gordon MN, Holcomb L, Jantzen PT et al (2002) Time course of the development of Alzheimer-like pathology in the doubly transgenic PS1 +APP mouse. Exp Neurol 173(2):183–195. doi:10.1006/exnr.2001.7754
10. Guo T, Noble W, Hanger DP (2017) Roles of tau protein in health and disease. Acta Neuropathol 133(5):665–704. doi:10.1007/s00401-017-1707-9
11. Han C, Jin J, Xu S et al (2010) Integrin CD11b negatively regulates TLR-triggered inflammatory responses by activating Syk and promoting degradation of MyD88 and TRIF via Cbl-b. Nat Immunol 11(8):734–742. doi:10.1038/ni.1908
12. Holcomb L, Gordon MN, McGowan E et al (1998) Accelerated Alzheimer-type phenotype in transgenic mice carrying both mutant amyloid precursor protein and presenilin 1 transgenes. Nat Med 4(1):97–100
13. Hsiao K, Chapman P, Nilsen S et al (1996) Correlative memory deficits, Abeta elevation, and amyloid plaques in transgenic mice. Science 274(5284):99–102
14. Huang Z-Y, Barreda DR, Worth RG et al (2006) Differential kinase requirements in human and mouse Fc-gamma receptor phagocytosis and endocytosis. J Leukoc Biol 80(6):1553–1562. doi:10.1189/jlb.0106019
15. Irizarry MC, McNamara M, Fedorchak K et al (1997) APPSw transgenic mice develop age-related a beta deposits and neuropil abnormalities, but no neuronal loss in CA1. J Neuropathol Exp Neurol 56(9):965–973
16. Kandalepas PC, Sadleir KR, Eimer WA et al (2013) The Alzheimer's beta-secretase BACE1 localizes to normal presynaptic terminals and to dystrophic presynaptic terminals surrounding amyloid plaques. Acta Neuropathol 126(3):329–352. doi:10.1007/s00401-013-1152-3
17. Kober DL, Brett TJ (2017) TREM2-Ligand interactions in health and disease. J Mol Biol 429(11):1607–1629. doi:10.1016/j.jmb.2017.04.004
18. Lanier LL, Bakker AB (2000) The ITAM-bearing transmembrane adaptor DAP12 in lymphoid and myeloid cell function. Immunol Today 21(12):611–614. doi:10.1016/S0167-5699(00)01745-X
19. Le Couteur DG, Hunter S, Brayne C (2016) Solanezumab and the amyloid hypothesis for Alzheimer's disease. BMJ 355:i6771. doi:10.1136/bmj.i6771
20. Lebouvier T, Scales TM, Williamson R et al (2009) The microtubule-associated protein tau is also phosphorylated on tyrosine. J Alzheimers Dis 18(1):1–9. doi:10.3233/JAD-2009-1116
21. Lin K-C, Huang D-Y, Huang D-W et al (2016) Inhibition of AMPK through Lyn-Syk-Akt enhances FcepsilonRI signal pathways for allergic response. J Mol Med (Berl) 94(2):183–194. doi:10.1007/s00109-015-1339-2
22. Lossos A, Reches A, Gal A et al (2003) Frontotemporal dementia and parkinsonism with the P301S tau gene mutation in a Jewish family. J Neurol 250(6):733–740. doi:10.1007/s00415-003-1074-4
23. McDonald DR, Brunden KR, Landreth GE (1997) Amyloid fibrils activate tyrosine kinase-dependent signaling and superoxide production in microglia. J Neurosci 17(7):2284–2294
24. McGeer PL, McGeer EG (2013) The amyloid cascade-inflammatory hypothesis of Alzheimer disease: implications for therapy. Acta Neuropathol 126(4):479–497. doi:10.1007/s00401-013-1177-7
25. Nisbet RM, Polanco J-C, Ittner LM et al (2015) Tau aggregation and its interplay with amyloid-beta. Acta Neuropathol 129(2):207–220. doi:10.1007/s00401-014-1371-2
26. Ossenkoppele R, van Berckel BN, Prins ND (2011) Amyloid imaging in prodromal Alzheimer's disease. Alzheimers Res Ther 3(5):26. doi:10.1186/alzrt88
27. Paloneva J, Manninen T, Christman G et al (2002) Mutations in two genes encoding different subunits of a receptor signaling complex result in an identical disease phenotype. Am J Hum Genet 71(3):656–662. doi:10.1086/342259
28. Paris D, Ait-Ghezala G, Bachmeier C et al (2014) The spleen tyrosine kinase (Syk) regulates Alzheimer amyloid-beta production and tau hyperphosphorylation. J Biol Chem 289(49):33927–33944. doi:10.1074/jbc.M114.608091
29. Prokop S, Miller KR, Heppner FL (2013) Microglia actions in Alzheimer's disease. Acta Neuropathol 126(4):461–477. doi:10.1007/s00401-013-1182-x
30. Sada K, Takano T, Yanagi S et al (2001) Structure and function of Syk protein-tyrosine Kinase. J Biochem 130(2):177–186
31. Sadleir KR, Kandalepas PC, Buggia-Prevot V et al. (2016) Presynaptic dystrophic neurites surrounding amyloid plaques are sites of microtubule disruption, BACE1 elevation, and increased Abeta generation in Alzheimer's disease. Acta Neuropathol doi:10.1007/s00401-016-1558-9
32. Sanchez-Varo R, Trujillo-Estrada L, Sanchez-Mejias E et al (2012) Abnormal accumulation of autophagic vesicles correlates with axonal and synaptic pathology in young Alzheimer's mice hippocampus. Acta Neuropathol 123(1):53–70. doi:10.1007/s00401-011-0896-x
33. Satoh J-I, Tabunoki H, Ishida T et al (2012) Phosphorylated Syk expression is enhanced in Nasu-Hakola disease brains. Neuropathology 32(2):149–157. doi:10.1111/j.1440-1789.2011.01256.x
34. Schindelin J, Arganda-Carreras I, Frise E et al (2012) Fiji: an open-source platform for biological-image analysis. Nat Methods 9(7):676–682. doi:10.1038/nmeth.2019
35. Schmidt ML, DiDario AG, Lee VM et al (1994) An extensive network of PHF tau-rich dystrophic neurites permeates neocortex and nearly all neuritic and diffuse amyloid plaques in Alzheimer disease. FEBS Lett 344(1):69–73

36. Shepherd C, McCann H, Halliday GM (2009) Variations in the neuropathology of familial Alzheimer's disease. Acta Neuropathol 118(1):37–52. doi:10.1007/s00401-009-0521-4
37. Siemers ER, Sundell KL, Carlson C et al (2016) Phase 3 solanezumab trials: secondary outcomes in mild Alzheimer's disease patients. Alzheimers Dement 12(2):110–120. doi:10.1016/j.jalz.2015.06.1893
38. Sperfeld AD, Collatz MB, Baier H et al (1999) FTDP-17: an early-onset phenotype with parkinsonism and epileptic seizures caused by a novel mutation. Ann Neurol 46(5):708–715
39. St-Amour I, Cicchetti F, Calon F (2016) Immunotherapies in Alzheimer's disease: too much, too little, too late or off-target? Acta Neuropathol 131(4):481–504. doi:10.1007/s00401-015-1518-9
40. Su JH, Cummings BJ, Cotman CW (1993) Identification and distribution of axonal dystrophic neurites in Alzheimer's disease. Brain Res 625(2):228–237
41. Thal DR, Walter J, Saido TC et al (2015) Neuropathology and biochemistry of Abeta and its aggregates in Alzheimer's disease. Acta Neuropathol 129(2):167–182. doi:10.1007/s00401-014-1375-y
42. Viola KL, Klein WL (2015) Amyloid beta oligomers in Alzheimer's disease pathogenesis, treatment, and diagnosis. Acta Neuropathol 129(2):183–206. doi:10.1007/s00401-015-1386-3
43. Yoshiyama Y, Higuchi M, Zhang B et al (2007) Synapse loss and microglial activation precede tangles in a P301S tauopathy mouse model. Neuron 53(3):337–351. doi:10.1016/j.neuron.2007.01.010
44. Yu Y, Gaillard S, Phillip JM et al (2015) Inhibition of spleen tyrosine Kinase potentiates Paclitaxel-induced Cytotoxicity in ovarian cancer cells by stabilizing microtubules. Cancer Cell 28(1):82–96. doi:10.1016/j.ccell.2015.05.009
45. Zhang X-M, Cai Y, Xiong K et al (2009) Beta-secretase-1 elevation in transgenic mouse models of Alzheimer's disease is associated with synaptic/axonal pathology and amyloidogenesis: implications for neuritic plaque development. Eur J Neurosci 30(12):2271–2283. doi:10.1111/j.1460-9568.2009.07017.x